

**Towards a coupled $\delta^{18}\text{O}$ sugar and $\delta^2\text{H}$ *n*-alkane
approach in paleoclimate research**

Dissertation

zur Erlangung des Grades Doktor der Naturwissenschaften

(Dr. rer. nat.)

an der Fakultät Biologie / Chemie / Geowissenschaften
der Universität Bayreuth

vorgelegt von

Mario Tuthorn

geb. am 23.12.1985 in Osijek, Kroatien

Betreuer: PD Dr. Michael Zech

Bayreuth, März 2014

Die vorliegende Arbeit wurde in der Zeit von 12/2011 bis 03/2014 in Bayreuth am Lehrstuhl für Geomorphologie und Abteilung Bodenphysik unter der Betreuung von Herrn PD Dr. Michael Zech angefertigt.

Vollständiger Abdruck der von der Fakultät für Biologie, Chemie and Geowissenschaften der Universität Bayreuth genehmigten Dissertation zur Erlangung des akademischen Grades eines Doktors der Naturwissenschaften (Dr. rer. nat.).

Dissertation eingereicht am: 12.03.2014

Zugelassen durch die Prüfungskommission: 19.03.2014

Wissenschaftliches Kolloquium: 25.07.2014

Amtierender Dekan: Prof. Dr. Rhett Kempe

Prüfungsausschuss:

1. PD Dr. Michael Zech (Erstgutachter)
2. Prof. Dr. Christiane Werner Pinto (Zweitgutachter)
3. Prof. Dr. Bernd Huwe (Vorsitz)
4. Prof. Dr. Ludwig Zöller

Contents

Contents.....	I
List of abbreviations.....	V
List of tables.....	IX
List of figures.....	XI
Abstract.....	XVII
Zusammenfassung.....	XIX
Extended Summary.....	1
1. Introduction and motivation.....	3
2. Method for compound-specific $\delta^{18}\text{O}$ analyses and first application to topsoils along a climate transect (Study 1).....	4
3. Plant physiology and climate aspects influence on $\delta^{18}\text{O}_{\text{hemicellulose}}$ (Studies 2 and 3).....	7
3.1 Validation of the $\delta^{18}\text{O}_{\text{hemicellulose}}$ proxy.....	7
3.2 Péclet modified Craig-Gordon model simulations.....	11
4. Coupling of $\delta^{18}\text{O}$ sugar and $\delta^2\text{H}$ lipid biomarkers (Study 4).....	13
4.1 $\delta^2\text{H}$ analyses of lipid biomarkers.....	13
4.2 Conceptual model for interpreting coupled $\delta^2\text{H}$ - $\delta^{18}\text{O}$ biomarker results.....	14
5. First application of the coupled $\delta^{18}\text{O}_{\text{sugar}}$ and $\delta^2\text{H}_{n\text{-alkane}}$ approach in paleolimnology (Studies 5 and 6).....	18
5.1 A 16 ka $\delta^{18}\text{O}_{\text{sugar}}$ and $\delta^2\text{H}_{n\text{-alkane}}$ biomarker records.....	18
5.2 Reconstruction of lake evaporation history.....	20
6. Conclusions.....	22
References.....	23
7. Contributions to the included manuscripts.....	29
Acknowledgments.....	32
Cumulative Study.....	33
Study 1:	
Natural abundance of ^{18}O of sugar biomarkers in topsoils along a climate transect over the Central Scandinavian Mountains, Norway.....	35
Abstract.....	36
1. Introduction.....	37
2. Material and methods.....	38
3. Results.....	40
4. Discussion.....	41
Acknowledgements.....	43
References.....	44

Study 2:

Oxygen isotope ratios ($^{18}\text{O}/^{16}\text{O}$) of hemicellulose-derived sugar biomarkers in plants, soils and sediments as paleoclimate proxy I: Insight from a climate chamber experiment

.....	47
Abstract	48
1. Introduction	50
2. Material and Methods.....	52
2.1 Climate chamber experiment	52
2.2 Sample preparation and compound-specific $\delta^{18}\text{O}$ analyses of hemicellulose-derived sugar biomarkers.....	54
2.3 Modeling.....	55
3. Results and Discussion.....	56
3.1 $\delta^{18}\text{O}$ results of hemicellulose-derived sugar biomarkers.....	56
3.2 Comparison of $\delta^{18}\text{O}_{\text{hemicellulose}}$ with modeled $\delta^{18}\text{O}_{\text{cellulose}}$ and measured $\delta^{18}\text{O}_{\text{leaf water}}$	57
3.3 Effect of RH, temperature and transpiration rate on $\delta^{18}\text{O}_{\text{hemicellulose}}$	59
4. A conceptual model for interpreting $\delta^{18}\text{O}_{\text{hemicellulose}}$ in sedimentary paleoclimate archives	63
Acknowledgements	66
References	67

Study 3:

Oxygen isotope ratios ($^{18}\text{O}/^{16}\text{O}$) of hemicellulose-derived sugar biomarkers in plants, soils and sediments as paleoclimate proxy II: Insight from a climate transect study.....

.....	73
Abstract	74
1. Introduction	76
2. Material and methods	77
2.1 Study area and topsoil samples	77
2.2 Compound-specific $\delta^{18}\text{O}$ analyses of the hemicellulose sugar biomarkers	79
2.3 Pécelet-modified Craig-Gordon model simulations.....	81
3. Results and discussion.....	83
3.1 Compound-specific $\delta^{18}\text{O}$ values of the hemicellulose biomarkers	83
3.2 Comparison of $\delta^{18}\text{O}_{\text{hemicellulose}}$ results with $\delta^{18}\text{O}_{\text{prec}}$	85
3.3 Relative air humidity as important controlling factor on $\delta^{18}\text{O}_{\text{leaf water}}$ and $\delta^{18}\text{O}_{\text{hemicellulose}}$ along the investigated Argentinian transect	86
3.4 Comparison between measured $\delta^{18}\text{O}_{\text{hemicellulose}}$ and modeled $\delta^{18}\text{O}_{\text{cellulose}}$ values.....	88
4. Conclusions and implications for paleoclimate studies	90
Acknowledgements	92
References	93

Study 4:

Coupled isotopes of plant wax and hemicellulose markers record information on relative humidity and isotopic composition of precipitation.....

.....	99
Abstract	100

Highlights	101
1. Introduction	102
2. Material and methods	104
2.1 Transect description and samples	104
2.2 Compound-specific $\delta^2\text{H}$ analyses of <i>n</i> -alkanes and fatty acids	105
2.3 Modeling of leaf water ^2H enrichment	106
3. Results and Discussion	108
3.1 Comparison of $\delta^2\text{H}_{n\text{-alkanes}}$ and $\delta^2\text{H}_{\text{fatty acids}}$	108
3.2 Evapotranspirative ^2H enrichment of leaf water	110
3.3 Combining $\delta^{18}\text{O}$ sugar and $\delta^2\text{H}$ <i>n</i> -alkane biomarker analyses	114
3.3.1 The conceptual model	114
3.3.2 Reconstructed RH values along the climate transect and comparison with actual RH values	116
3.3.3 Comparison of reconstructed and actual $\delta^2\text{H}_{\text{prec}}$ and $\delta^{18}\text{O}_{\text{prec}}$ values	118
4. Conclusions	119
Acknowledgements	120
References	121

Study 5:

A 16-ka $\delta^{18}\text{O}$ record of lacustrine sugar biomarkers from the High Himalaya reflects Indian Summer Monsoon variability

Abstract	130
1. Introduction	132
1.1 Site description and modern climate	133
2. Materials and methods	135
2.1 Sampling, TOC analyses and radiocarbon dating	135
2.2 Compound-specific $\delta^{18}\text{O}$ analyses of sugar biomarkers	136
2.3 Pollen analyses and calculation of a pollen-based index reflecting the Indian Summer Monsoon (ISM) strengt	138
3. Results	139
3.1 Chronostratigraphy and TOC contents	139
3.2 Lake Panch Pokhari $\delta^{18}\text{O}$ sugar biomarker results	140
4. Discussion	141
4.1 Interpretation of the $\delta^{18}\text{O}$ sugar biomarker record of Lake Panch Pokhari	141
4.2 Comparison with other $\delta^{18}\text{O}$ records and modern precipitation	142
4.3 Amount effect and source effect as influencing factors	143
4.4 Evaporative ^{18}O enrichment as an influencing factor	145
4.5 Driving mechanisms and North Atlantic – Indian Summer Monsoon teleconnections	147
5. Conclusions	148
Acknowledgements	148
References	149

Study 6:

Coupled ^{18}O and ^2H isotopes of biomarkers record lake evaporation history and allow reconstructing the isotopic composition of precipitation.....

Highlights	156
Abstract	157
1. Introduction	158
2. Material and methods	159
2.1 Study area – Lake Panch Pokhari, Helambu Himal, Nepal	159
2.2 Compound-specific $\delta^2\text{H}$ analyses of <i>n</i> -alkanes	160
3. Theory/calculation.....	162
3.1 $\delta^{18}\text{O}$ - $\delta^2\text{H}$ diagram.....	162
3.2 Model-based reconstruction of $\delta^{18}\text{O}_{\text{prec}}$ and $\delta^2\text{H}_{\text{prec}}$ values	162
4. Results and Discussion.....	164
4.1 Lake Panch Pokhari $\delta^2\text{H}_{n\text{-alkane}}$ record and comparison with the $\delta^{18}\text{O}_{\text{sugar}}$ record.....	164
4.2 Interpretation – $\delta^2\text{H}_{n\text{-alkane}}$ and $\delta^{18}\text{O}_{\text{sugar}}$ reflect lake water	167
4.3 Coupling $\delta^{18}\text{O}_{\text{sugar}}$ and $\delta^2\text{H}_{n\text{-alkane}}$ biomarker results of Lake Panch Pokhari	169
4.3.1 Deuterium-excess as proxy for lake water evaporation losses	169
4.3.2 Reconstructed $\delta^{18}\text{O}_{\text{prec}}$ and $\delta^2\text{H}_{\text{prec}}$ values	172
5. Conclusions	173
Acknowledgements	174
References	175
Additional peer-reviewed publications	182
(Eidesstattliche) Versicherungen und Erklärungen.....	183

List of abbreviations

^{12}C	stable carbon atom with atomic mass 12
^{13}C	stable carbon atom with atomic mass 13
^{14}C	radioactive carbon atom with atomic mass 14
^{14}N	stable nitrogen atom with atomic mass 14
^{15}N	stable nitrogen atom with atomic mass 15
^{16}O	stable oxygen atom with atomic mass 16
^{18}O	stable oxygen atom with atomic mass 18
a.s.l.	above sea level
A horizon	mineral topsoil horizon
ara	arabinose
BP	before present (1950)
BSTFA	bis(trimethylsilyl)trifluoroacetamide
C	molar concentration of water
C/N	carbon/nitrogen ratio
CO	carbon monoxide
CSIA	compound-specific isotope analysis
d-excess (d)	deuterium excess
D	diffusivity of H_2^{18}O
DCM	dichlorometane
E	transpiration rate
e_a	water vapour pressure of the atmosphere
e_i	water vapour pressure in the intercellular spaces
EASM	East Asian Summer Monsoon
EL	evaporation line

FAME	fatty acid methyl ester
fuc	fucose
GC-Py-IRMS	gas chromatography-pyrolysis-isotope ratio mass spectrometer
GC-FID	gas chromatograph with flame ionization detector
glu	glucose
GMWL	global meteoric water line
HF	hydrofluoric acid
HI	hydrogen index
h_N	relative humidity normalized to the ground temperature
I_{TOT}	total inflow (precipitation, surface water and groundwater)
ISM	Indian Summer Monsoon
L	effective path length
LEL	local evaporation line
LW	leaf water
MBA	methylboronic acid
MeOH	methanol
M_{source}	isotopic composition of atmospheric water vapor
myo-ino	myo-inositol
n	turbulence parameter
OM	organic matter
P/E	precipitation/evaporation ratio
PMCG model	Péclet-modified Craig-Gordon model
PIT	principle of “Identical Treatment”
R	correlation coefficient

RH	relative air humidity
R_{sample} and R_{standard}	ratio of a heavier to a lighter isotope in a sample or a standard, respectively
S_{LEL}	slope of a local evaporation line
SW	stem water
T	temperature
T_{air}	air temperature
TC/EA-IRMS	thermal conversion/elemental analyses-isotope ratio mass spectrometer
TFA	trifluoroacetic acid
TOC	total organic carbon
V SMOW	Vienna Standard Mean Ocean Water
WV	water vapour
XW	xylem water
xyl	xylose
α_k	kinetic fractionation factor
α^*	equilibrium fractionation factor
δ_{LS}	isotopic composition of lake water under steady state conditions
δ_{IT}	isotopic composition of the total inflow components
$\delta^{13}\text{C}$	natural abundance of ^{13}C
$\delta^{15}\text{N}$	natural abundance of ^{15}N
$\delta^{18}\text{O}$	natural abundance of ^{18}O

$\delta^{18}\text{O}_{\text{hemicellulose}}$	weighted mean $\delta^{18}\text{O}$ value of the most abundant sugar biomarkers arabinose and xylose, and sometimes additionally fucose
$\delta^{18}\text{O}_{\text{prec}}$	oxygen isotopic composition of precipitation
Δd	difference in deuterium excess between leaf-water and source water
$\Delta\varepsilon$	kinetic isotopic enrichment
$\Delta^{18}\text{O}_{\text{leaf water}}$	evapotranspirative ^{18}O enrichment of leaf water
$\Delta^{18}\text{O}_e$	^{18}O evaporative enrichment of leaf water above source water
$\delta^2\text{H}$	natural abundance of deuterium
$\delta^2\text{H}_{\text{prec}}$	deuterium isotopic composition of precipitation
$\alpha_{L/V}$	temperature dependent equilibrium fractionation factor
ε	apparent fractionation
ε^+	equilibrium fractionation
ε_k	kinetic fractionation
Θ	advection parameter
\wp	Péclet number

List of tables

Study 2

Table 1: Climatic conditions (temperature and relative air humidity) of the eight climate chambers, oxygen isotopic composition of soil water ($\delta^{18}\text{O}_{\text{SW}}$)^{a,b}, stem water ($\delta^{18}\text{O}_{\text{XW}}$)^b, leaf water ($\delta^{18}\text{O}_{\text{LW}}$)^b and atmospheric water vapor ($\delta^{18}\text{O}_{\text{WV}}$)^{a,b}, transpiration rates (E)^{a,b}, modeled $\delta^{18}\text{O}_{\text{cellulose}}$, $\delta^{18}\text{O}_{\text{arabinose}}$, and $\delta^{18}\text{O}_{\text{xylose}}$. (p. 53)

Study 3

Table 1: Geographical description of the 20 sampling localities, mean (n=3) total organic carbon (TOC) contents of the investigated topsoil samples and soil type classification. (p. 78)

Table 2: Compound-specific $\delta^{18}\text{O}$ results for the hemicellulose biomarkers arabinose, fucose and xylose. Standard deviations are given for the field replications. $\delta^{18}\text{O}$ values of annual precipitation were retrieved from The Online Isotopes in Precipitation Calculator (Bowen, 2012). (p. 84)

Study 4

Table 1: $\delta^2\text{H}$ values of individual leaf wax *n*-alkanes and fatty acids. Measurements were carried out in at least triplicate (sd = standard deviation). (p. 109)

Study 5

Table 1: Radiocarbon data obtained for sediment cores N1 and N2 from Lake Panch Pokhari. (p. 136)

Table 2: Arboreal pollen taxa grouped according to their modern distribution. (p. 138)

Study 6

Table 1: $\delta^2\text{H}$ values of individual *n*-alkanes. Measurements were carried out in triplicate (sd = standard deviation). (p. 166)

List of figures

Extended summary

Fig. 1: Scheme of GC-Py-IRMS compound-specific $\delta^{18}\text{O}$ analyses of plant-derived sugar biomarkers in soils (from Zech *et al.*, 2011). (p. 5)

Fig. 2: Comparison of $\delta^{18}\text{O}_{\text{arabinose}}$ and $\delta^{18}\text{O}_{\text{xylose}}$ with modelled $\delta^{18}\text{O}_{\text{cellulose}}$, measured $\delta^{18}\text{O}_{\text{leaf water}}$, $\delta^{18}\text{O}_{\text{xylem water}}$, $\delta^{18}\text{O}_{\text{soil water}}$, and transpiration rate (E). Additionally, temperature and relative air humidity are displayed (from Zech *et al.*, 2014a). (p. 8)

Fig. 3: A) Sampling localities along the investigated Argentinian climate transect and interpolated $\delta^{18}\text{O}$ estimates of annual precipitation (from Bowen, 2012). B) Vegetational zonation in the study area (from Tuthorn *et al.*, 2014). (p. 9)

Fig. 4: A) Comparison of measured $\delta^{18}\text{O}_{\text{hemicellulose}}$ values of arabinose, fucose and xylose with modeled $\delta^{18}\text{O}_{\text{prec}}$, $\delta^{18}\text{O}_{\text{leaf water}}$, $\delta^{18}\text{O}_{\text{stem cellulose}}$, and $\delta^{18}\text{O}_{\text{leaf cellulose}}$. B) Mean annual precipitation and temperature characterizing the investigated sampling sites (from Tuthorn *et al.*, 2014). (p. 10)

Fig. 5: Conceptual diagram illustrating the major variables influencing $\delta^{18}\text{O}_{\text{hemicellulose}}$ (from Zech *et al.*, 2014a). (p. 12)

Fig. 6: Comparison of measured $\delta^2\text{H}_{n\text{-alkanes}}$ (weighted mean of $n\text{-C}_{29}$ and $n\text{-C}_{31}$) and $\delta^2\text{H}_{\text{fatty acids}}$ (weighted mean of $n\text{-C}_{22}$, $n\text{-C}_{24}$, $n\text{-C}_{26}$, $n\text{-C}_{28}$, and $n\text{-C}_{30}$), inferred isotopic composition of leaf water, and $\delta^2\text{H}_{\text{prec}}$ (from Tuthorn *et al.*, to be submitted to BGD). (p. 14)

Fig. 7: $\delta^{18}\text{O}$ - $\delta^2\text{H}$ diagram illustrating the global meteoric water line (GMWL) and an evaporation line (EL). Data for the $\delta^{18}\text{O}$ values of hemicellulose-derived sugars (mean of arabinose, fucose, and xylose) and the mean $\delta^2\text{H}$ values of leaf wax-derived n -

alkanes (mean of $n\text{-C}_{29}$ and $n\text{-C}_{31}$) are displayed (from Tuthorn *et al.*, to be submitted to BGD). (p. 16)

Fig. 8: Reconstructed biomarker-based $\delta^{18}\text{O}_{\text{prec}}$ and $\delta^2\text{H}_{\text{prec}}$ results and comparison with actual modern $\delta^{18}\text{O}_{\text{prec}}$ and $\delta^2\text{H}_{\text{prec}}$ values, respectively (from Tuthorn *et al.*, to be submitted to BGD). (p. 17)

Fig. 9: Age profiles for analytical results from the sediment cores of Lake Panch Pokhari and comparison with $\delta^{18}\text{O}$ records of Chinese speleothemes (P/E- ratio of precipitation to evaporation, ISM- Indian Summer Monsoon; from Tuthorn *et al.*, submitted to JOH). (p. 19)

Fig. 10: Comparison of (a) C/N ratio (from Krstic *et al.*, 2011), (b) Hydrogen Index (HI), and (c) deuterium-excess as proxies for evaporation history of Lake Panch Pokhari (from Tuthorn *et al.*, submitted to JOH). (p. 21)

Study 1

Fig. 1: Location of the study areas in the W and E part of the Central Scandinavian Mountains, respectively. Mean annual precipitation (MAP) illustrates the strong climate gradient (from NMI, 2012). (p. 38)

Fig. 2: Measured $\delta^{18}\text{O}$ values of precipitation, bulk soil and plant-derived sugar biomarkers arabinose and xylose along an altitudinal and climate transect over the Central Scandinavian Mountains, Norway. Additionally, the mean apparent isotopic fractionation $\epsilon_{\text{prec/sugars}}$ is calculated as proxy for evapotranspirative ^{18}O enrichment of leaf water by transpiration. 1) no soil samples were available for ^{18}O analyses. (p. 41)

Study 2

Fig. 1: Results for $\delta^{18}\text{O}_{\text{arabinose}}$ and $\delta^{18}\text{O}_{\text{xylose}}$ and comparison with modeled $\delta^{18}\text{O}_{\text{cellulose}}$, $\delta^{18}\text{O}_{\text{leaf water}}$, $\delta^{18}\text{O}_{\text{xylem water}}$, $\delta^{18}\text{O}_{\text{soil water}}$, transpiration rate (E) and the climate parameters temperature and relative air humidity. 1) from Mayr (2002). (p. 57)

Fig. 2: 3D-Scatterplot and multiple regression analysis describing the dependence of $\delta^{18}\text{O}_{\text{hemicellulose}}$ on the climate parameters temperature and relative air humidity in the climate chamber experiment. (p. 59)

Fig. 3: Results of model sensitivity tests showing the dependency of $\delta^{18}\text{O}_{\text{leaf water}}$ on (A) RH, (B) temperature, (C) transpiration rate and (D) leaf-air temperature difference. The model used for these simulations is from Barbour et al. (2004). (p. 61)

Fig. 4: Conceptual diagram illustrating the major factors influencing the oxygen isotopic composition of hemicellulose-derived sugar biomarkers. (p. 63)

Study 3

Fig. 1: A) Sampling localities along the investigated Argentinian climate transect and interpolated $\delta^{18}\text{O}$ estimates of annual precipitation (from Bowen, 2012). B) Vegetational zonation in the study area (from Olson et al., 2001). (p. 79)

Fig. 2: A) Comparison of measured $\delta^{18}\text{O}_{\text{hemicellulose}}$ values of arabinose, fucose, and xylose extracted from topsoils along the Argentinian climate transect with modeled $\delta^{18}\text{O}_{\text{prec.}}$, $\delta^{18}\text{O}_{\text{leaf water}}$, $\delta^{18}\text{O}_{\text{stem cellulose}}$, and $\delta^{18}\text{O}_{\text{leaf cellulose}}$. B) Mean annual precipitation and temperature characterizing the investigated sampling sites. (p. 85)

Fig. 3: Model sensitivity tests based on a Péclet-modified Craig-Gordon model (Kahmen et al., 2011) showing the dependency of $\delta^{18}\text{O}_{\text{leaf water}}$ on relative air humidity and temperature changes. (p. 88)

Fig. 4: Conceptual diagram illustrating the major factors influencing the oxygen isotopic composition of hemicellulose sugar biomarkers (from Zech et al., 2014). (p. 92)

Study 4

Fig. 1: Sampling localities along the investigated transect in Argentina. The colors illustrate the gradient in $\delta^2\text{H}_{\text{prec}}$, and mean annual T and precipitation are shown below. (p. 104)

Fig. 2: Comparison of $\delta^2\text{H}$ results of individual leaf wax *n*-alkanes and *n*-alkanoic (fatty) acids along the investigated transect. (p. 110)

Fig. 3: Comparison of measured $\delta^2\text{H}_{n\text{-alkanes}}$ (weighted mean of *n*-C₂₉ and *n*-C₃₁) and $\delta^2\text{H}_{\text{fatty acids}}$ (weighted mean of *n*-C₂₂, *n*-C₂₄, *n*-C₂₆, *n*-C₂₈, and *n*-C₃₀), inferred isotopic composition of leaf water, and $\delta^2\text{H}_{\text{prec}}$ (Bowen, 2012). (p. 111)

Fig. 4: Results of $\delta^2\text{H}_{\text{leaf water}}$ model simulations and comparison with measured $\delta^2\text{H}_{n\text{-alkanes}}$ and $\delta^2\text{H}_{\text{fatty acids}}$. Sensitivity tests for $\delta^2\text{H}_{\text{leaf water}}$ are shown for changes in RH and air temperature for all 20 sites along the transect. (p. 113)

Fig. 5: $\delta^{18}\text{O}$ - $\delta^2\text{H}$ diagram representing the global meteoric water line (GMWL) and an evaporation line (EL). Data for the $\delta^{18}\text{O}$ values of hemicellulose-derived sugars (mean of arabinose, fucose, and xylose) and the mean $\delta^2\text{H}$ values of leaf wax-derived *n*-alkanes (mean of *n*-C₂₉ and *n*-C₃₁) are displayed. $\delta^2\text{H}$ and $\delta^{18}\text{O}$ values of leaf water are reconstructed using biosynthetic fractionation factors and $\delta^2\text{H}$ and $\delta^{18}\text{O}$ values of precipitation are calculated as intersection of the individual ELs with the GMWL. (p. 114)

Fig. 6: Comparison of reconstructed humidity based on a normalized Craig-Gordon model accounting for deuterium excess and temperature with modern humidity data retrieved for the investigated sites (GeoINTA, 2012). Deuterium excess values were calculated using $\delta^{18}\text{O}_{\text{leaf water}}$ reconstructed from terrestrial sugars (Tuthorn et al., 2014) and $\delta^2\text{H}_{\text{leaf water}}$ reconstructed from *n*-alkanes. (p. 116)

Fig. 7: Correlation of $\delta^{18}\text{O}_{\text{prec}}$ and $\delta^2\text{H}_{\text{prec}}$ reconstructed from the biomarkers with actual modern $\delta^{18}\text{O}_{\text{prec}}$ and $\delta^2\text{H}_{\text{prec}}$ (from Bowen, 2012), a and b, respectively. (p. 119)

Study 5

Fig. 1: Location of Lake Panch Pokhari on a mountain ridge in the Helambu Himal, Nepal. a) Northward and b) eastward oblique view over the Panch Pokhari catchment that is indicated by dotted white lines (modified from Google Earth). c) The research area is predominantly influenced by the Indian Summer Monsoon (ISM) and to some degree by winter precipitation provided by the Westerlies. EASM = East Asian Summer Monsoon. The EASM exerts the pivotal climatic influence on Hulu Cave. (p. 134)

Fig. 2: Typical GC-Py-IRMS chromatogram for the sediment samples from Lake Panch Pokhari (sample 490 cm depth). Whereas the lower part of the figure shows the signal intensity of m/z 28 ($^{12}\text{C}^{16}\text{O}$), the upper part shows the ratio of m/z 30 to m/z 28 ($^{12}\text{C}^{18}\text{O}$ to $^{12}\text{C}^{16}\text{O}$). (p.137)

Fig. 3: Depth profiles for analytical results from the sediment cores of Lake Panch Pokhari. Total organic carbon (TOC) contents for sediment cores N1 and N2 are shown with the calibrated radiocarbon data given to the right. The $\delta^{18}\text{O}$ results of hemicellulose and polysaccharide sugar biomarkers (arabinose, fucose and xylose) extracted from core N1 (grey lines show all data, dark lines show the 3-point running mean) reflect the ratio of precipitation to evaporation (P/E). In addition, a pollen-based index of the strength of the Indian Summer Monsoon (ISM) and the July insolation at 30°N (Berger and Loutre 1991) are shown. The periods of deglaciation and Younger Dryas are depicted with horizontal blue bars. (p. 140)

Fig. 4: Comparison of the Lake Panch Pokhari $\delta^{18}\text{O}$ record with other $\delta^{18}\text{O}$ records. a) The grey line shows the weighted average for arabinose, fucose and xylose; the dark line shows the 3-point running mean for the weighted average. b) Hulu stalagmites H82 and PD (Wang et al. 2001) and c) Greenland ice core $\delta^{18}\text{O}$ record (NGRIP members 2005) plotted versus time. Vertical blue bars highlight the periods of deglaciation and the

Younger Dryas. Calibrated radiocarbon ages and errors are plotted for sediment cores N1 and N2. VSMOW = Vienna Standard Mean Ocean Water, VPDB = Vienna Pee Dee Belemnite. (p. 143)

Study 6

Fig. 1: Location of Lake Panch Pokhari, Helambu Himalaya, Nepal. The most prominent atmospheric circulation pattern influencing the study area are additionally depicted (Westerlies, ISM - Indian Summer Monsoon, EASM - East Asian Summer Monsoon). (p. 160)

Fig. 2: Comparison of (a) the Lake Panch Pokhari $\delta^2\text{H}_{n\text{-alkane}}$ record (weighted mean of $n\text{-C}25$, $n\text{-C}27$, $n\text{-C}29$, and $n\text{-C}31$) with (b) the $\delta^{18}\text{O}_{\text{sugar}}$ record (from Zech *et al.*, 2014), (c, d) the reconstructed $\delta^2\text{H}_{\text{prec}}$ and $\delta^{18}\text{O}_{\text{prec}}$ records and (e) the $\delta^{18}\text{O}$ records of Chinese speleothems (Wang *et al.*, 2001; Dykoski *et al.* 2005). P/E = ratio of precipitation to evaporation; S_{LEL} = slope of the evaporation line; H82, PD, D4 = identification of Chinese speleothems. (p. 167)

Fig. 3: $\delta^{18}\text{O}$ - $\delta^2\text{H}$ diagram illustrating the isotopic deviation of lake water (defined as deuterium-(d-)excess) from the Global Meteoric Water Line (GMWL). $\delta^{18}\text{O}$ values of hemicellulose-derived sugars (mean of arab, fuc, and xyl; from Zech *et al.*, 2014) and $\delta^2\text{H}$ values of wax-derived $n\text{-alkanes}$ (mean of $n\text{-C}25$, $n\text{-C}27$, $n\text{-C}29$, and $n\text{-C}31$) are used for reconstruction of the isotopic composition of Panch Pokhari lake water. $\delta^2\text{H}$ and $\delta^{18}\text{O}$ values of precipitation are calculated as intersections of the individual local evaporation lines (LEL) with the GMWL using a slope value of 4.2. (p. 170)

Fig. 4: Comparison of (a) C/N ratio (from Krstic *et al.*, 2011) (b) Hydrogen Index (HI) and (c) deuterium-excess of lake water as proxies for evaporation history of Lake Panch Pokhari. (p. 171)

Abstract

The oxygen and hydrogen isotopic composition of (hemi)cellulose and leaf wax-derived lipids, respectively, are increasingly used in paleohydrological and -climate reconstructions. However, previous studies found it challenging to disentangle the effects of past changes in $\delta^{18}\text{O}$ and $\delta^2\text{H}$ of precipitation ($\delta^{18}\text{O}_{\text{prec}}$ and $\delta^2\text{H}_{\text{prec}}$, respectively) and changes due to evapotranspirative enrichment of leaf water.

In this dissertation, a possible solution for the above given constraint is presented, namely a coupled $\delta^{18}\text{O}$ sugar and $\delta^2\text{H}$ *n*-alkane biomarker approach. Sugar biomarkers were extracted hydrolytically from plant and soil samples and measured for $\delta^{18}\text{O}$ using gas chromatography-pyrolysis-isotope ratio mass spectrometry (GC-Py-IRMS). Prior to coupling of the $\delta^{18}\text{O}$ sugar and $\delta^2\text{H}$ *n*-alkane results, the recently developed method for compound-specific $\delta^{18}\text{O}$ analyses of the hemicellulose-derived sugars had to be validated. First $\delta^{18}\text{O}_{\text{hemicellulose}}$ results obtained from topsoils investigated along two climate transects (Norway and Argentina) enabled detecting and evaluating climate variables that are influencing the isotopic imprint in sugar biomarkers. Accordingly, the sugar biomarkers reflect the $\delta^{18}\text{O}$ isotopic composition of precipitation altered by evapo(transpi)rative ^{18}O enrichment of leaf and soil water. Both the results of modeling analyses of $\delta^{18}\text{O}_{\text{leaf water}}$ and a climate chamber experiment corroborate this interpretation. Furthermore, these studies suggest that the degree of evapotranspirative ^{18}O enrichment is most rigorously controlled by relative air humidity (RH), whereas temperature is of minor importance.

A coupled $\delta^{18}\text{O}_{\text{sugar}}\text{-}\delta^2\text{H}_{\text{n-alkane}}$ approach on topsoils was applied for the first time to the above mentioned Argentinian climate transect. Based on the premise that the sugar and *n*-alkane biomarkers are primarily leaf-derived, $\delta^{18}\text{O}_{\text{leaf water}}$ and $\delta^2\text{H}_{\text{leaf water}}$ were reconstructed and used to assess the deuterium excess of leaf water. The calculated deuterium excess proved to be a suitable proxy for RH, revealing a systematic trend towards more negative values in

the southern, more arid part of the transect. Using a Péclet modified Craig-Gordon model allows reconstructing biomarker-based RH values which correlate significantly with the actual RH values along the transect. Likewise, $\delta^{18}\text{O}_{\text{prec}}$ and $\delta^2\text{H}_{\text{prec}}$ can be calculated using the coupled biomarker approach and the Craig-Gordon model; they, too, correlate significantly with the actual $\delta^{18}\text{O}$ and $\delta^2\text{H}$ values of modern precipitation, thus validating the suggested coupled $\delta^{18}\text{O}$ - $\delta^2\text{H}$ biomarker approach.

Finally, a first paleoclimatic application of the $\delta^{18}\text{O}_{\text{sugar}}\text{-}\delta^2\text{H}_{n\text{-alkane}}$ approach to a lacustrine archive is presented for Lake Panch Pokhari, Nepal. The established 16 ka $\delta^{18}\text{O}_{\text{prec}}$ and $\delta^2\text{H}_{\text{prec}}$ records reflect well the variability of the Indian Summer Monsoon (ISM) and the established deuterium excess record of lake water allows reconstructing the evaporation history of Panch Pokhari Lake.

Conclusively, the newly developed and validated coupled $\delta^{18}\text{O}$ - $\delta^2\text{H}$ biomarker approach presented in this dissertation offers great and intriguing potential for more quantitative paleoclimate research, both on terrestrial and lacustrine sedimentary archives.

Zusammenfassung

Zur Rekonstruktion paläohydrologischer und paläoklimatischer Bedingungen finden zunehmend stabile Sauerstoff- und Wasserstoffisotope (^{18}O , ^2H) aus Blattwachs-bürtigen (Hemi-)Zellulosen und Lipiden Anwendung. Bislang war es aber nicht möglich, mit Sicherheit zwischen den Ursachen der ^{18}O und ^2H Anreicherung in den Biomarker zu differenzieren, da diese durch die $\delta^{18}\text{O}$ und $\delta^2\text{H}$ Signatur des Niederschlags ($\delta^{18}\text{O}_{\text{Niederschlag}}$ und $\delta^2\text{H}_{\text{Niederschlag}}$) wie auch durch eine Anreicherung des Blattwassers während der Verdunstung verursacht werden können. In der vorliegenden Dissertation wird eine Methode vorgestellt, diese Differenzierungsschwierigkeiten mit Hilfe einer gekoppelten $\delta^{18}\text{O}$ Zucker und $\delta^2\text{H}$ *n*-Alkane Analyse zu überwinden. Dabei werden die Zuckerbiomarker hydrolytisch aus Pflanzen- und Bodenproben extrahiert und $\delta^{18}\text{O}$ mit Hilfe der Gas Chromatographie-Pyrolyse-Isotopenverhältnis Massenspektrometrie (GC-Py-IRMS) bestimmt. Bevor jedoch die $\delta^{18}\text{O}$ Zucker und $\delta^2\text{H}$ *n*-Alkan Ergebnisse kombiniert werden können, musste die neu entwickelte substanzspezifische $\delta^{18}\text{O}$ Analyse von Hemizellulose-bürtigen Zuckern validiert werden. Dazu wurden $\delta^{18}\text{O}_{\text{Hemizellulose}}$ Daten von Oberböden entlang zweier Klimatransekte (Norwegen und Argentinien) untersucht und Klimavariablen, die Einfluss auf die Isotopie der Zuckerbiomarker haben, erfasst und evaluiert. Es konnte gezeigt werden, dass Zuckerbiomarker die $\delta^{18}\text{O}$ Isotopie des Niederschlags einbauen und demzufolge auch teilweise widerspiegeln. Zusätzlich spielt jedoch auch die ^{18}O Anreicherung von Blatt- und Bodenwasser durch evapotranspirative Prozesse eine entscheidende Rolle. Dieser Befund konnte durch die Ergebnisse einer $\delta^{18}\text{O}_{\text{Blattwasser}}$ Modellierung und eines Klimakammerexperimentes bestätigt werden. Des Weiteren deuten die vorliegenden Studien darauf hin, dass der Grad der ^{18}O Anreicherung durch Verdunstung meist ausschließlich durch die relative Luftfeuchte (RH) kontrolliert wird, während die Temperatur nur von geringer Bedeutung zu sein scheint. Der kombinierte $\delta^{18}\text{O}_{\text{Zucker}}-\delta^2\text{H}_{\text{Lipid}}$ Ansatz wurde zuerst auf die

Oberböden des oben genannten argentinischen Klimatransekts angewandt. Basierend auf der Annahme, dass die Zucker- und *n*-Alkanbiomarker vorrangig blattbürtig sind, wurden $\delta^{18}\text{O}_{\text{Blattwasser}}$ und $\delta^2\text{H}_{\text{Blattwasser}}$ rekonstruiert und genutzt, um den Deuterium-Excess des Blattwassers zu ermitteln. Die Eignung von Deuterium-Excess als Proxie für RH wurde durch einen starken systematischen Trend zu negativeren Werten im südlichen und trockeneren Teil des Transekts nachgewiesen.

Die Anwendung eines Pécelet modifizierten Craig-Gordon Modells erlaubt darüber hinaus die Rekonstruktion biomarkerbasierter RH Werte. Diese korrelieren über das gesamte Transekt signifikant mit den aktuellen RH Werten. Weiterhin können $\delta^{18}\text{O}_{\text{Niederschlag}}$ und $\delta^2\text{H}_{\text{Niederschlag}}$ mit Hilfe des kombinierten Biomarkeransatzes und des Craig-Gordon Modells berechnet werden. Diese Werte korrelieren ebenfalls signifikant mit aktuellen $\delta^{18}\text{O}$ und $\delta^2\text{H}$ Werten des heutigen Niederschlags und eignen sich damit zur Validierung des vorgeschlagenen kombinierten $\delta^{18}\text{O}$ - $\delta^2\text{H}$ Biomarkeransatzes.

Abschließend wird eine Studie vorgestellt, die erstmals eine paläoklimatische Anwendung des kombinierten $\delta^{18}\text{O}_{\text{Zucker}}$ - $\delta^2\text{H}_{\text{Lipid}}$ Ansatzes auf ein lakustrisches Archiv darstellt. Die für den Panch Pokhari See in Nepal etablierten 16 ka $\delta^{18}\text{O}_{\text{Niederschlag}}$ und $\delta^2\text{H}_{\text{Niederschlag}}$ Rekords spiegeln demnach die Variabilität des Indischen Sommermonsuns wider, und der Deuterium-Excess Rekord des Seewassers erlaubt die Rekonstruktion der Verdunstungsgeschichte des Panch Pokhari Sees.

Zusammenfassend und ausblickend ist festzuhalten, dass die im Rahmen dieser Dissertation entwickelte und validierte Methode des kombinierten $\delta^{18}\text{O}$ - $\delta^2\text{H}$ Biomarkeransatzes vielversprechende innovative Möglichkeiten für eine zukünftige quantitativere Paläoklimaforschung bietet, die sich sowohl auf terrestrische als auch auf lakustrische Sedimentarchive anwenden lässt.

**Towards a coupled $\delta^{18}\text{O}$ sugar and $\delta^2\text{H}$ *n*-alkane
approach in paleoclimate research**

Extended Summary

1. Introduction and motivation

Stable oxygen ($^{18}\text{O}/^{16}\text{O}$) and hydrogen ($^2\text{H}/^1\text{H}$) analyses are contemporary research topics in the field of paleohydrology (Barbour, 2007; Sachse *et al.*, 2012). Small variations in oxygen-18 and deuterium composition in the water molecule are associated with isotopic fractionation occurring during phase changes in the hydrological cycle, as light isotopes (^{16}O and ^1H) evaporate more rapidly than their heavier counterparts. The interpretation of $\delta^{18}\text{O}$ and $\delta^2\text{H}$ records from various climate archives (e.g. lacustrine and marine sediments, ice cores, speleothems, and tree-rings) on the global scale is based on geographical effects (latitude, altitude, continentality), temperature dependence, the amount effect, and rainout of air masses (Dansgaard, 1964; Rozanski *et al.*, 1993; Araguas-Araguas *et al.*, 2000). All together, these climatic factors define the $\delta^{18}\text{O}$ and $\delta^2\text{H}$ isotopic composition of paleoprecipitation ($\delta^{18}\text{O}_{\text{prec}}$ and $\delta^2\text{H}_{\text{prec}}$, respectively) which furthermore represents the source water for biosynthesis of diverse plants compounds (e.g. (hemi)cellulose and lipids). This allows inferring paleoclimate information by analysing variations of stable isotope ratios of oxygen and hydrogen from (hemi)cellulose-derived sugar and leaf wax-derived lipid biomarkers, respectively.

While compound specific $\delta^2\text{H}$ analyses of lipid biomarkers are nowadays widely applied in paleoclimate and -hydrological research (Sauer *et al.*, 2001a; Schefuss *et al.*, 2005; Pagani *et al.*, 2006; Eglinton and Eglinton, 2008; Tierney *et al.*, 2008; Zech *et al.*, 2013a), compound-specific $\delta^{18}\text{O}$ analyses are hardly applied so far due to analytical challenges (Hener *et al.*, 1998; Juchelka *et al.*, 1998; Jung *et al.*, 2007; Greule *et al.*, 2008). However, a recently developed method for compound-specific $\delta^{18}\text{O}$ analyses of individual hemicellulose-derived sugar biomarkers (Zech and Glaser, 2009) overcomes the limitations of previously applied $\delta^{18}\text{O}$ analyses of soils and sediments. Given that experimental findings and theoretical mechanistic considerations suggest stability of $\delta^{18}\text{O}$ signature of sugars (Zech *et al.*, 2012) and $\delta^2\text{H}$ of lipids (Radke *et al.*, 2005; Eglinton and Eglinton, 2008), combining these proxies

has great potential for paleoclimate and -hydrological reconstructions. However, prior to coupling of $\delta^{18}\text{O}_{\text{sugars}}$ and $\delta^2\text{H}_{\text{lipids}}$ it is important to validate the newly developed method for $\delta^{18}\text{O}$ analyses of sugars and disentangle climatic and plant-physiological factors influencing the $\delta^{18}\text{O}$ signal recorded in these hemicellulose-derived biomarkers.

The aims of this dissertation are to (i) validate $\delta^{18}\text{O}_{\text{hemicellulose}}$ as climate proxy through climate chamber and transect studies, (ii) evaluate the potential of the combined $\delta^{18}\text{O}_{\text{sugars}}$ - $\delta^2\text{H}_{\text{lipids}}$ conceptual model in hydrological research, and (iii) apply the novel combined approach to a promising lacustrine paleoclimate archive.

2. Method for compound-specific $\delta^{18}\text{O}$ analyses and first application to topsoils along a climate transect (Study 1)

Publications reporting on the natural abundance of $\delta^{18}\text{O}$ in soils are sparse (Balabane, 1983; Zech and Glaser, 2009). This can be ascribed to analytical and methodological challenges which include thermal conversion/elemental analysis – isotope-ratio mass spectrometry (TC/EA-IRMS) for bulk, and gas chromatography – pyrolysis – isotope-ratio mass spectrometry (GC-Py-IRMS) for compound specific $\delta^{18}\text{O}$ analyses. Moreover, applied bulk analyses make it challenging to discriminate the origin of oxygen in soils (inorganic/organic), and whether it reflects a climate signal or not. The instrumental coupling of GC-Py-IRMS simplified compound specific $\delta^{18}\text{O}$ measurements, but it has been hardly applied so far (Jung *et al.*, 2005; Jung *et al.*, 2007; Greule *et al.*, 2008). Zech and Glaser (2009) optimised the GC-Py-IRMS $\delta^{18}\text{O}$ method for sugar biomarkers and reported on its potential for the application in soils and sediments (Fig. 1). Briefly, hemicellulose monosaccharides such as arabinose and xylose are extracted from soil/plant/sediment samples using trifluoroacetic acid and further purified with cation exchange columns (XAD and

Dowex). The freeze-dried samples are derivatised with methylboronic acid and measured for compound specific $\delta^{18}\text{O}$ using a GC-Py-IRMS system. The $\delta^{18}\text{O}$ measurements are carried out on pyrolytically produced carbon monoxide (CO) for each individual sugar biomarker. All $\delta^{18}\text{O}$ results are expressed in the δ -nomenclature as per mil (‰) deviation relative to the internationally accepted standard Vienna Standard Mean Ocean Water, (V SMOW; Coplen *et al.*, 1996). In the following $\delta^{18}\text{O}_{\text{hemicellulose}}$ refers to the weighted mean $\delta^{18}\text{O}$ value of the most abundant sugar biomarkers. These are arabinose and xylose, sometimes additionally fucose.

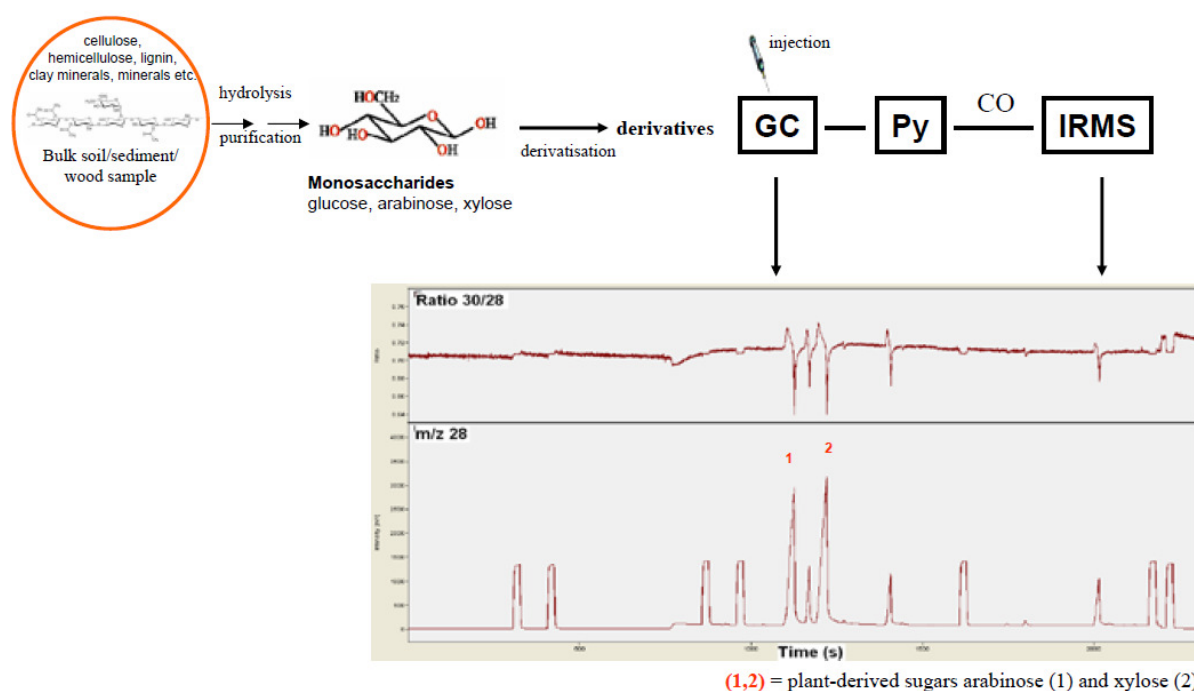


Fig. 1: Scheme of GC-Py-IRMS compound-specific $\delta^{18}\text{O}$ analyses of plant-derived sugar biomarkers in soils (from Zech *et al.*, 2011).

Experimentally, it was confirmed that litter and soil organic matter degradation does not affect $\delta^{18}\text{O}_{\text{hemicellulose}}$ values (Zech *et al.*, 2012). Accordingly, $\delta^{18}\text{O}$ of hemicellulose-derived sugars has the potential to be used as paleoclimate proxy. In order to determine which paleoclimatic information are recorded in sugar biomarkers extracted from soils, first compound-specific $\delta^{18}\text{O}_{\text{hemicellulose}}$ analyses were applied on topsoils in Study 1. Nine sampling sites along a strong east-west climate transect over the Central Scandinavian

Mountains, Norway were analysed. While the climate is very wet along the western slopes (approx. 2250 mm y⁻¹), it becomes more arid along the eastern slopes due to rain-shadow effects (approx. 445 mm y⁻¹).

Since oxygen atoms of plant-biosynthesized sugars originate from water (Schmidt *et al.*, 2001), it can be expected that hemicellulose, like cellulose, reflects the isotopic composition of precipitation (Gray and Thompson, 1976; Libby *et al.*, 1976; Gray and Thompson, 1977; Burk and Stuiver, 1981). The isotopic composition of precipitation over the Norwegian transect reflects more negative $\delta^{18}\text{O}_{\text{prec}}$ values with increasing altitude and longitudinal shift in east-west direction (so called “altitude” and “continental” effects, respectively; Dansgaard, 1964). However, the bulk $\delta^{18}\text{O}$ values and $\delta^{18}\text{O}$ values of hemicelluloses (arabinose and xylose) do not reflect the same trend. This implies that other variables exert an additional important control on $\delta^{18}\text{O}$ of sugar biomarkers. Increased aridity along the transect can be assumed to cause higher evapotranspirative ¹⁸O enrichment of leaf water which results in higher apparent isotopic fractionation between $\delta^{18}\text{O}_{\text{prec}}$ and $\delta^{18}\text{O}_{\text{hemicellulose}}$ observed in the more arid eastern part of the transect. This finding is in agreement with studies reporting that $\delta^{18}\text{O}_{\text{cellulose}}$ is additionally strongly influenced by evaporative ¹⁸O enrichment of leaf water due to transpiration (Dongmann *et al.*, 1974; Flanagan *et al.*, 1991; Roden *et al.*, 2000; Barbour *et al.*, 2004; Pendall *et al.*, 2005).

3. Plant physiology and climate aspects influence on $\delta^{18}\text{O}_{\text{hemicellulose}}$ (Studies 2 and 3)

3.1 Validation of the $\delta^{18}\text{O}_{\text{hemicellulose}}$ proxy

Study 1 shows that evapotranspiration leads to leaf water enrichment in ^{18}O compared to plant source water (precipitation). It is known that the degree of ^{18}O enrichment depends on plant physiological and climate factors (Barbour, 2007; Farquhar *et al.*, 2007). It is crucial to disentangle the influence of plant physiological variables (e.g. leaf temperature and transpiration) and primary climatic drivers (air temperature and relative air humidity, RH) on $\delta^{18}\text{O}_{\text{hemicellulose}}$ in order to use it as a climate proxy. Therefore, a conjoint research was conducted consisting of a climate chamber experiment (Study 2) and a climate transect study (Study 3).

In Study 2, the investigated plants (*Eucalyptus globulus*, *Vicia faba* and *Brassica oleracea*) were grown in climate chambers under different climatic conditions following diurnal variations in temperature (14 – 30 °C) and RH (20% – 70%) (Fig. 2). Sugar biomarkers were extracted from the stem material and analysed for compound-specific $\delta^{18}\text{O}$. The $\delta^{18}\text{O}$ values of arabinose and xylose correlate significantly with measured $\delta^{18}\text{O}_{\text{leaf water}}$ and with modelled $\delta^{18}\text{O}_{\text{cellulose}}$ values (R=0.66, p<0.001, n=24 and R=0.80, p<0.001, n=24, respectively). Hence, these chamber experiment results corroborate the interpretation of Study 1 suggesting that hemicellulose-derived biomarkers reflect the oxygen isotopic composition of plant source water altered by evapotranspirative ^{18}O enrichment of leaf water. Furthermore, model sensitivity tests demonstrate that RH rigorously controls the evapotranspirative enrichment, while a direct temperature effect is much smaller.

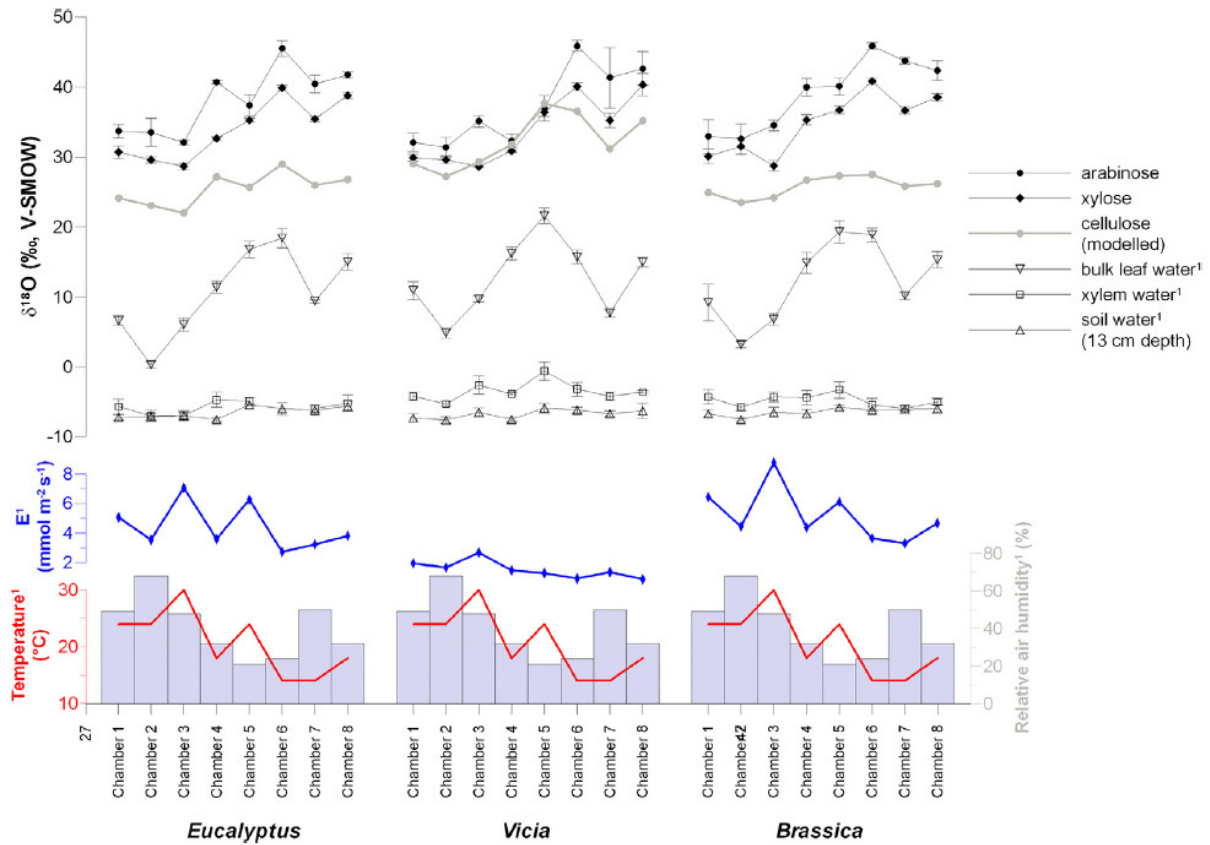


Fig. 2: Comparison of $\delta^{18}\text{O}_{\text{arabinose}}$ and $\delta^{18}\text{O}_{\text{xylose}}$ with modelled $\delta^{18}\text{O}_{\text{cellulose}}$, measured $\delta^{18}\text{O}_{\text{leaf water}}$, $\delta^{18}\text{O}_{\text{xylem water}}$, $\delta^{18}\text{O}_{\text{soil water}}$, and transpiration rate (E). Additionally, temperature and relative air humidity are displayed (from Zech *et al.*, 2014a).

Although negligible direct influence of temperature was reported in Study 2, it needs to be noted that temperature influences the transpiration rate, which affects evapotranspirative enrichment of leaf water due to the so-called Péclet effect. This effect accounts for the flux of source water entering the leaf through the transpiration flow opposed by backward diffusion of isotopically enriched water (Farquhar and Lloyd, 1993). In automatically irrigated systems where plant source water is no limiting factor (e.g. chambers used in Study 2), at higher temperature also the transpiration rate is higher, which causes less effective opposing diffusion of isotopically enriched water from the evaporative front into the xylem. This is reflected in lower enrichment of leaf water, arabinose, and xylose in ^{18}O compared to the values from chambers with lower temperature (Fig. 2).

The influence of air temperature and relative air humidity is furthermore investigated in Study 3 along an Argentinian transect spanning from ~32°S to 47°S and comprising 20 sampling localities (Fig. 3).

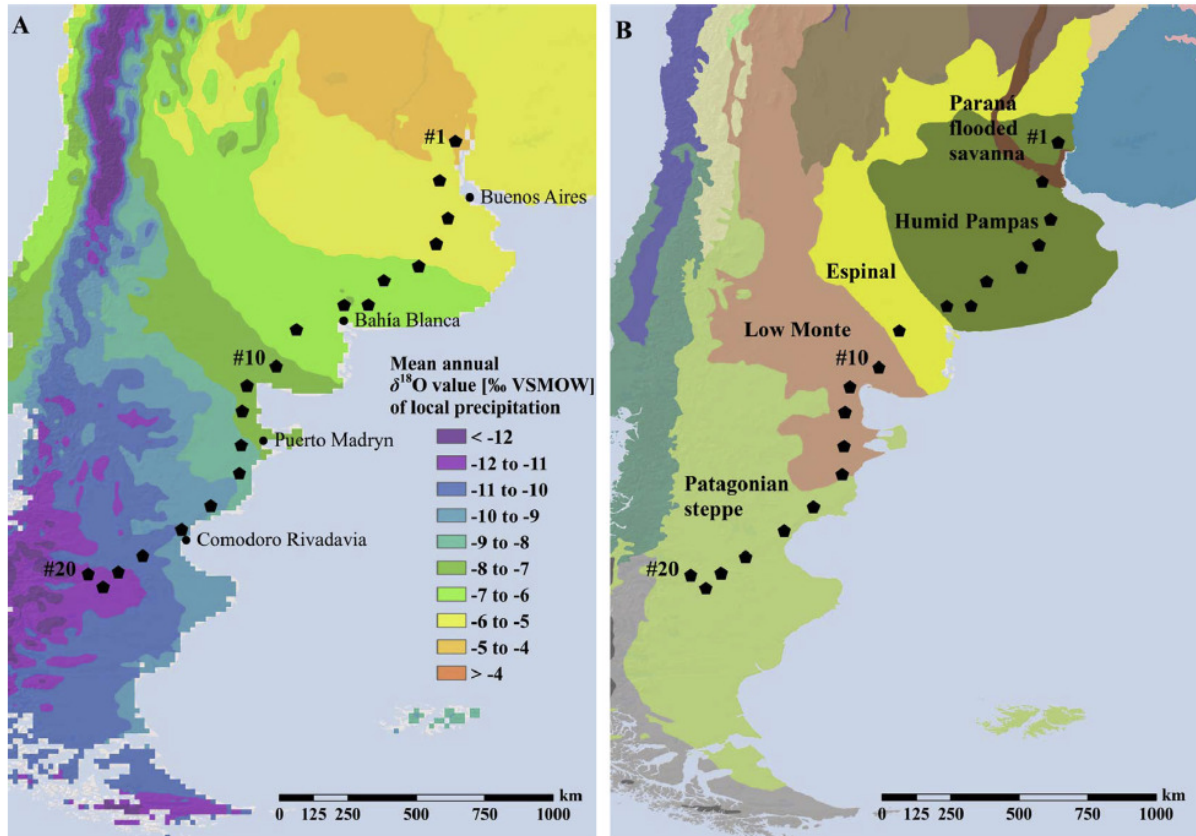


Fig. 3: A) Sampling localities along the investigated Argentinian climate transect and interpolated $\delta^{18}\text{O}$ estimates of annual precipitation (Bowen, 2012). B) Vegetational zonation in the study area (from Tuthorn *et al.*, 2014).

The investigated sites cover a large climate gradient with warm humid subtropical conditions in the north, distinct arid conditions in the middle part and cool temperate conditions in the south. Pronounced contrasting climate conditions are reflected in the vegetation zones of the study area (Fig. 3B), changing from Humid/Dry Pampa in the north to the Espinal vegetation zone that prevails under semi-arid climate (Burgos and Vidal, 1951), Low Monte semi-desert/desert in the most arid region of Argentina (Fernández and Busso,

1997), and Patagonian Steppe in the southernmost part of the transect (Le Hou  rou, 1996; Paruelo *et al.*, 1998).

$\delta^{18}\text{O}_{\text{prec}}$ values (from Bowen, 2012) reveal a systematic trend southwards, getting more depleted (Fig. 3A and Fig. 4). This trend most likely reflects the so called ‘‘temperature effect’’ on $\delta^{18}\text{O}_{\text{prec}}$ (Dansgaard, 1964).

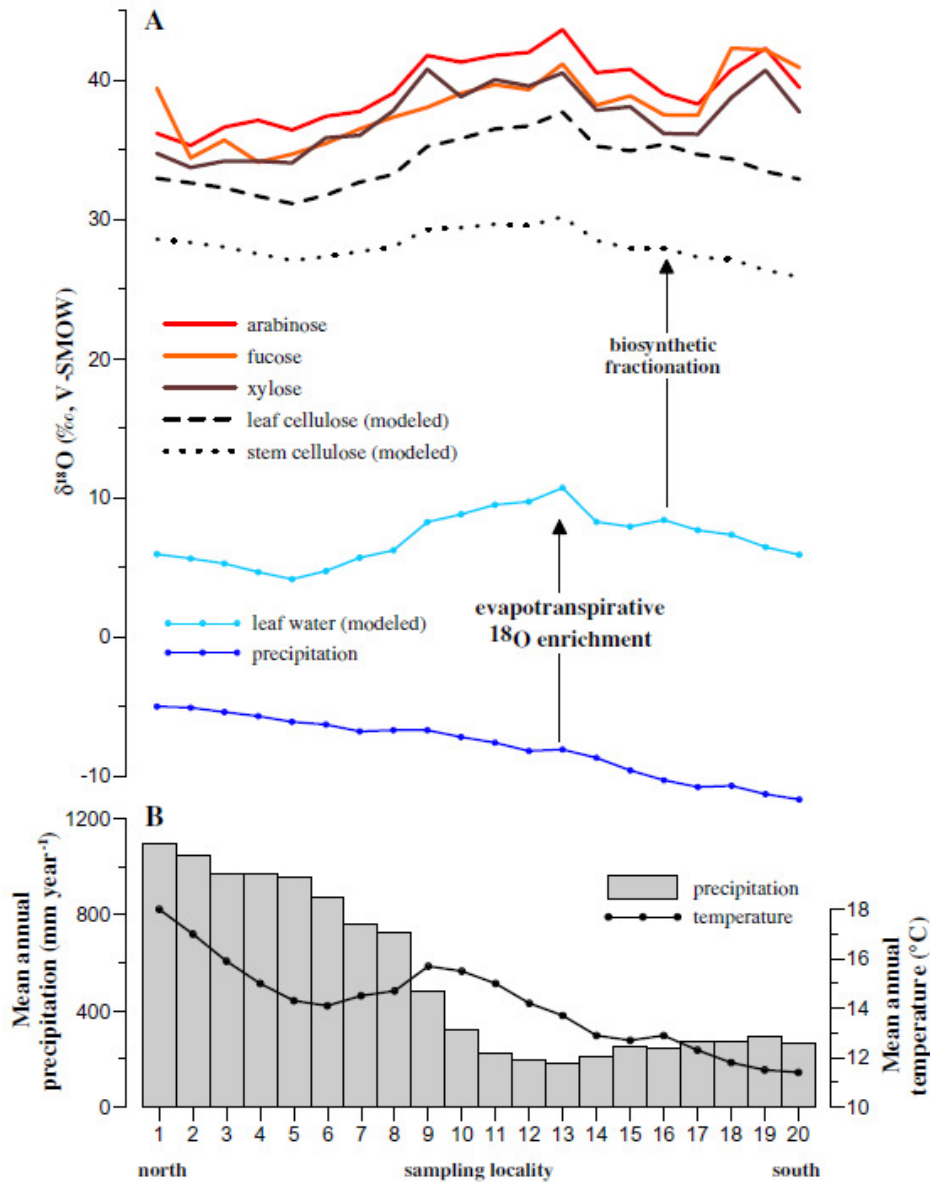


Fig. 4: A) Comparison of measured $\delta^{18}\text{O}_{\text{hemicellulose}}$ values of arabinose, fucose and xylose with modeled $\delta^{18}\text{O}_{\text{prec}}$, $\delta^{18}\text{O}_{\text{leaf water}}$, $\delta^{18}\text{O}_{\text{stem cellulose}}$, and $\delta^{18}\text{O}_{\text{leaf cellulose}}$. B) Mean annual precipitation and temperature characterizing the investigated sampling sites (from Tuthorn *et al.*, 2014).

The $\delta^{18}\text{O}$ values of all three hemicellulose sugar biomarkers are significantly correlated with each other, especially arabinose and xylose ($r=0.96$, $p<0.001$, $n=20$), and reveal systematic trends over the investigated transect with maximum values in the middle and southernmost part (Fig. 4). The comparison of $\delta^{18}\text{O}_{\text{hemicellulose}}$ with $\delta^{18}\text{O}_{\text{prec}}$ (from Bowen, 2012) shows that they do not follow the same trend southwards (Fig. 4). These results indicate that increasing aridity along the climatic gradient cause enhanced evapotranspirative enrichment of leaf water, which is especially pronounced and well depicted in measured $\delta^{18}\text{O}_{\text{hemicellulose}}$ values of the Espinal and Low Monte area.

Furthermore, the empirical data analyses were combined with mechanistic model simulations of $\delta^{18}\text{O}_{\text{leaf water}}$ in order to better detect and evaluate how the dominant climate variables (air temperature and relative air humidity) influence $\delta^{18}\text{O}_{\text{hemicellulose}}$.

3.2 Péclet modified Craig-Gordon model simulations

Evapotranspirative ^{18}O enrichment of leaf water can be predicted by using a mechanistic model originally developed for fractionation processes of water surfaces by Craig and Gordon (1965) and adapted for plants by Dongmann *et al.* (1974) and subsequently by Farquhar and Lloyd (1993).

Accordingly, $\delta^{18}\text{O}_{\text{leaf water}}$ can be estimated as follows:

$$\delta^{18}\text{O}_{\text{leaf water}} = \Delta^{18}\text{O}_{\text{leaf water}} + \delta^{18}\text{O}_{\text{SW}} \quad (\text{Eqn. 1}),$$

where $\Delta^{18}\text{O}_{\text{leaf water}}$ is the bulk leaf water evaporative enrichment and $\delta^{18}\text{O}_{\text{SW}}$ is the oxygen isotope composition source or xylem water. Calculation of $\Delta^{18}\text{O}_{\text{leaf water}}$ accounts for the Péclet effect and evaporative enrichment of leaf water above the plant's source water in ^{18}O at the sites of evaporation (according to Craig and Gordon, 1965 and Botting and Craig, 1969). The

model was optimised by Kahmen *et al.* (2011), reducing the necessary model input data to the primary variables: air temperature, relative air humidity, and the isotopic composition of source water (precipitation).

The modeled $\delta^{18}\text{O}_{\text{leaf water}}$ values for the Argentinian transect correlate significantly with the measured $\delta^{18}\text{O}_{\text{hemicellulose}}$ values ($r=0.81$, $p<0.001$, $n=20$) which corroborates that the investigated hemicelluloses-derived biomarkers reflect $\delta^{18}\text{O}_{\text{leaf water}}$, i.e. $\delta^{18}\text{O}_{\text{prec}}$ altered by evaporative ^{18}O enrichment during transpiration. In additional sensitivity tests mean RH was varied up to $\pm 20\%$ and mean annual temperature up to $\pm 5^\circ\text{C}$. The respective results indicate that reasonable changes in RH strongly influence $\delta^{18}\text{O}_{\text{leaf water}}$ (shifts of $\pm 12.8 - \pm 14.0 \text{‰}$), whereas changes in T_{air} have only a marginal effect (shifts of $\pm 0.5 - \pm 1.2 \text{‰}$).

Based on the results of the Argentinian transect study and the climate chamber experiment a conceptual model for interpreting $\delta^{18}\text{O}_{\text{hemicellulose}}$ in paleoclimate studies is suggested (Fig. 5).

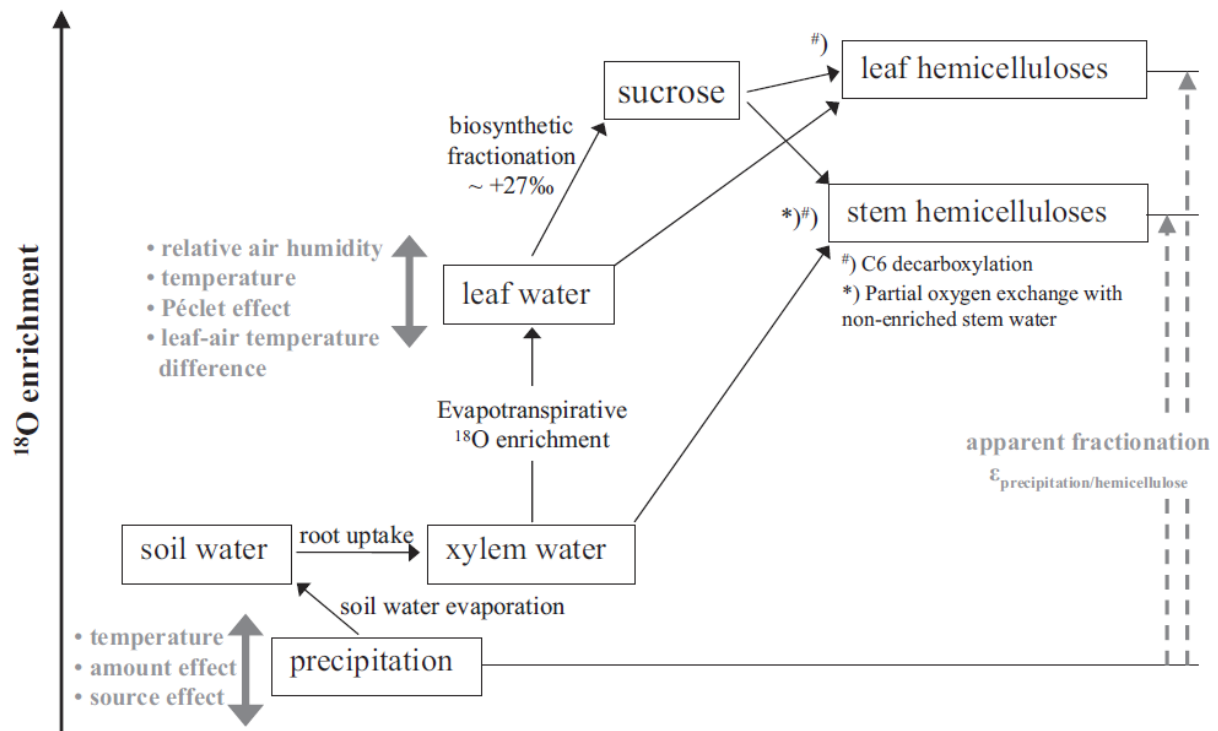


Fig. 5: Conceptual diagram illustrating the major variables influencing $\delta^{18}\text{O}_{\text{hemicellulose}}$ (from Zech *et al.*, 2014a).

Accordingly, $\delta^{18}\text{O}_{\text{hemicellulose}}$ values in plants and soils depend primarily on:

- $\delta^{18}\text{O}_{\text{prec}}$ which in turn depends on climatic and geographical effects,
- evapotranspirative ^{18}O enrichment of leaf water which is most rigorously controlled by relative air humidity, and
- the biosynthetic fractionation factor and its potential temperature dependency.

4. Coupling of $\delta^{18}\text{O}$ sugar and $\delta^2\text{H}$ lipid biomarkers (Study 4)

4.1 $\delta^2\text{H}$ analyses of lipid biomarkers

Leaf wax-derived lipids show a great potential to be used in paleohydrology and - climate reconstruction (Eglinton and Eglinton, 2008). In Study 4, $\delta^2\text{H}$ of *n*-alkanes and fatty acids were analysed in topsoils along the previously described transect (chapter 3.1., Study 3) spanning a climate gradient in Argentina. Similar to sugar biomarkers, these results prove that although leaf wax biomarker $\delta^2\text{H}$ isotopic composition primarily reflects $\delta^2\text{H}_{\text{source water}}$ (precipitation), it is additionally modulated by evapotranspirative enrichment (Fig. 6). This was only recently considered in respective paleoclimate studies (Zech, R. *et al.*, 2013c). The analytical results are additionally supported by mechanistic model simulations (Péclet modified Craig-Gordon model) of $\delta^2\text{H}_{\text{leaf water}}$ revealing a positive correlation between modeled values and measured $\delta^2\text{H}_{\text{lipids}}$. This highlights the role of aridity for evapotranspiration and isotopic enrichment of leaf waxes and lends support to prior studies on the topic (Sachse *et al.*, 2006; Feakins and Sessions, 2010; Kahmen *et al.*, 2013).

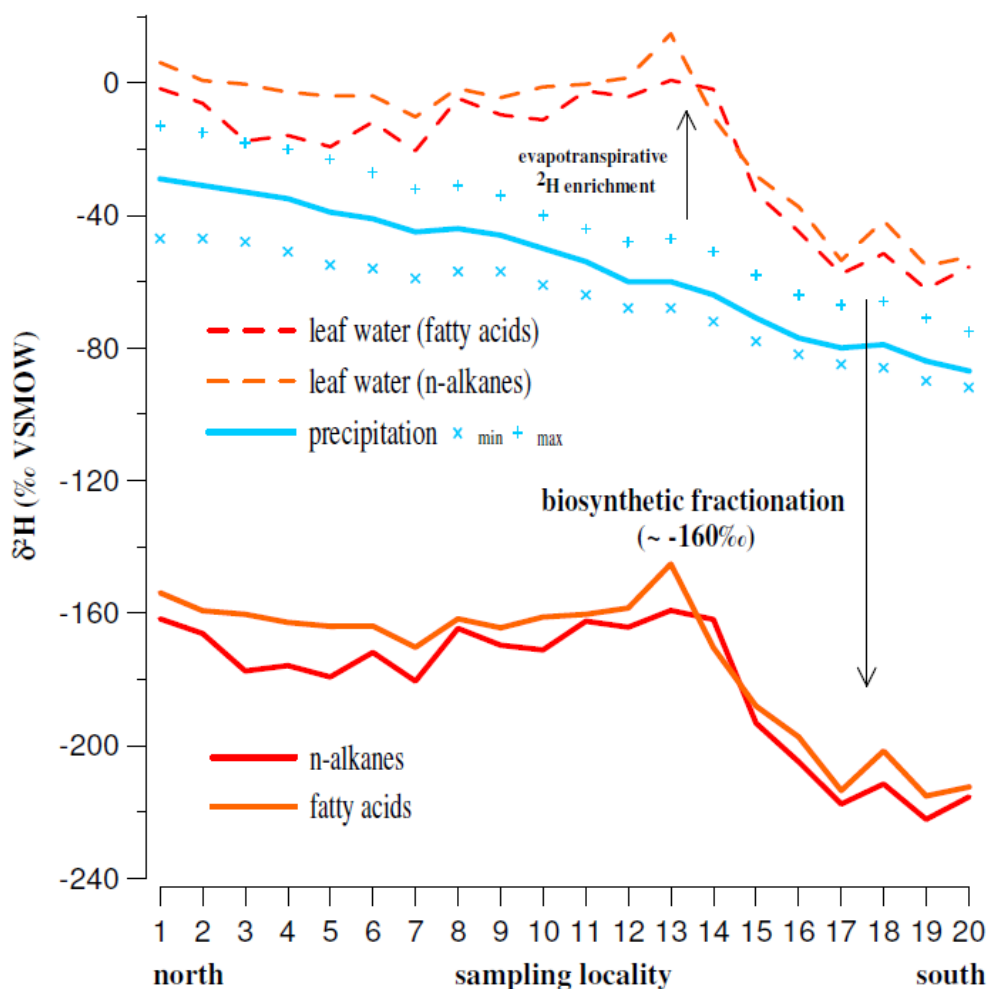


Fig. 6: Comparison of measured $\delta^2\text{H}_{n\text{-alkanes}}$ (weighted mean of $n\text{-C}_{29}$ and $n\text{-C}_{31}$) and $\delta^2\text{H}_{\text{fatty acids}}$ (weighted mean of $n\text{-C}_{22}$, $n\text{-C}_{24}$, $n\text{-C}_{26}$, $n\text{-C}_{28}$, and $n\text{-C}_{30}$), inferred isotopic composition of leaf water, and $\delta^2\text{H}_{\text{prec}}$ (from Tuthorn *et al.*, to be submitted to BGD).

4.2 Conceptual model for interpreting coupled $\delta^2\text{H}$ - $\delta^{18}\text{O}$ biomarker results

Based on the $\delta^{18}\text{O}$ or $\delta^2\text{H}$ biomarker records alone, it is challenging to disentangle whether the isotopic composition of these biomarkers is a consequence of changing isotopic composition of precipitation or changes in evapotranspirative enrichment of leaf water. The possibly variable degree of evapotranspirative enrichment can make it challenging to reconstruct the isotopic composition of precipitation. In order to overcome this limitation, a coupled sugar $\delta^{18}\text{O}$ and $n\text{-alkane}$ $\delta^2\text{H}$ approach for reconstructing the deuterium excess (d-

excess) of leaf water is introduced. d-Excess quantifies the isotopic deviation from the Global Meteoric Water Line (GMWL) and has the potential to be used as paleoclimate proxy for relative air humidity. Furthermore, the coupled $\delta^{18}\text{O}$ and $\delta^2\text{H}$ biomarker approach allows reconstructing the isotopic composition of precipitation ($\delta^{18}\text{O}_{\text{prec}}$ and $\delta^2\text{H}_{\text{prec}}$).

The $\delta^{18}\text{O}$ - $\delta^2\text{H}$ conceptual model (Fig. 7) presented in Study 4 is based on the assumption that the investigated sugar and *n*-alkane biomarkers are primarily leaf-derived and reflect the isotopic composition of leaf water. Taking fractionation factors during hemicellulose and *n*-alkane biosynthesis into account (DeNiro and Epstein, 1981; Sternberg, 1986; Sessions *et al.*, 1999; Schmidt *et al.*, 2001), the model allows reconstructing the leaf water isotopic composition and subsequently the d-excess of leaf water from sedimentary archives.

The calculated d-excess reveals a systematic trend towards more negative values in the southern, arid part of the transect. Using a Craig-Gordon model adapted by Gat and Bowser (1991) relative air humidity (RH) was reconstructed as follows:

$$RH = 1 - \frac{\Delta d}{(\epsilon_2^* - 8 \cdot \epsilon_{18}^* + C_k^2 - 8 \cdot C_k^{18})} \quad (\text{Eqn. 2})$$

where Δd represents the difference in d-excess between leaf-water and source water. According to Merlivat (1978), the kinetic isotope fractionation equals 25.1 ‰ and 28.5 ‰ for C_k^2 and C_k^{18} , respectively. Equilibrium isotope enrichments ϵ_2^* and ϵ_{18}^* as functions of temperature can be calculated using empirical equations of Horita and Wesolowski (1994).

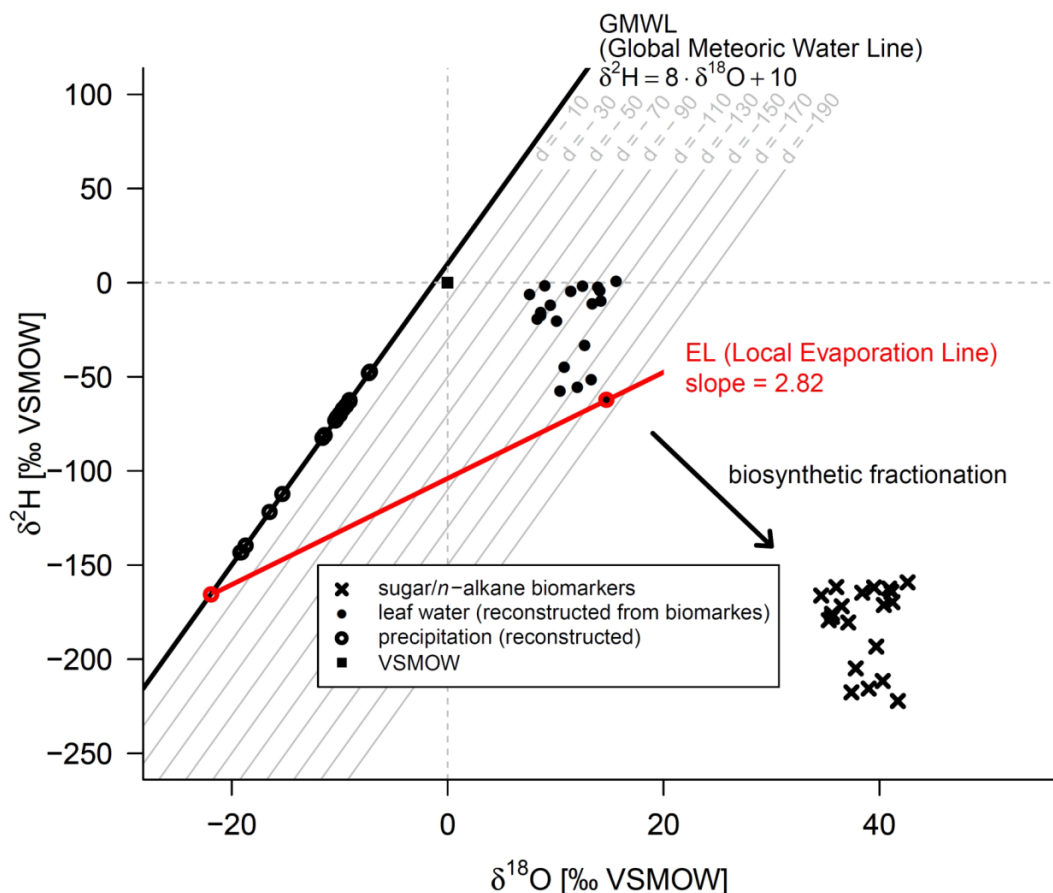


Fig. 7: $\delta^{18}\text{O}$ - $\delta^2\text{H}$ diagram illustrating the global meteoric water line (GMWL) and an evaporation line (EL). Data for the $\delta^{18}\text{O}$ values of hemicellulose-derived sugars (mean of arabinose, fucose, and xylose) and the mean $\delta^2\text{H}$ values of leaf wax-derived n -alkanes (mean of $n\text{-C}_{29}$ and $n\text{-C}_{31}$) are displayed (from Tuthorn *et al.*, to be submitted to BGD).

Reconstructed RH follows the systematic d-excess trend and correlates significantly ($r=0.79$, $p<0.001$, $n=20$) with empirical modern relative humidity (retrieved from GeoINTA 2012) along the transect, which generally validates the $\delta^{18}\text{O}$ - $\delta^2\text{H}$ conceptual model.

Similarly, the $\delta^{18}\text{O}$ and $\delta^2\text{H}$ values of precipitation, calculated as intersection of the individual ELs with the GMWL, correlate significantly with, but systematically underestimate the $\delta^{18}\text{O}$ and $\delta^2\text{H}$ values of modern precipitation, respectively (Fig. 8). This can be attributed to seasonality effect on investigated area, but also further effects need to be considered such as influence of evaporative enrichment of soil water, changing vegetation (grass versus trees

or shrubs), seasonality of biomarker synthesis, and the accuracy of the biosynthetic fractionation factors.

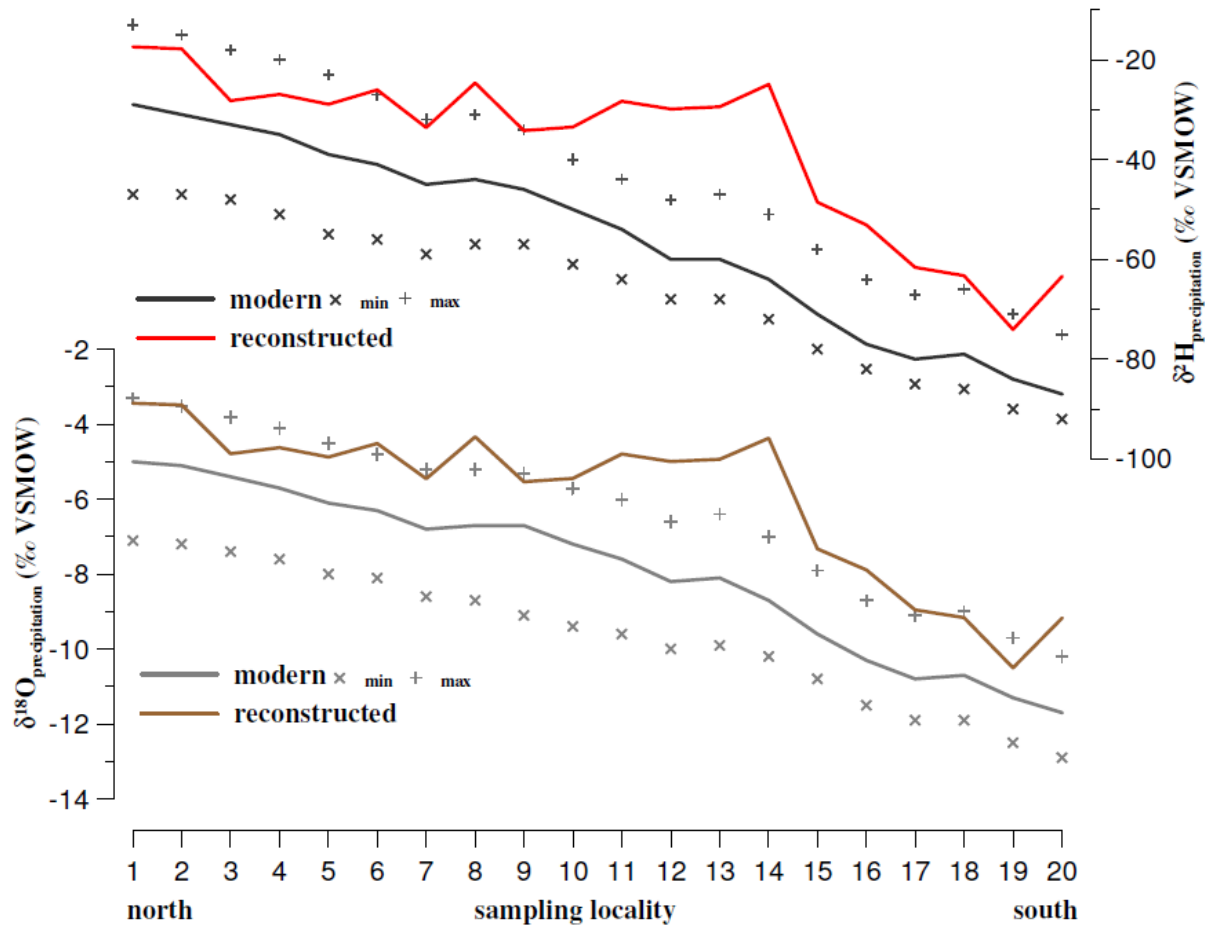


Fig. 8: Reconstructed biomarker-based $\delta^{18}\text{O}_{\text{prec}}$ and $\delta^2\text{H}_{\text{prec}}$ results and comparison with actual modern $\delta^{18}\text{O}_{\text{prec}}$ and $\delta^2\text{H}_{\text{prec}}$ values, respectively (from Tuthorn *et al.*, to be submitted to BGD).

Recently, the proposed coupled $\delta^{18}\text{O}$ - $\delta^2\text{H}$ biomarker approach was applied successfully to a terrestrial paleoclimate archive, namely a ~220 ka permafrost paleosol sequence in NE-Siberia (Zech *et al.*, 2013a). Similar potential for the application of the coupled $\delta^{18}\text{O}$ - $\delta^2\text{H}$ biomarker approach is offered also by lacustrine sediments, which are known to be valuable paleoclimate archives, too (Sauer *et al.*, 2001b; Huang *et al.*, 2004; Sachse *et al.*, 2004; Wissel *et al.*, 2008; Chaplignin *et al.*, 2012; Zech *et al.*, 2014b).

5. First application of the coupled $\delta^{18}\text{O}_{\text{sugar}}$ and $\delta^2\text{H}_{n\text{-alkane}}$ approach in paleolimnology (Studies 5 and 6)

5.1 A 16 ka $\delta^{18}\text{O}_{\text{sugar}}$ and $\delta^2\text{H}_{n\text{-alkane}}$ biomarker records

While biomarkers extracted from soils or terrestrial sediment archives reflect the isotopic composition of precipitation modified by evapo(transpi)rative enrichment of soil and leaf water (Zech *et al.*, 2013b; Tuthorn *et al.*, 2014), aquatic biomarkers reflect lake water isotopic composition. Notably, lake water does not necessarily simply reflect the isotopic composition of precipitation as lake water is becoming enriched in ^{18}O and ^2H due to evaporation and involving isotopic fractionation processes. This offers the possibility to reconstruct lake water evaporation history (e.g. Mayr *et al.*, 2007; Muegler *et al.*, 2008; Aichner *et al.*, 2010). However, based on $\delta^{18}\text{O}$ or $\delta^2\text{H}$ records alone, it is hard to distinguish between changes of the precipitation signal and changes of evaporation. By contrast, the coupled $\delta^{18}\text{O}$ - $\delta^2\text{H}$ approach proposed in this dissertation offers the intriguing possibility to disentangle between these two factors.

The first application of the coupled $\delta^{18}\text{O}$ - $\delta^2\text{H}$ biomarker approach in paleolimnology was carried out on Late Glacial – Holocene lacustrine sediments from Lake Panch Pokhari. This lake is of glacial origin and located at 4,050 m a.s.l. about 100 km north of Kathmandu in Central Nepal, Helambu Himalaya (28°02.533'N; 85°42.822'E). The area is influenced by the Indian Summer Monsoon causing heavy rainfall between May and September and Westerlies causing minor winter precipitation.

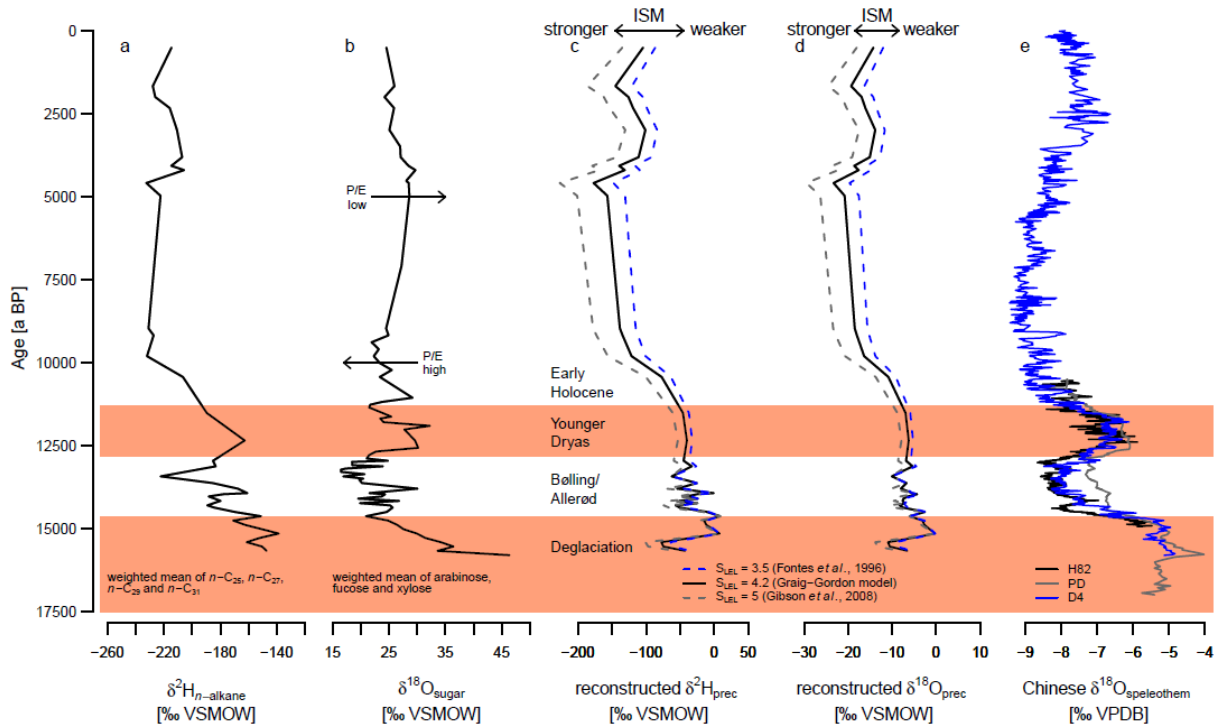


Fig. 9: Age profiles for analytical results from the sediment cores of Lake Panch Pokhari and comparison with $\delta^{18}\text{O}$ records of Chinese speleothemes (P/E- ratio of precipitation to evaporation, ISM- Indian Summer Monsoon; from Tuthorn *et al.*, submitted to Journal of Hydrology).

The weighted mean of the three investigated sugar biomarkers arabinose, fucose, and xylose reveals lower $\delta^{18}\text{O}$ values coinciding with the Bølling-Allerød and the early Holocene, and higher $\delta^{18}\text{O}$ values coinciding with the deglaciation and the Younger Dryas (Fig. 9). The $\delta^{18}\text{O}$ sugar biomarker record is controlled by “amount” and “source” effects, and evaporative enrichment of lake water. Additionally, a lacustrine $\delta^2\text{H}$ record based on n -alkane biomarkers is established in Study 6. The $\delta^2\text{H}_{n\text{-alkane}}$ record reveals similarities with the $\delta^{18}\text{O}_{\text{sugar}}$ record with high values characterising the deglaciation and the Older and the Younger Dryas, and lower values characterising the Bølling and the Allerød periods (Fig. 9). However, certain discrepancies between the records are revealed, too. For instance, the $\delta^2\text{H}_{n\text{-alkane}}$ values are very negative throughout the Holocene, whereas the Holocene $\delta^{18}\text{O}_{\text{sugars}}$ values are well within the range of the Late Glacial $\delta^{18}\text{O}_{\text{sugar}}$ values.

5.2 Reconstruction of lake evaporation history

A major prerequisite for the interpretation of the coupled $\delta^{18}\text{O}_{\text{sugar}}$ and $\delta^2\text{H}_{n\text{-alkane}}$ record of Lake Panch Pokhari is the assumption that the investigated sedimentary organic matter is primarily of autochthonous, aquatic origin. This seems justified given that (i) the catchment is very small and sparsely vegetated, (ii) the C/N ratios are relatively low (<12) and (iii) sugar biomarker patterns show high abundance of fucose indicating aquatic origin (Study 6).

Study 6 suggests that the d-excess of lake water, which is reconstructed from the aquatic *n*-alkane and sugar biomarkers, can serve as proxy for the evaporation history of Lake Panch Pokhari. For the validation of this hypothesis, the reconstructed d-excess values were compared with other proxies that can be used as lake level indicators, such as the C/N ratio and the hydrogen index (HI) (Talbot and Livingstone, 1989) (Fig. 10). All three evaporation proxies reveal minimum values during the deglaciation, the Older Dryas and the Younger Dryas, when presumably precipitation was reduced. This is in agreement with the $\delta^{18}\text{O}$ records of Asian speleothems (Wang *et al.*, 2001; Dykoski *et al.*, 2005) and $\delta^{18}\text{O}_{\text{hemicellulose}}$ (Zech *et al.*, 2014b) indicating weak Indian Summer Monsoon during the deglaciation and the Younger Dryas, and a strengthened monsoon during the Bølling-Allerød and the early Holocene (Fig. 9).

Furthermore, the d-excess indicates high evaporative enrichment of lake water also during the Middle Holocene, when the lake did not desiccate according to C/N ratio and HI proxy. This can be explained with overall higher temperatures and thus higher evaporation during the Holocene compared to the Late Glacial.

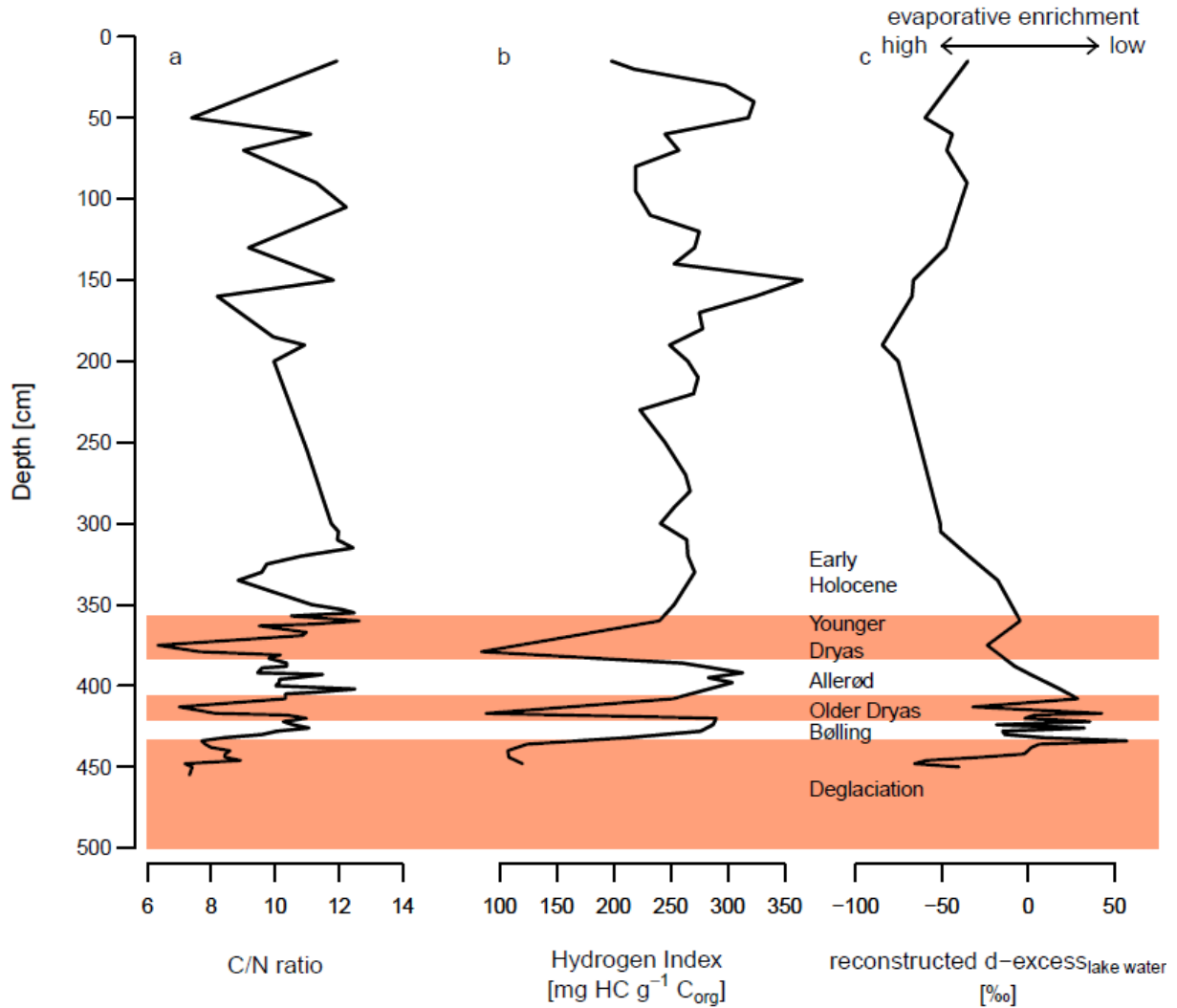


Fig. 10: Comparison of (a) C/N ratio (from Krstic et al., 2011), (b) Hydrogen Index (HI), and (c) deuterium-excess as proxies for evaporation history of Lake Panch Pokhari (from Tuthorn *et al.*, submitted to Journal of Hydrology).

The proposed interpretation of the d-excess record in terms of an intensive or weak Indian Summer Monsoon is additionally corroborated by the reconstructed $\delta^{18}\text{O}_{\text{prec}}$ and $\delta^2\text{H}_{\text{prec}}$ records. As depicted in Fig. 9, these records strongly resemble the Chinese speleothem $\delta^{18}\text{O}$ records and suggest that the Indian Summer Monsoon as well as the East Asian Summer Monsoon were very weak both during the deglaciation and the Younger Dryas.

6. Conclusions

Within this dissertation it was shown that compound-specific $\delta^{18}\text{O}$ values of hemicellulose-derived sugar biomarkers of modern topsoils do not simply reflect $\delta^{18}\text{O}_{\text{prec}}$ (Study 1). The results of a climate chamber experiment (Study 2), an Argentinian climate transect study (Study 3) and a modeling approach (Studies 2 and 3) suggest that, apart from $\delta^{18}\text{O}_{\text{prec}}$, evapotranspirative ^{18}O enrichment of leaf water exerts a dominant control on $\delta^{18}\text{O}_{\text{sugar}}$ of plants and soils. This enrichment is most rigorously controlled by relative air humidity, whereas temperature has only a marginal effect.

As possible solution for disentangling between varying $\delta^{18}\text{O}_{\text{prec}}$ and varying evapotranspirative ^{18}O enrichment, a coupled $\delta^{18}\text{O}$ sugar and $\delta^2\text{H}$ *n*-alkane biomarker approach is proposed (Study 4). This approach is validated using the Argentinian topsoil transect. Accordingly, *d*-excess of leaf water can be assessed by analyzing the sugar and *n*-alkane biomarkers and it can be used as proxy for relative humidity. Furthermore, $\delta^{18}\text{O}_{\text{prec}}$ and $\delta^2\text{H}_{\text{prec}}$ can be reconstructed from the biomarker results using a modified Craig-Gordon model. Finally, the intriguing possibilities for future paleoclimate research using the proposed coupled $\delta^{18}\text{O}$ sugar and $\delta^2\text{H}$ *n*-alkane biomarker approach were presented and evaluated for a first application to a lacustrine sediment archive (Studies 5 and 6). Accordingly, the established 16 ka *d*-excess record for Lake Panch Pokhari, Nepal, allows reconstructing the lake evaporation history and moreover the reconstruction of the $\delta^{18}\text{O}_{\text{prec}}$ record that is reflecting the Indian Summer Monsoon variability.

Further studies are needed to inquire whether the fractionation factors during biomarker biosynthesis are temperature-dependent or not, and to improve our understanding of possible species and seasonality effects.

References

- Aichner B., Herzsuh U., Wilkes H., Vieth A., and Boehner J. (2010) δD values of n-alkanes in Tibetan lake sediments and aquatic macrophytes - A surface sediment study and application to a 16 ka record from Lake Koucha. *Organic Geochemistry* **41**(8), 779-790.
- Araguas-Araguas L., Froehlich K., and Rozanski K. (2000) Deuterium and oxygen-18 isotope composition of precipitation and atmospheric moisture. *Hydrological Processes* **14**(8), 1341-1355.
- Balabane M. (1983) Oxygen-18, deuterium and carbon-13 content of organic matter from litter and humus layers in Podzolic soils. *CATENA* **10**(1-2), 159-166.
- Barbour M. M. (2007) Stable oxygen isotope composition of plant tissue: a review. *Functional Plant Biology* **34**(2), 83-94.
- Barbour M. M., Roden J. S., Farquhar G. D., and Ehleringer J. R. (2004) Expressing leaf water and cellulose oxygen isotope ratios as enrichment above source water reveals evidence of a Péclet effect. *Oecologia* **138**(3), 426-435.
- Bottinga Y. and Craig H. (1969) Oxygen isotope fractionation between CO₂ and water, and the isotopic composition of marine atmospheric CO₂. *Earth and Planetary Science Letters* **5**, 285-295.
- Bowen G. J. (2012) The Online Isotopes in Precipitation Calculator, version 2.2. <http://www.waterisotopes.org>.
- Burgos J. J. and Vidal A. L. (1951) Los climas de la República Argentina, según la nueva clasificación de Thornthwaite. *Meteoros* **1**, 1-32.
- Burk R. L. and Stuiver M. (1981) Oxygen isotope ratios in trees reflect mean annual temperature and humidity. *Science* **211**(4489), 1417-1419.
- Chapligin B., Meyer H., Swann G. E. A., Meyer-Jacob C., and Hubberten H.-W. (2012) A 250 ka oxygen isotope record from diatoms at Lake El'gygytgyn, far east Russian Arctic. *Climate of the Past* **8**(2), 1169-1207.
- Coplen T. B., De Bièvre P., Krouse H. R., Vocke R. D., Groening M., and Rozanski K. (1996) Ratios for light-element isotopes standardized for better interlaboratory comparison. *Eos, Transactions American Geophysical Union* **77**(27), 255.
- Craig H. and Gordon L. I. (1965) Deuterium and oxygen-18 variations in the ocean and the marine atmosphere. *Conference on Stable Isotopes in Oceanographic Studies and Paleotemperatures*, 9-130.

- Dansgaard W. (1964) Stable isotopes in precipitation. *Tellus* **16**(4), 436-468.
- DeNiro M. J. and Epstein S. (1981) Isotopic composition of cellulose from aquatic organisms. *Geochimica et Cosmochimica Acta* **45**(10), 1885-1894.
- Dongmann G., Nürnberg H. W., Förstel H., and Wagener K. (1974) On the enrichment of $H_2^{18}O$ in the leaves of transpiring plants. *Radiation and Environmental Biophysics* **11**(1), 41-52.
- Dykoski C. A., Edwards R. L., Cheng H., Yuan D., Cai Y., Zhang M., Lin Y., Qing J., An Z., and Revenaugh J. (2005) A high-resolution, absolute-dated Holocene and deglacial Asian monsoon record from Dongge Cave, China. *Earth and Planetary Science Letters* **233**(1-2), 71-86.
- Eglinton T. I. and Eglinton G. (2008) Molecular proxies for paleoclimatology. *Earth and Planetary Science Letters* **275**, 1-16.
- Farquhar G. D., Cernusak L. A., and Barnes B. (2007) Heavy Water Fractionation during Transpiration. *Plant Physiology* **143**(1), 11-18.
- Farquhar G. D. and Lloyd J. (1993) Carbon and oxygen isotope effects in the exchange of carbon dioxide between terrestrial plants and the atmosphere. In *Stable isotopes and plant carbon-water relations* (ed. J. R. Ehleringer, A. E. Hall, and G. D. Farquhar), pp. 47-70. Academic Press, Inc.
- Feakins S. J. and Sessions A. L. (2010) Controls on the D/H ratios of plant leaf waxes in an arid ecosystem. *Geochimica et Cosmochimica Acta* **74**(7), 2128-2141.
- Flanagan L. B., Comstock J. P., and Ehleringer J. R. (1991) Comparison of modeled and observed environmental influences on the stable oxygen and hydrogen isotope composition of leaf water in *Phaseolus vulgaris* L. *Plant Physiology* **96**(2), 588-596.
- Gat J. R. and Bowser C. (1991) The heavy isotope enrichment of water in coupled evaporative systems. In *Stable Isotope Geochemistry: A Tribute to Samuel Epstein* (ed. H. P. Taylor, J. R. O'Neil, and I. R. Kaplan), pp. 159-168. The Geochemical Society.
- GeoINTA. (2012) Instituto Nacional de Tecnologia Agropecuaria Visualizador Integrado. Available online at: <http://geointa.inta.gov.ar/visor/> . Accessed 01.08.2012.
- Gray J. and Thompson P. (1977) Climatic information from $^{18}O/^{16}O$ analysis of cellulose, lignin and whole wood from tree rings. *Nature* **270**(5639), 708-709.
- Greule M., Hänsel C., Bauermann U., and Mosandl A. (2008) Feed additives: authenticity assessment using multicomponent-/multielement-isotope ratio mass spectrometry. *European Food Research and Technology* **227**(3), 767-776.

- Hener U., Brand W. A., Hilker A. W., Juchelka D., Mosandl A., and Podebrad F. (1998) Simultaneous on-line analysis of $^{18}\text{O}/^{16}\text{O}$ and $^{13}\text{C}/^{12}\text{C}$ ratios of organic compounds using GC-pyrolysis-IRMS. *Zeitschrift für Lebensmitteluntersuchung und -Forschung A* **206**(3), 230-232.
- Horita J. and Wesolowski D. J. (1994) Liquid-vapor fractionation of oxygen and hydrogen isotopes of water from the freezing to the critical temperature. *Geochimica et Cosmochimica Acta* **58**(16), 3425-3437.
- Huang Y., Shuman B., Wang Y., and Webb T. (2004) Hydrogen isotope ratios of individual lipids in lake sediments as novel tracers of climatic and environmental change: a surface sediment test. *Journal of Paleolimnology* **31**(3), 363-375.
- Juchelka D., Beck T., Hener U., Dettmar F., and Mosandl A. (1998) Multidimensional Gas Chromatography Coupled On-Line with Isotope Ratio Mass Spectrometry (MDGC-IRMS): Progress in the Analytical Authentication of Genuine Flavor Components. *Journal of High Resolution Chromatography* **21**(3), 145-151.
- Jung J., Puff B., Eberts T., Hener U., and Mosandl A. (2007) Reductive ester cleavage of acyl glycerides-GC-C/P-IRMS measurements of glycerol and fatty alcohols. *European Food Research and Technology* **225**(2), 191-197.
- Jung J., Sewenig S., Hener U., and Mosandl A. (2005) Comprehensive authenticity assessment of lavender oils using multielement/multicomponent isotope ratio mass spectrometry analysis and enantioselective multidimensional gas chromatography-mass spectrometry. *European Food Research and Technology* **220**(2), 232-237.
- Kahmen A., Sachse D., Arndt S. K., Tu K. P., Farrington H., Vitousek P. M., and Dawson T. E. (2011) Cellulose $\delta^{18}\text{O}$ is an index of leaf-to-air vapor pressure difference (VPD) in tropical plants. *Proceedings of the National Academy of Sciences* **108**(5), 1981-1986.
- Kahmen A., Schefuß E., and Sachse D. (2013) Leaf water deuterium enrichment shapes leaf wax n-alkane δD values of angiosperm plants I: Experimental evidence and mechanistic insights. *Geochimica et Cosmochimica Acta* **111**, 39-49.
- Le Houérou H. N. (1996) Climate change, drought and desertification. *Journal of Arid Environments* **34**, 133-185.
- Libby L. M., Pandolfi L. J., Payton P. H., Marshall J., Becker B., and Giertz-Sienbenlist V. (1976) Isotopic tree thermometers. *Nature* **261**(5558), 284-288.
- Mayr C., Luecke A., Stichler W., Trimborn P., Ercolano B., Oliva G., Ohlendorf C., Soto J., Fey M., Haberzettl T., Janssen S., Schaebitz F., Schleser G. H., Wille M., and Zolitschka B. (2007) Precipitation origin and evaporation of lakes in semi-arid Patagonia

- (Argentina) inferred from stable isotopes ($\delta^{18}\text{O}$, $\delta^2\text{H}$). *Journal of Hydrology* **334**(1-2), 53-63.
- Merlivat L. (1978) Molecular diffusivities of H_2^{16}O , HD^{16}O , and H_2^{18}O in gases. *The Journal of Chemical Physics* **69**(6), 2864-2871.
- Muegler I., Sachse D., Werner M., Xu B., Wu G., Yao T., and Gleixner G. (2008) Effect of lake evaporation on δD values of lacustrine n-alkanes: A comparison of Nam Co (Tibetan Plateau) and Holzmaar (Germany). *Organic Geochemistry* **39**(6), 711-729.
- Pagani M., Pedentchouk N., Huber M., Sluijs A., and Schouten S. (2006) Arctic hydrology during global warming at the Paleocene/Eocene thermal maximum. *Nature* **442**, 671-675.
- Paruelo J. M., Beltrán A., Jobbágy E., Sala O. E., and Golluscio R. A. (1998) The climate of Patagonia: general patterns and controls on biotic processes. *Ecologia Austral* **8**, 85-101.
- Pendall E., Williams D., and Leavitt S. (2005) Comparison of measured and modeled variations in pinon pine leaf water isotopic enrichment across a summer moisture gradient. *Oecologia* **145**(4), 605-618.
- Radke J., Bechtel A., Gaupp R., Püttmann W., Schwark L., Sachse D., and Gleixner G. (2005) Correlation between hydrogen isotope ratios of lipid biomarkers and sediment maturity. *Geochimica et Cosmochimica Acta* **69**(23), 5517-5530.
- Roden J. S., Lin G., and Ehleringer J. R. (2000) A mechanistic model for interpretation of hydrogen and oxygen isotope ratios in tree-ring cellulose. *Geochimica et Cosmochimica Acta* **64**(1), 21-35.
- Rozanski K., Araguás-Araguás L., and Gonfiantini R. (1993) Isotopic patterns in modern global precipitation. In *Climate Change in Continental Isotopic Records*, pp. 1-36. AGU.
- Sachse D., Billault I., Bowen G. J., Chikaraishi Y., Dawson T. E., Feakins S. J., Freeman K. H., Magill C. R., McInerney F. A., van der Meer M. T. J., Polissar P., Robins R. J., Sachs J. P., Schmidt H.-L., Sessions A. L., White J. W. C., West J. B., and Kahmen A. (2012) Molecular Paleohydrology: Interpreting the Hydrogen-Isotopic Composition of Lipid Biomarkers from Photosynthesizing Organisms. *Annual Review of Earth and Planetary Sciences* **40**(1), 221-249.
- Sachse D., Radke J., and Gleixner G. (2006) δD values of individual n-alkanes from terrestrial plants along a climatic gradient - Implications for the sedimentary biomarker record. *Organic Geochemistry* **37**(4), 469-483.
- Sauer P. E., Eglinton T. I., Hayes J. M., Schimmelmann A., and Sessions A. L. (2001a) Compound-specific D/H ratios of lipid biomarkers from sediments as a proxy for

- environmental and climatic conditions. *Geochimica et Cosmochimica Acta* **65**(2), 213-222.
- Sauer P. E., Miller G. H., and Overpeck J. T. (2001b) Oxygen isotope ratios of organic matter in arctic lakes as a paleoclimate proxy: field and laboratory investigations. *Journal of Paleolimnology* **25**(1), 43-64.
- Schefuss E., Schouten S., and Schneider R. R. (2005) Climatic controls on central African hydrology during the past 20,000 years. *Nature* **437**, 1003-1006.
- Schmidt H.-L., Werner R. A., and Rossmann A. (2001) ^{18}O pattern and biosynthesis of natural plant products. *Phytochemistry* **58**(1), 9-32.
- Sessions A. L., Burgoyne T. W., Schimmelmann A., and Hayes J. M. (1999) Fractionation of hydrogen isotopes in lipid biosynthesis. *Organic Geochemistry* **30**(9), 1193-1200.
- Sternberg L., DeNiro M. J., and Savidge R. A. (1986) Oxygen isotope exchange between metabolites and water during biochemical reactions leading to cellulose synthesis. *Plant Physiology* **82**, 423-427.
- Talbot M. R. and Livingstone D. A. (1989) Hydrogen index and carbon isotopes of lacustrine organic matter as lake level indicators. *Palaeogeography, Palaeoclimatology, Palaeoecology* **70**(1-3), 121-137.
- Tierney J. E., Russel J. M., Huang Y., Sinninghe Damsté J. S., Hopmans E. C., and Cohen A. S. (2008) Northern Hemisphere Controls on Tropical Southeast African Climate During the Past 60,000 Years. *Science* **322**, 252-255.
- Tuthorn M., Hepp J., Zech R., Muegler I., Gleixner G., Zech W., and Zech M. Coupled ^2H and ^{18}O isotopes of biomarkers record lake evaporation history and allow distinguishing precipitation versus evaporation signal. *Submitted to Journal of Hydrology*.
- Tuthorn M., Zech M., Ruppenthal M., Oelmann Y., Kahmen A., Valle H. c. F. d., Wilcke W., and Glaser B. (2014) Oxygen isotope ratios ($^{18}\text{O}/^{16}\text{O}$) of hemicellulose-derived sugar biomarkers in plants, soils and sediments as paleoclimate proxy II: Insight from a climate transect study. *Geochimica et Cosmochimica Acta* **126**, 624-634.
- Tuthorn M., Zech R., Ruppenthal M., Oelmann Y., Kahmen A., del Valle H. F., Eglinton T. I., and Zech M. Coupled isotopes of plant wax and hemicellulose markers record information on relative humidity and isotopic composition of precipitation. *To be submitted to Biogeosciences Discussions*.
- Wang Y. J., Cheng H., Edwards R. L., An Z. S., Wu J. Y., Shen C.-C., and Dorale J. A. (2001) A High-Resolution Absolute-Dated Late Pleistocene Monsoon Record from Hulu Cave, China. *Science* **294**, 2345-2348.

- Wissel H., Mayr C., and Luecke A. (2008) A new approach for the isolation of cellulose from aquatic plant tissue and freshwater sediments for stable isotope analysis. *Organic Geochemistry* **39**(11), 1545-1561.
- Zech M. and Glaser B. (2009) Compound-specific $\delta^{18}\text{O}$ analyses of neutral sugars in soils using gas chromatography-pyrolysis-isotope ratio mass spectrometry: problems, possible solutions and a first application. *Rapid Communications in Mass Spectrometry* **23**(22), 3522-3532.
- Zech M., Mayr C., Tuthorn M., Leiber-Sauheitl K., and Glaser B. (2014a) Oxygen isotope ratios ($^{18}\text{O}/^{16}\text{O}$) of hemicellulose-derived sugar biomarkers in plants, soils and sediments as paleoclimate proxy I: Insight from a climate chamber experiment. *Geochimica et Cosmochimica Acta* **126**, 614-623.
- Zech M., Tuthorn M., Detsch F., Rozanski K., Zech R., Zoeller L., Zech W., and Glaser B. (2013a) A 220 ka terrestrial $\delta^{18}\text{O}$ and deuterium excess biomarker record from an eolian permafrost paleosol sequence, NE-Siberia. *Chemical Geology* **360-361**, 220-230.
- Zech M., Tuthorn M., Glaser B., Amelung W., Huwe B., Zech W., Zöller L., and Löffler J. (2013b) Natural abundance of ^{18}O of sugar biomarkers in topsoils along a climate transect over the Central Scandinavian Mountains, Norway. *Journal of Plant Nutrition and Soil Science* **176**(1), 12-15.
- Zech M., Tuthorn M., Zech R., Schluetz F., Zech W., and Glaser B. (2014b) A 16-ka $\delta^{18}\text{O}$ record of lacustrine sugar biomarkers from the High Himalaya reflects Indian Summer Monsoon variability. *Journal of Paleolimnology* **51**(2), 241-251.
- Zech M., Werner R. A., Juchelka D., Kalbitz K., Buggle B., and Glaser B. (2012) Absence of oxygen isotope fractionation/exchange of (hemi-) cellulose derived sugars during litter decomposition. *Organic Geochemistry* **42**, 1470-1475.
- Zech M., Zech R., Buggle B., and Zoeller L. (2011) Novel methodological approaches in loess research - interrogating biomarkers and compound-specific stable isotopes. *Quaternary Science Journal* **60**(1), 170-187.
- Zech R., Zech M., Markovic S., Hambach U., and Huang Y. (2013c) Humid glacials, arid interglacials? Critical thoughts on pedogenesis and paleoclimate based on multi-proxy analyses of the loess-paleosol sequence Crvenka, Northern Serbia. *Palaeogeography, Palaeoclimatology, Palaeoecology* **387**, 165-175.

7. Contributions to the included manuscripts

The publications and manuscripts included in the here presented cumulative PhD thesis were prepared in cooperation with co-authors. The specific contributions of all authors are estimated as follows:

Study 1: Natural abundance of ^{18}O of sugar biomarkers in topsoils along a climate transect over the Central Scandinavian Mountains, Norway

- M. Zech: laboratory work, discussion of results, manuscript preparation (51%)
- M. Tuthorn: laboratory work, discussion of results, comments on the manuscript (20%)
- B. Glaser: discussion of results, comments on the manuscript (5%)
- W. Amelung: discussion of results, comments on the manuscript (5%)
- B. Huwe: discussion of results, comments on the manuscript (3%)
- W. Zech: discussion of results, comments on the manuscript (3%)
- L. Zöller: discussion of results, comments on the manuscript (3%)
- J. Löffler: field work, discussion of results, comments on the manuscript (10%)

Study 2: Oxygen isotope ratios ($^{18}\text{O}/^{16}\text{O}$) of hemicellulose-derived sugar biomarkers in plants, soils and sediments as paleoclimate proxy I: Insight from a climate chamber experiment

- M. Zech: laboratory work, discussion of results, manuscript preparation (60%)
- C. Mayr: climate chamber experiment, comments on the manuscript (10%)
- M. Tuthorn: discussion of results, comments on the manuscript (20%)
- K. Leiber-Sauheitl: laboratory work, comments on the manuscript (5%)
- B. Glaser: discussion of results, comments on the manuscript (5%)

Study 3: Oxygen isotope ratios ($^{18}\text{O}/^{16}\text{O}$) of hemicellulose-derived sugar biomarkers in plants, soils and sediments as paleoclimate proxy II: Insight from a climate transect study

M. Tuthorn: laboratory work, modeling, data analyses, discussion of results, manuscript preparation (55%)

M. Zech: discussion of results, comments on the manuscript (20%)

M. Ruppenthal: climosequence design and field work, comments on the manuscript (5%)

Y. Oelmann: climosequence design and field work, comments on the manuscript (5%)

A. Kahmen: assistance with modeling discussion, comments on the manuscript (5%)

H. del Valle: field work, comments on the manuscript (4%)

W. Wilcke: comments on the manuscript (3%)

B. Glaser: comments on the manuscript (3%)

Study 4: Coupled isotopes of plant wax and hemicellulose markers record information on relative humidity and isotopic composition of precipitation

M. Tuthorn: laboratory work, modeling, data analyses, discussion of results, manuscript preparation (59%)

R. Zech: laboratory work, discussion of results, comments on the manuscript (10%)

M. Ruppenthal: climosequence design and field work, comments on the manuscript (5%)

Y. Oelmann: climosequence design and field work, comments on the manuscript (5%)

A. Kahmen: assistance with modeling, $\delta^2\text{H}_{n\text{-alkanes}}$ analyses, comments on the manuscript (5%)

H. del Valle: field work, comments on the manuscript (3%)

T. Eglinton: comments on the manuscript (3%)

M. Zech: discussion of results, comments on the manuscript (10%)

Study 5: A 16-ka $\delta^{18}\text{O}$ record of lacustrine sugar biomarkers from the High Himalaya reflects Indian Summer Monsoon variability

- M. Zech: laboratory work, discussion of results, manuscript preparation (63%)
- M. Tuthorn: laboratory work, discussion of results, comments on the manuscript (15%)
- R. Zech: field work, discussion of results, comments on the manuscript (7%)
- F. Schlütz: pollen analyses, discussion of results, comments on the manuscript (5%)
- W. Zech: field work, comments on the manuscript (5%)
- B. Glaser: discussion of results, comments on the manuscript (5%)

Study 6: Coupled ^2H and ^{18}O isotopes of biomarkers record lake evaporation history and allow distinguishing precipitation versus evaporation signal

- M. Tuthorn: data analyses, assistance with modelling and laboratory work, discussion of results, manuscript preparation (55%)
- J. Hepp: discussion of results, modeling, comments on the manuscript (20%)
- R. Zech: discussion of results, comments on the manuscript (5%)
- I. Mügler: measurements, data preparation, comments on the manuscript (5%)
- W. Zech: field work, comments on the manuscript (5%)
- M. Zech: laboratory work, discussion of results, comments on the manuscript (10%)

Acknowledgments

First of all, I am eternally grateful to my mentor Michael. You have been a great support and it was such a pleasure working with you. Thank you for all the freedom of the choice you gave me, for always supporting my interests, and for all the appreciation you have shown. You are a true friend and a highly appreciated mentor.

I am very grateful to Prof. B. Glaser, Prof. L. Zöllner, and Prof. B. Huwe for their logistic support and for allowing me to use laboratory and institutional infrastructure at the University of Bayreuth and the Martin-Luther University Halle-Wittenberg. I am very thankful to Prof. C. Werner Pinto for her support and advices. I thank the DFG, the DAAD and the SIBAE COST Action for financial support.

I thank all of my co-authors, colleagues, and students who helped me in my research work, providing highly appreciated scientific support. Especially, I thank Prof. A. Kahmen, Prof. Y. Oelmann, M. Ruppenthal, and J. Hepp for successful cooperation and discussions.

I am very thankful to Roland, for pushing me further when needed, and to Wolfgang for all the kindness and support. I wish to thank all my friends and colleagues; it was a pleasure sharing my days with you. Michaela, Silke, Anna, and Maren thank you for your help and all the sheer joy we shared. Maja and Ana thank you for your great support.

I am very grateful to my family; everything I value the most in my life, they've given me. I wish to thank my Mum, for she has been my pillar and my guide. I admire you and I am eternally in debt with you for all the love, advising, and kindness you are giving me. I am very thankful to my father and brother, for their care and understanding. Goranka, thank you for always believing in me.

My special thanks go to Dejan, Janne, and Christian for their love, patience, and unconditional support. You are my motivation and strength, and I am blessed to have you in my life.

**Towards a coupled $\delta^{18}\text{O}$ sugar and $\delta^2\text{H}$ *n*-alkane
approach in paleoclimate research**

Cumulative Study

Study 1

Natural abundance of ^{18}O of sugar biomarkers in topsoils along a climate transect over the Central Scandinavian Mountains, Norway

Michael Zech^{1,2,3,*}, Mario Tuthorn^{1,2,3}, Bruno Glaser³, Wulf Amelung⁴, Bernd Huwe¹, Wolfgang Zech⁵, Ludwig Zöller², Jörg Löffler⁶

This paper is dedicated to Dr. Sonja Brodowski[†]

¹) Department of Soil Physics, University of Bayreuth, Universitätsstr. 30, 95440 Bayreuth, Germany

²) Chair of Geomorphology, University of Bayreuth, Universitätsstr. 30, 95440 Bayreuth, Germany

³) Department of Terrestrial Biogeochemistry, Martin-Luther University Halle-Wittenberg, Von-Seckendorff-Platz 3, 06120 Halle, Germany

⁴) Institute of Crop Science and Resource Conservation, Soil Science and Soil Ecology, University of Bonn, Nussallee 13, 53115 Bonn, Germany

⁵) Institute of Soil Science and Soil Geography, University of Bayreuth, Universitätsstr. 30, 95440 Bayreuth, Germany

⁶) Department of Geography, University of Bonn, Meckenheimer Allee 166; 53115 Bonn, Germany

^{*}) corresponding author: michael_zech@gmx.de

Journal of Plant Nutrition and Soil Science

(2013) 176, 12-15

Abstract

Precipitation and topsoil samples from a climate transect over the Scandinavian Mountains, Norway, were analyzed for bulk and compound-specific $\delta^{18}\text{O}$ values. The natural abundance of ^{18}O in the plant-derived hemicellulose biomarkers arabinose and xylose correlates positively with $\delta^{18}\text{O}$ of bulk soil, but not with $\delta^{18}\text{O}$ of precipitation. This suggests that other factors than $\delta^{18}\text{O}_{\text{prec}}$, such as evaporative ^{18}O enrichment of leaf water, exert a strong influence on the natural abundance of ^{18}O in soils.

Keywords: mountain soils, biomarkers, hemicelluloses, sugars, oxygen isotopes, evaporative ^{18}O enrichment.

1. Introduction

While stable carbon ($^{13}\text{C}/^{12}\text{C}$) and nitrogen ($^{15}\text{N}/^{14}\text{N}$) isotope analyses, particularly compound-specific isotope analyses (CSIA), have become widely applied and powerful tools in plant and soil sciences during the last decades (*Glaser, 2005; Amelung et al., 2008; Sauheitl et al., 2009*), there are hardly any publications reporting on the natural abundance of ^{18}O in soils, so far (*Balabane, 1983*). This can be attributed to several reasons. First, oxygen in soils occurs in several inorganic (e.g. carbonates, clay minerals, silicates) and organic (e.g. plant-derived, microbial-derived) pools. Some of these pools are exchangeable with soil water (e.g. the oxygen atoms forming carbonyl groups), others are not (e.g. oxygen atoms forming hydroxyl groups). Some of these pools reflect a climate signal (e.g. plant-derived cellulose), other do not (e.g. lignin phenols; *Schmidt et al., 2001*). Second, ^{18}O analysis requires conversion of the oxygen atoms of a sample into carbon monoxide via pyrolysis. Respective ‘online’ instrumental facilities both for bulk (via thermal conversion/elemental analysis – isotope ratio mass spectrometry = TC/EA – IRMS) and compound-specific (via gas chromatography – pyrolysis – isotope ratio mass spectrometry = GC – Py – IRMS) $\delta^{18}\text{O}$ analysis is relatively young (*Werner et al., 1996; Hener et al., 1998; Juchelka et al., 1998*) and challenging compared to $\delta^{13}\text{C}$ and $\delta^{15}\text{N}$ analysis. Only recently, a methodological approach for determining $\delta^{18}\text{O}$ of plant-derived biomarkers from soils was suggested (*Zech and Glaser 2009*). And third, the potential applications of $\delta^{18}\text{O}$ analyses in soils, presumably ranging from paleoclimate reconstructions to labelling experiments, are not yet elaborated.

Here we present a first ^{18}O dataset from a climate transect over the Southern Scandinavian Mountains, Norway, comprising the natural abundances of ^{18}O in precipitation, bulk soil, and

the hemicellulose biomarkers arabinose and xylose. The objective of this study is to answer the question whether soils reflect $\delta^{18}\text{O}$ of precipitation.

2. Material and methods

The Central Scandinavian Mountains in Southern Norway, culminating in the 2469 m a.s.l. high summit of Mt. Galdhøpiggen, feature a strong climate transect from the windward westerly exposed slopes to the leeward easterly exposed slopes (Fig. 1). The climate is very wet along the western slopes (2250 mm/year in Bergen), and becomes more arid on the eastern slopes due to rain shadow effects (445 mm/year in Kongsvoll in Oppdal (Dovrefjell); *NMI*, 2012).

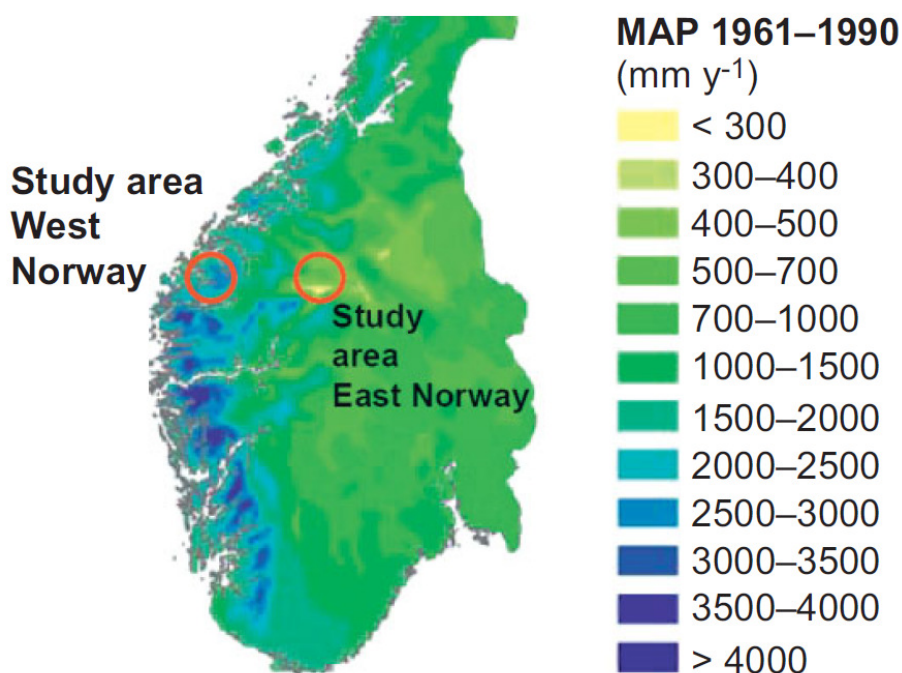


Fig. 1: Location of the study areas in the W and E part of the Central Scandinavian Mountains, respectively. Mean annual precipitation (MAP) illustrates the strong climate gradient (from *NMI*, 2012).

In August 2010, nine composite precipitation samples, reflecting the precipitation of a typical rainy summer season according to the long-year on-site experience of AG *Löffler*, were collected for one week using storage rain gauges. The gauges were installed within a long-term alpine ecosystem research project (*Löffler et al.*, 2006; *Pape et al.*, 2009) along a climate transect ranging from 930 m a.s.l. in western part (N62°04', E6°24') to 340 m. a.s.l. in the eastern part (N61°53', E9°32') of the Central Scandinavian Mountains (Fig. 1 and 2). Representative mixed topsoil samples (0 – 5 cm depth, total organic carbon contents ranging from 3.1 to 6.7%, sieved < 2 mm, roots removed using tweezers, finely ground) from six of these sites were analyzed for bulk and compound-specific $\delta^{18}\text{O}$.

Bulk water and soil $\delta^{18}\text{O}$ analyses were carried out in the Laboratory of Isotope Biogeochemistry of the Bayreuth Center of Ecology and Environmental Research (University of Bayreuth, Germany). Note that bulk soil $\delta^{18}\text{O}$ analyses do not only capture oxygen bound in organic matter, but partly although often not quantitatively also oxygen from inorganic compounds like clay minerals, silicates, and carbonates (*Werner*, 2003). For the TC/EA-IRMS system, a pyrolysis oven (HEKAtech, Wegberg, Germany) was coupled via a ConFlo III Interface (Thermo Fisher Scientific) with a Delta V Plus isotope ratio mass spectrometer (Thermo Fisher Scientific). The standard deviation of bulk $\delta^{18}\text{O}$ analysis is typically $\pm 1\%$. For compound-specific $\delta^{18}\text{O}$ analysis, the hemicelluloses of the 6 topsoil samples were hydrolyzed using 4M TFA according to *Amelung et al.* (1996). After purifying the monosaccharides over XAD and Dowex columns, they were derivatized with methylboronic acid (MBA) and measured at the University of Halle according to the procedure described in detail by *Zech and Glaser* (2009). The GC-Py-IRMS system consisted of a Trace GC 2000 gas chromatograph (Thermo Fisher Scientific, Bremen, Germany) coupled with a Delta V Advantage isotope ratio mass spectrometer (Thermo Fisher Scientific) via a pyrolysis reactor and a GC/TC III interface (Thermo Fisher Scientific). All oxygen isotope values are

expressed in per mil (‰) relative to the Vienna Standard Mean Ocean Water (VSMOW). The relative abundance of the exclusively plant-derived sugar biomarkers arabinose and xylose was much higher than for other sugars (e.g. fucose and rhamnose). This is in agreement with findings of *Zech and Glaser (2009)* and *Zech et al. (2012)* and we therefore only focus on $\delta^{18}\text{O}$ of arabinose and xylose in this study.

3. Results

The natural abundance of ^{18}O in precipitation over the investigated mountain transect features two well known effects. First, the $\delta^{18}\text{O}$ values become more negative with increasing altitude both in the western (from -9.3 to -10.7‰) and in the eastern part (from -11.6 to -14.6‰) of the transect (Fig. 2). This is called the “altitude effect” (*Dansgaard, 1964*). Second, the leeward eastern part of the transect is characterized by systematically more negative $\delta^{18}\text{O}$ values compared to the western part of the transect (Fig. 2). This can be attributed to the preferential rainout of isotopically heavy water molecules when the air masses are crossing the mountain range (called “continent effect”).

The plant-derived sugar biomarkers arabinose and xylose have very similar $\delta^{18}\text{O}$ values ($R=0.92$) but do not reflect $\delta^{18}\text{O}_{\text{prec}}$. In fact, none of the two effects described above (altitude and continent effect) is confirmed and the $\delta^{18}\text{O}$ amplitudes are conspicuously higher than those of $\delta^{18}\text{O}_{\text{prec}}$ (Fig. 2). Bulk $\delta^{18}\text{O}$ values of the topsoil samples correlate positively with compound-specific $\delta^{18}\text{O}$ values of arabinose ($R=0.58$, $n=6$, $p=0.23$) and xylose ($R=0.80$, $n=6$, $p=0.06$), but the absolute values are considerably less positive and the $\delta^{18}\text{O}$ amplitude is dampened.

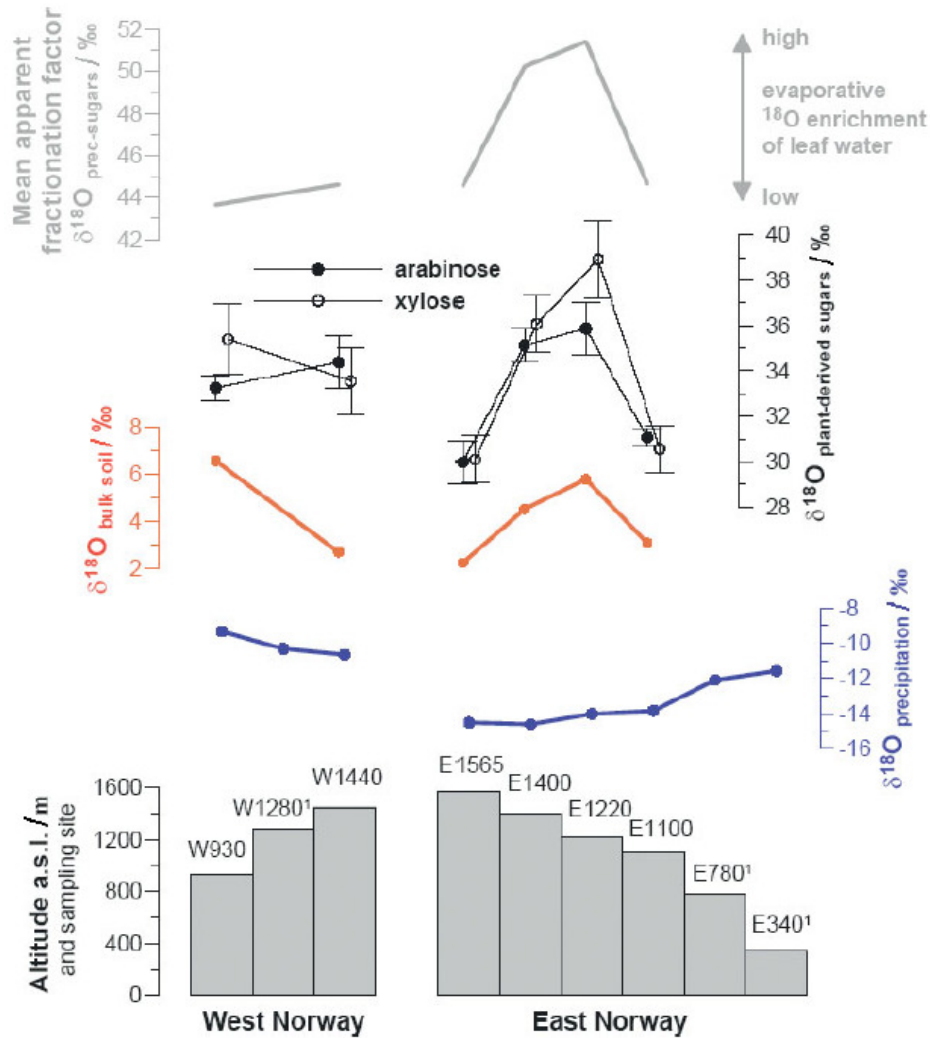


Fig. 2: Measured $\delta^{18}\text{O}$ values of precipitation, bulk soil and plant-derived sugar biomarkers arabinose and xylose along an altitudinal and climate transect over the Central Scandinavian Mountains, Norway. Additionally, the mean apparent isotopic fractionation $\epsilon_{\text{prec/sugars}}^{18\text{O}}$ is calculated as proxy for evaporative ^{18}O enrichment of leaf water by transpiration. 1) no soil samples were available for ^{18}O analyses.

4. Discussion

The plant-derived sugar biomarkers arabinose and xylose in topsoils obviously do not reflect $\delta^{18}\text{O}$ of precipitation. Given that Zech et al. (2012) demonstrated that $\delta^{18}\text{O}$ values of sugar biomarkers do not change during litter decomposition, this finding cannot be explained with different edaphic conditions. In fact, it is well known amongst plant physiologists that

plants do not simply incorporate the oxygen isotope signal of source water, i.e. of precipitation and soil water. Transpiration results in an evaporative ^{18}O enrichment of leaf water, where plant sugars are assimilated. Furthermore, a biosynthetic fractionation factor of approximately +27‰ has to be considered for sugars (*Barbour, 2007; Ferrio et al., 2009*). Figure 2 illustrates that the mean apparent fractionation factor $\delta^{18}\text{O}_{\text{prec} - \text{sugars}}$ for arabinose and xylose reveals a clear maximum in the more arid eastern part of the transect (rain shadow effect). Note that the highest site along the eastern transect (E1565) is often cloudy, thus confirming that this site is still characterized by high relative air humidity. Hence, we conclude that evaporative ^{18}O enrichment of leaf water by transpiration due to increasing aridity from west to east is the most plausible explanation for the very positive $\delta^{18}\text{O}$ values at the sites E1400 and E1220 (Fig. 2).

At the current state of research, we can only speculate why the lowermost study site E1100 on the eastern slopes does not confirm this trend. Presumably, specific microclimatic conditions affecting evaporative ^{18}O enrichment such as overall reduced wind-speed, reduced wind-speed due to denser shrub vegetation, etc. have to be considered. Indeed, site E1100 is characterized by the highest abundance of dwarf-shrubs. Furthermore, a species effect cannot be excluded, because different plants can vary in their transpiration rate and hence their evaporative ^{18}O enrichment under the same climatic conditions. Possibly also a higher input of root-derived hemicelluloses to the soils compared to above-ground litter could be relevant. Site E1100 has a higher root density compared to the sites at higher altitude (unpublished data by J. Löffler). Given that *Gessler et al. (2009)* reported that up to 40% of the oxygen atoms of assimilated sugars are not transferred into wood cellulose because they exchange with xylem water, we suppose that also root hemicelluloses do not show the same ^{18}O enrichment as do leave hemicelluloses.

The compound-specific $\delta^{18}\text{O}$ results are partly confirmed by bulk $\delta^{18}\text{O}$ (Fig. 2). Both the more negative bulk $\delta^{18}\text{O}$ values and the reduced amplitude can be explained with dilution effects. On the one hand, not all plant products incorporate oxygen from leaf water and thus carry a climatic signal. For instance, lignin phenols incorporate atmospheric oxygen and show $\delta^{18}\text{O}$ values near +5‰ (Schmidt et al., 2001). On the other hand, soils contain mineral and clay mineral oxygen pools with a very different oxygen isotope signature compared to plant-derived organic matter.

We are not aware of any other study focussing on the natural abundance of ^{18}O in soil organic matter except for Balabane (1983). Applying a novel analytical method based on GC-Py-IRMS, we have demonstrated that plant-derived sugar biomarkers and bulk soils do not simply reflect $\delta^{18}\text{O}$ of precipitation, but are in all likelihood strongly affected by evaporative ^{18}O enrichment of leaf water during transpiration.

Acknowledgements

We are very grateful to A. Mergner and S. Bösel for support during CSIA and to Prof. G. Gebauer, University of Bayreuth, and his team for conducting the bulk $\delta^{18}\text{O}$ analyses. Our manuscript greatly profited from constructive comments provided by Dr. D. Sauer and two anonymous reviewers. Financial support was provided by the German Research Foundation. M. Zech also greatly acknowledges the support given by the Alexander von Humboldt-Foundation.

References

- Amelung, W., Brodowski, S., Sandhage-Hofmann, A., Bol, R., 2008. Combining Biomarker with Stable Isotope Analyses for Assessing the Transformation and Turnover of Soil Organic Matter. In: D.L. Sparks (Editor), *Advances in Agronomy*. Academic Press, Burlington, pp. 155-250.
- Amelung, W., Cheshire, M.V., Guggenberger, G. (1996): Determination of neutral and acidic sugars in soil by capillary gas-liquid chromatography after trifluoroacetic acid hydrolysis. *Soil Biol Biochem* 28(12), 1631-1639.
- Balabane, M. (1983): Oxygen-18, deuterium and carbon-13 content of organic matter from litter and humus layers in podzolic soils. *Catena* 10, 159-166.
- Barbour, M. (2007): Stable oxygen isotope composition of plant tissue: a review. *Funct Plant Biol* 34, 83-94.
- Dansgaard, P. (1964): Stable isotopes in precipitation. *Tellus* 16, 436-468.
- Ferrio, J.P., Cuntz, M., Offermann, C., Siegwolf, R., Saurer, M., Gessler, A. (2009): Effect of water availability on leaf water isotopic enrichment in beech seedlings shows limitations of current fractionation models. *Plant Cell Environ* 32, 1285-1296.
- Gessler, A., Brandes, E., Buchmann, N., Helle, G., Rennenberg, H., Barnard, R. (2009): Tracing carbon and oxygen isotope signals from newly assimilated sugars in the leaves to the tree-ring archive. *Plant Cell Environ* 32(7), 780-795.
- Glaser, B. (2005): Compound-specific stable-isotope ($\delta^{13}\text{C}$) analysis in soil science. *J. Plant Nutr. Soil Sci.* 168, 633-648.
- Hener, U., Brand, W.A., Hilker, A.W., Juchelka, D., Mosandl, A., Podebrad, F. (1998): Simultaneous on-line analysis of $^{18}\text{O}/^{16}\text{O}$ and $^{13}\text{C}/^{12}\text{C}$ ratios of organic compounds using GC-pyrolysis-IRMS. *Z Lebensm Unters F A* 206(3), 230-232.
- Juchelka, D., Beck, T., Hener, U., Dettmar, F., Mosandl, A. (1998): Multidimensional Gas Chromatography Coupled On-Line with Isotope Ratio Mass Spectrometry (MDGC-IRMS): Progress in the Analytical Authentication of Genuine Flavor Components. *J High Res Chromatog* 21, 145-151.
- Löffler, J., Pape, R., Wundram, D. (2006): The climatologic significance of topography, altitude and region in high mountains – A survey of oceanic-continental differentiations of the Scandes. *Erdkunde* 60, 15-24.

- NMI, 2012: Norwegian Meteorological Institute. Available online at http://met.no/English/Climate_in_Norway/.
- Pape, R., Wundram, D., Löffler, J. (2009): Modelling near-surface temperature conditions in high mountain environments - An appraisal. *Climate Research* 39, 99-109.
- Sauheitl, L., Glaser, B., Weigelt, A. (2009): Uptake of intact amino acids by plants depends on soil amino acid concentrations. *Environ Exp Bot* 66(2), 145-152.
- Schmidt, H.-L., Werner, R., Roßmann, A. (2001): ^{18}O Pattern and biosynthesis in natural plant products. *Phytochem* 58, 9-32.
- Werner, R.A. (2003): The online $^{18}\text{O}/^{16}\text{O}$ analysis: development and application. *Isot Environ Healt S* 39(2), 85-104.
- Werner, R.A., Kornxl, B.E., Roßmann, A., Schmidt, H.-L. (1996): On-line determination of $\delta^{18}\text{O}$ values of organic substances. *Anal Chim Acta* 319, 159-164.
- Zech, M., Glaser, B. (2009): Compound-specific $\delta^{18}\text{O}$ analyses of neutral sugars in soils using GC-Py-IRMS: problems, possible solutions and a first application. *Rapid Commun Mass Sp* 23, 3522-3532.
- Zech, M., Werner, R., Juchelka, D., Kalbitz, K., Buggle, B., Glaser, B. (2012): Absence of oxygen isotope fractionation/exchange of (hemi-) cellulose derived sugars during litter decomposition. *Org Geoch* 42, 1470-1475.

Study 2

Oxygen isotope ratios ($^{18}\text{O}/^{16}\text{O}$) of hemicellulose-derived sugar biomarkers in plants, soils and sediments as paleoclimate proxy I: Insight from a climate chamber experiment

Michael Zech^{1,2,3,*}, Christoph Mayr^{4,5}, Mario Tuthorn^{1,2}, Katharina Leiber-Sauheitl⁶ and Bruno Glaser³

¹) Chair of Geomorphology, University of Bayreuth, Universitätsstr. 30, 95440 Bayreuth, Germany

²) Department of Soil Physics, University of Bayreuth, Universitätsstr. 30, 95440 Bayreuth, Germany

³) Institute of Agronomy and Nutritional Sciences, Soil Biogeochemistry, Martin-Luther University Halle-Wittenberg, Weidenplan 14, 06120 Halle, Germany

⁴) Institute of Geography, Friedrich-Alexander University Erlangen-Nürnberg, Kochstr. 4/4, 91054 Erlangen, Germany

⁵) GeoBio-Center, Institute of Paleontology and Geobiology, Ludwig Maximilians Universität München, Richard_Wagner-Str. 10, 80333 München, Germany

⁶) Thünen Institute of Climate-Smart Agriculture, Bundesallee 50, 38116 Braunschweig, Germany

^{*}) corresponding author: michael_zech@gmx.de

Geochimica et Cosmochimica Acta

(2014) 126, 614-623

Abstract

The oxygen isotopic composition of cellulose is a valuable proxy in paleoclimate research. However, its application to sedimentary archives is challenging due to extraction and purification of cellulose. Here we present compound-specific $\delta^{18}\text{O}$ results of hemicellulose-derived sugar biomarkers determined using gas chromatography-pyrolysis-isotope ratio mass spectrometry, which is a method that overcomes the above-mentioned analytical challenges. The biomarkers were extracted from stem material of different plants (*Eucalyptus globulus*, *Vicia faba* and *Brassica oleracea*) grown in climate chamber experiments under different climatic conditions.

The $\delta^{18}\text{O}$ values of arabinose and xylose range from 31.4 to 45.9‰ and from 28.7 to 40.8‰, respectively, and correlate highly significantly with each other ($R=0.91$, $p<0.001$). Furthermore, $\delta^{18}\text{O}_{\text{hemicellulose}}$ (mean of arabinose and xylose) correlate highly significantly with $\delta^{18}\text{O}_{\text{leaf water}}$ ($R=0.66$, $p<0.001$) and significantly with modeled $\delta^{18}\text{O}_{\text{cellulose}}$ ($R=0.42$, $p<0.038$), as well as with relative air humidity ($R=-0.79$, $p<0.001$) and temperature ($R=-0.66$, $p<0.001$). These findings confirm that the hemicellulose-derived sugar biomarkers, like cellulose, reflect the oxygen isotopic composition of plant source water altered by climatically controlled evapotranspirative ^{18}O enrichment of leaf water. While relative air humidity controls most rigorously the evapotranspirative ^{18}O enrichment, the direct temperature effect is less important. However, temperature can indirectly exert influence via plant physiological reactions, namely by influencing the transpiration rate which affects $\delta^{18}\text{O}_{\text{leaf water}}$ due to the Péclet effect. In a companion paper (Tuthorn et al., this issue) we demonstrate the applicability of the hemicellulose-derived sugar biomarker $\delta^{18}\text{O}$ method to soils and provide evidence from a climate transect study confirming that relative air humidity exerts the dominant control on evapotranspirative ^{18}O enrichment of leaf water.

Finally, we present a conceptual model for the interpretation of $\delta^{18}\text{O}_{\text{hemicellulose}}$ records and propose that a combined $\delta^{18}\text{O}_{\text{hemicellulose}}$ and $\delta^2\text{H}_{n\text{-alkane}}$ biomarker approach is promising for disentangling $\delta^{18}\text{O}_{\text{precipitation}}$ variability from evapotranspirative ^{18}O enrichment variability in future paleoclimate studies.

Keywords: climate chamber experiment, stable oxygen isotopes, biomarkers, evaporative ^{18}O enrichment, plant physiology, paleoclimatology, Péclet effect

1. Introduction

The natural abundance of stable oxygen isotopes ($^{18}\text{O}/^{16}\text{O}$) is a well known proxy in paleoclimate research. It is successfully applied to a wide range of different climate archives such as ice cores, deep sea and lacustrine sediments, speleothems and tree-rings (Epica Members, 2004; Ngrip Members, 2004; Lisiecki and Raymo, 2005; Spötl et al., 2006; Mischke et al., 2010; Rozanski et al., 2010). This can be partly attributed to the finding that the isotopic composition of precipitation is mainly controlled by climatic factors, namely the “temperature effect” in high latitudes and the “amount effect” in tropical and particularly in monsoon regions. Other influencing factors are continentality, altitude and changes in the source area of the moisture-bearing air masses (Dansgaard, 1964; Rozanski et al., 1993; Araguas-Araguas et al., 2000).

In lacustrine sediment and tree-ring archives, it is often cellulose which is used as recorder of the isotopic composition of lake water (Wolfe et al., 2007; Wissel et al., 2008; Rozanski et al., 2010) and leaf water (Danis et al., 2006; Boettger et al., 2007; Gessler et al., 2009; Kress et al., 2010), respectively. While typical $\delta^{18}\text{O}$ values of ground water range from -10 to +2‰ and those of leaf water from -5 to +10‰, cellulose is generally enriched in ^{18}O by ~+27‰ relative to the water present during biosynthesis (Schmidt et al., 2001). Measurements are commonly carried out on purified cellulose using thermal conversion/elemental analysis – isotope ratio mass spectrometry (TC/EA-IRMS) (Werner et al., 1996; Saurer and Siegwolf, 2004). However, analytical challenges concerning extraction, purification and measurement (due to hygroscopicity of cellulose) exist (Saurer and Siegwolf, 2004; Wissel et al., 2008) and hamper an adaptation of this method to soils and terrestrial sediments. These limitations may be overcome by an alternative, recently developed method (Zech and Glaser, 2009; Zech et al., 2013), which is based on compound-specific $\delta^{18}\text{O}$ analyses of hemicellulose-derived sugar

biomarkers such as arabinose, fucose, xylose, and rhamnose using gas chromatography – pyrolysis – isotope ratio mass spectrometry (GC-Py-IRMS) (Zech et al., 2011). The sugar biomarkers are thereby released hydrolytically from the samples and purified highly efficiently after derivatisation using gas chromatography. Given that Zech et al. (2012) found no evidence for oxygen isotope exchange reactions and ^{18}O fractionation affecting the isotopic composition of hemicelluloses during litter degradation, they proposed that this method has potential to become a valuable tool in paleoclimate research.

Like cellulose, hemicelluloses are structural components of plant cell walls and should reflect the oxygen isotopic composition of source water (= soil water) altered by evaporative ^{18}O enrichment due to transpiration (Epstein et al., 1977; Schmidt et al., 2001; Barbour, 2007; Farquhar et al., 2007). The degree of evaporative ^{18}O enrichment of leaf water is known to depend on plant physiological and climate parameters. Respective models, based on the conceptual framework for the isotope effects accompanying the evaporation process, laid down by Craig and Gordon (1965), have been developed and refined during the last decades (Dongmann et al., 1974; Flanagan et al., 1991; Roden et al., 2000; Barbour et al., 2004; Cuntz et al., 2007; Kahmen et al., 2011).

The aim of this study was to take advantage of plant material (*Eucalyptus globulus*, *Vicia faba* and *Brassica oleracea*) grown in climate chamber experiments in order to (i) determine the $\delta^{18}\text{O}$ values of hemicellulose-derived sugar biomarkers ($\delta^{18}\text{O}_{\text{hemicellulose}}$) and to compare them with $\delta^{18}\text{O}_{\text{leaf water}}$ and modeled $\delta^{18}\text{O}_{\text{cellulose}}$ results, (ii) to investigate the effect of relative air humidity, temperature and transpiration rate on $\delta^{18}\text{O}_{\text{hemicellulose}}$ and (iii) to draw implications for paleoclimate studies applying GC-Py-IMRS $\delta^{18}\text{O}$ analyses in soil and sediment archives.

2. Material and Methods

2.1 Climate chamber experiment

The experiment was conducted in winter 2000/01 in the climate chambers of the GSF, Neuherberg, Germany. The experimental design was described in detail previously (Mayr, 2002). In brief, seedlings of *Eucalyptus globulus*, *Vicia faba* and *Brassica oleracea* were grown for 56 days in eight climate chambers under seven different climatic conditions (identical in chamber 4 and 8; Table 1). Diurnal variations followed typical natural conditions. Temperature and relative air humidity from 11 a. m. to 16 p. m. were set to 14°C, 18°C, 24°C and 30°C and to 20%, 30%, 50% and 70%, respectively. The actual temperature and relative air humidity were measured; accordingly, only minor deviations (<5%) from set relative air humidity was observed. Uniform irrigation conditions were ensured by an automatic irrigation system using tensiometers in 9 cm substrate depth. The irrigation water, provided by a water tank, was sampled regularly over the period of the experiment and showed only minor variability in its oxygen isotopic composition ($\delta^{18}\text{O} = -10.7\text{‰} \pm 0.3\text{‰}$). Similarly, soil water and atmospheric water vapour were sampled regularly for $\delta^{18}\text{O}$ analyses (using suction cups in 13 cm substrate depth and cryo traps, respectively) and transpiration rates were determined (Table 1 and Fig. 1). At the end of the experiment, the plants were harvested for $\delta^{18}\text{O}$ analyses of leaf and stem water (vacuum distillation). Although stem water is strictly speaking the mixture of xylem and phloem water, stem water basically reflects the $\delta^{18}\text{O}$ values of soil water (Fig. 1). In simplification, we therefore refer to xylem water (XW) in the following. For further details on the experiment and $\delta^{18}\text{O}$ water analyses the reader is referred to Mayr (2002).

Table 1
Climatic conditions (temperature and relative air humidity) of the eight climate chambers, oxygen isotopic composition of soil water ($\delta^{18}\text{O}_{\text{SW}}$)^{a,b}, stem water ($\delta^{18}\text{O}_{\text{SW}}$)^{a,b}, leaf water ($\delta^{18}\text{O}_{\text{LW}}$)^b and atmospheric water vapor ($\delta^{18}\text{O}_{\text{WV}}$)^{a,b}, transpiration rates (E)^{a,b}, modeled $\delta^{18}\text{O}_{\text{cellulose}}$, $\delta^{18}\text{O}_{\text{arabinose}}$ and $\delta^{18}\text{O}_{\text{xylose}}$.

Chamber	1	2	3	4	5	6	7	8
Temperature (°C)	24	24	30	18	24	14	14	18
Relative air humidity (%)	49	68	48	32	21	24	50	32
$\delta^{18}\text{O}_{\text{WV}}$ (‰)	-16.9	-15.2	-15.1	-22.9	-19.4	-21.7	-16.9	-18.9
Eucalyptus								
$\delta^{18}\text{O}_{\text{SW}}$ (‰)	-7.2 ± 0.4	-7.1 ± 0.5	-7.0 ± 0.5	-7.5 ± 0.3	-5.4 ± 0.2	-6.0 ± 0.9	-6.2 ± 0.7	-5.6 ± 0.7
$\delta^{18}\text{O}_{\text{XW}}$ (‰)	-5.7 ± 1.1	-7.0 ± 0.8	-7.0 ± 0.7	-4.7 ± 1.1	-4.9 ± 0.5	-	-6.0 ± 0.5	-5.2 ± 1.2
$\delta^{18}\text{O}_{\text{LW}}$ (‰)	6.6 ± 0.7	0.3 ± 0.5	6.0 ± 0.9	11.4 ± 0.9	16.8 ± 1.2	18.4 ± 1.4	9.4 ± 0.3	15.0 ± 1.2
E ($\text{mmol m}^{-2}\text{s}^{-1}$)	5.1 ± 1.1	3.5 ± 1.1	7.1 ± 1.3	3.6 ± 1.2	6.3 ± 0.5	2.7 ± 0.5	3.2 ± 0.2	3.8 ± 0.5
$\delta^{18}\text{O}_{\text{cellulose}}$ (‰) ^c	24.3	23.1	22.0	27.1	25.7	29.0	25.9	26.8
$\delta^{18}\text{O}_{\text{arabinose}}$ (‰)	33.6 ± 0.9	33.5 ± 2.0	32.1 ± 0.3	40.7 ± 0.3	37.4 ± 1.6	45.5 ± 1.1	40.4 ± 1.3	41.7 ± 0.4
$\delta^{18}\text{O}_{\text{xylose}}$ (‰)	30.7 ± 0.9	29.6 ± 0.5	28.7 ± 0.4	32.7 ± 0.3	35.3 ± 0.3	39.9 ± 0.4	35.5 ± 0.4	38.8 ± 0.5
Vicia								
$\delta^{18}\text{O}_{\text{SW}}$ (‰)	-7.3 ± 0.6	-7.6 ± 0.5	-6.5 ± 0.6	-7.5 ± 0.3	-5.9 ± 0.7	-6.2 ± 0.4	-6.7 ± 0.4	-6.3 ± 1.1
$\delta^{18}\text{O}_{\text{XW}}$ (‰)	-4.2 ± 0.6	-5.3 ± 0.4	-2.6 ± 1.3	-3.9 ± 0.2	-0.6 ± 1.3	-3.2 ± 1.0	-4.2 ± 0.6	-3.6 ± 0.2
$\delta^{18}\text{O}_{\text{LW}}$ (‰)	10.9 ± 1.3	4.8 ± 0.7	9.7 ± 0.4	16.2 ± 0.9	21.6 ± 1.1	15.7 ± 1.0	7.7 ± 0.6	15.0 ± 0.7
E ($\text{mmol m}^{-2}\text{s}^{-1}$)	2.0 ± 1.0	1.7 ± 0.9	2.7 ± 0.4	1.5 ± 0.7	1.3 ± 0.6	0.9 ± 0.1	1.3 ± 0.6	0.9 ± 0.7
$\delta^{18}\text{O}_{\text{cellulose}}$ (‰) ^c	29.0	27.2	29.3	31.8	37.6	36.5	31.1	35.2
$\delta^{18}\text{O}_{\text{arabinose}}$ (‰)	32.1 ± 1.4	31.4 ± 1.5	35.1 ± 0.8	32.3 ± 1.0	37.0 ± 1.8	45.9 ± 0.8	41.3 ± 4.3	42.6 ± 2.4
$\delta^{18}\text{O}_{\text{xylose}}$ (‰)	29.9 ± 0.5	29.6 ± 0.6	28.6 ± 0.2	30.9 ± 0.2	36.4 ± 0.6	40.1 ± 0.6	35.2 ± 1.0	40.3 ± 1.6
Brassica								
$\delta^{18}\text{O}_{\text{SW}}$ (‰)	-6.7 ± 0.5	-7.5 ± 0.2	-6.5 ± 0.7	-6.7 ± 0.6	-5.8 ± 0.4	-6.2 ± 0.5	-6.1 ± 0.6	-6.0 ± 0.6
$\delta^{18}\text{O}_{\text{XW}}$ (‰)	-4.3 ± 1.0	-5.8 ± 0.5	-4.3 ± 0.7	-4.4 ± 1.0	-3.3 ± 1.2	-5.4 ± 0.9	-6.0 ± 0.3	-5.0 ± 0.5
$\delta^{18}\text{O}_{\text{LW}}$ (‰)	9.2 ± 2.6	3.2 ± 0.9	6.8 ± 0.9	14.9 ± 1.5	19.3 ± 1.6	18.9 ± 1.0	10.2 ± 0.5	15.3 ± 1.2
E ($\text{mmol m}^{-2}\text{s}^{-1}$)	6.4 ± 0.7	4.4 ± 1.2	8.8 ± 0.4	4.4 ± 1.2	6.1 ± 0.2	3.6 ± 0.4	3.3 ± 0.3	4.7 ± 1.2
$\delta^{18}\text{O}_{\text{cellulose}}$ (‰) ^c	24.9	23.5	24.2	26.7	27.3	27.5	25.8	26.2
$\delta^{18}\text{O}_{\text{arabinose}}$ (‰)	32.9 ± 2.4	32.6 ± 2.1	34.5 ± 0.8	40.0 ± 1.3	40.1 ± 1.3	45.9 ± 0.5	$43.8 \pm \pm 0.5$	42.4 ± 1.4
$\delta^{18}\text{O}_{\text{xylose}}$ (‰)	30.1 ± 1.0	31.5 ± 1.2	28.7 ± 0.8	35.3 ± 0.7	36.7 ± 0.5	40.8 ± 0.5	36.7 ± 0.5	38.5 ± 0.5

^a Mean values and standard deviations over the period of the experiment.

^b Data from Mayr (2002).

^c Modeled.

2.2 Sample preparation and compound-specific $\delta^{18}\text{O}$ analyses of hemicellulose-derived sugar biomarkers

Sample preparation for hemicellulose-derived sugar biomarker analyses was carried out on dry and finely grinded stem material of the climate chamber experiment at the Department of Soil Physics, University of Bayreuth, Germany, and followed a slightly modified procedure described in detail by Zech and Glaser (2009). The hemicellulose sugars were extracted hydrolytically (105 °C, 4 h) from sample aliquots containing ~10 mg total organic carbon with 10 mL 4 M trifluoroacetic acid (TFA) as proposed by Amelung et al. (1996); the extracted monosaccharides were purified using XAD-7 and Dowex 50WX8 columns. For derivatization of the freeze-dried sugars we added 4 mg methylboronic acid (MBA) in 400 μL dry pyridine and heated the samples to 60 °C for 1 h. The originally included second derivatization step with bis(trimethylsilyl)trifluoroacetamide (BSTFA), which is necessary for the remaining hydroxyl groups of hexoses, was skipped because Zech and Glaser (2009) found not reproducible derivatization results. For the investigated pentoses arabinose and xylose and the deoxyhexoses fucose and rhamnose the MBA derivatization ensures that each sugar yields only one peak in the chromatograms and furthermore oxygen addition by the derivatization reagent is avoided (Pizer and Tihal, 1992).

Compound-specific $\delta^{18}\text{O}$ measurements were performed in the Isotope Laboratory of the Institute of Agronomy and Nutritional Sciences, Martin-Luther-University Halle-Wittenberg, Germany. The GC-Py-IRMS system consisted of a Trace GC 2000 gas chromatograph (Thermo Fisher Scientific, Bremen, Germany) coupled to a Delta V Advantage isotope ratio mass spectrometer (Thermo Fisher Scientific) via an ^{18}O -pyrolysis reactor and a GC/TC III interface (Thermo Fisher Scientific). The sample batches were run in six-fold replication with co-derivatized sugar standard batches with varying sugar concentrations and known $\delta^{18}\text{O}$ values embedded in-between in order to allow for corrections

of an amount dependence of the $\delta^{18}\text{O}$ measurements if necessary (Zech and Glaser, 2009) and in order to ensure the ‘Principle of Identical Treatment’ of samples and standards (Werner and Brand, 2001). Results are presented as $\delta^{18}\text{O}$ values (in permil, ‰), which is the deviation of the oxygen isotope ratio of a sample relative to that of an international standard (Coplen, 2011)

$$\delta^{18}\text{O} = \left(\frac{R_{\text{sample}}}{R_{\text{standard}}} \right) - 1 \quad (\text{Eqn. 1}),$$

where R_{sample} and R_{standard} represent the isotope ratio $^{18}\text{O}/^{16}\text{O}$ of the sample and the Vienna Standard Mean Ocean Water (V-SMOW), respectively. Mean standard errors for the replication measurements of all samples are 1.3‰ and 0.6‰ for arabinose (n=3) and xylose (n=6), respectively. Note that three replication measurements could not be evaluated for arabinose due to a slight drift of the retention times during the run of the sequence and a resulting arabinose peak overlap with a reference gas peak.

2.3 Modeling

In order to compare our experimental findings with modeling results we used the Péclet modified Craig Gordon leaf water model of Barbour et al. (2004) and conducted model sensitivity tests for changing temperatures, relative air humidities, transpiration rates and leaf-air temperature differences. For these tests, the $\delta^{18}\text{O}$ value of the source water (= stem water) was set to -5‰ and the $\delta^{18}\text{O}$ value of the atmospheric water vapour was set to -17.6‰.

3. Results and Discussion

3.1 $\delta^{18}\text{O}$ results of hemicellulose-derived sugar biomarkers

The investigated plant stem material of *Eucalyptus*, *Vicia* and *Brassica* contains considerably higher relative abundances of the pentoses arabinose and xylose compared to the deoxyhexoses fucose and rhamnose. This is in agreement with findings of Jia et al. (2008) and Zech et al. (2012) and hampered a reliable evaluation of fucose and rhamnose. The $\delta^{18}\text{O}$ values of arabinose and xylose range from 31.4 to 45.9‰ and from 28.7 to 40.8‰, respectively, and are highly significantly correlated with each other ($R=0.91$, $p<0.001$, $n=24$). They reveal similar and systematic patterns for *Eucalyptus*, *Vicia* and *Brassica* depending on the climatic conditions adjusted in the eight chambers (Table 1 and Fig. 1). For comparison, soil water in 13 cm depth, which is slightly enriched in ^{18}O relative to the irrigation water (-10.7‰), shows small variability ranging from -7.6 to -5.4‰ (Table 1 and Fig. 1). Atmospheric water vapour, by contrast, is slightly depleted in ^{18}O relative to the irrigation water. $\delta^{18}\text{O}$ values range from -22.9 to -15.1‰ (chamber 4 and 3, respectively, see Table 1) and are positively correlated with relative air humidity ($R=0.80$, $p=0.017$, $n=8$).

Slightly but systematically more positive $\delta^{18}\text{O}_{\text{arabinose}}$ values compared to $\delta^{18}\text{O}_{\text{xylose}}$ values were also reported by Tuthorn et al. (this issue) and Zech et al. (submitted), but not by Zech and Glaser (2009) and Zech et al. (2012; 2013). Both pentoses are biosynthesized in plants by the decarboxylation of C6 carbon atoms from glucose (Altermatt and Neish, 1956; Harper and Bar-Peled, 2002; Burget et al., 2003). Given that arabinose is an epimerase product of xylose and the intermediate UDP-4-keto-xylose (Purich and Allison, 2002) could be able to exchange oxygen isotopes with the aqueous phase, the observed difference may be attributed to a slight biosynthetic ^{18}O fractionation or ^{18}O exchange. In the following we use the mean of $\delta^{18}\text{O}_{\text{arabinose}}$ and $\delta^{18}\text{O}_{\text{xylose}}$ and refer to it as $\delta^{18}\text{O}_{\text{hemicellulose}}$.

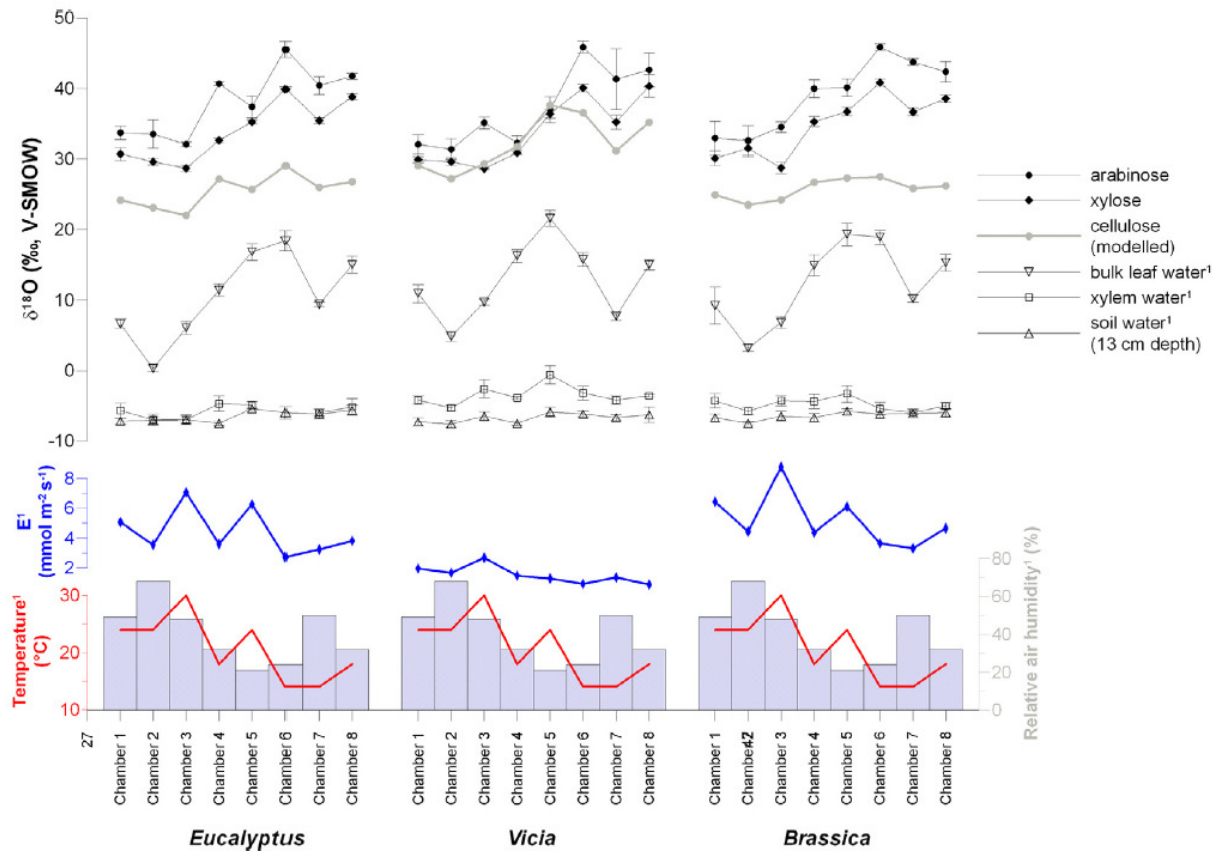


Fig. 1: Results for $\delta^{18}\text{O}_{\text{arabinose}}$ and $\delta^{18}\text{O}_{\text{xylose}}$ and comparison with modeled $\delta^{18}\text{O}_{\text{cellulose}}$, $\delta^{18}\text{O}_{\text{leaf water}}$, $\delta^{18}\text{O}_{\text{xylem water}}$, $\delta^{18}\text{O}_{\text{soil water}}$, transpiration rate (E) and the climate parameters temperature and relative air humidity. 1) from Mayr (2002).

3.2 Comparison of $\delta^{18}\text{O}_{\text{hemicellulose}}$ with modeled $\delta^{18}\text{O}_{\text{cellulose}}$ and measured $\delta^{18}\text{O}_{\text{leaf water}}$

The $\delta^{18}\text{O}_{\text{hemicellulose}}$ values correlate highly significantly with the $\delta^{18}\text{O}_{\text{leaf water}}$ values (Mayr, 2002) ($R=0.66$, $p<0.001$, $n=24$) and significantly with the modeled $\delta^{18}\text{O}_{\text{cellulose}}$ values ($R=0.42$, $p<0.038$, $n=24$). Furthermore, Fig. 1 depicts that the amplitude of $\delta^{18}\text{O}_{\text{leaf water}}$ is by several per mil higher compared to the amplitude of $\delta^{18}\text{O}_{\text{hemicellulose}}$ and modeled $\delta^{18}\text{O}_{\text{cellulose}}$. This can be reasonably attributed to the fact that stem material and not leaf material was investigated in our study. Leaf water is enriched in ^{18}O compared to plant source water ($\delta^{18}\text{O}_{\text{xylem water}}$) due to isotope effects accompanying the evaporation/transpiration process

(Craig and Gordon, 1965; Dongmann et al., 1974; Flanagan et al., 1991; Farquhar et al., 2007). Although with a biosynthetic ^{18}O fractionation of $\sim +27\text{‰}$ (Cernusak et al., 2003), sugars which are biosynthesized in leaves reflect the oxygen isotopic composition of leaf water and thus its evapotranspirative ^{18}O enrichment (Schmidt et al., 2001; Barbour, 2007). However, it is known that up to 40% of the oxygen atoms of sucrose, which is the most important transport sugar in plants, are isotopically exchanged with non-enriched xylem water during cellulose synthesis (Sternberg et al., 1986; Gessler et al., 2009). Indeed, our $\delta^{18}\text{O}_{\text{hemicellulose}}$ values obtained for stem material are enriched in ^{18}O by only $\sim +24\text{‰}$ on average relative to the leaf water, indicating that part of the leaf water ^{18}O enrichment is lost. It is noteworthy that the $\delta^{18}\text{O}_{\text{hemicellulose}}$ values tend to be more positive than the modeled $\delta^{18}\text{O}_{\text{cellulose}}$ values (Fig. 1), because as mentioned above, pentoses are biosynthesized by a decarboxylation of the C6 carbon atoms from glucose (Altermatt and Neish, 1956; Harper and Bar-Peled, 2002; Burget et al., 2003) and because Sternberg et al. (2006) found evidence for non-uniform isotope distributions of oxygen atoms attached to different carbon atoms in glucose as postulated already by Schmidt et al. (1995). Hence, more positive $\delta^{18}\text{O}_{\text{hemicellulose}}$ values than $\delta^{18}\text{O}_{\text{cellulose}}$ values (also observed in our companion study presented by Tuthorn et al., this issue) might indicate that the oxygen atom in C6 position of glucose building up cellulose is more depleted in ^{18}O than the average of the oxygen atoms in positions C2 to C5. This interpretation is in agreement with the recent finding of Waterhouse et al. (2013) that about 80% of the oxygen atoms in C6 position are isotopically exchanged during heterotrophic cellulose synthesis and have hence lost the evapotranspirative ^{18}O enrichment signal of leaf water.

Overall, our findings suggest that $\delta^{18}\text{O}_{\text{hemicellulose}}$ of stem material, like $\delta^{18}\text{O}_{\text{cellulose}}$, reflects slightly dampened the climatically controlled evapotranspirative ^{18}O enrichment of leaf water.

3.3 Effect of RH, temperature and transpiration rate on $\delta^{18}\text{O}_{\text{hemicellulose}}$

The $\delta^{18}\text{O}_{\text{hemicellulose}}$ values do not only correlate highly significantly with $\delta^{18}\text{O}_{\text{leaf water}}$, but also with the climate variables relative air humidity ($R=-0.79$, $p<0.001$, $n=24$) and temperature ($R=-0.66$, $p<0.001$, $n=24$) (Fig. 1). Fig. 2 illustrates in form of a 3D-scatterplot that the correlation is even better when a multiple regression analysis is carried out with $\delta^{18}\text{O}_{\text{hemicellulose}}$ depending on the variables RH and temperature ($R=0.89$, $p<<0.001$, $n=24$). Accordingly, the lower RH and temperature are in our climate chamber experiment, the more positive the $\delta^{18}\text{O}_{\text{hemicellulose}}$ values become.

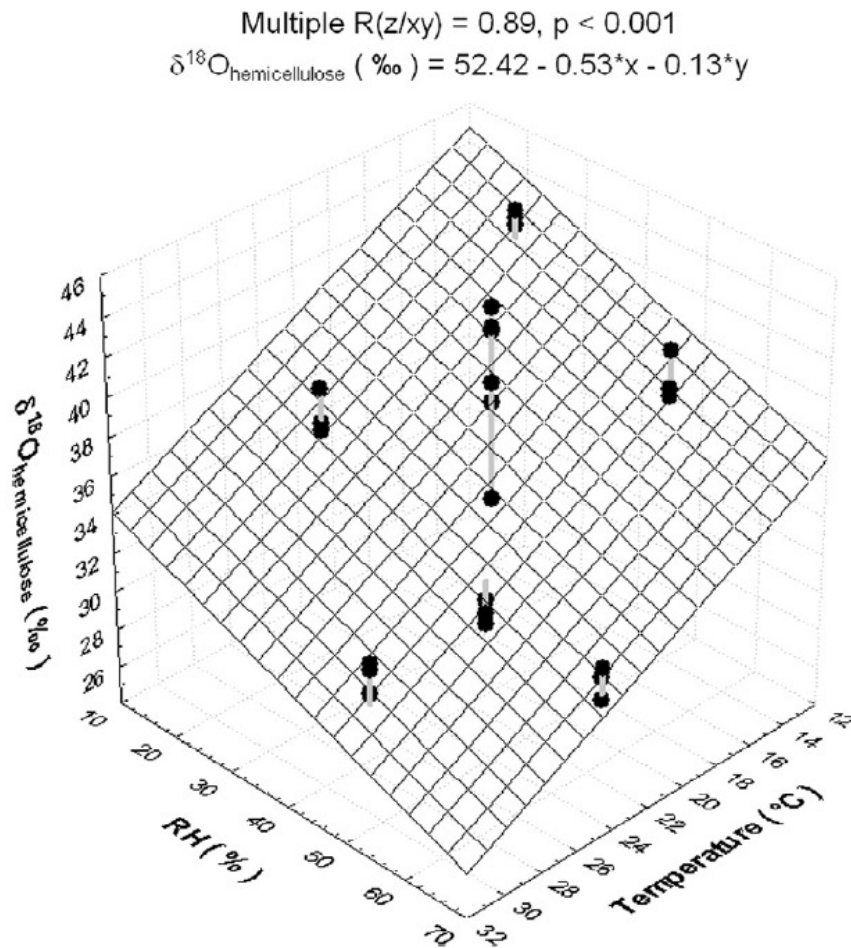


Fig. 2: 3D-Scatterplot and multiple regression analysis describing the dependence of $\delta^{18}\text{O}_{\text{hemicellulose}}$ on the climate parameters temperature and relative air humidity in the climate chamber experiment.

The strong dependence of evapotranspirative ^{18}O enrichment of leaf water on RH, which is reflected in our $\delta^{18}\text{O}_{\text{hemicellulose}}$ results (Fig. 2), is well known and included in respective models, for instance in the equation (Eqn. 2) of Flanagan et al. (1991)

$$R_{lw} = \alpha^* \left[\alpha_k R_{xw} \left(\frac{e_i - e_a}{e_i} \right) + R_a \left(\frac{e_a}{e_i} \right) \right] \quad (\text{Eqn. 2}),$$

where R is the $^{18}\text{O}/^{16}\text{O}$ ratio of leaf water (lw), xylem water (xw) and atmospheric water vapour, respectively, and e_i and e_a is the water vapour partial pressures in the intercellular spaces and the atmosphere, respectively. Both the kinetic ^{18}O fractionation factor α_k and the equilibrium ^{18}O fractionation factor α^* are temperature-dependent (Merlivat, 1978). However, when compared with the strong effect that changing RH has, the effect of temperature on $\delta^{18}\text{O}_{\text{leaf water}}$ according to Eqn. 2 is negligible and can hence not explain this part of our findings.

Further modifications of the model introducing boundary layer effects, the Péclet effect, and leaf-air temperature differences (Roden et al., 2000; Barbour et al., 2004; Kahmen et al., 2011) confirm that RH is the most important and rigorous climatic factor controlling evapotranspirative ^{18}O enrichment of leaf water. Fig. 3A illustrates this strong dependency using the model of Barbour et al. (2004) for different transpiration rates. By contrast, the direct effect of pure temperature changes on evapotranspirative ^{18}O enrichment of leaf water remains negligible (Fig. 3B). However, model sensitivity tests highlight that transpiration rate changes have a very strong effect on $\delta^{18}\text{O}_{\text{leaf water}}$ with more negative values resulting from higher transpiration rates (Fig. 3A and C). This can be attributed to a Péclet effect (Farquhar and Lloyd, 1993), with the Péclet number \wp describing the ratio of convection to diffusion according to Eqn. 3:

$$\phi = \frac{LE}{CD} \quad (\text{Eqn. 3}),$$

where L is the effective length, C is the molar density of water and D the diffusivity of H_2^{18}O . Accordingly, at higher transpiration rates the backward diffusion of ^{18}O -enriched water from the evaporating sites opposing the transpirational convection is less effective and $\delta^{18}\text{O}_{\text{leaf water}}$ becomes more negative due to the dilution with not ^{18}O -enriched xylem water.

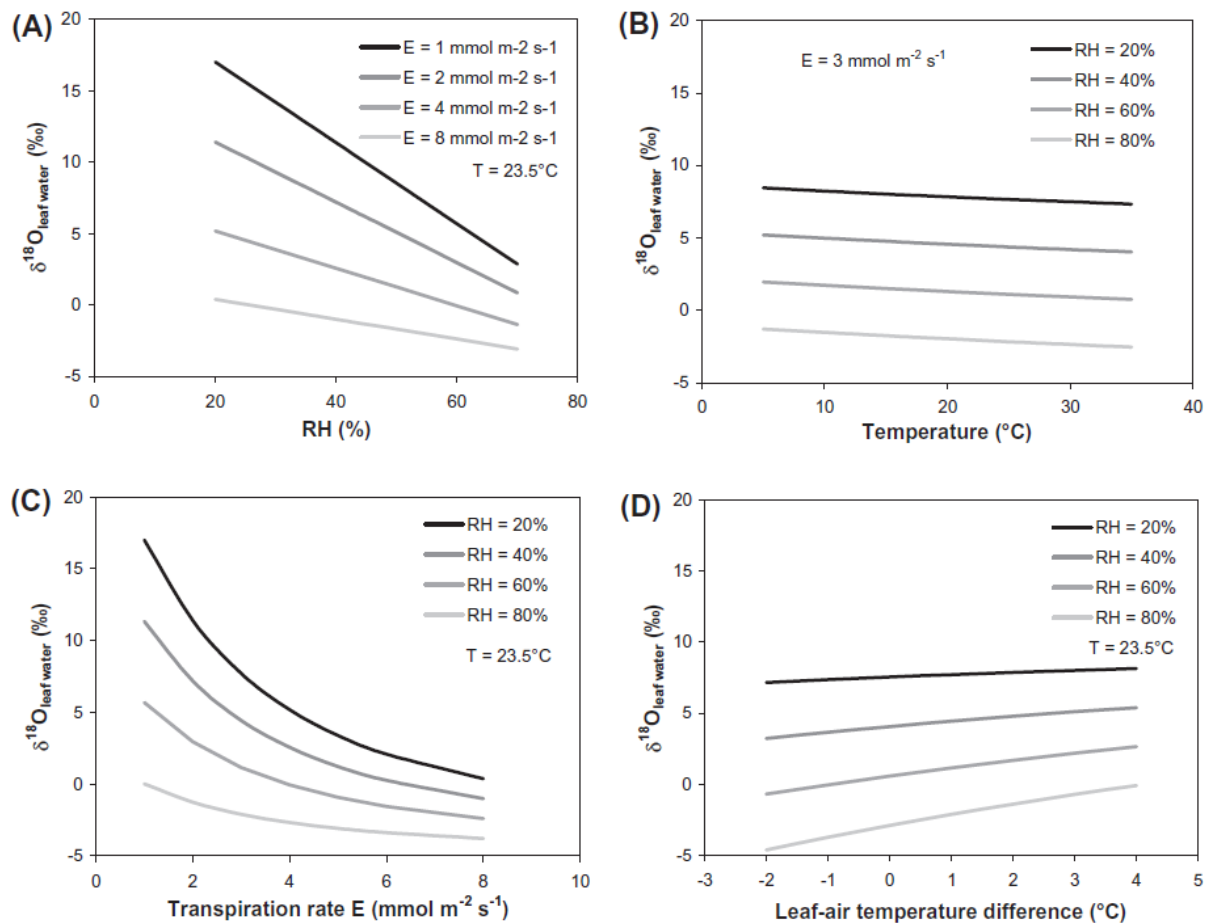


Fig. 3: Results of model sensitivity tests showing the dependency of $\delta^{18}\text{O}_{\text{leaf water}}$ on (A) RH, (B) temperature, (C) transpiration rate, and (D) leaf-air temperature difference. The model used for these simulations is from Barbour et al. (2004).

A prerequisite for the Péclet effect to be effective is a good water supply of the plants as it was ensured in our climate chamber experiment by the installed automatic irrigation system. One of the factors influencing transpiration is temperature and indeed there is a significant positive correlation for all three investigated plant species with correlation coefficients of $R=0.86$ ($p=0.006$), $R=0.82$ ($p=0.013$) and $R=0.91$ ($p=0.002$, $n=8$ for all) for *Eucalyptus*, *Vicia* and *Brassica*, respectively (Fig. 1). Hence, although there is only a negligible direct temperature effect, there is a strong indirect temperature effect on our $\delta^{18}\text{O}_{\text{hemicellulose}}$ results (Fig. 2) by varying transpiration rates and the Péclet effect.

The Péclet effect can also help explaining the observed and at first glimpse unexpected large differences of $\delta^{18}\text{O}_{\text{arabinose}}$ and $\delta^{18}\text{O}_{\text{xylose}}$ for *Vicia* between chamber 4 and 8 (Fig. 1). Despite the climatic conditions in those two chambers were identical, stem material from *Vicia* in chamber 4 is characterized by significantly more negative $\delta^{18}\text{O}_{\text{arabinose}}$ and $\delta^{18}\text{O}_{\text{xylose}}$ values. Mayr (2002) found that *Vicia* in chamber 4 was characterized by considerable higher transpiration rates ($E=1.5 \pm 0.7 \text{ mmol m}^{-2} \text{ s}^{-1}$) than *Vicia* in chamber 8 ($E=0.9 \pm 0.7 \text{ mmol m}^{-2} \text{ s}^{-1}$), which involves a stronger Péclet effect for the plants in chamber 4. Given that the climatic conditions in the chambers 4 and 8 were identical, plant physiological differences likely account for the different transpiration rates. Indeed, Mayr (2002) reported that the stomatal conductance for water ($g_{\text{H}_2\text{O}}$) and the net photosynthetic rate (A) of *Vicia* were considerably higher in chamber 4 compared to chamber 8 ($g_{\text{H}_2\text{O}}=74 \pm 8$ versus $32 \pm 30 \text{ mmol m}^{-2} \text{ s}^{-1}$ and $A=7.7 \pm 0.9$ versus $2.9 \pm 2.6 \text{ } \mu\text{mol m}^{-2} \text{ s}^{-1}$).

4. A conceptual model for interpreting $\delta^{18}\text{O}_{\text{hemicellulose}}$ in sedimentary paleoclimate archives

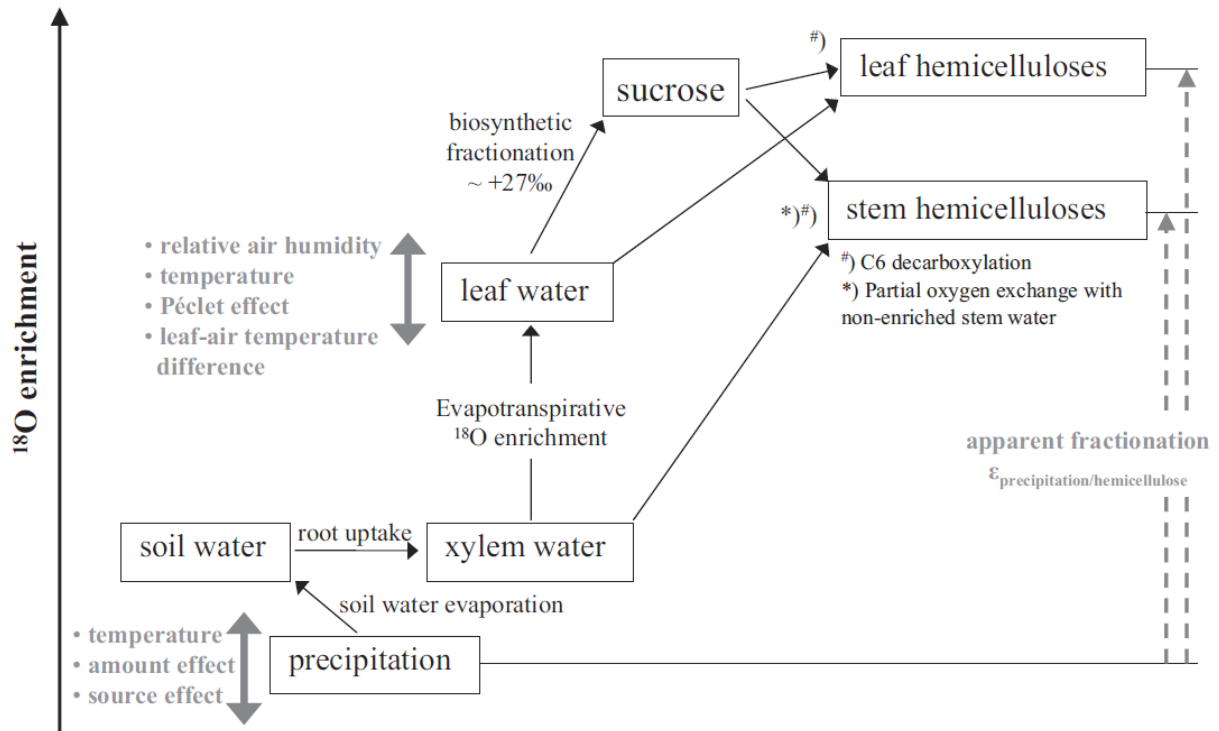


Fig. 4: Conceptual diagram illustrating the major factors influencing the oxygen isotopic composition of hemicellulose-derived sugar biomarkers.

The above presented results and discussion suggest that plant hemicellulose sugars are a valuable recorder of $\delta^{18}\text{O}_{\text{leaf water}}$ comparable to cellulose. Investigating $\delta^{18}\text{O}$ of hemicellulose-derived sugar biomarkers in soil and sediment archives by applying the method proposed by Zech and Glaser (2009) has therefore potential for paleoclimate studies, particularly because Zech et al. (2012) found no evidence for degradation effects on $\delta^{18}\text{O}_{\text{hemicellulose}}$.

- One major factor influencing $\delta^{18}\text{O}_{\text{hemicellulose}}$ is the oxygen isotopic composition of the plant source water (Fig. 4). Basically, it depends on $\delta^{18}\text{O}_{\text{precipitation}}$ which can vary over time due

to temperature, amount and/or source effects (Dansgaard, 1964; Rozanski et al., 1993; Araguas-Araguas et al., 2000). While it is generally accepted that the uptake of water by roots is not associated with a ^{18}O fractionation (Wershaw et al., 1966; Dawson et al., 2002), other factors may need careful consideration. For instance, the uptake of ground water depleted in ^{18}O by deep rooting plants versus uptake of soil water enriched in ^{18}O by evaporation (Fig. 4), seasonality of $\delta^{18}\text{O}_{\text{precipitation}}$ (growing season) (see also our companion study presented by Tuthorn et al., this issue) or uptake of permafrost meltwater (Sugimoto et al., 2002).

- A second major influencing factor is evapotranspirative ^{18}O enrichment of leaf water (Fig. 4). It is most rigorously controlled by relative air humidity (Fig. 3A), whereas the direct physical effect of temperature on evapotranspirative ^{18}O enrichment is much smaller (Fig. 3B). However, temperature can indirectly exert influence via plant physiological reactions, namely by affecting the transpiration rate which strongly controls $\delta^{18}\text{O}_{\text{leaf water}}$ due to the Péclet effect at least under very arid climatic conditions (Fig. 3C). While this effect is highlighted in the here presented climate chamber study with an automatic irrigation system, the relevance of the temperature and the Péclet effect in paleoclimate studies where water supply is actually often limited is presumably considerably lower than the relevance of relative air humidity. This assumption is confirmed by a climate transect study on $\delta^{18}\text{O}_{\text{hemicellulose}}$ of modern topsoils presented in the companion paper by Tuthorn et al. (this issue).
- Thirdly, a biosynthetic ^{18}O fractionation of $\sim+27\text{‰}$ (Sternberg et al., 1986; Cernusak et al., 2003; Gessler et al., 2009) causes newly assimilated sugars and leaf cellulose to be systematically enriched in ^{18}O compared to leaf water (Fig. 4). Recently, Sternberg and Ellsworth (2011) suggested that the biochemical ^{18}O fractionation during cellulose synthesis is not constant but increases at lower temperatures to values of $\sim+31\text{‰}$. However,

this conclusion is based on the assumption that the percentage of oxygen atoms exchanging during cellulose synthesis (p_{ex}) is constant and 42%. This assumption may not hold true, because although not statistically significant ($p=0.10$, $n=6$), there is a clear trend indicating that p_{ex} is not constant but temperature-dependent (ranging from ~40% to ~45%). Calculating the biosynthetic ^{18}O fractionation with the temperature-dependent p_{ex} values (Table S1 of Sternberg and Ellsworth, 2011) actually does not support the conclusion that the biosynthetic ^{18}O fractionation is statistically significant temperature-dependent ($p=0.22$, $n=6$).

- Significant input of stem or root-derived hemicelluloses rather than leaf-derived hemicelluloses to sedimentary archives results in a dampening of the leaf water ^{18}O enrichment signal. This is caused by the above mentioned partial oxygen isotope exchange (p_{ex}) with xylem water that is not enriched in ^{18}O , during stem (hemi-)cellulose synthesis (Fig. 4).
- First results (this study and Tuthorn et al., this issue) indicate that hemicelluloses are slightly enriched compared to cellulose. This points to the loss of a relatively depleted oxygen atom attached to C6 during pentose biosynthesis (C6 decarboxylation; Altermatt and Neish, 1956; Harper and Bar-Peled, 2002; Burget et al., 2003) and is in agreement with the recent finding that about 80% of the oxygen atoms in C6 position are isotopically exchanged during cellulose synthesis (Waterhouse et al., 2013).
- It is worth mentioning that in paleolimnological studies dealing with lacustrine sediments, no evapotranspirative ^{18}O enrichment of leaf water has to be considered provided that the hemicelluloses are primarily of aquatic origin (Zech et al., accepted). In cases where evaporative ^{18}O enrichment of lake water is negligible and lake water resembles precipitation, this can largely simplify the paleoclimatic interpretation because then the

apparent ^{18}O fractionation between precipitation and the lacustrine $\delta^{18}\text{O}_{\text{hemicellulose}}$ record can be assumed to have been constant (Fig. 4).

- By contrast, in terrestrial records it will be challenging or even impossible to disentangle $\delta^{18}\text{O}_{\text{precipitation}}$ variability from possible variability of evapotranspirative ^{18}O enrichment of leaf water based on $\delta^{18}\text{O}_{\text{hemicellulose}}$ records alone. Zech et al. (submitted) therefore suggested that the most promising approach in biomarker-based paleohydrology and paleoclimate research may be the combination of $\delta^{18}\text{O}_{\text{hemicellulose}}$ and $\delta^2\text{H}_{n\text{-alkane}}$ records, with n -alkanes serving as leaf wax-derived lipid biomarkers. Such a combined approach allows estimating the evapotranspirative ^{18}O and ^2H leaf water enrichment by using an Craig-Gordon-modelled evaporation line and thus in turn allows reconstructing $\delta^{18}\text{O}_{\text{precipitation}}$ and $\delta^2\text{H}_{\text{precipitation}}$.

Acknowledgements

We thank S. Bösel and A. Mergner for laboratory and technical support, Prof. B. Huwe, Prof. S. Markovic and Prof. L. Zöller for logistic support and M. Dippold and M. Dubbert for valuable discussions. Prof. J. Roden kindly provided the EXCEL spreadsheet with the leaf water ^{18}O enrichment model including the Péclet effect published in Barbour et al. (2004). We thank AE R. Prof. R. Pancost and two anonymous reviewers for constructive comments and suggestions on the manuscript. This study was partly funded by the German Research foundation (DFG ZE 844/1-1). M. Zech also greatly acknowledges the support provided by the Alexander von Humboldt-Foundation.

References

- Altermatt H. A. and Neish A. C. (1956) The biosynthesis of cell wall carbohydrates: III: Further studies on formation of cellulose and xylan from labeled monosaccharides in wheat plants. *Canadian Journal of Biochemistry and Physiology* **34**(3), 405-413.
- Amelung W., Cheshire M. V., and Guggenberger G. (1996) Determination of neutral and acidic sugars in soil by capillary gas-liquid chromatography after trifluoroacetic acid hydrolysis. *Soil Biology and Biochemistry* **28**(12), 1631-1639.
- Araguas-Araguas L., Froehlich K., and Rozanski K. (2000) Deuterium and oxygen-18 isotope composition of precipitation and atmospheric moisture. *Hydrological Processes* **14**, 1341-1355.
- Barbour M. (2007) Stable oxygen isotope composition of plant tissue: a review. *Functional Plant Biology* **34**, 83-94.
- Barbour M., Roden J. S., Farquhar G., and Ehleringer J. R. (2004) Expressing leaf water and cellulose oxygen isotope ratios as enrichment above source water reveals evidence of a Péclet effect. *Oecologia* **138**, 426-435.
- Boettger T., Haupt M., Knöller K., Weise S., Waterhouse J., Rinne K., Loader N., Sonninen E., Jungner H., Masson-Delmotte V., Stievenard M., Guillemain M. T., Pierre M., Pazdur A., Leuenberger M., Filot M., Saurer M., Reynolds C., Helle G., and Schleser G. (2007) Wood Cellulose Preparation Methods and Mass Spectrometric Analyses of $\delta^{13}\text{C}$, $\delta^{18}\text{O}$, and Nonexchangeable $\delta^2\text{H}$ Values in Cellulose, Sugar, and Starch: An Interlaboratory Comparison. *Analytical Chemistry* **79**, 4603-4612.
- Burget E., Verma R., Mølhøj M., and Reiter W. (2003) The biosynthesis of L-arabinose in plants: molecular cloning and characterization of a golgi-localized UDPD-xylose 4-epimerase encoded by the MUR4 gene of arabidopsis. *The Plant Cell* **15**, 523-531.
- Cernusak L., Wong S., and Farquhar G. (2003) Oxygen isotope composition of phloem sap in relation to leaf water in *Ricinus communis*. *Functional Plant Biology* **30**(10), 1059-1070.
- Coplen T. B. (2011) Guidelines and recommended terms for expression of stableisotope-ratio and gas-ratio measurement results. *Rapid Communications in Mass Spectrometry* **25**, 2538-2560.

- Craig H. and Gordon L. I. (1965) Deuterium and oxygen-18 variations in the ocean and the marine atmosphere. In *Stable Isotopes in Oceanographic Studies and Paleotemperatures* (ed. E. Tongiorgi), pp. 1-122. Lab. Geol. Nucl.
- Cuntz M., Ogée J., Farquhar G., Peylin P., and Cernusak L. (2007) Modelling advection and diffusion of water isotopologues in leaves. *Plant, Cell and Environment* **30**, 892-909.
- Danis P. A., Masson-Delmotte V., Stievenard M., Guillemin M. T., Daux V., Naveau P., and von Grafenstein U. (2006) Reconstruction of past precipitation $\delta^{18}\text{O}$ using tree-ring cellulose $\delta^{18}\text{O}$ and $\delta^{13}\text{C}$: a calibration study near Lac d'Annecy, France. *Earth and Planetary Science Letters* **243**, 439-448.
- Dansgaard P. (1964) Stable isotopes in precipitation. *Tellus* **16**, 436-468.
- Dawson T. E., Mambelli S., Plamboeck A. H., Templer P. H., and Tu K. P. (2002) Stable isotopes in plant ecology. *Annual Review of Ecology and Systematics* **33**, 507-559.
- Dongmann G., Nurnberg H. W., Förstel H., and Wagener K. (1974) On the enrichment of H_2^{18}O in the leaves of transpiring plants. *Radiation and Environmental Biophysics* **11**, 41-52.
- EPICA members. (2004) Eight glacial cycles from an Antarctic ice core. *Nature* **429**(6992), 623-628.
- Epstein S., Thompson P., and Yapp C. J. (1977) Oxygen and hydrogen isotopic ratios in plants cellulose. *Science* **198**, 1209-1215.
- Farquhar G., Cernusak L., and Barnes B. (2007) Heavy water fractionation during transpiration. *Plant Physiology* **143**, 11-18.
- Farquhar G. D. and Lloyd J. (1993) Carbon and oxygen isotope effects in the exchange of carbon dioxide between terrestrial plants and the atmosphere. In *Stable isotopes and plant carbon-water relations* (ed. J. R. Ehleringer, A. E. Hall, and G. D. Farquhar), pp. 47-70. Academic Press.
- Flanagan L. B., Marshall J. D., and Ehleringer J. R. (1991) Comparison of modeled and observed environmental influences on the stable oxygen and hydrogen isotope composition of leaf water in *Phaseolus vulgaris* L. *Plant Physiology* **96**, 623-631.
- Gessler A., Brandes E., Buchmann N., Helle G., Rennenberg H., and Barnard R. (2009) Tracing carbon and oxygen isotope signals from newly assimilated sugars in the leaves to the tree-ring archive. *Plant, Cell and Environment* **32**(7), 780-795.
- Harper A. and Bar-Peled M. (2002) Biosynthesis of UDP-xylose. Cloning and characterization of a novel Arabidopsis gene family, UXS, encoding soluble and putative

- membrane-bound UDP-glucuronic acid decarboxylase isoforms. *Plant Physiology* **130**(4), 2188-2198.
- Jia G., Dungait J. A. J., Bingham E. M., Valiranta M., Korhola A., and Evershed R. P. (2008) Neutral monosaccharides as biomarker proxies for bog-forming plants for application to palaeovegetation reconstruction in ombrotrophic peat deposits. *Organic Geochemistry* **39**, 1790-1799.
- Kahmen A., Sachse D., Arndt S., Tu K. P., Farrington H., Vitousek P., and Dawson T. E. (2011) Cellulose $\delta^{18}\text{O}$ is an index of leaf-to air vapor pressure difference (VPD) in tropical plants. *PNAS* **108**(5), 1981-1986.
- Kress A., Saurer M., Siegwolf R., Frank D., Esper J., and Bugmann H. (2010) A 350 year drought reconstruction from Alpine tree ring stable isotopes. *Global Biogeochemical Cycles* **24**, doi:10.1029/2009GB003613.
- Lisiecki L. E. and Raymo M. E. (2005) A Pliocene-Pleistocene stack of 57 globally distributed benthic $\delta^{18}\text{O}$ records. *Paleoceanography* **20**(PA1003), 17 PP.
- Mayr C. (2002) Möglichkeiten der Klimarekonstruktion im Holozän mit $\delta^{13}\text{C}$ - und $\delta^2\text{H}$ -Werten von Baum-Jahrringen auf der Basis von Klimakammerversuchen und Rezentstudien, Ludwig-Maximilians-Universität München.
- Merlivat L. (1978) Molecular diffusivities of H_2^{16}O , HD^{16}O , H_2^{18}O in gases. *The Journal of Chemical Physics* **69**, 2864-2871.
- Mischke S., Aichner B., Diekmann B., Herzsuh U., Plessen B., Wünnemann B., and Zhang C. (2010) Ostracods and stable isotopes of a late glacial and Holocene lake record from the NE Tibetan Plateau. *Chemical Geology* **276**, 95-103.
- NGRIP members. (2004) High-resolution record of Northern Hemisphere climate extending into the last interglacial period. *Nature* **431**, 147-151.
- Pizer R. and Tihai C. (1992) Equilibria and Reaction Mechanism of the Complexation of Methylboronic Acid with Polyols. *Inorganic Chemistry* **31**, 3243-3247.
- Purich D. L. and Allison R. D. (2002) *The enzyme reference - a comprehensive guidebook to enzyme nomenclature, reactions and methods*. Academic Press.
- Roden J. S., Lin G., and Ehleringer J. R. (2000) A mechanistic model for interpretation of hydrogen and oxygen isotope ratios in tree-ring cellulose. *Geochimica and Cosmochimica Acta* **64**, 21-35.
- Rozanski K., Araguas-Araguas L., and Gonfiantini R. (1993) Isotopic patterns in modern global precipitation. In *Climate Change in Continental Isotopic Records* (ed. P.K. Swart et al.), pp. 1-37. Geophysical Monograph 78, American Geophysical Union.

-
- Rozanski K., Klisch M., Wachniew P., Gorczyca Z., Goslar T., Edwards T. W. D., and Shemesh A. (2010) Oxygen-isotope geothermometers in lacustrine sediments: New insights through combined $\delta^{18}\text{O}$ analyses of aquatic cellulose, authigenic calcite and biogenic silica in Lake Gołcisz, central Poland. *Geochimica et Cosmochimica Acta* **74**, 2957-2969.
- Saurer M. and Siegwolf R. (2004) Pyrolysis Techniques for Oxygen Isotope Analysis of Cellulose. In *Handbook of Stable Isotope Analytical Techniques*, Vol. Volume 1 (ed. P. A. de Groot). Elsevier B.V.
- Schmidt H.-L., Werner R., and Roßmann A. (2001) ^{18}O Pattern and biosynthesis in natural plant products. *Phytochemistry* **58**, 9-32.
- Schmidt H. L., Kexel H., Butzenlechner M., Schwarz S., Gleixner G., Thimet S., Werner R., and Gensler M. (1995) Non-statistical isotope distributions in natural compounds: mirror of their biosynthesis and key for their origin assignment. In *Stable isotopes in the Biosphere* (ed. E. Wada, T. Yoneyama, M. Minagawa, T. Ando, and B. D. Fry), pp. 17-35. Kyoto University Press.
- Spötl C., Mangini A., and Richards D. (2006) Chronology and paleoenvironment of Marine Isotope Stage 3 from two high-elevation speleothems, Austrian Alps. *Quaternary Science Reviews* **25**(9-10), 1127-1136.
- Sternberg L., DeNiro M. J., and Savidge R. A. (1986) Oxygen isotope exchange between metabolites and water during biochemical reactions leading to cellulose synthesis. *Plant Physiology* **82**, 423-427.
- Sternberg L. and Ellsworth P. (2011) Divergent biochemical fractionation, not convergent temperature, explains cellulose oxygen isotope enrichment across latitudes. *Plos ONE* **6**(11), e28040. doi:10.1371/journal.pone.0028040.
- Sternberg L., Pinzon M., Anderson W. T., and Jahren A. (2006) Variation in oxygen isotope fractionation during cellulose synthesis: intramolecular and biosynthetic effects. *Plant, Cell and Environment* **29**, 1881-1889.
- Sugimoto A., Yanagisawa N., Naito D., Fujita N., and Maximov T. C. (2002) Importance of permafrost as a source of water for plants in east Siberian taiga. *Ecological Research* **17**, 493-503.
- Tuthorn M., Zech M., Ruppenthal M., Oelmann Y., Kahmen A., Wilke W., and Glaser B. (this issue) Oxygen isotope ratios ($^{18}\text{O}/^{16}\text{O}$) of hemicellulose-derived sugar biomarkers in plants, soils and sediments as paleoclimate proxy II: Insight from a climate transect study. *Geochimica et Cosmochimica Acta* **this issue**.

- Waterhouse J. S., Cheng S., Juchelka D., Loader N., McCarroll D., Switsur V., and Gautam L. (2013) Position-specific measurement of oxygen isotope ratios in cellulose: Isotopic exchange during heterotrophic cellulose synthesis. *Geochimica et Cosmochimica Acta* **112**, 178-191.
- Werner R. A. and Brand W. A. (2001) Referencing strategies and techniques in stable isotope ratio analysis. *Rapid Communications in Mass Spectrometry* **15**, 501-519.
- Werner R. A., Kornexl B. E., Roßmann A., and Schmidt H.-L. (1996) On-line determination of $\delta^{18}\text{O}$ values of organic substances. *Analytica Chimica Acta* **319**, 159-164.
- Wershaw R. L., Friedman I., and Heller S. (1966) Hydrogen isotope fractionation of water passing through trees. In *Advances in Organic Geochemistry* (ed. F. Hobson and M. Speers), pp. 55-67. Pergamon.
- Wissel H., Mayr C., and Lücke A. (2008) A new approach for the isolation of cellulose from aquatic plant tissue and freshwater sediments for stable isotope analysis. *Organic Geochemistry* **39**, 1545-1561.
- Wolfe B. B., Falcone M., Clogg-Wright K., Mongeon C., Yi Y., Brock B., Amour N., Mark W., and Edwards T. W. D. (2007) Progress in isotope paleohydrology using lake sediment cellulose. *Journal of Paleolimnology* **37**, 221-231.
- Zech M. and Glaser B. (2009) Compound-specific $\delta^{18}\text{O}$ analyses of neutral sugars in soils using GC-Py-IRMS: problems, possible solutions and a first application. *Rapid Communications in Mass Spectrometry* **23**, 3522-3532.
- Zech M., Tuthorn M., Detsch F., Rozanski K., Zech R., Zöllner L., Zech W., and Glaser B. (submitted) A 220 ka terrestrial $\delta^{18}\text{O}$ and deuterium excess biomarker record from an eolian permafrost paleosol sequence, NE-Siberia. *Chemical Geology* **submitted**.
- Zech M., Tuthorn M., Glaser B., Amelung W., Huwe B., Zech W., Zöllner L., and Löffler J. (2013) Natural abundance of ^{18}O of sugar biomarkers in topsoils along a climate transect over the Central Scandinavian Mountains, Norway. *Journal of Plant Nutrition and Soil Science* **176**, 12-15.
- Zech M., Tuthorn M., Zech R., Schlütz F., Zech W., and Glaser B. (accepted) A 16 ka lacustrine $\delta^{18}\text{O}$ sugar biomarker record from the High Himalaya reflecting the Indian Monsoon variability. *Journal of Paleolimnology* **accepted**.
- Zech M., Werner R., Juchelka D., Kalbitz K., Buggle B., and Glaser B. (2012) Absence of oxygen isotope fractionation/exchange of (hemi-) cellulose derived sugars during litter decomposition. *Organic Geochemistry* **42**, 1470-1475.

Zech M., Zech R., Bugge B., and Zöller L. (2011) Novel methodological approaches in loess research - interrogating biomarkers and compound-specific stable isotopes. *Eiszeitalter und Gegenwart - Quaternary Science Journal* **60**(1), 170-187.

Study 3

Oxygen isotope ratios ($^{18}\text{O}/^{16}\text{O}$) of hemicellulose-derived sugar biomarkers in plants, soils and sediments as paleoclimate proxy II: Insight from a climate transect study

Mario Tuthorn^{1,*}, Michael Zech^{1,2}, Marc Ruppenthal³, Yvonne Oelmann³, Ansgar Kahmen⁴, Héctor Francisco del Valle⁵, Wolfgang Wilcke⁶, Bruno Glaser²

¹⁾ Department of Soil Physics and Chair of Geomorphology, University of Bayreuth, Universitätsstr. 30, D-95440 Bayreuth, Germany

²⁾ Institute of Agronomy and Nutritional Sciences, Soil Biogeochemistry, Martin-Luther University Halle-Wittenberg, von-Seckendorff-Platz 3, D-06120 Halle, Germany

³⁾ Geoecology University of Tübingen, Rümelinstr. 19-23, D-72070 Tübingen, Germany

⁴⁾ Department of Environmental Sciences –Botany, University of Basel, Schönbeinstrasse 6, CH-4056 Basel, Switzerland

⁵⁾ Ecología Terrestre, Centro Nacional Patagónico (CENPAT), Consejo Nacional de Investigaciones Científicas y Técnicas (CONICET), Boulevard Brown 2825, U9120ACF Puerto Madryn, Argentina

⁶⁾ Soil Science Group, Geographic Institute, University of Bern, Hallerstrasse 12, 3012 Bern, Switzerland

^{*}) corresponding author: mariothrn@windowslive.com

Geochimica et Cosmochimica Acta

(2014) 126, 624-634

Abstract

The oxygen isotopic composition of precipitation ($\delta^{18}\text{O}_{\text{prec}}$) is well known to be a valuable (paleo-)climate proxy. Paleosols and sediments and hemicelluloses therein have the potential to serve as archives recording the isotopic composition of paleoprecipitation. In a companion paper (Zech et al., this issue) we investigated $\delta^{18}\text{O}_{\text{hemicellulose}}$ values of plants grown under different climatic conditions in a climate chamber experiment. Here we present results of compound-specific $\delta^{18}\text{O}$ analyses of arabinose, fucose, and xylose extracted from modern topsoils (n=56) along a large humid-arid climate transect in Argentina in order to answer the question whether hemicellulose biomarkers in soils reflect $\delta^{18}\text{O}_{\text{prec}}$.

The results from the field replications indicate that the homogeneity of topsoils with regard to $\delta^{18}\text{O}_{\text{hemicellulose}}$ is very high for most of the 20 sampling sites. Standard deviations for the field replications are 1.5 ‰, 2.2 ‰ and 1.7 ‰, for arabinose, fucose, and xylose, respectively. Furthermore, all three hemicellulose biomarkers reveal systematic and similar trends along the climate gradient. However, the $\delta^{18}\text{O}_{\text{hemicellulose}}$ values (mean of the three sugars) do not correlate positively with $\delta^{18}\text{O}_{\text{prec}}$ ($r=-0.54$, $p<0.014$, $n=20$). By using a Pécelet-modified Craig-Gordon (PMCG) model it can be shown that the $\delta^{18}\text{O}_{\text{hemicellulose}}$ values correlate highly significantly with modeled $\delta^{18}\text{O}_{\text{leaf water}}$ values ($r=0.81$, $p<0.001$, $n=20$). This finding suggests that hemicellulose biomarkers in (paleo-)soils do not simply reflect $\delta^{18}\text{O}_{\text{prec}}$ but rather $\delta^{18}\text{O}_{\text{prec}}$ altered by evaporative ^{18}O enrichment of leaf water due to evapotranspiration. According to the modeling results, evaporative ^{18}O enrichment of leaf water is relatively low (~10 ‰) in the humid northern part of the Argentinian transect and much higher (up to 19 ‰) in the arid middle and southern part of the transect. Model sensitivity tests corroborate that changes in relative air humidity exert a dominant control on evaporative ^{18}O enrichment of leaf water and thus $\delta^{18}\text{O}_{\text{hemicellulose}}$, whereas the effect of temperature changes is of minor importance. While oxygen exchange and degradation effects

seem to be negligible, further factors needing consideration when interpreting $\delta^{18}\text{O}_{\text{hemicellulose}}$ values obtained from (paleo-)soils are evaporative ^{18}O enrichment of soil water, seasonality effects, wind effects, and in case of abundant stem/root-derived organic matter input a partial loss of the evaporative ^{18}O enrichment of leaf water.

Overall, our results prove that compound-specific $\delta^{18}\text{O}$ analyses of hemicellulose biomarkers in soils and sediments are a promising tool for paleoclimate research. However, disentangling the two major factors influencing $\delta^{18}\text{O}_{\text{hemicellulose}}$, namely $\delta^{18}\text{O}_{\text{prec}}$ and relative air humidity controlled evaporative ^{18}O enrichment of leaf water, is challenging based on $\delta^{18}\text{O}$ analyses alone.

Keywords: stable oxygen isotopes, hemicellulose biomarkers, sugars, evaporative enrichment, plant physiology, paleoclimate

1. Introduction

Stable oxygen isotope ($^{18}\text{O}/^{16}\text{O}$) analysis has become one of the most important tools in hydrology and paleoclimate research. This is based on the observation that the isotopic composition of precipitation ($\delta^{18}\text{O}_{\text{prec}}$ and $\delta^2\text{H}_{\text{prec}}$) is mainly controlled by climatic factors (Araguas-Araguas et al., 2000; Dansgaard, 1964). Various kinds of archives are studied in order to reconstruct the isotopic composition of precipitation and thus to reconstruct paleoclimate; for instance speleothems (Cruz et al., 2005; McDermott et al., 2011), ice-cores (Dansgaard et al., 1993; Thompson et al., 2005), lake sediments (Sauer et al., 2001; Wissel et al., 2008) and plant cellulose (Danis et al., 2006; Li et al., 2011; Loader et al., 2008). Recently, Zech and Glaser (2009) and Zech et al. (2013) developed and applied a method based on gas chromatography-pyrolysis-isotope ratio mass spectrometry (GC-Py-IRMS), which allows compound-specific $\delta^{18}\text{O}$ analyses of plant-derived hemicellulose sugar biomarkers extracted from soils and sediments. Given that Zech et al. (2012) report absence of isotope fractionation during decomposition as well as absence of oxygen exchange reactions affecting the $\delta^{18}\text{O}$ signature of sugar molecules based on experimental findings and on theoretical biochemical mechanistic considerations, this method has potential to be applied to soil/sedimentary climate archives for paleoclimate research.

Oxygen atoms of plant-biosynthesized sugars originate from water (Schmidt et al., 2001). Therefore, like cellulose, hemicelluloses can be expected to reflect the isotopic composition of precipitation (Burk and Stuiver, 1981; Gray and Thompson, 1976; Gray and Thompson, 1977; Libby et al., 1976). However, it is well acknowledged that $\delta^{18}\text{O}_{\text{cellulose}}$ is additionally strongly influenced by evaporative ^{18}O enrichment of leaf water due to transpiration (Barbour et al., 2004; Dongmann et al., 1974; Flanagan et al., 1991; Pendall et al., 2005; Roden et al., 2000). The degree of evaporative ^{18}O enrichment of leaf water

depends on plant physiological and climatic conditions, such as relative air humidity, temperature and transpiration rate. In a companion paper (Zech et al., this issue) we report the results of an experimental study based on climate chamber experiments that investigate the effect of the above mentioned plant physiological and climate conditions on $\delta^{18}\text{O}_{\text{hemicellulose}}$.

In the study presented here, we take advantage of an Argentinian climate transect in order to answer the question “do hemicellulose biomarkers in soils reflect the $^{18}\text{O}/^{16}\text{O}$ isotopic composition of precipitation?”. Furthermore, we use a Péclet-modified Craig-Gordon (PMCG) model to model the isotopic composition of leaf water ($\delta^{18}\text{O}_{\text{leaf water}}$) and leaf cellulose ($\delta^{18}\text{O}_{\text{leaf cellulose}}$) and to test if additional environmental variables influence $\delta^{18}\text{O}$ values of hemicellulose biomarkers. By combining empirical data analyses with the mechanistic model simulations we aim to detect and evaluate the dominant climate variables influencing $\delta^{18}\text{O}_{\text{hemicellulose}}$ along the investigated transect and to draw implications for paleoclimate studies applying the $\delta^{18}\text{O}_{\text{hemicellulose}}$ method.

2. Material and methods

2.1 Study area and topsoil samples

The investigated Argentinian transect comprises 20 sampling localities (Fig. 1 and Table 1). It ranges from $\sim 32^\circ$ to 47° southern latitude and covers a large climate gradient with warm humid subtropical conditions in the north (Zárate, Buenos Aires Province), pronounced arid conditions in the middle part of the transect and cool temperate conditions in the south (Bajo Caracoles, Santa Cruz Province). Mean annual temperature and mean annual precipitation at the sampling sites range from 11.4°C to 18.0°C and from 185 mm year^{-1} to 1100 mm year^{-1} , respectively (Fig. 2B) (GeoINTA, 2012).

Table 1: Geographical description of the 20 sampling localities, mean (n=3) total organic carbon (TOC) contents of the investigated topsoil samples and soil type classification.

Sampling locality	Latitude	Longitude	Altitude (m)	TOC (%)	Soil type*
1	32°46'19"S	58°38'11"W	26	1.7	Vertisol
2	34°03'39"S	59°09'30"W	22	1.8	Phaeozem
3	35°18'10"S	58°53'02"W	29	1.8	Planosol
4	36°08'50"S	59°16'04"W	42	2.2	Phaeozem
5	36°52'43"S	59°50'23"W	154	3.9	Chernozem
6	37°20'55"S	60°58'42"W	198	2.1	Kastanozem
7	38°08'57"S	61°29'45"W	314	2.7	Kastanozem
8	38°09'34"S	62°17'15"W	257	1.0	Chernozem
9	38°57'51"S	63°51'12"W	100	1.3	Kastanozem
10	40°10'19"S	64°31'05"W	102	0.9	Solonetz
11	40°48'47"S	65°28'14"W	165	0.6	Solonetz
12	41°38'44"S	65°37'51"W	348	1.0	Leptosol
13	42°44'45"S	65°39'43"W	119	0.9	Calcisol
14	43°40'46"S	65°43'21"W	250	0.6	Calcisol
15	44°44'29"S	66°39'56"W	453	1.0	Solonetz
16	45°31'33"S	67°37'28"W	625	1.1	Solonetz
17	46°23'19"S	68°53'41"W	632	1.4	Luvisol
18	46°55'10"S	69°41'43"W	501	0.8	Luvisol
19	46°59'15"S	70°41'29"W	736	1.5	Vertisol
20	47°24'35"S	70°11'57"W	962	2.2	Planosol

* WRB Classification.

Figure 1A depicts that according to the interpolated $\delta^{18}\text{O}$ estimates retrieved from Bowen (2012), $\delta^{18}\text{O}_{\text{prec}}$ along the investigated transect is characterized by a systematic trend towards more negative values in the south.

The large range of different climatic conditions is reflected in the vegetation zones of the study area (Fig. 1B). The northernmost sampling sites are located in the Humid Pampa (grasslands featuring a humid-subhumid climate with incipient water excess). Further south, the Dry Pampa under subhumid-arid climate forms the transition to the Espinal vegetation zone that prevails under semi-arid climate (Burgos and Vidal, 1951). The Low Monte vegetation zone prevails in the most arid region of Argentina (total annual precipitation of 100 – 350 mm) (Fernández and Busso, 1997) and the Patagonian Steppe in the southernmost part of the transect under cool-temperate, arid climate (Le Houérou, 1996; Paruelo et al., 1998).

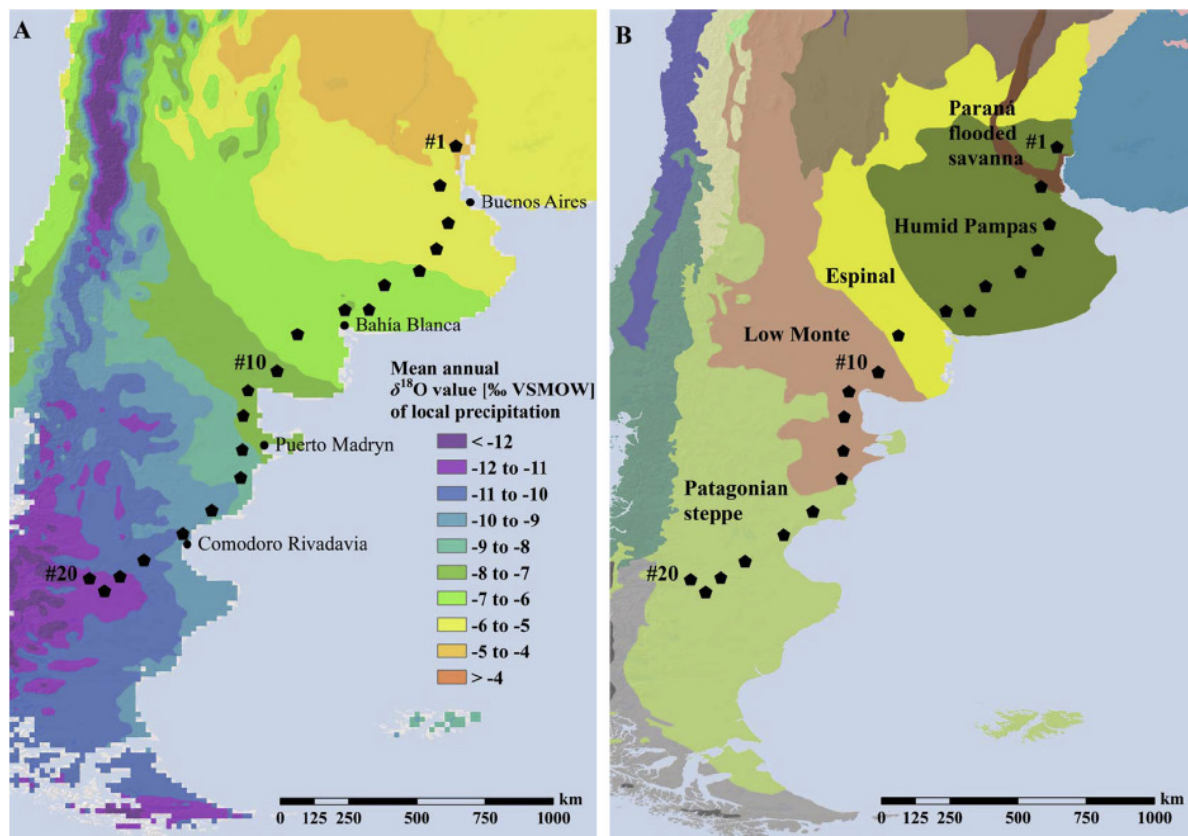


Fig. 1: A) Sampling localities along the investigated Argentinian climate transect and interpolated $\delta^{18}\text{O}$ estimates of annual precipitation (from Bowen, 2012). B) Vegetational zonation in the study area (from Olson et al., 2001).

During a field campaign in March and April 2010, a total of 56 mixed topsoil (A horizon) samples from maximum 51 cm depth were taken from the 20 sampling localities. Sampling in triplicates (duplicates for locations No. 1 and 18 – 20) at a distance of ~100 m was conducted in order to investigate possible topsoil heterogeneities at each sampling locality. The soil samples were air-dried in the field and later dried in an oven at 50 °C.

2.2 Compound-specific $\delta^{18}\text{O}$ analyses of the hemicellulose sugar biomarkers

Extraction and purification of the hemicellulose sugars from grinded soil samples was performed according to the method described by Amelung et al. (1996) and Zech and Glaser (2009). Accordingly, 4M trifluoroacetic acid (TFA) was used at 105 °C for 4 h in order to

liberate the monosaccharides from hemicelluloses and other non-cellulose polysaccharides. The extracted monosaccharides were filtered through glass fibre filters and purified using XAD columns to remove dissolved humic substances and Dowex cation exchange columns to remove cations like iron and also amino sugars. After freeze drying, the samples were dissolved in pyridine and derivatised with methylboronic acid (MBA) (Knapp, 1979). The originally included second derivatization step with bis(trimethylsilyl)trifluoroacetamide (BSTFA), which is necessary for derivatising the remaining hydroxyl groups of hexoses, was skipped because no reproducible derivatization results were found in previous studies (Zech and Glaser, 2009). For the investigated pentoses arabinose and xylose, as well as for the deoxyhexose fucose, the MBA derivatization ensures that no foreign oxygen is additionally introduced and that each sugar yields only one peak in the chromatograms. Rhamnose was present in too low concentrations in most samples and could therefore not be evaluated.

The compound-specific $\delta^{18}\text{O}$ measurements were performed on a GC-Py-IRMS system for which a Trace GC 2000 gas chromatograph (Thermo Fisher Scientific, Bremen, Germany) was coupled to a Delta plus isotope ratio mass spectrometer (Thermo Fisher Scientific) via a pyrolysis reactor and a GC/TC III interface (Thermo Fisher Scientific). Oxygen from the analytes was converted ‘online’ into carbon monoxide (CO) in the pyrolysis reactor (Thermo Fisher Scientific) which was preconditioned with iso-octane in order to ensure C surplus in the reactor and full conversion of oxygen in CO. $\delta^{18}\text{O}$ measurements were carried out on CO by monitoring the ion currents at m/z 28, 29 and 30. For further details on the principle of compound-specific $\delta^{18}\text{O}$ analyses, the reader is referred to Zech et al. (2011). The Argentinian sample batches were measured at least in quadruplicate replication with batches of external sugars standard concentration series being measured in-between. This procedure ensures compliance with the principle of “Identical Treatment” (PIT) of samples and standards (Werner and Brand, 2001) and allows checking and correcting if necessary for

an amount dependence of the $\delta^{18}\text{O}$ measurements. The hydrolytically introduced oxygen atoms in C1 position of the sugars are mathematically corrected as described in Zech and Glaser (2009).

All $\delta^{18}\text{O}$ results presented in the following are expressed in the δ notation as per mil (‰) deviation from the internationally accepted standard according to the equation (Eqn. 1):

$$\delta = (R_{\text{sample}} - R_{\text{standard}})/R_{\text{standard}} \quad (\text{Eqn. 1}),$$

where R_{sample} and R_{standard} are the isotope ratio ($^{18}\text{O}/^{16}\text{O}$) in the sample and the Vienna Standard Mean Ocean water (V-SMOW), respectively. Mean standard errors for all $\delta^{18}\text{O}$ measurements (56 samples done in quadruplicate to fivefold replication) of arabinose, fucose and xylose were 0.57 ‰, 0.71 ‰ and 0.41 ‰, respectively. Rhamnose was excluded from data evaluation because the respective peaks in the chromatograms were either too low to be evaluated reliably or not detected at all.

2.3 Péclet-modified Craig-Gordon model simulations

As mentioned above, leaf water is typically enriched in ^{18}O compared to the source water of plants due to evapotranspiration. This process is primarily driven by the water vapor pressure of the atmosphere (e_a), air temperature (T_{air}), the isotopic composition of atmospheric water vapor ($\delta^{18}\text{O}_{\text{prec}}$) (Kahmen et al., 2011) and in addition by different plant physiological variables (e.g. leaf temperature and transpiration) (Barbour, 2007; Farquhar et al., 2007). The ^{18}O enrichment of leaf water through evapotranspiration can be predicted by using a mechanistic model originally developed for fractionation processes of water surfaces by Craig and Gordon (1965) and adapted for plants by Dongmann et al. (1974) and subsequently Farquhar and Lloyd (1993).

The model allows estimating $\delta^{18}\text{O}_{\text{leaf water}}$ according to Eqn. 2

$$\delta^{18}\text{O}_{\text{leaf water}} = \Delta^{18}\text{O}_{\text{leaf water}} + \delta^{18}\text{O}_{\text{SW}} \quad (\text{Eqn. 2}),$$

where $\Delta^{18}\text{O}_{\text{leaf water}}$ is the bulk leaf water evaporative enrichment and $\delta^{18}\text{O}_{\text{SW}}$ is the oxygen isotope composition source or xylem water. $\Delta^{18}\text{O}_{\text{leaf water}}$ can be calculated as follows:

$$\Delta^{18}\text{O}_{\text{leafwater}} = \frac{\Delta^{18}\text{O}_e (1 - e^{-\wp})}{\wp} \quad (\text{Eqn. 3}).$$

$\Delta^{18}\text{O}_e$ is the evaporative enrichment of leaf water above the plant's source water in ^{18}O at the sites of evaporation and is calculated as follows:

$$\Delta^{18}\text{O}_e = \varepsilon^+ + \varepsilon_k + (\Delta^{18}\text{O}_{\text{wv}} - \varepsilon_k) \frac{e_a}{e_i} \quad (\text{Eqn. 4}),$$

where ε^+ is the equilibrium fractionation between liquid water and vapor at the air-water interface (Bottinga and Craig, 1969), ε_k is the kinetic fractionation, $\Delta^{18}\text{O}_{\text{wv}}$ is the isotope composition of water vapor and e_a/e_i is the ratio of ambient to intercellular vapor pressures (Craig and Gordon, 1965). The Péclet effect accounts for flux of source water entering the leaf through the transpiration flow opposed by backward diffusion of isotopically enriched water (Farquhar and Lloyd, 1993). The Péclet number was determined as follows:

$$\wp = EL/CD \quad (\text{Eqn. 5}),$$

where E is the transpiration rate, L is effective path length, C is the molar concentration of water and D is the diffusivity of H_2^{18}O . Transpiration rate was calculated using relative

humidity, air temperature and atmospheric pressure at each sampling site and mean stomatal conductance of 0,15 mol/m²/s. For L we used an average value of 20 mm that we kept constant across the transect. A L-value of 20 mm reflects an average value based on reports for a large number of species in the literature (Kahmen et al., 2008; Kahmen et al., 2009; Song et al., 2013).

Under field conditions, e_a , T_{air} and $\delta^{18}O_{prec}$ are primary climatic drivers of the model with additional influences of secondary variables (O-isotope composition of source water, O-isotope composition of water vapor, leaf temperature, rates of stomatal conductance to water vapor loss and transpiration) (Craig and Gordon, 1965; Cuntz et al., 2007; Dongmann et al., 1974; Farquhar and Cernusak, 2005; Kahmen et al., 2011; Kahmen et al., 2008). Functional relationships between primary and secondary variables were analyzed and optimized by Kahmen et al. (2011), which reduces the necessary model input data to the primary variables. An isotopic equilibrium between precipitation and water vapor was assumed in order to calculate $\delta^{18}O_{wv}$ (included in Eqn. 4) and subsequently leaf water evapotranspirative enrichment. For our simulations, the primary drivers (e_a , T_{air} and $\delta^{18}O_{prec}$) for the 20 sites were obtained from Bowen (2012) or GeoINTA (2012).

3. Results and discussion

3.1 Compound-specific $\delta^{18}O$ values of the hemicellulose biomarkers

The $\delta^{18}O$ values obtained for arabinose, fucose and xylose range from 35.3 – 43.6 ‰, 34.1 – 42.3 ‰ and 33.7 – 40.8 ‰, respectively, and reveal systematic trends over the investigated transect (Table 2 and Fig. 2A).

Table 2: Compound-specific $\delta^{18}\text{O}$ results for the hemicellulose biomarkers arabinose, fucose and xylose. Standard deviations are given for the field replications. $\delta^{18}\text{O}$ values of annual precipitation were retrieved from The Online Isotopes in Precipitation Calculator (Bowen, 2012).

Sampling locality	$\delta^{18}\text{O}$ Arabinose (‰ V-SMOW)	Standard deviation Arabinose	$\delta^{18}\text{O}$ Fucose (‰ V-SMOW)	Standard deviation Fucose	$\delta^{18}\text{O}$ Xylose (‰ V-SMOW)	Standard deviation Xylose	$\delta^{18}\text{O}$ Precipitation (‰ V-SMOW)	Coincidence intervals (95%) precipitation
1	36.2	1.5	39.4	4.5	34.7	1.0	-5	0.3
2	35.3	0.6	34.4	1.7	33.7	1.1	-5.1	0.3
3	36.6	0.6	35.7	1.1	34.2	2.4	-5.4	0.3
4	37.1	0.4	34.1	2.2	34.2	0.3	-5.7	0.2
5	36.4	0.4	34.7	1.3	34.1	0.3	-6.1	0.2
6	37.4	0.8	35.5	1.7	35.9	0.9	-6.3	0.2
7	37.7	1.6	36.5	0.7	36.0	2.5	-6.8	0.2
8	39.1	1.6	37.3	2.0	37.8	1.3	-6.7	0.2
9	41.8	2.3	38.0	0.7	40.8	3.9	-6.7	0.2
10	41.3	1.1	39.1	0.3	38.8	1.2	-7.2	0.3
11	41.8	0.6	39.7	1.6	40.0	1.0	-7.6	0.3
12	42.0	0.6	39.3	1.6	39.6	1.1	-8.2	0.4
13	43.6	1.3	41.2	0.6	40.5	0.4	-8.1	0.4
14	40.5	1.9	38.2	1.3	37.8	0.9	-8.7	0.4
15	40.8	1.9	38.9	2.8	38.1	2.5	-9.6	0.6
16	39.0	1.1	37.5	1.5	36.2	1.5	-10.3	0.8
17	38.3	1.7	37.5	2.5	36.1	1.8	-10.8	1.2
18	40.7	0.6	42.3	6.4	38.8	1.1	-10.7	1.2
19	42.3	5.7	42.2	4.9	40.7	6.2	-11.3	1.2
20	39.5	3.5	40.9	4.2	37.7	3.2	-11.7	1.2

The northern sampling sites are characterized by the lowest $\delta^{18}\text{O}_{\text{hemicellulose}}$ values whereas $\delta^{18}\text{O}_{\text{hemicellulose}}$ maxima characterize the middle and southernmost part of the transect. Standard deviations for the field replications are 1.5 ‰, 2.2 ‰ and 1.7 ‰, for arabinose, fucose and xylose, respectively. This finding suggests that the overall homogeneity of topsoils with regard to $\delta^{18}\text{O}_{\text{hemicellulose}}$ is high. As an exception, the mean standard deviation for fucose at the sampling site 18 and the mean standard errors for all three hemicelluloses at the sampling sites 19 and 20 are higher with up to 6.4 ‰, indicating lower homogeneity of the topsoil replications.

The $\delta^{18}\text{O}$ values (in the following we refer to the means of the field replications) of all three hemicellulose sugar biomarkers are highly significantly correlated with each other, especially arabinose and xylose ($r=0.96$, $p<0.001$, $n=20$). Slightly but systematically more positive $\delta^{18}\text{O}$ values of arabinose (Table 2 and Fig. 2A) compared to xylose were also

reported in our companion paper (Zech et al., this issue) but not by Zech and Glaser (2009) and Zech et al. (2013; 2012). Both pentoses (arabinose and xylose) are biosynthesized in plants by the decarboxylation of the C6 carbon atoms from glucose (Altermatt and Neish, 1956; Burget et al., 2003; Harper and Bar-Peled, 2002). Given that arabinose is an epimerase product of xylose, more positive $\delta^{18}\text{O}$ values of arabinose could reflect a biosynthetic fractionation.

3.2 Comparison of $\delta^{18}\text{O}_{\text{hemicellulose}}$ results with $\delta^{18}\text{O}_{\text{prec}}$

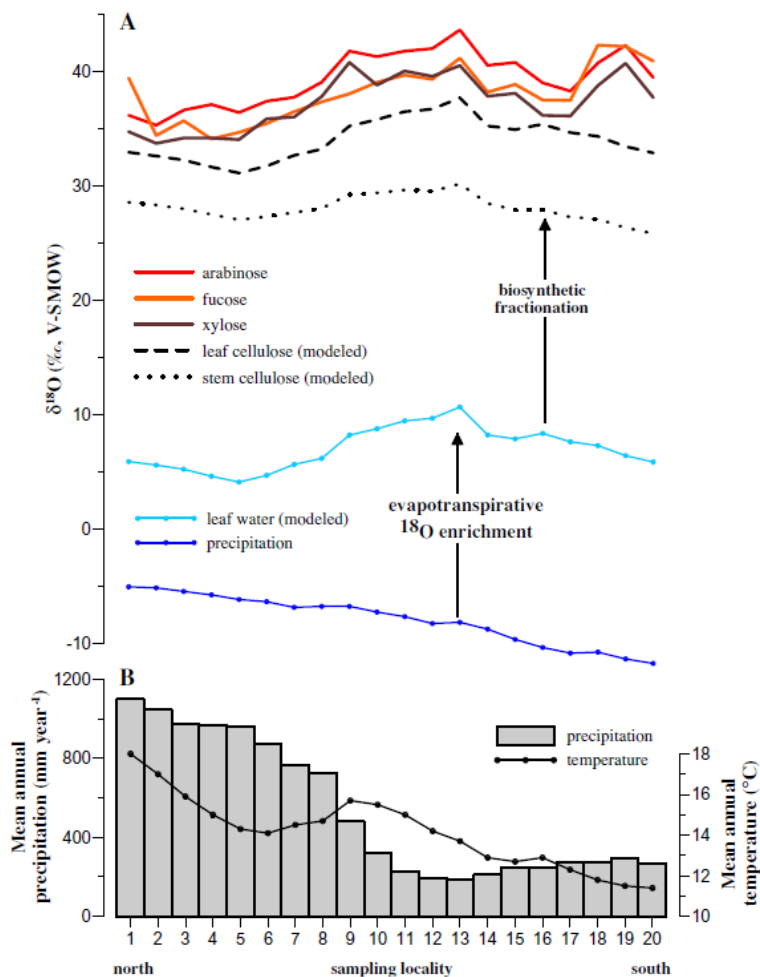


Fig. 2: A) Comparison of measured $\delta^{18}\text{O}_{\text{hemicellulose}}$ values of arabinose, fucose, and xylose extracted from topsoils along the Argentinian climate transect with modeled $\delta^{18}\text{O}_{\text{prec}}$, $\delta^{18}\text{O}_{\text{leaf water}}$, $\delta^{18}\text{O}_{\text{stem cellulose}}$, and $\delta^{18}\text{O}_{\text{leaf cellulose}}$. B) Mean annual precipitation and temperature characterizing the investigated sampling sites.

The $\delta^{18}\text{O}$ values of annual precipitation retrieved from The Online Isotopes in Precipitation Calculator (Bowen, 2012), calculated from a global data set according to an algorithm published by Bowen and Revenaugh (2003), reveal a systematic trend ranging from -5 ‰ in the north to -11.7 ‰ in the south (Table 2 and Fig. 2A). This trend most likely reflects the “temperature effect” on $\delta^{18}\text{O}_{\text{prec}}$ (Dansgaard, 1964). Since oxygen in hemicelluloses, like in cellulose, originates from plant water (e.g. Schmidt et al., 2001) and thus ultimately from precipitation, $\delta^{18}\text{O}_{\text{prec}}$ values represent without doubt an important variable influencing $\delta^{18}\text{O}_{\text{hemicellulose}}$ values. One might thus expect hemicellulose biomarkers in soils to reflect $\delta^{18}\text{O}_{\text{prec}}$. However, in our study the weighted mean $\delta^{18}\text{O}$ values of arabinose, fucose and xylose are negatively correlated with $\delta^{18}\text{O}_{\text{prec}}$ ($r=-0.54$, $p<0.014$, $n=20$) and do not reflect $\delta^{18}\text{O}_{\text{prec}}$ along the transect.

3.3 Relative air humidity as important controlling factor on $\delta^{18}\text{O}_{\text{leaf water}}$ and $\delta^{18}\text{O}_{\text{hemicellulose}}$ along the investigated Argentinian transect

The above finding highlights that in addition to $\delta^{18}\text{O}_{\text{prec}}$ another variable exerts an important control on $\delta^{18}\text{O}_{\text{hemicellulose}}$. Indeed, amongst plant physiologists it is well known that evapotranspiration results in an ^{18}O enrichment of leaf water and that this signal is incorporated in newly assimilated sugars and in leaf- and stem cellulose (Barbour, 2007; Farquhar et al., 2007; Flanagan et al., 1991; Kahmen et al., 2011; Roden et al., 2000). As well, our experimental investigations presented in the companion paper (Zech et al., this issue) report that $\delta^{18}\text{O}_{\text{hemicellulose}}$ reflect slightly dampened the climatically controlled evapotranspirative ^{18}O enrichment of leaf water. Several climatic and plant physiological variables such as relative air humidity, temperature and transpiration rate influence the degree of evaporative ^{18}O enrichment of leaf water.

In order to evaluate the effect of air temperature and relative air humidity on $\delta^{18}\text{O}_{\text{hemicellulose}}$, a Péclet-Modified Craig-Gordon Model was used to model $\delta^{18}\text{O}_{\text{leaf water}}$ along the investigated Argentinian transect and to conduct sensitivity tests. Modeled results for $\delta^{18}\text{O}_{\text{leaf water}}$ with e_a , T_{air} and $\delta^{18}\text{O}_{\text{prec}}$ values from GeoINTA (2012) and Bowen (2012) are shown in Fig. 2A. Accordingly, the general $\delta^{18}\text{O}_{\text{prec}}$ trend towards more negative values from north to south is not reflected in modeled $\delta^{18}\text{O}_{\text{leaf water}}$. Rather, the modeled $\delta^{18}\text{O}_{\text{leaf water}}$ values correlate highly significantly with the measured $\delta^{18}\text{O}_{\text{hemicellulose}}$ values ($r=0.81$, $p<0.001$, $n=20$), corroborating that our hemicellulose biomarker results reflect $\delta^{18}\text{O}_{\text{leaf water}}$, i.e. $\delta^{18}\text{O}_{\text{prec}}$ altered by evaporative ^{18}O enrichment during transpiration rather than $\delta^{18}\text{O}_{\text{prec}}$ alone.

Leaf water $\delta^{18}\text{O}$ is driven in model simulations by three primary variables; temperature, relative humidity and $\delta^{18}\text{O}_{\text{prec}}$. To test if leaf water is more sensitive to relative humidity or temperature, we performed a sensitivity analysis with the model where mean annual humidity and mean annual T_{air} were varied by 10 and 20 % and by 2.5 and 5.0 °C (Fig. 3). These model sensitivity tests demonstrate that reasonable changes in relative humidity strongly influence $\delta^{18}\text{O}_{\text{leaf water}}$ resulting in shifts of 12.8 – 14.0 ‰ depending on the sampling site, whereas changes in T_{air} have only a marginal effect in the range of 0.5 – 1.2 ‰ on $\delta^{18}\text{O}_{\text{leaf water}}$. The same was observed in a previous study for alpha cellulose (Kahmen et al., 2011) and in our chamber experiments presented in the companion paper for hemicelluloses (Zech et al., this issue). Given the large relative air humidity gradient prevailing along the investigated Argentinian transect (ranging from 48.0 to 73.2 ‰), this finding helps to explain why $\delta^{18}\text{O}_{\text{hemicellulose}}$ values do not reflect $\delta^{18}\text{O}_{\text{prec}}$ values. Evaporative ^{18}O enrichment of leaf water is relatively low (~10 ‰) in the humid northern part of the transect and high (up to ~19 ‰) in the arid middle and southern part of the transect (Fig. 2A).

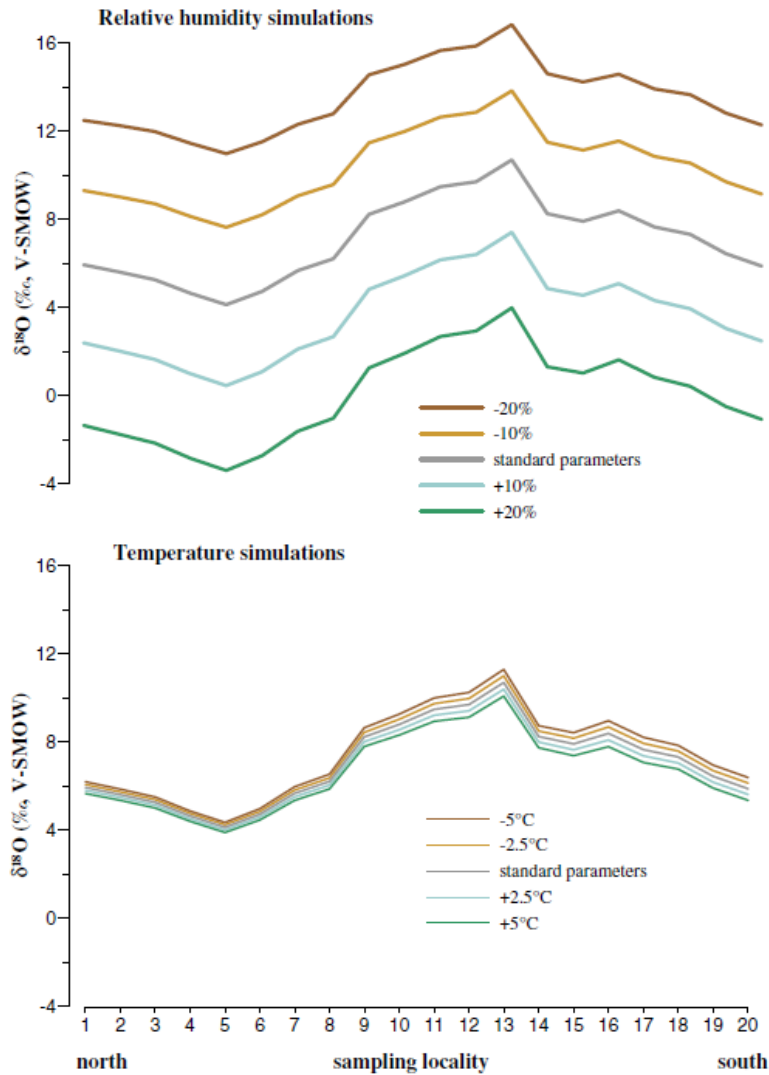


Fig. 3: Model sensitivity tests based on a Péclet-modified Craig-Gordon model (Kahmen et al., 2011) showing the dependency of $\delta^{18}\text{O}_{\text{leaf water}}$ on relative air humidity and temperature changes.

3.4 Comparison between measured $\delta^{18}\text{O}_{\text{hemicellulose}}$ and modeled $\delta^{18}\text{O}_{\text{cellulose}}$ values

Based on the notion that $\delta^{18}\text{O}$ values of primary assimilates (glucose and ultimately sucrose) are approximately 27 ‰ more enriched compared to leaf water (Sternberg et al., 1986; Yakir and DeNiro, 1990), the PMCG model also allows calculating values for $\delta^{18}\text{O}_{\text{leaf cellulose}}$ and $\delta^{18}\text{O}_{\text{stem cellulose}}$ by accounting for 40 % of exchangeable oxygen atoms during cellulose formation with leaf water (for leaf cellulose) and xylem water (for stem cellulose)

(Roden et al., 2000). Calculated values represent the maximum possible difference between leaf and stem cellulose. The modelling results range from 31.14 ‰ to 37.70 ‰ and 25.85 ‰ to 30.18 ‰ for $\delta^{18}\text{O}_{\text{leaf cellulose}}$ and $\delta^{18}\text{O}_{\text{stem cellulose}}$, respectively, and show weaker ^{18}O enrichment than the measured $\delta^{18}\text{O}_{\text{hemicellulose}}$ values (Fig. 2A). We acknowledge that the measured $\delta^{18}\text{O}_{\text{hemicellulose}}$ values reflect a mixture of leaf and stem/root organic matter. Stem/root (hemi)celluloses are depleted in ^{18}O compared to leaf (hemi)celluloses because approximately 40 % of the O atoms during stem cellulose synthesis are exchanging with not enriched stem water (Sternberg et al., 1986). Hence, it can be expected that varying input of leaf vs. stem/root (hemi)celluloses results in varying $\delta^{18}\text{O}$ (hemi)cellulose values in soils. In fact, modeled stem cellulose is depleted in ^{18}O by approximately 7 ‰ compared to modeled leaf cellulose (Fig. 2A). While it is difficult to address the question leaf- versus stem-derived qualitatively at the current state of research, based on the model simulations we would consider that leaf input in soil organic matter along here investigated transect is greater compared to stem/root input.

The observed systematic offset between modeled cellulose and measured hemicellulose values might be attributed to inaccurate model input variables. Neither relative air humidity, nor temperature nor the isotopic composition of atmospheric water vapor ($\delta^{18}\text{O}_{\text{prec}}$) are actually measured values but interpolated values from GeoINTA (2012) and from Bowen (2012). For the interpolated $\delta^{18}\text{O}_{\text{prec}}$ values used in the PMCG model, Bowen and Revenaugh (2003) show a confidence intervals (95 %) ranging from 0.2 to 1.2 ‰. Furthermore, evaporative ^{18}O enrichment of soil water is not considered in the model results and can potentially cause a considerable positive offset of the actual $\delta^{18}\text{O}_{\text{hemicellulose}}$ values.

The companion experimental study by Zech et al. (this issue) has also reported more positive $\delta^{18}\text{O}_{\text{hemicellulose}}$ compared to $\delta^{18}\text{O}_{\text{cellulose}}$ values. This feature can possibly be attributed to position-specific $\delta^{18}\text{O}$ differences of oxygen atoms in glucose molecules forming (hemi-)

cellulose. Sternberg et al. (2006) reported that the fractionation factor for the oxygen atoms in C2 position is 19.6 ‰, while for the oxygen atoms associated with the carbon atoms C3-C6 it is on average 28.8 ‰. Since pentoses are biosynthesized by the decarboxylation of the C6 carbon atoms from glucose (Altermatt and Neish, 1956; Burget et al., 2003; Harper and Bar-Peled, 2002), more positive $\delta^{18}\text{O}_{\text{hemicellulose}}$ values would indicate that the oxygen atoms in C6 position of glucose building up cellulose are isotopically depleted compared to the average of the oxygen atoms in position C2 – C5. This is in agreement with recent study by Waterhouse et al. (2013) indicating that oxygen atoms at C6 position undergo around 80 ‰ exchange with medium water during heterotrophic cellulose synthesis.

Finally, two additional factors may help explaining the increased offset between measured $\delta^{18}\text{O}_{\text{hemicellulose}}$ and modeled $\delta^{18}\text{O}_{\text{cellulose}}$ values characterizing the three southernmost sampling sites (18-20). First, while modeling is carried out with mean annual climate values, the growing season (when biosynthesis of hemicelluloses actually occurs) for these sites does not coincide with the months when precipitation falls, i.e. during the winter months (Jobbágy et al., 2002). Taking this seasonality effect into account, the PMCG model yields by 1-2 ‰ more positive $\delta^{18}\text{O}_{\text{cellulose}}$ values. Second, Patagonia is characterized by dry westerly winds (foehn) (Beltrán, 1997), which presumably additionally contribute to higher evaporative ^{18}O enrichment of leaf water.

4. Conclusions and implications for paleoclimate studies

Investigating the compound-specific $\delta^{18}\text{O}$ values of hemicellulose sugar biomarkers of modern topsoils along a climate transect in Argentina allows drawing conclusions, which have implications for the interpretation of $\delta^{18}\text{O}$ values of hemicellulose sugars derived from paleosols for the reconstruction of climate history.

- Although oxygen in hemicelluloses derives from water and thus ultimately from precipitation, the hemicellulose biomarkers arabinose, fucose and xylose do not simply reflect $\delta^{18}\text{O}_{\text{prec}}$ but rather $\delta^{18}\text{O}_{\text{leaf water}}$. The correlation between measured $\delta^{18}\text{O}_{\text{hemicellulose}}$ and modeled $\delta^{18}\text{O}_{\text{leaf water}}$ is highly significant ($r=0.81$, $p<0.001$, $n=20$).
- This finding can be attributed to the evaporative ^{18}O enrichment of leaf water during transpiration. Model sensitivity tests using a Péclet-modified Craig-Gordon (PMCG) model corroborate that relative air humidity is a very rigorous climate parameter influencing $\delta^{18}\text{O}_{\text{leaf water}}$, whereas temperature is of minor importance.
- While oxygen exchange and degradation effects on $\delta^{18}\text{O}$ values of hemicelluloses sugar biomarkers seem to be negligible (Zech et al., 2012), further effects that need to be considered when interpreting $\delta^{18}\text{O}_{\text{hemicellulose}}$ values obtained from (paleo-)soils are evaporative ^{18}O enrichment of soil water, seasonality effects, wind effects and in case of abundant stem/root-derived organic matter input a partial loss of the evaporative ^{18}O enrichment of leaf water.
- Overall, our Argentinian climate transect study is in agreement with an experimental study conducted on plant material from a climate chamber experiment presented in the companion paper (Zech et al., this issue). Our results corroborate the conceptual model proposed by Zech et al. (this issue) for interpreting $\delta^{18}\text{O}_{\text{hemicellulose}}$ results in paleoclimate studies (Fig. 4).

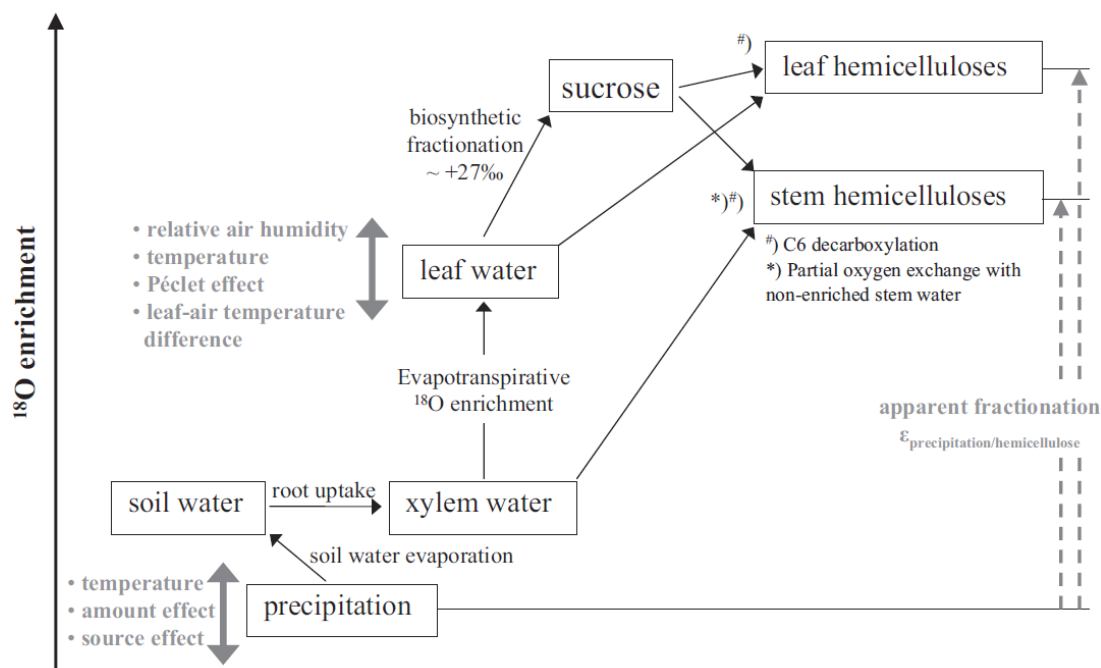


Fig. 4: Conceptual diagram illustrating the major factors influencing the oxygen isotopic composition of hemicellulose sugar biomarkers (from Zech et al., this issue).

Acknowledgements

We would like to thank Prof. B. Huwe and Prof. L. Zöller for logistic support. We thank S. Bösel for assistance during GC-Py-IRMS measurements at the Isotope Laboratory of Halle and A. Mergner and H. Fasold for support during laboratory work. Our study also greatly profited from constructive discussions with M. Dippold, M. Dubbert and Dr. R. Zech. We furthermore thank AE Prof. R. Pancost and two anonymous reviewers for constructive comments and suggestions on the manuscript. This study was partly financed by the SIBAE COST Action ES0806 and the German Research Foundation (DFG Oe516/2-1 and ZE 844/1-2).

References

- Altermatt H. A. and Neish A. C. (1956) The biosynthesis of cell wall carbohydrates: III. further studies on formation of cellulose and xylan from labeled monosaccharides in wheat plants. *Canadian Journal of Biochemistry and Physiology* **34**(3), 405-413.
- Amelung W., Cheshire M. V., and Guggenberger G. (1996) Determination of neutral and acidic sugars in soil by capillary gas-liquid chromatography after trifluoroacetic acid hydrolysis. *Soil Biology and Biochemistry* **28**, 1631-1639.
- Araguas-Araguas L., Froehlich K., and Rozanski K. (2000) Deuterium and oxygen-18 isotope composition of precipitation and atmospheric moisture. *Hydrological Processes* **14**(8), 1341-1355.
- Barbour M. M. (2007) Stable oxygen isotope composition of plant tissue: a review. *Functional Plant Biology* **34**(2), 83-94.
- Barbour M. M., Roden J. S., Farquhar G. D., and Ehleringer J. R. (2004) Expressing leaf water and cellulose oxygen isotope ratios as enrichment above source water reveals evidence of a Péclet effect. *Oecologia* **138**(3), 426-435.
- Beltrán A. (1997) Caracterización microclimática del Distrito Occidental de la estepa patagónica. Magister Thesis, Universidad de Buenos Aires.
- Bottinga Y. and Craig H. (1969) Oxygen isotope fractionation between CO₂ and water and isotopic composition of marine atmospheric CO₂. *Earth and Planetary Science Letters* **5**, 285-295.
- Bowen G. J. (2012) The Online Isotopes in Precipitation Calculator, version 2.2. <http://www.waterisotopes.org>.
- Bowen G. J. and Revenaugh J. (2003) Interpolating the isotopic composition of modern meteoric precipitation. *Water Resources Research* **39**(10), 1299.
- Burget E., Verma R., Mølhøj M., and Reiter W. (2003) The biosynthesis of L-arabinose in plants: molecular cloning and characterization of a golgi-localized UDP-D-xylose 4-epimerase encoded by the MUR4 gene of arabidopsis. *The Plant Cell* **15**, 523-531.
- Burgos J. J. and Vidal A. L. (1951) Los climas de la República Argentina, según la nueva clasificación de Thornthwaite. *Meteoros* **1**, 1-32.
- Burk R. L. and Stuiver M. (1981) Oxygen isotope ratios in trees reflect mean annual temperature and humidity. *Science* **211**(4489), 1417-1419.

- Craig H. and Gordon L. I. (1965) Deuterium and oxygen-18 variations in the ocean and the marine atmosphere. *Conference on Stable Isotopes in Oceanographic Studies and Paleotemperatures*, 9-130.
- Cruz F. W., Burns S. J., Karmann I., Sharp W. D., Vuille M., Cardoso A. O., Ferrari J. A., Silva Dias P. L., and Viana O. (2005) Insolation-driven changes in atmospheric circulation over the past 116,000 years in subtropical Brazil. *Nature* **434**(7029), 63-66.
- Cuntz M., Ogée J., Farquhar G. D., Peylin P., and Cernusak L. A. (2007) Modelling advection and diffusion of water isotopologues in leaves. *Plant, Cell & Environment* **30**(8), 892-909.
- Danis P. A., Masson-Delmotte V., Stievenard M., Guillemin M. T., Daux V., Naveau P., and von Grafenstein U. (2006) Reconstruction of past precipitation $\delta^{18}\text{O}$ using tree-ring cellulose $\delta^{18}\text{O}$ and $\delta^{13}\text{C}$: A calibration study near Lac d'Annecy, France. *Earth and Planetary Science Letters* **243**(3-4), 439-448.
- Dansgaard W. (1964) Stable isotopes in precipitation. *Tellus* **16**(4), 436-468.
- Dansgaard W., Johnsen S. J., Clausen H. B., Dahl-Jensen D., Gundestrup N. S., Hammer C. U., Hvidberg C. S., Steffensen J. P., Sveinbjörnsdóttir A. E., Jouzel J., and Bond G. (1993) Evidence for general instability of past climate from a 250-kyr ice-core record. *Nature* **364**, 218-220.
- Dongmann G., Nürnberg H. W., Förstel H., and Wagener K. (1974) On the enrichment of H_2^{18}O in the leaves of transpiring plants. In *Radiation and Environmental Biophysics*, Vol. 11, pp. 41-52. Springer Berlin / Heidelberg.
- Farquhar G. D. and Cernusak L. A. (2005) On the isotopic composition of leaf water in the non-steady state. *Functional Plant Biology* **32**(4), 293-303.
- Farquhar G. D., Cernusak L. A., and Barnes B. (2007) Heavy water fractionation during transpiration. *Plant Physiology* **143**(1), 11-18.
- Farquhar G. D. and Lloyd J. (1993) Carbon and oxygen isotope effects in the exchange of carbon dioxide between terrestrial plants and the atmosphere. In *Stable isotopes and plant carbon-water relations* (ed. J. R. Ehleringer, A. E. Hall, and G. D. Farquhar), pp. 47-70. Academic Press, Inc.
- Fernández O. A. and Busso C. A. (1997) Arid and semi-arid rangelands: two thirds of Argentina, pp. 41-60. RALA Report 200.
- Flanagan L. B., Comstock J. P., and Ehleringer J. R. (1991) Comparison of modeled and observed environmental influences on the stable oxygen and hydrogen isotope composition of leaf water in *Phaseolus vulgaris* L. *Plant Physiology* **96**(2), 588-596.

- GeoINTA. (2012) Instituto Nacional de Tecnologia Agropecuaria Visualizador Integrado. Available online at: <http://geointa.inta.gov.ar/visor/> . Accessed 01.08.2012.
- Gray J. and Thompson P. (1976) Climatic information from $^{18}\text{O}/^{16}\text{O}$ ratios of cellulose in tree rings. *Nature* **262**(5568), 481-482.
- Gray J. and Thompson P. (1977) Climatic information from $^{18}\text{O}/^{16}\text{O}$ analysis of cellulose, lignin and whole wood from tree rings. *Nature* **270**(5639), 708-709.
- Harper A. and Bar-Peled M. (2002) Biosynthesis of UDP-xylose. Cloning and characterization of a novel Arabidopsis gene family, UXS, encoding soluble and putative membrane-bound UDP-glucuronic acid decarboxylase isoforms. *Plant Physiology* **130**(4), 2188-2198.
- Jobbágy E. G., Sala O. E., and Paruelo J. M. (2002) Patterns and controls of primary production in the Patagonian steppe: a remote sensing approach. *Ecology* **83**(2), 307-319.
- Kahmen A., Sachse D., Arndt S. K., Tu K. P., Farrington H., Vitousek P. M., and Dawson T. E. (2011) Cellulose $\delta^{18}\text{O}$ is an index of leaf-to-air vapor pressure difference (VPD) in tropical plants. *Proceedings of the National Academy of Sciences* **108**(5), 1981-1986.
- Kahmen A., Simonin K., Tu K., Goldsmith G. R., and Dawson T. E. (2009) The influence of species and growing conditions on the ^{18}O enrichment of leaf water and its impact on "effective path length". *New Phytologist* **184**, 619-630.
- Kahmen A., Simonin K., Tu K. P., Merchant A., Callister A., Siegwolf R., Dawson T. E., and Arndt S. K. (2008) Effects of environmental parameters, leaf physiological properties and leaf water relations on leaf water $\delta^{18}\text{O}$ enrichment in different Eucalyptus species. *Plant, Cell & Environment* **31**(6), 738-751.
- Knapp D. R. (1979) *Handbook of Analytical Derivatization reactions*. John Wiley & Sons, Inc.
- Le Houérou H. N. (1996) Climate change, drought and desertification. *Journal of Arid Environments* **34**, 133-185.
- Li Q., Nakatsuka T., Kawamura K., Liu Y., and Song H. (2011) Regional hydroclimate and precipitation $\delta^{18}\text{O}$ revealed in tree-ring cellulose $\delta^{18}\text{O}$ from different tree species in semi-arid Northern China. *Chemical Geology* **282**, 19-28.
- Libby L. M., Pandolfi L. J., Payton P. H., Marshall J., Becker B., and Giertz-Sienbenlist V. (1976) Isotopic tree thermometers. *Nature* **261**(5558), 284-288.
- Loader N. J., Santillo P. M., Woodman-Ralph J. P., Rolfe J. E., Hall M. A., Gagen M., Robertson I., Wilson R., Froyd C. A., and McCarroll D. (2008) Multiple stable isotopes

- from oak trees in southwestern Scotland and the potential for stable isotope dendroclimatology in maritime climatic regions. *Chemical Geology* **252**, 62-71.
- McDermott F., Atkinson T. C., Fairchild I. J., Baldini L. M., and Matthey D. P. (2011) A first evaluation of the spatial gradients in $\delta^{18}\text{O}$ recorded by European Holocene speleothems. *Global and Planetary Change* **79**(3-4), 275-287.
- Olson D. M., Dinerstein E., Wikramanayake E. D., Burgess N. D., Powell G. V. N., Underwood E. C., D'amico J. A., Itoua I., Strand H. E., Morrison J. C., Loucks C. J., Allnutt T. F., Ricketts T. H., Kura Y., Lamoreux J. F., Wettengel W. W., Hedao P., and Kassem K. R. (2001) Terrestrial ecoregions of the world: a new map of life on earth. *BioScience* **51**(11), 933-938.
- Paruelo J. M., Beltrán A., Jobbágy E., Sala O. E., and Golluscio R. A. (1998) The climate of Patagonia: general patterns and controls on biotic processes. *Ecologia Austral* **8**, 85-101.
- Pendall E., Williams D., and Leavitt S. (2005) Comparison of measured and modeled variations in pinon pine leaf water isotopic enrichment across a summer moisture gradient. *Oecologia* **145**(4), 605-618.
- Roden J. S., Lin G., and Ehleringer J. R. (2000) A mechanistic model for interpretation of hydrogen and oxygen isotope ratios in tree-ring cellulose. *Geochimica et Cosmochimica Acta* **64**(1), 21-35.
- Sauer P. E., Miller G. H., and Overpeck J. T. (2001) Oxygen isotope ratios of organic matter in arctic lakes as a paleoclimate proxy: field and laboratory investigations. In *Journal of Paleolimnology*, Vol. 25, pp. 43-64. Springer Netherlands.
- Schmidt H.-L., Werner R. A., and Rossmann A. (2001) ^{18}O pattern and biosynthesis of natural plant products. *Phytochemistry* **58**(1), 9-32.
- Song X., Barbour M. M., Farquhar G. D., Vann D. R., and Helliker B. R. (2013) Transpiration rate relates to within- and across-species variations in effective path length in a leaf water model of oxygen isotope enrichment. *Plant, Cell and Environment* **36**, 1338-1351.
- Sternberg L., DeNiro M. J., and Savidge R. A. (1986) Oxygen isotope exchange between metabolites and water during biochemical reactions leading to cellulose synthesis. *Plant Physiology* **82**, 423-427.
- Sternberg L., Pinzon M., Anderson W. T., and Jahren A. (2006) Variation in oxygen isotope fractionation during cellulose synthesis: intramolecular and biosynthetic effects. *Plant, Cell & Environment* **29**, 1881-1889.

-
- Thompson L. G., Davis M. E., Mosley-Thompson E., Lin P.-N., Henderson K. A., and Mashiotta T. A. (2005) Tropical ice core records: evidence for asynchronous glaciation on Milankovitch timescales. *Journal of Quaternary Science* **20**(7-8), 723-733.
- Waterhouse J. S., Cheng S., Juchelka D., Loader N., McCarroll D., Swistur V., and Gautam L. (2013) Position-specific measurement of oxygen isotope ratios in cellulose: Isotopic exchange during heterotrophic cellulose synthesis. *Geochimica et Cosmochimica Acta* **112**, 178-191.
- Werner R. A. and Brand W. A. (2001) Referencing strategies and techniques in stable isotope ratio analysis. *Rapid Communications in Mass Spectrometry* **15**, 501-519.
- Wissel H., Mayr C., and Lücke A. (2008) A new approach for the isolation of cellulose from aquatic plant tissue and freshwater sediments for stable isotope analysis. *Organic Geochemistry* **39**(11), 1545-1561.
- Yakir D. and DeNiro M. J. (1990) Oxygen and hydrogen isotope fractionation during cellulose metabolism in *Lemna gibba* L. *Plant Physiology* **93**(1), 325-332.
- Zech M. and Glaser B. (2009) Compound-specific $\delta^{18}\text{O}$ analyses of neutral sugars in soils using gas chromatography-pyrolysis-isotope ratio mass spectrometry: problems, possible solutions and a first application. *Rapid Communications in Mass Spectrometry* **23**(22), 3522-3532.
- Zech M., Mayr C., Tuthorn M., Leiber-Sauheitl K., and Glaser B. (this issue) Oxygen isotope ratios ($^{18}\text{O}/^{16}\text{O}$) of hemicellulose derived sugar biomarkers in plants, soils and sediments as paleoclimate proxy I: Insight from a climate chamber experiment. *Geochimica et Cosmochimica Acta*, **this issue**.
- Zech M., Tuthorn M., Glaser B., Amelung W., Huwe B., W. Z., Zöller L., and Löffler J. (2013) Natural abundance of ^{18}O of sugar biomarkers in topsoils along a climate transect over the Central Scandinavian Mountains, Norway. *Journal of Plant Nutrition and Soil Science* **176**, 12-15.
- Zech M., Werner R. A., Juchelka D., Kalbitz K., Buggle B., and Glaser B. (2012) Absence of oxygen isotope fractionation/exchange of (hemi-) cellulose derived sugars during litter decomposition. *Organic Geochemistry* **42**, 1470-1475.
- Zech M., Zech R., Buggle B., and Zöller L. (2011) Novel methodological approaches in loess research - interrogating biomarkers and compound-specific stable isotopes. *Quaternary Science Journal* **60**(1), 170-187.

Study 4

Coupled isotopes of plant wax and hemicellulose markers record information on relative humidity and isotopic composition of precipitation

Mario Tuthorn^{1,*}, Roland Zech², Marc Ruppenthal³, Yvonne Oelmann³, Ansgar Kahmen⁴, Héctor Francisco del Valle⁵, Timothy Eglinton², Michael Zech^{1,6}

¹⁾ Department of Soil Physics and Chair of Geomorphology, University of Bayreuth, Universitätsstr. 30, D-95440 Bayreuth, Germany

²⁾ Geological Institute, ETH Zurich, Sonneggstrasse 5, CH-8092 Zurich, Switzerland

³⁾ Geoecology, University of Tübingen, Rümelinstr. 19-23, D-72070 Tübingen, Germany

⁴⁾ Departement of Environmental Sciences - Botany, University of Basel, Schönbeinstrasse 6, CH-4056 Basel, Switzerland

⁵⁾ Ecología Terrestre, Centro Nacional Patagónico (CENPAT), Consejo Nacional de Investigaciones Científicas y Técnicas (CONICET), Boulevard Brown 2825, U9120ACF Puerto Madryn, Argentina

⁶⁾ Institute of Agronomy and Nutritional Sciences, Soil Biogeochemistry, Martin-Luther University Halle-Wittenberg, von-Seckendorff-Platz 3, D-06120 Halle, Germany

*) corresponding author: mariothrn@windowslive.com

To be submitted to Biogeosciences Discussions

Abstract

The $\delta^2\text{H}$ isotopic composition of leaf waxes is used increasingly for paleohydrological and -climate reconstructions. However, it is challenging to disentangle past changes in the isotopic composition of precipitation and changes in evapotranspirative enrichment of leaf water. For this study, we analyzed $\delta^2\text{H}$ on *n*-alkanes and fatty acids in topsoils along a transect spanning a climate gradient in Argentina, for which we had previously measured $\delta^{18}\text{O}$ on plant-derived sugars. Our results indicate that leaf wax biomarker $\delta^2\text{H}$ values ($\delta^2\text{H}_{\text{lipids}}$) primarily reflect $\delta^2\text{H}_{\text{source water}}$ (precipitation), but are modulated by evapotranspirative enrichment. A mechanistic model is able to produce the main trends in $\delta^2\text{H}_{\text{lipids}}$ along the transect, but seems to slightly underestimate evapotranspirative enrichment in arid regions and overestimate it in grass-dominated ecosystems.

Assuming constant biosynthetic fractionation, and combining $\delta^2\text{H}$ of lipids and $\delta^{18}\text{O}$ of plant-derived sugar biomarkers, the isotopic composition of leaf water can be calculated. This also yields the deuterium excess (d-excess), which mainly reflects evapotranspirative enrichment, and can be converted to relative air humidity (RH). The high correlation with measured RH, as well as the good agreement between reconstructed and actual $\delta^2\text{H}$ and $\delta^{18}\text{O}$ of precipitation along the transect lends support for our approach and highlights the value of combined $\delta^2\text{H}$ and $\delta^{18}\text{O}$ measurement of lipid and sugar biomarkers for paleoclimate research. Future studies are needed to evaluate the biosynthetic fractionation factors, the degree of soil water enrichment, seasonality, and the role of grasslands.

Keywords: paleoclimate proxies, hemicellulose sugars, *n*-alkanes, leaf water enrichment, deuterium-excess, relative air humidity.

Highlights

- Leaf wax lipids reflect $\delta^2\text{H}$ of precipitation and evapotranspirative enrichment
- Combining $\delta^2\text{H}$ and $\delta^{18}\text{O}$ from lipids and sugars yields d-excess of leaf water
- d-Excess of leaf water is a promising novel proxy for relative air humidity
- $\delta^2\text{H}_{\text{prec}}$ and $\delta^{18}\text{O}_{\text{prec}}$ can also be reconstructed by combining both biomarker proxies

1. Introduction

Long chain *n*-alkanes and fatty acids are important components of the epicuticular leaf waxes of terrestrial plants (Eglinton, 1967). As leaf waxes can be preserved in sedimentary archives over a long time (Radke *et al.*, 2005; Samuels *et al.*, 2008), they can serve as valuable biomarkers for paleo-environmental and -climate reconstructions (Eglinton and Eglinton, 2008; Zech *et al.*, 2011). The $\delta^2\text{H}$ isotopic composition of leaf waxes is of particular interest in this regard, because, at least to a first order, it reflects the isotopic composition of precipitation (Sauer *et al.*, 2001; Sachse *et al.*, 2004; Rao *et al.*, 2009), which in turn depends on temperature, humidity, atmospheric circulation, etc. (Gat, 1996; Araguas-Araguas *et al.*, 2000). While there is probably no fractionation of hydrogen isotopes during water uptake by the roots (Ehleringer and Dawson, 1992), several studies have shown that leaf water is enriched in ^2H compared to the source water or precipitation (Flanagan *et al.*, 1991; Yakir, 1992; Sachse *et al.*, 2006; Smith & Freeman, 2006; Farquhar *et al.*, 2007; Feakins & Sessions, 2010). This ^2H enrichment, which is also recorded in the leaf waxes, can be explained by evapotranspiration and is mainly controlled by relative air humidity (RH), temperature and the isotopic composition of atmospheric water vapor. Potential variations in the degree of evapotranspirative enrichment in the past can make it challenging to reconstruct the isotopic composition of paleoprecipitation from $\delta^2\text{H}$ biomarker records alone.

Compound-specific $\delta^2\text{H}$ of lipid biomarkers, especially *n*-alkanes due to their good preservation, are already widely applied in paleoclimate and -hydrological research (Sauer *et al.*, 2001; Schefuss *et al.*, 2005; Pagani *et al.*, 2006; Tierney *et al.*, 2008; Zech *et al.*, 2013c). Comparison of $\delta^2\text{H}_{n\text{-alkanes}}$ with $\delta^2\text{H}_{\text{fatty acids}}$ in such research is hardly done so far but may provide additional merits of using fatty acids as an alternative to *n*-alkanes. Similarly, compound-specific $\delta^{18}\text{O}$ analyses of sugars remain in their infancy, yet hold significant

promise (Hener *et al.*, 1998; Juchelka *et al.*, 1998; Werner, 2003; Jung *et al.*, 2005; Jung *et al.*, 2007; Greule *et al.*, 2008; Zech & Glaser, 2009; Zech *et al.*, 2012). Similar to leaf waxes, hemicellulose-derived sugars record the isotopic composition of water used for metabolism, i.e. the isotopic composition of precipitation altered by evapotranspirative ^{18}O enrichment of soil and leaf water (Zech *et al.*, 2013b). Hemicellulose residues can persist in soils (Zech *et al.*, 2012), and combined plant wax $\delta^2\text{H}$ and hemicellulose sugar $\delta^{18}\text{O}$ measurements offer the potential of reconstructing the deuterium excess of leaf water. The d-excess quantifies the isotopic deviation of water from the Global Meteoric Water Line (GMWL) and may serve as valuable proxy for evapotranspirative enrichment and RH. Furthermore, if leaf water values are defined in a $\delta^2\text{H}$ - $\delta^{18}\text{O}$ diagram, by using a leaf water evaporation line (EL) sugar and *n*-alkane isotopic information may enable reconstruction of the isotopic composition of precipitation in paleohydrological studies (Zech *et al.*, 2013a).

This study describes the application of a combined $\delta^2\text{H}$ and $\delta^{18}\text{O}$ biomarker approach to modern topsoils sampled along a climate transect in Argentina. The aims of this investigation are to

- (i) compare the $\delta^2\text{H}$ values of *n*-alkanes with those of fatty acids, modeled *n*-alkane $\delta^2\text{H}$ values and $\delta^{18}\text{O}$ values of sugars and evaluate the dominant climate factors influencing these values,
- (ii) reconstruct d-excess using $\delta^2\text{H}$ values of *n*-alkanes and $\delta^{18}\text{O}$ values of sugars and assess the potential of reconstructed d-excess of leaf water as paleoclimate proxy for RH, and
- (iii) evaluate the potential of the combined $\delta^{18}\text{O}$ and $\delta^2\text{H}$ biomarker approach to reconstruct the isotopic composition of precipitation.

2. Material and methods

2.1 Transect description and samples

The investigated transect in Argentina spans from $\sim 32^\circ\text{S}$ to 47°S , and encompasses 20 sampling localities spanning a large climate and altitudinal (22 – 964 m) gradient (Fig. 1).

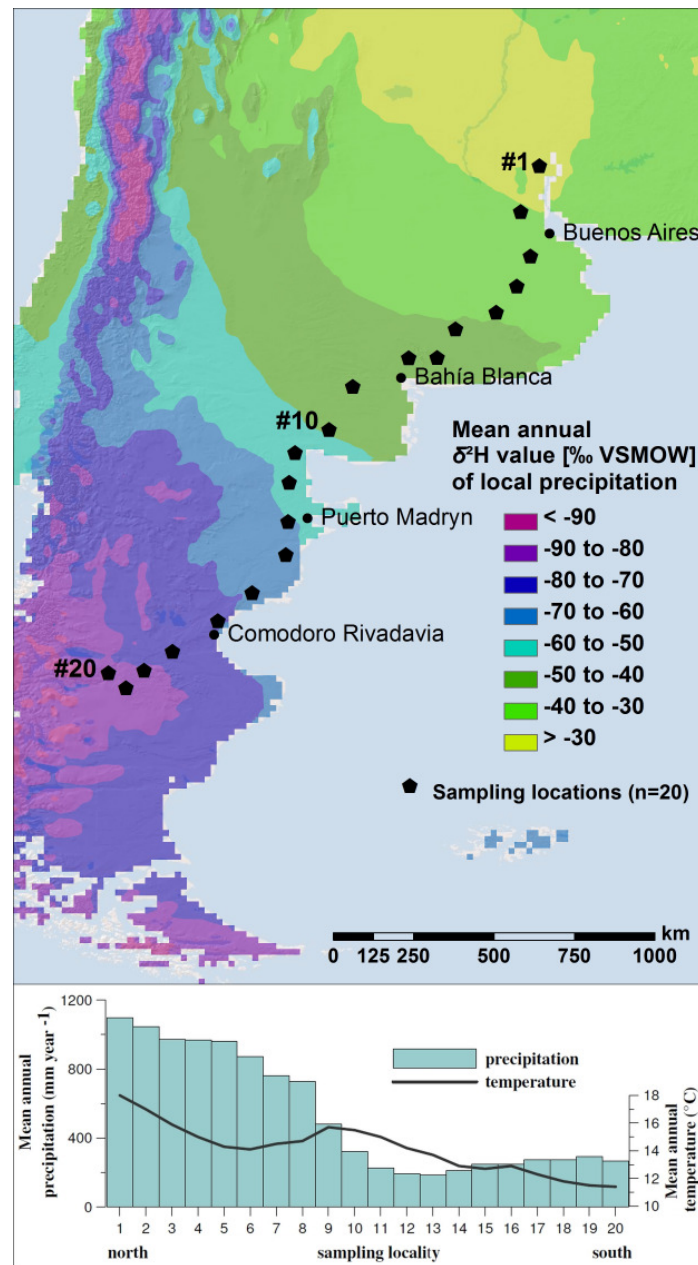


Fig. 1: Sampling localities along the investigated transect in Argentina. The colors illustrate the gradient in $\delta^2\text{H}_{\text{prec}}$, and mean annual temperature and precipitation are shown below.

Mean annual temperature ranges from 11.4 °C to 18.0 °C and mean annual precipitation from 185 mm to 1100 mm. Precipitation shows a systematic southward trend towards more negative $\delta^{18}\text{O}$ and $\delta^2\text{H}$ values ($\delta^{18}\text{O}_{\text{prec}}$ and $\delta^2\text{H}_{\text{prec}}$, respectively) (Bowen, 2012; GeoINTA, 2012). The transect is described in detail by Tuthorn *et al.* (2014). Briefly, it is characterized by warm humid subtropical conditions in the north (Zárate, Buenos Aires Province), pronounced arid conditions in the middle part of the transect and cool temperate conditions in the south (Las Heras, Santa Cruz Province). These markedly contrasting climate conditions are reflected in the vegetation zones of the study area, changing from Humid/Dry Pampa in the north to the Espinal vegetation zone that prevails under semi-arid climate (Burgos and Vidal, 1951), Low Monte semidesert/desert in the most arid region of Argentina (Fernández and Busso, 1997), and Patagonian Steppe in the southernmost part of the transect (Le Houérou, 1996; Paruelo *et al.*, 1998).

During a field campaign in March and April 2010, mixed topsoil samples (A_h -horizons) were collected from the 20 sample sites along the transect. The soil samples were air-dried in the field and later in an oven at 50°C.

2.2 Compound-specific $\delta^2\text{H}$ analyses of *n*-alkanes and fatty acids

For $\delta^2\text{H}$ analyses of *n*-alkane and fatty acid biomarkers, an Accelerated Solvent Extractor (Dionex ASE 200) was used to extract free lipids from the dried soil samples with dichloromethane (DCM) and methanol (MeOH; 9:1). The total lipid extracts were separated over pipette columns filled with ~2 g aminopropyl. *n*-Alkanes were eluted with hexane, more polar lipids with DCM:MeOH (1:1), and free fatty acids with diethyl ether:acetic acid (19:1). The *n*-alkanes were further purified using zeolite (Geokleen) pipette columns. The zeolite was dried and dissolved in HF after eluting branched- and cyclo-alkyl compounds with hexane, and the straight-chain (*n*-alkyl) compounds were then recovered by liquid-liquid extraction

with hexane. For samples 1 – 12, an additional purification step with silver nitrate columns was carried out in order to eliminate unsaturated compounds.

Fatty acids were methylated using 5% HCl in methanol at 80°C for 12 hours. Subsequently, liquid-liquid extraction with 5% NaCl and hexane was used to retrieve fatty acid methyl esters (FAMES). FAMES were purified by elution with dichloromethane over SiO₂ columns (~2 g).

5 α androstane and hexamethylbenzene was used for quantification of the compounds on an Agilent Technologies 7890A gas chromatograph (GC) equipped with a VF1 column (30 m, 0.25 mm i.d., 0.25 μ m film thickness) and a flame ionization detector (FID). Compound-specific $\delta^2\text{H}$ values of the long-chain *n*-alkanes and FAMES were determined based on at least triplicate analyses on a gas chromatograph-pyrolysis-isotope ratio mass spectrometer (GC-pyrolysis-IRMS, Delta V, ThermoFisher Scientific, Bremen, Germany). The A4 standard mixture (provided by Arndt Schimmelmann, Indiana University, USA) was run three times per sequence at three different concentrations. All results are reported after normalization using multi-linear regression (Paul *et al.*, 2007) and simple mass-balance correction of the FAMES for the isotopic composition of the methanol used for derivatisation. Long-term precision of the analyses was monitored using a laboratory standard (oak, *n*-C₂₉). The standard was analyzed in every sequence and yielded a mean value of -147.2 with a standard deviation of ± 1.7 ‰ across all sequences run for this study.

2.3 Modeling of leaf water ²H enrichment

The ²H enrichment of leaf water due to evapotranspiration can be predicted by using mechanistic models originally developed for isotope fractionation processes associated with evaporation from water surfaces by Craig and Gordon (1965). These models were adapted for plants by Dongmann *et al.* (1974) and subsequently Farquhar and Lloyd (1993). Evaporative

enrichment of the leaf water (Δ^2H_e) at the evaporative surface in the mesophyll is given by the equation:

$$\Delta^2H_e = \varepsilon^+ + \varepsilon_k + (\Delta^2H_{wv} - \varepsilon_k) \frac{e_a}{e_i}, \quad (\text{Eqn. 1})$$

where ε^+ is the equilibrium fractionation between liquid water and vapor at the air-water interfaces (Bottinga and Craig, 1969), ε_k is the kinetic fractionation during water vapor diffusion from leaf intercellular air space to the atmosphere, Δ^2H_{wv} is the isotopic difference of the water vapor and the source water, and e_a/e_i is the ratio of ambient to intercellular vapor pressure (Craig and Gordon, 1965). This basic calculation was modified by including a Péclet effect that accounts for opposing fluxes of source water entering the leaf through the transpiration flow and the back-diffusion of isotopically enriched water from the sites of evaporation (Farquhar and Lloyd, 1993):

$$\Delta^2H_{\text{leafwater}} = \frac{\Delta^2H_e (1 - e^{-\rho})}{EL/CD}. \quad (\text{Eqn. 2})$$

The quotient of EL/CD represents the Péclet number (ρ) where E is the transpiration rate, L is the effective path length, C is the molar concentration of water and D is the diffusivity of $^2\text{H}_2\text{O}$. The approach we used for our estimates of ^2H enrichment of leaf water followed that of Kahmen *et al.* (2011b), where the Péclet-modified Craig Gordon model is reduced to three input variables: air temperature, atmospheric vapour pressure and source water $\delta^2\text{H}$. This simplified model is based on the assumption that leaf temperature equals air temperature and that atmospheric vapor $\delta^2\text{H}$ is in equilibrium with source water $\delta^2\text{H}$ (Kahmen *et al.* 2011b). Transpiration rate is estimated using relative humidity and air temperature (retrieved from GeoINTA, 2012) and atmospheric pressure at each sampling site and assuming a mean stomatal conductance of $0.15 \text{ mol/m}^2/\text{s}$. Based on reports for a large number of species in the literature (Kahmen *et al.*, 2008; Kahmen *et al.*, 2009; Song *et al.*, 2013), we used an average value of 20 mm for L and kept it constant across the transect. For our

simulation of leaf water $\delta^2\text{H}$ values we obtained the model input variables air temperature, atmospheric vapor pressure and source water $\delta^2\text{H}$ from GeoINTA (2012) and Bowen (2012). The isotopic composition of the leaf water can be estimated according to Eqn. 3:

$$\delta^2\text{H}_{\text{leaf water}} = \Delta^2\text{H}_{\text{leaf water}} + \delta^2\text{H}_{\text{SW}} \quad (\text{Eqn.3}),$$

where $\Delta^2\text{H}_{\text{leaf water}}$ is the bulk leaf water evaporative enrichment and $\delta^2\text{H}_{\text{SW}}$ is the hydrogen isotope ratio of source/xylem water.

3. Results and Discussion

3.1 Comparison of $\delta^2\text{H}_{n\text{-alkanes}}$ and $\delta^2\text{H}_{\text{fatty acids}}$

The C_{29} and C_{31} *n*-alkane homologues were sufficiently abundant in all samples to be measured for their hydrogen isotopic composition. The $\delta^2\text{H}$ values range from -155 to -222 ‰ and reveal a similar trend between *n*- C_{29} and *n*- C_{31} along the investigated transect (Table 1 and Fig. 2). While the northern and middle part of the transect is characterized by relatively high $\delta^2\text{H}$ values (~ -160 ‰), the southern part of the transect is characterized by considerably more negative $\delta^2\text{H}$ values (~ -210 ‰).

The $\delta^2\text{H}$ values of the fatty acids *n*- C_{22} , *n*- C_{24} , *n*- C_{26} , *n*- C_{28} and *n*- C_{30} range from -128 to -225 ‰ (Table 1 and Fig. 2). Interestingly, the longer homologues *n*- C_{28} and *n*- C_{30} are systematically enriched by a few per mil compared to the *n*-alkanes. Reasons for this trend remain vague at this point, but may be relate to metabolic pathways, seasonal differences in homologue production, or differences in homologue sources. Roots, for example, have also been suggested as a source of long-chain *n*-fatty acids (Bull *et al.*, 2000). Shorter homologues, for have been suggested to be not only plant-derived, but also of bacterial origin (Matsumoto

et al., 2007; Bianchi and Canuel, 2011). Similarly, soil microbial overprinting of long chain *n*-alkanes and fatty acids cannot be excluded (Nguyen Tu *et al.*, 2011; Zech *et al.*, 2011).

Table 1: $\delta^2\text{H}$ values of individual leaf wax *n*-alkanes and fatty acids. Measurements were carried out in at least triplicate (sd = standard deviation).

sampling locality	$\delta^2\text{H}_{n\text{-alkanes}}$				$\delta^2\text{H}_{\text{fatty acids}}$									
	C ₂₉		C ₃₁		C ₂₂		C ₂₄		C ₂₆		C ₂₈		C ₃₀	
	mean (‰)	sd	mean (‰)	sd	mean (‰)	sd	mean (‰)	sd	mean (‰)	sd	mean (‰)	sd	mean (‰)	sd
1	-157	2	-164	2	-155	1	-157	1	-151	1	-153	1	-153	2
2	-166	0	-166	1	-150	0	-155	1	-165	1	-163	1	-161	3
3	-175	1	-179	1	-162	0	-161	1	-165	1	-159	1	-155	0
4	-176	1	-176	1	-162	2	-163	1	-166	1	-165	1	-158	2
5	-178	1	-180	2	-164	0	-165	1	-168	2	-162	1	-159	1
6	-171	2	-172	0	-166	0	-165	2	-169	1	-161	1	-158	1
7	-179	0	-182	0	-170	0	-172	1	-177	0	-169	1	-157	0
8	-162	1	-167	1	-161	1	-161	1	-166	1	-161	1	-158	2
9	-173	1	-168	1	-163	1	-164	0	-168	1	-169	0	-156	1
10	-173	2	-170	2	-159	1	-167	1	-168	0	-159	1	-137	2
11	-170	2	-156	2	-158	0	-169	0	-167	2	-153	4	-147	4
12	-155	1	-176	0	-158	1	-168	1	-172	1	-148	1	-133	1
13	-157	2	-161	1	-158	1	-153	0	-140	1	-135	1	-128	1
14	-158	1	-166	0	-168	1	-183	0	-181	2	-160	2	-147	1
15	-194	2	-193	1	-194	0	-197	0	-191	1	-176	2	-168	2
16	-203	1	-211	1	-204	1	-198	0	-201	0	-193	0	-189	1
17	-218	1	-217	1	-219	1	-220	1	-217	0	-205	1	-204	1
18	-213	1	-202	4	-211	0	-203	1	-204	0	-196	0	-194	0
19	-222	1	-222	1	-220	0	-210	0	-225	1	-212	1	-204	1
20	-220	1	-212	1	-225	0	-221	1	-211	1	-193	3	-195	2

There is a good overall agreement between the *n*-alkanes and the fatty acids ($R=0.96$, $p<0.001$, $n=20$; for the weighted means), both showing much more negative $\delta^2\text{H}$ values in the south than in the northern and middle portions of the transect (Table 1, Fig. 2). The consistent $\delta^2\text{H}$ pattern revealed by the *n*-alkanes along the north-south climate transect does not solely reflect the $\delta^2\text{H}$ isotopic composition of precipitation, with $\delta^2\text{H}$ of the fatty acids exhibiting similar behavior. Especially in the middle part of the transect, $\delta^2\text{H}$ of the lipid biomarkers shows a pronounced offset (Fig. 3). Given that *n*-alkanes are considered to primarily reflect leaf signals and are most widely applied in paleoclimate and paleohydrological studies, we will principally refer to $\delta^2\text{H}$ of long chain *n*-alkanes in further discussion and calculations.

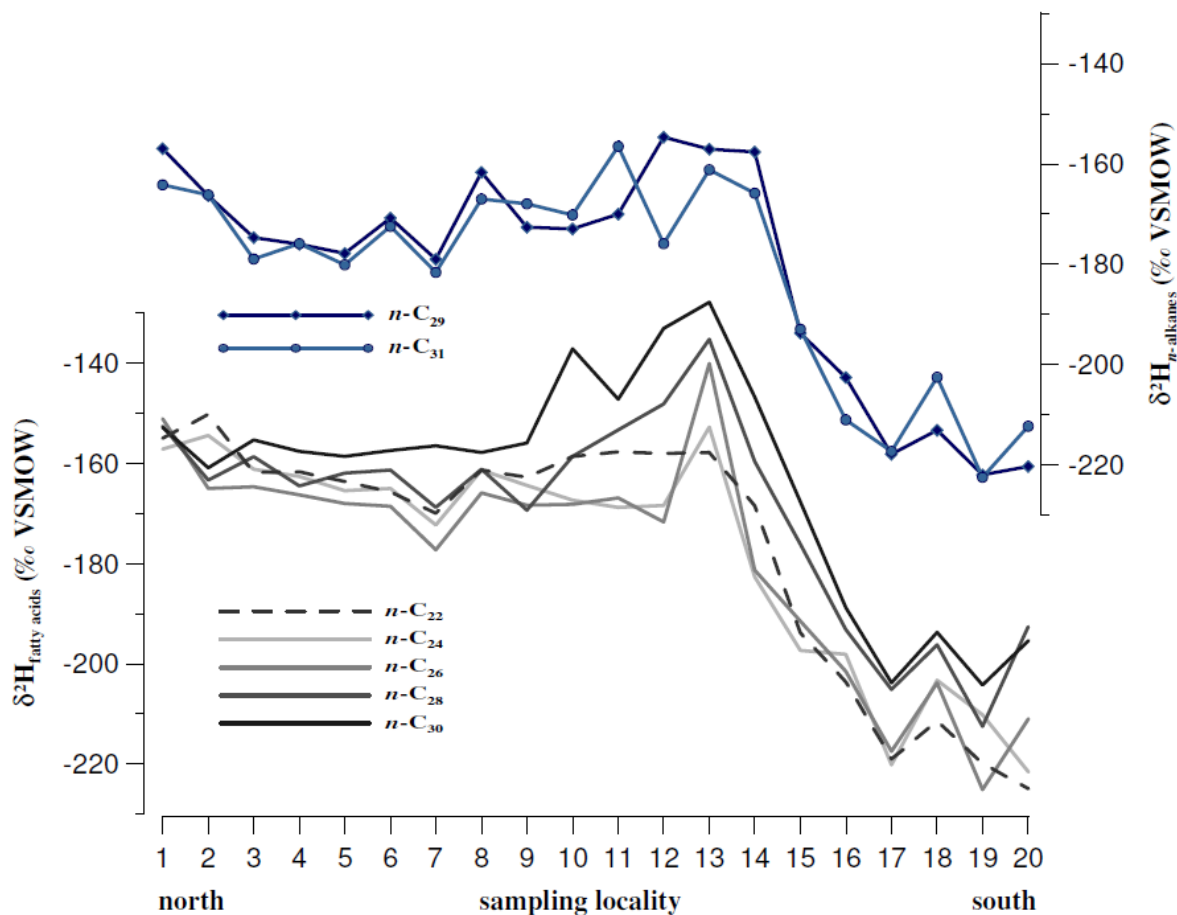


Fig. 2: Comparison of $\delta^2\text{H}$ results of individual leaf wax n -alkanes and n -alkanoic (fatty) acids along the investigated transect.

3.2 Evapotranspirative ^2H enrichment of leaf water

Assuming a constant biosynthetic fractionation of -160‰ for the n -alkane and fatty acids biosynthesis in plants (Sessions *et al.*, 1999; Sachse *et al.*, 2006), we estimate the isotopic composition of leaf water using our n -alkane and fatty acids $\delta^2\text{H}$ values along the transect/gradient (Fig. 3). Note that an average biosynthetic fractionation factor of $\sim -200\text{‰}$ was reported by Sessions *et al.* (1999) for short- and mid-chained fatty acids synthesized mostly by unicellular/multicellular marine algae. By contrast, there are hardly any biosynthetic fractionation factors reported for long-chained fatty acids of higher plants. Given that our $\delta^2\text{H}$

n-alkanes and fatty acids values are very similar, using a biosynthetic fractionation factor of -160 ‰ for both lipids seems appropriate.

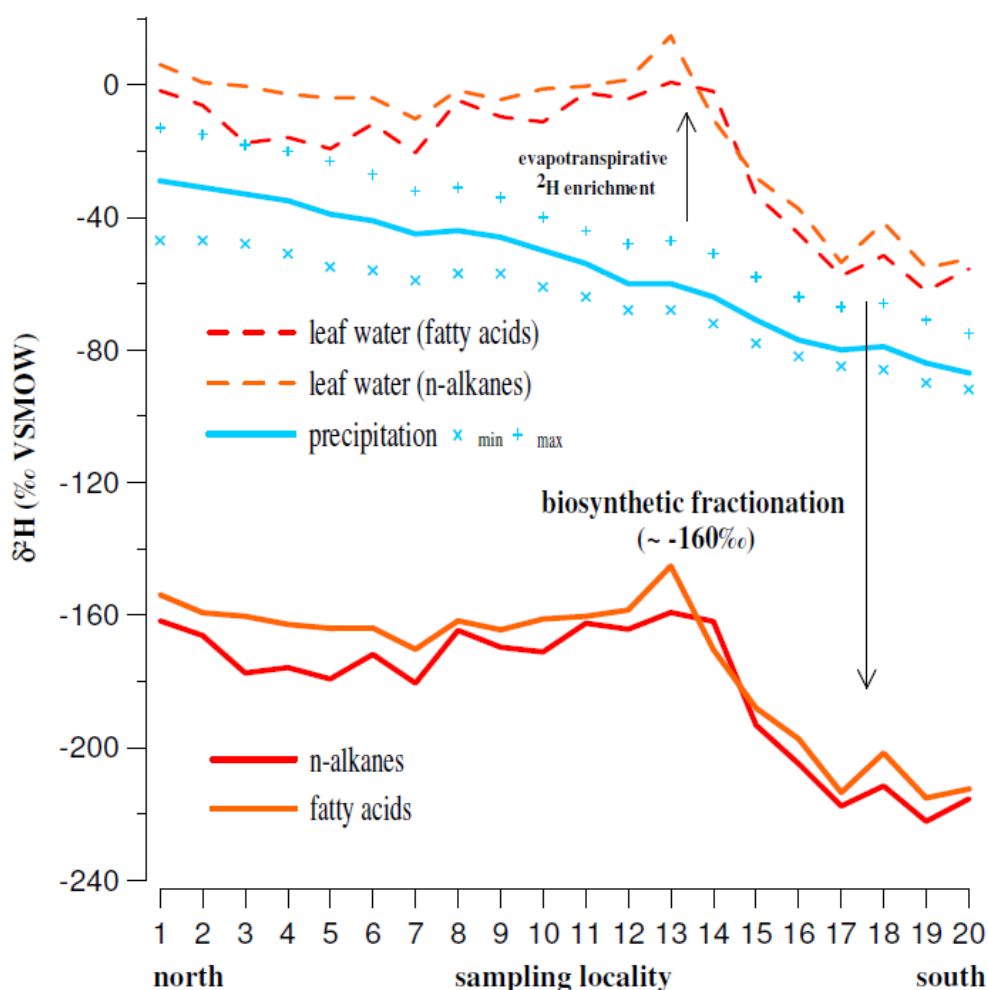


Fig. 3: Comparison of measured $\delta^2\text{H}_{n\text{-alkanes}}$ (weighted mean of $n\text{-C}_{29}$ and $n\text{-C}_{31}$) and $\delta^2\text{H}_{\text{fatty acids}}$ (weighted mean of $n\text{-C}_{22}$, $n\text{-C}_{24}$, $n\text{-C}_{26}$, $n\text{-C}_{28}$, and $n\text{-C}_{30}$), inferred isotopic composition of leaf water, and $\delta^2\text{H}_{\text{prec}}$ (Bowen, 2012).

Estimated leaf water $\delta^2\text{H}$ values suggest a pronounced ^2H enrichment of leaf water compared to precipitation (up to +62 ‰). This finding highlights the role of aridity for evapotranspiration and isotopic enrichment of leaf waxes, in good agreement with prior studies (Sachse *et al.*, 2006; Feakins and Sessions, 2010; Douglas *et al.*, 2012; Kahmen *et al.*, 2013a).

Figure 4 illustrates the overall good agreement between $\delta^2\text{H}_{\text{leaf water}}$ values inferred from the measured *n*-alkanes and fatty acids, and $\delta^2\text{H}_{\text{leaf water}}$ values calculated using the Pecllet-modified Graig-Gordon model. The correlations are highly significant ($r=0.88$, $p<0.001$, $n=20$, for *n*-alkanes and $r=0.93$, $p<0.001$, $n=20$ for fatty acids), suggesting that the model correctly implements the most relevant processes related to evapotranspirative enrichment of leaf water. While predicting the overall trend in leaf water $\delta^2\text{H}$ along the transect with reasonable accuracy, the model does not capture site-to-site excursions in the *n*-alkane-derived leaf water $\delta^2\text{H}$ values from this overall trend. Additional influences that are not captured by the model, such as evaporative ^2H enrichment of soil water can possibly explain the underestimation of the modeled $\delta^2\text{H}_{\text{leaf water}}$ values in the middle part of the transect (Fig. 4). In contrast, the model might overestimate $\delta^2\text{H}_{\text{leaf water}}$ in the northern and the southern part of the transect. The corresponding ecosystems, the Humid Pampa and the Patagonian Steppe, respectively, are grasslands, whereas the middle part of the transect is dominated by shrubland. Grass-derived lipids have been shown to be less strongly affected by evapotranspirative leaf water enrichment than those of trees or shrubs (McInerney *et al.*, 2011; Yang *et al.*, 2011; Sachse *et al.*, 2012; Kahmen *et al.*, 2013b), and hence the overestimation of the model may be due to plant species effects (Pedentchouk *et al.*, 2008; Douglas *et al.*, 2012). The more pronounced offsets in Patagonia could additionally be attributed to a seasonality effect. The growing season in Patagonia is not year-round but mainly in spring.

In order to assess the sensitivity of the model to the input parameters, we varied vapor pressure of air by +/- 5 hPa and mean annual temperature by +/- 5°C. While changes in temperature have only negligible effects on the modeled $\delta^2\text{H}$ isotopic composition of leaf water, changes in RH yield difference of up to ~30 ‰ (Fig. 4). Different climatic conditions

during the spring growing season in Patagonia could thus readily explain the overestimation of the evapotranspirative enrichment in the model.

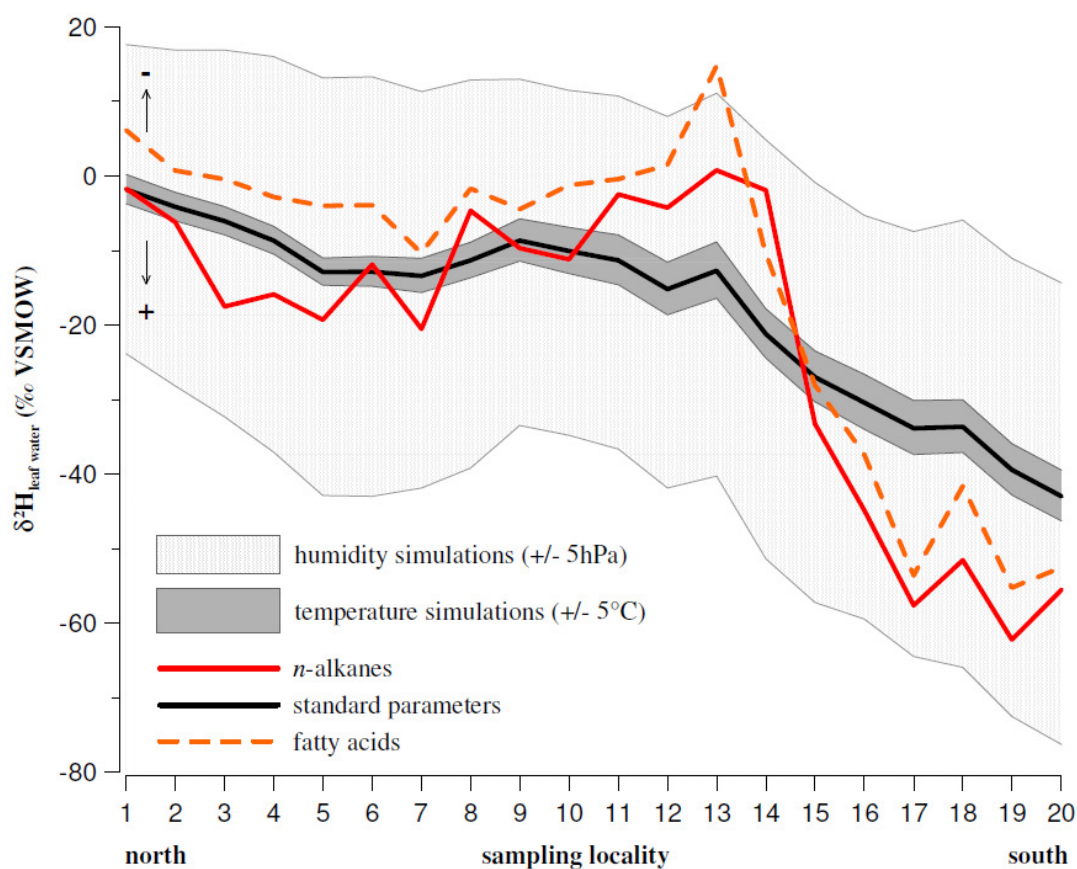


Fig. 4: Results of $\delta^2\text{H}_{\text{leaf water}}$ model simulations and comparison with measured $\delta^2\text{H}_{n\text{-alkanes}}$ and $\delta^2\text{H}_{\text{fatty acids}}$. Sensitivity tests for $\delta^2\text{H}_{\text{leaf water}}$ are shown for changes in RH and air temperature for all 20 sites along the transect.

Evapotranspirative enrichment of leaf water has also been observed in $\delta^{18}\text{O}$ values of hemicellulose-derived arabinose, fucose and xylose analysed in topsoils along the investigated transect (Tuthorn *et al.*, 2014). Model sensitivity tests of ^{18}O enrichment of leaf water using PMCG model corroborate the observations presented here that air humidity is the key factor defining the $^{18}\text{O}/^2\text{H}$ enrichment of leaf water.

3.3 Combining $\delta^{18}\text{O}$ sugar and $\delta^2\text{H}$ n -alkane biomarker analyses

3.3.1 The conceptual model

A conceptual model for the combined interpretation of $\delta^2\text{H}_{n\text{-alkane}}$ and $\delta^{18}\text{O}_{\text{sugar}}$ biomarkers can be illustrated in a $\delta^{18}\text{O}$ - $\delta^2\text{H}$ diagram (Fig. 5). The model is based on the assumption that the investigated n -alkane and hemicellulose biomarkers are primarily leaf-derived and reflect the isotopic composition of leaf water. With regard to the topsoil transect investigated here, this assumption is reasonable and supported by leaf water modeling (for $\delta^2\text{H}$ in Section 3.2, and for $\delta^{18}\text{O}$ see Tuthorn *et al.*, 2014).

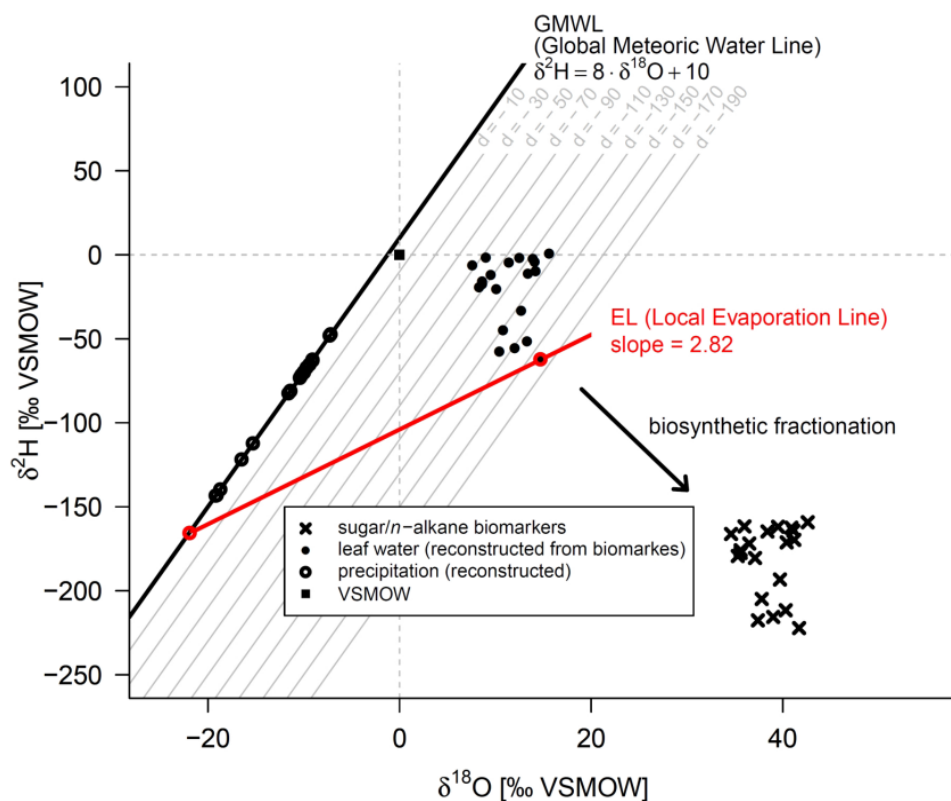


Fig. 5: $\delta^{18}\text{O}$ - $\delta^2\text{H}$ diagram representing the global meteoric water line (GMWL) and an evaporation line (EL). Data for the $\delta^{18}\text{O}$ values of hemicellulose-derived sugars (mean of arabinose, fucose, and xylose) and the mean $\delta^2\text{H}$ values of leaf wax-derived n -alkanes (mean of $n\text{-C}_{29}$ and $n\text{-C}_{31}$) are displayed. $\delta^2\text{H}$ and $\delta^{18}\text{O}$ values of leaf water are reconstructed using biosynthetic fractionation factors and $\delta^2\text{H}$ and $\delta^{18}\text{O}$ values of precipitation are calculated as intersection of the individual ELs with the GMWL.

Accordingly, the isotopic composition of leaf water can be reconstructed from the isotopic composition of the biomarkers by applying an average value according to various studies of the biosynthetic fractionation factors resulting in -160 ‰ (Sessions *et al.*, 1999; Sachse *et al.*, 2006) and +27 ‰ (Sternberg *et al.*, 1986; Yakir and DeNiro, 1990; Schmidt *et al.*, 2001; Cernusak *et al.*, 2003) for $\delta^2\text{H}$ and $\delta^{18}\text{O}$, respectively (Fig. 5).

In the $\delta^{18}\text{O}$ - $\delta^2\text{H}$ diagram, the distance of reconstructed leaf water to the Global Meteoric Water Line (GMWL) defines the deuterium excess ($d = \delta^2\text{H} - 8 \cdot \delta^{18}\text{O}$). Observed deviation is caused by the kinetic effect resulting in slower diffusivity of the $^1\text{H}^1\text{H}^{18}\text{O}$ molecules compared to the $^2\text{H}^1\text{H}^{16}\text{O}$ molecules. More humid conditions and less evapotranspiration are reflected by lower d values, and more arid conditions and more evapotranspiration are reflected by higher d values. Using a Craig-Gordon model adapted by Gat and Bowser (1991), the d -excess of leaf water can be used to calculate RH values normalized to the temperature of leaf-water:

$$RH = 1 - \frac{\Delta d}{(\epsilon_2^* - 8 \cdot \epsilon_{18}^* + C_k^2 - 8 \cdot C_k^{18})} \quad (\text{Eqn. 4})$$

where Δd represents the difference in d -excess between leaf-water and source water. According to Merlivat (1978), the kinetic isotope fractionation equals 25.1 ‰ and 28.5 ‰ for C_k^2 and C_k^{18} , respectively, considering that these are the maximum values of kinetic fractionation during molecular diffusion of water through stagnant air. Equilibrium isotope enrichments ϵ_2^* and ϵ_{18}^* as functions of temperature can be calculated using empirical equations of Horita and Wesolowski (1994).

The combined $\delta^{18}\text{O}$ - $\delta^2\text{H}$ biomarker approach also allows reconstruction of the isotopic composition of plant source water, which can be considered as an approximation for $\delta^2\text{H}_{\text{prec}}$ and $\delta^{18}\text{O}_{\text{prec}}$. In Figure 5 these are given by the intersects of the individual evaporation lines (EL) with the GMWL. The slope value of 2.82 that is used for the EL has been observed in

previous experiments on evaporating leaf water (Allison *et al.*, 1985; Walker and Brunel, 1990; Bariac *et al.*, 1994; Zech *et al.*, 2013a).

3.3.2 Reconstructed RH values along the climate transect and comparison with actual RH values

The reconstructed d-excess values of leaf water along the investigated transect range from -67 to -178 ‰ and reveal a systematic trend towards more negative values in the south (Fig. 6). The reconstructed RH values calculated using the leaf water d-excess values according to the above-described Craig-Gordon model range from 16 to 65 %, with one extremely low value of 5 % (Fig. 6). They follow the systematic d-excess trend and correlate significantly ($r=0.79$, $p<0.001$, $n=20$) with the actual modern RH values retrieved from GeoINTA (2012), which generally validates the $\delta^{18}\text{O}$ - $\delta^2\text{H}$ conceptual model.

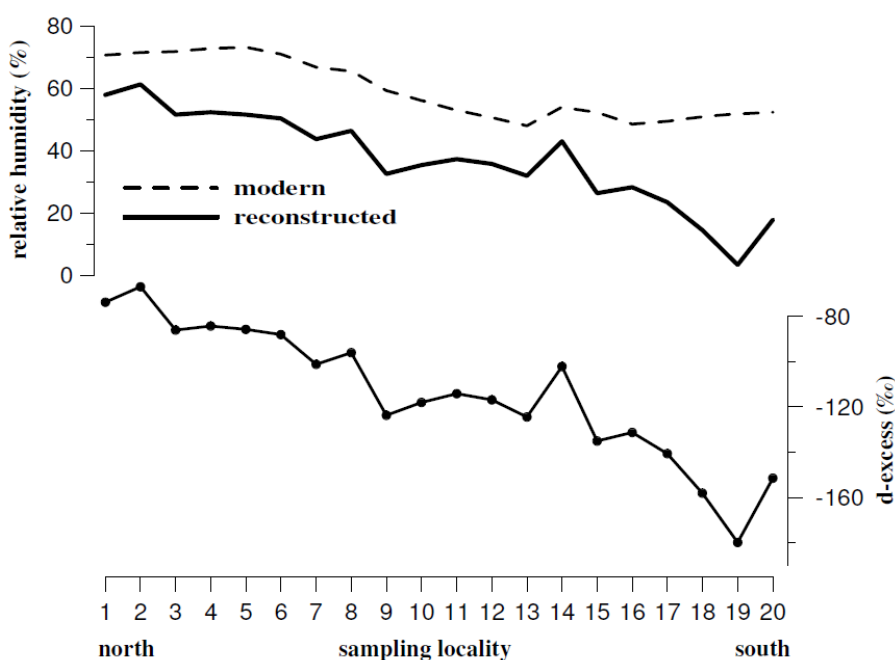


Fig. 6: Comparison of reconstructed humidity based on a normalized Craig-Gordon model accounting for deuterium excess and temperature with modern humidity data retrieved for the investigated sites (GeoINTA, 2012). Deuterium excess values were calculated using $\delta^{18}\text{O}_{\text{leaf water}}$ reconstructed from terrestrial sugars (Tuthorn *et al.*, 2014) and $\delta^2\text{H}_{\text{leaf water}}$ reconstructed from *n*-alkanes.

However, as depicted by Fig. 6, the reconstructed RH values systematically underestimate the actual (modern) RH values. This is especially pronounced for the three southernmost locations (18-20) and may be attributed to several causes. First, the applied model calculations do not account for evaporative enrichment of soil water. In the $\delta^{18}\text{O}$ - $\delta^2\text{H}$ diagram, the soil water enrichment shifts the source water (simplified to ‘reconstructed precipitation’ in Fig. 5 and our model) along the evaporation line and thus leads to too negative d-excess values and an underestimation of RH. Second, the reconstructed source water lies on the GMWL in the model, while local meteoric water lines and thus actual precipitation may have a d-excess offset from the GMWL (d-excess of GMWL = 10 ‰). In our case, this effect should be negligible, as d-excess values of precipitation along the transect are only on the order of 4.8 – 11 ‰ (Bowen, 2012). Third, given that leaf waxes considered to be formed mostly during early stages of leaf ontogeny (Kolattukudy, 1970; Riederer & Markstaedter, 1996; Kahmen *et al.*, 2011a; Tipple *et al.*, 2012) they may not necessarily reflect the mean annual isotopic composition of precipitation in regions with pronounced seasonality, but rather the isotopic composition of precipitation during the growing season. As well, compared to the annual (modern) RH values, growing season RH yields up to 9% (CRU, 2013) lower values in Patagonia where seasonality is especially pronounced. Fourth, reconstructed RH values will be also underestimated if *n*-alkanes do not fully incorporate the evapotranspirative ^2H enrichment of leaf water (section 3.2; McInerney *et al.*, 2011; Kahmen *et al.*, 2013b). In the $\delta^{18}\text{O}$ - $\delta^2\text{H}$ diagram, leaf water would thus plot lower than the simple Craig-Gordon model predicts, and d-excess would be too negative.

Finally, the $\delta^{18}\text{O}$ biosynthetic fractionation factor of $\sim +27$ ‰, which has been reported for cellulose, may underestimate the actual fractionation factor of hemicelluloses (Tuthorn *et al.*, 2014; Zech *et al.*, 2014), which would result in reconstructed leaf water values plotting too far to the right in the $\delta^{18}\text{O}$ - $\delta^2\text{H}$ diagram. This can be explained with the loss of a relatively

^{18}O -depleted oxygen atom attached to C-6 during pentose biosynthesis (C-6 decarboxylation; Altermatt and Neish, 1956; Harper and Bar-Peled, 2002; Burget *et al.*, 2003), and is in agreement with the recent finding that about 80% of the oxygen atoms at the C-6 position are isotopically exchanged during cellulose synthesis (Waterhouse *et al.*, 2013). In contrast, the value of +27 ‰ would be an overestimation in cases where significant amounts of stem or root-derived sugars contribute to the soil sugar pool, because up to 40% of the oxygen atoms being biosynthesized in leaves are exchanging with non-enriched root/stem water during cellulose biosynthesis in roots/stems (Sternberg *et al.*, 1986; Gessler *et al.*, 2009). However, given that this would result in an overestimation of reconstructed RH values (the opposite is observed, Fig. 6), we suggest that the majority of the sugar biomarkers along the topsoil transect investigated here are leaf-derived and not stem-/root-derived.

3.3.3 Comparison of reconstructed and actual $\delta^2\text{H}_{\text{prec}}$ and $\delta^{18}\text{O}_{\text{prec}}$ values

Values of $\delta^{18}\text{O}_{\text{prec}}$ and $\delta^2\text{H}_{\text{prec}}$ reconstructed as the intercepts of the individual evaporation lines (EL) with the GMWL in the $\delta^{18}\text{O}$ - $\delta^2\text{H}$ diagram (Fig. 5) range from -7 to -22 ‰ and from -47 to -166 ‰, respectively. They correlate significantly (Fig. 7; $r=0.90$, $p<0.001$, $n=20$, and $r=0.88$, $p<0.001$, $n=20$ for $\delta^{18}\text{O}_{\text{prec}}$ and $\delta^2\text{H}_{\text{prec}}$, respectively) with the actual $\delta^2\text{H}_{\text{prec}}$ and $\delta^{18}\text{O}_{\text{prec}}$ values as derived from Bowen (2012). While the reconstructed $\delta^{18}\text{O}_{\text{prec}}$ and $\delta^2\text{H}_{\text{prec}}$ values, like the reconstructed RH values, generally validate our conceptual model, they appear to systematically underestimate the actual $\delta^{18}\text{O}$ and $\delta^2\text{H}$ values of the precipitation water (Fig. 7).

The uncertainties discussed above for the observed offset of reconstructed versus actual RH values can also affect the accuracy of reconstructed $\delta^{18}\text{O}_{\text{prec}}$ and $\delta^2\text{H}_{\text{prec}}$ values. As well, the actual values for the isotopic composition of precipitation as reported by Bowen (2012) show a confidence interval (95%) ranging from 0.2‰ to 1.2‰, and from 2‰ to 11‰ for $\delta^2\text{H}_{\text{prec}}$ and $\delta^{18}\text{O}_{\text{prec}}$, respectively.

Here, we would like to emphasize the possible influence of seasonality. Leaf waxes and sugar biomarkers likely reflect the humidity and the isotopic composition of spring and summer precipitation rather than mean annual values. Accounting for these seasonality effects, the apparent offsets would be reduced. Future modeling studies should therefore pay particular attention to seasonality, and consider using climate parameters of the growing season instead of annual means.

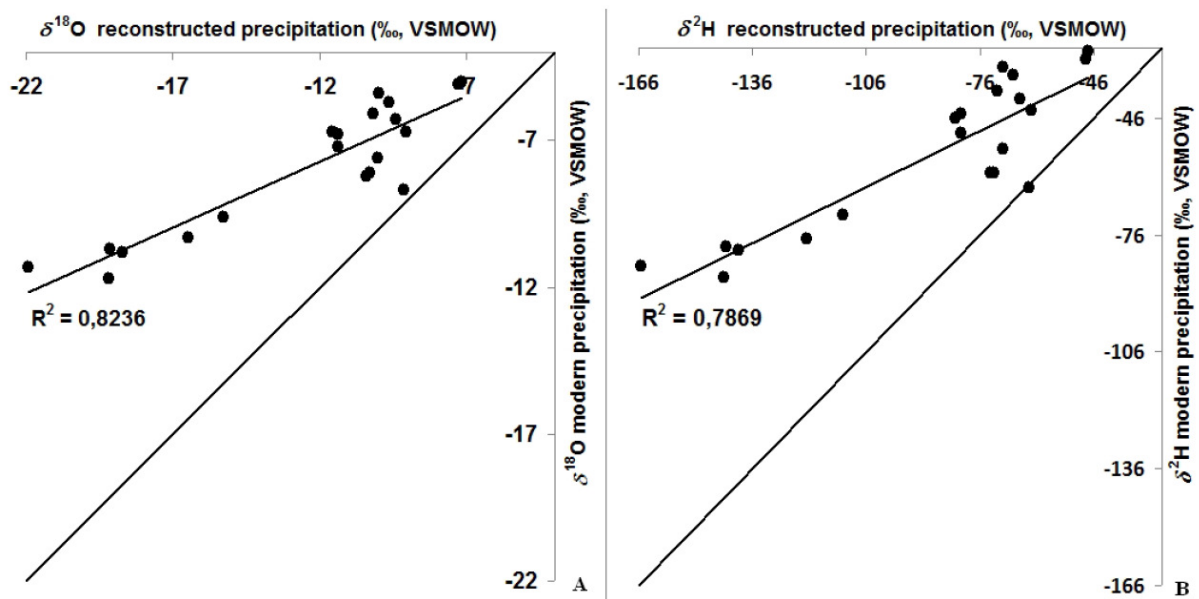


Fig. 7: Correlation of $\delta^{18}\text{O}_{\text{prec}}$ and $\delta^2\text{H}_{\text{prec}}$ reconstructed from the biomarkers with actual modern $\delta^{18}\text{O}_{\text{prec}}$ and $\delta^2\text{H}_{\text{prec}}$ (from Bowen, 2012), a and b, respectively.

4. Conclusions

The hydrogen isotopic composition of leaf wax *n*-alkanes and *n*-alkanoic (fatty) acids extracted from topsoils along a transect in Argentina varies significantly, with $\delta^2\text{H}$ values ranging from -155 to -222 ‰ and -128 to -225 ‰, respectively. These $\delta^2\text{H}$ values broadly parallel variations in the hydrogen isotopic composition of precipitation, but are modulated by evapotranspirative enrichment of leaf water. A mechanistic leaf water model correctly simulates the overall trends, but our data suggest that it might slightly underestimate the evapotranspirative leaf water ^2H enrichment in arid environments, while it might overestimate

the evapotranspirative enrichment in grass-dominated ecosystems. Sensitivity tests show that RH exerts a stronger influence on evapotranspirative enrichment than temperature.

Based on the premise that *n*-alkanes and hemicellulose biomarkers are primarily leaf-derived, we use their oxygen and hydrogen isotopic compositions to reconstruct $\delta^{18}\text{O}_{\text{leaf water}}$ and $\delta^2\text{H}_{\text{leaf water}}$, which in turn allows assessment of the d-excess of leaf water. The large calculated range in d-excess along the transect (-67 to -178 ‰) can be used to calculate values for RH, and the latter are found to correlate significantly with empirical modern RH along the transect. Despite this overall correlation, we observe a systematic underestimation of RH, which we attribute to limitations of the model. Similarly, $\delta^{18}\text{O}_{\text{prec}}$ and $\delta^2\text{H}_{\text{prec}}$ calculated from biomarker isotopic compositions significantly correlate with, but systematically underestimate the $\delta^{18}\text{O}$ and $\delta^2\text{H}$ values of modern precipitation.

The novel combined $\delta^2\text{H}$ - $\delta^{18}\text{O}$ biomarker approach has great potential for paleo-hydrological and paleo-climate reconstructions. In principle, it allows determination of d-excess of past leaf water, thus constraining evapotranspirative enrichment and aridity, as well as the isotopic signal of past precipitation. Further studies are needed to understand the observed systematic offsets, which point to the possible influence of evaporative enrichment of soil water, changing vegetation (grass versus trees or shrubs), seasonality of biomarker synthesis, and the accuracy of the biosynthetic fractionation factors.

Acknowledgements

We kindly thank Prof. B. Huwe (University Bayreuth) and Prof. L. Zöller (University Bayreuth) for logistic support. This study was partly financed by the SIBAE COST Action ES0806, the German Research Foundation (DFG Oe516/2-1 and ZE 844/1-2), and the Swiss National Science Foundation (SNF Ambizione PZ00P2_131670).

References

- Allison G. B., Gat J. R., and Leaney F. W. J. (1985) The relationship between deuterium and oxygen-18 delta values in leaf water. *Chemical Geology* **58**, 145-156.
- Altermatt H. A. and Neish A. C. (1956) The biosynthesis of cell wall carbohydrates: III. further studies on formation of cellulose and xylan from labeled monosaccharides in wheat plants. *Canadian Journal of Biochemistry and Physiology* **34**(3), 405-413.
- Araguas-Araguas L., Froehlich K., and Rozanski K. (2000) Deuterium and oxygen-18 isotope composition of precipitation and atmospheric moisture. *Hydrological Processes* **14**(8), 1341-1355.
- Bariac T., Gonzales-Dunia J., Katerji N., Bethenod O., Bertolini J. M., and Mariotti A. (1994) Spatial variation of the isotopic composition of water (^{18}O , ^2H) in the soil-plant-atmosphere system. *Chemical Geology* **115**, 317-333.
- Bianchi T. and Canuel E. A. (2011) *Chemical Biomarkers in Aquatic Ecosystems*. Princeton University Press.
- Bottinga Y. and Craig H. (1969) Oxygen isotope fractionation between CO_2 and water, and the isotopic composition of marine atmospheric CO_2 . *Earth and Planetary Science Letters* **5**, 285-295.
- Bowen G. J. (2012) The Online Isotopes in Precipitation Calculator, version 2.2. <http://www.waterisotopes.org>.
- Bull I. D., Nott C. J., van Bergen P. F., Poulton P. R., and Evershed R. P. (2000) Organic geochemical studies of soils from the Rothamsted classical experiments - VI. The occurrence and source of organic acids in an experimental grassland soil. *Soil Biology and Biochemistry* **32**(10), 1367-1376.
- Burget E., Verma R., Mølhøj M., and Reiter W. (2003) The biosynthesis of L-arabinose in plants: molecular cloning and characterization of a golgi-localized UDP-D-xylose 4-epimerase encoded by the MUR4 gene of arabidopsis. *The Plant Cell* **15**, 523-531.
- Burgos J. J. and Vidal A. L. (1951) Los climas de la República Argentina, según la nueva clasificación de Thornthwaite. *Meteoros* **1**, 1-32.
- Cernusak L. A., Wong S. C., and Farquhar G. D. (2003) Oxygen isotope composition of phloem sap in relation to leaf water in *Ricinus communis*. *Functional Plant Biology* **30**(10), 1059-1070.

-
- Craig H. and Gordon L. I. (1965) Deuterium and oxygen-18 variations in the ocean and the marine atmosphere. *Conference on Stable Isotopes in Oceanographic Studies and Paleotemperatures*, 9-130.
- CRU. (2013) University of East Anglia-Climate Research Unit, Relative humidity data. Available at: <http://www.cru.uea.ac.uk/cru/data/hrq/tmc/>. Accessed 28.11.2013, Vol. 2013.
- Dongmann G., Nürnberg H. W., Förstel H., and Wagener K. (1974) On the enrichment of H₂¹⁸O in the leaves of transpiring plants. *Radiation and Environmental Biophysics* **11**(1), 41-52.
- Douglas P. M. J., Pagani M., Brenner M., Hodell D. A., and Curtis J. H. (2012) Aridity and vegetation composition are important determinants of leaf-wax δD values in southeastern Mexico and Central America. *Geochimica et Cosmochimica Acta* **97**, 24-45.
- Eglinton G. and Hamilton R. J. (1967) Leaf Epicuticular Waxes. *Science* **156**(3780), 1322-1335.
- Eglinton T. I. and Eglinton G. (2008) Molecular proxies for paleoclimatology. *Earth and Planetary Science Letters* **275**(1-2), 1-16.
- Ehleringer J. R. and Dawson T. E. (1992) Water uptake by plants: perspectives from stable isotope composition. *Plant, Cell & Environment* **15**(9), 1073-1082.
- Farquhar G. D., Cernusak L. A., and Barnes B. (2007) Heavy Water Fractionation during Transpiration. *Plant Physiology* **143**(1), 11-18.
- Farquhar G. D. and Lloyd J. (1993) Carbon and oxygen isotope effects in the exchange of carbon dioxide between terrestrial plants and the atmosphere. In *Stable isotopes and plant carbon-water relations* (ed. J. R. Ehleringer, A. E. Hall, and G. D. Farquhar), pp. 47-70. Academic Press, Inc.
- Feakins S. J. and Sessions A. L. (2010) Controls on the D/H ratios of plant leaf waxes in an arid ecosystem. *Geochimica et Cosmochimica Acta* **74**(7), 2128-2141.
- Fernández O. A. and Busso C. A. (1997) Arid and semi-arid rangelands: two thirds of Argentina, pp. 41-60. RALA Report 200.
- Flanagan L. B., Comstock J. P., and Ehleringer J. R. (1991) Comparison of modeled and observed environmental influences on the stable oxygen and hydrogen isotope composition of leaf water in *Phaseolus vulgaris* L. *Plant Physiology* **96**(2), 588-596.
- Gat J. R. (1996) Oxygen and Hydrogen Isotopes in the Hydrologic Cycle. *Annual Review of Earth and Planetary Sciences* **24**, 225-262.

-
- Gat J. R. and Bowser C. (1991) The heavy isotope enrichment of water in coupled evaporative systems. In *Stable Isotope Geochemistry: A Tribute to Samuel Epstein* (ed. H. P. Taylor, J. R. O'Neil, and I. R. Kaplan), pp. 159-168. The Geochemical Society.
- GeoINTA. (2012) Instituto Nacional de Tecnologia Agropecuaria Visualizador Integrado. Available online at: <http://geointa.inta.gov.ar/visor/> . Accessed 01.08.2012.
- Greule M., Hänsel C., Bauermann U., and Mosandl A. (2008) Feed additives: authenticity assessment using multicomponent-/multielement-isotope ratio mass spectrometry. *European Food Research and Technology* **227**(3), 767-776.
- Harper A. and Bar-Peled M. (2002) Biosynthesis of UDP-xylose. Cloning and characterization of a novel Arabidopsis gene family, UXS, encoding soluble and putative membrane-bound UDP-glucuronic acid decarboxylase isoforms. *Plant Physiology* **130**(4), 2188-2198.
- Hener U., Brand W. A., Hilker A. W., Juchelka D., Mosandl A., and Podebrad F. (1998) Simultaneous on-line analysis of $^{18}\text{O}/^{16}\text{O}$ and $^{13}\text{C}/^{12}\text{C}$ ratios of organic compounds using GC-pyrolysis-IRMS. *Zeitschrift für Lebensmitteluntersuchung und -Forschung A* **206**(3), 230-232.
- Horita J. and Wesolowski D. J. (1994) Liquid-vapor fractionation of oxygen and hydrogen isotopes of water from the freezing to the critical temperature. *Geochimica et Cosmochimica Acta* **58**(16), 3425-3437.
- Huang Y., Shuman B., Wang Y., and Webb T. (2004) Hydrogen isotope ratios of individual lipids in lake sediments as novel tracers of climatic and environmental change: a surface sediment test. *Journal of Paleolimnology* **31**(3), 363-375.
- Juchelka D., Beck T., Hener U., Dettmar F., and Mosandl A. (1998) Multidimensional Gas Chromatography Coupled On-Line with Isotope Ratio Mass Spectrometry (MDGC-IRMS): Progress in the Analytical Authentication of Genuine Flavor Components. *Journal of High Resolution Chromatography* **21**(3), 145-151.
- Jung J., Puff B., Eberts T., Hener U., and Mosandl A. (2007) Reductive ester cleavage of acyl glycerides-GC-C/P-IRMS measurements of glycerol and fatty alcohols. *European Food Research and Technology* **225**(2), 191-197.
- Jung J., Sewenig S., Hener U., and Mosandl A. (2005) Comprehensive authenticity assessment of lavender oils using multielement/multicomponent isotope ratio mass spectrometry analysis and enantioselective multidimensional gas chromatography-mass spectrometry. *European Food Research and Technology* **220**(2), 232-237.

-
- Kahmen A., Dawson T. E., Vieth A., and Sachse D. (2011) Leaf wax n-alkane δD values are determined early in the ontogeny of *Populus trichocarpa* leaves when grown under controlled environmental conditions. *Plant, Cell & Environment* **34**(10), 1639-1651.
- Kahmen A., Hoffmann B., Schefuss E., Arndt S. K., Cernusak L. A., West J. B., and Sachse D. (2013a) Leaf water deuterium enrichment shapes leaf wax n-alkane δD values of angiosperm plants II: Observational evidence and global implications. *Geochimica et Cosmochimica Acta* **111**, 50-63.
- Kahmen A., Schefuß E., and Sachse D. (2013b) Leaf water deuterium enrichment shapes leaf wax n-alkane δD values of angiosperm plants I: Experimental evidence and mechanistic insights. *Geochimica et Cosmochimica Acta* **111**, 39-49.
- Kahmen A., Simonin K., Tu K. P., Merchant A., Callister A., Siegwolf R., Dawson T. E., and Arndt S. K. (2008) Effects of environmental parameters, leaf physiological properties and leaf water relations on leaf water $\delta^{18}O$ enrichment in different Eucalyptus species. *Plant, Cell & Environment* **31**(6), 738-751.
- Kolattukudy P. (1970) Cutin biosynthesis in *Vicia faba* leaves - effect of age. *Plant Physiology* **46**, 759-760.
- Le Hou rou H. N. (1996) Climate change, drought and desertification. *Journal of Arid Environments* **34**, 133-185.
- Matsumoto K., Kawamura K., Uchida M., and Shibata Y. (2007) Radiocarbon content and stable carbon isotopic ratios of individual fatty acids in subsurface soils: Implication for selective microbial degradation and modification of soil organic matter. *Geochemical Journal* **41**, 483-492.
- McInerney F. A., Helliker B. R., and Freeman K. H. (2011) Hydrogen isotope ratios of leaf wax n-alkanes in grasses are insensitive to transpiration. *Geochimica et Cosmochimica Acta* **75**(2), 541-554.
- Merlivat L. (1978) Molecular diffusivities of $H_2^{16}O$, $HD^{16}O$, and $H_2^{18}O$ in gases. *The Journal of Chemical Physics* **69**(6), 2864-2871.
- Nguyen Tu T. T., Egasse C. I., Zeller B., Bardoux G. r., Biron P., Ponge J.-F. o., David B., and Derenne S. (2011) Early degradation of plant alkanes in soils: A litterbag experiment using ^{13}C -labelled leaves. *Soil Biology and Biochemistry* **43**(11), 2222-2228.
- Pagani M., Pedentchouk N., Huber M., Sluijs A., and Schouten S. (2006) Arctic hydrology during global warming at the Paleocene/Eocene thermal maximum. *Nature* **442**, 671-675.

-
- Paruelo J. M., Beltrán A., Jobbágy E., Sala O. E., and Golluscio R. A. (1998) The climate of Patagonia: general patterns and controls on biotic processes. *Ecologia Austral* **8**, 85-101.
- Paul D., Skrzypek G., and Fórizs I. (2007) Normalization of measured stable isotopic compositions to isotope reference scales - a review. *Rapid Communications in Mass Spectrometry* **21**(18), 3006-3014.
- Pedentchouk N., Sumner W., Tipple B., and Pagani M. (2008) delta C-13 and delta D compositions of n-alkanes from modern angiosperms and conifers: An experimental set up in central Washington State, USA. *Organic Geochemistry* **39**(8), 1066-1071.
- Radke J., Bechtel A., Gaupp R., Püttmann W., Schwark L., Sachse D., and Gleixner G. (2005) Correlation between hydrogen isotope ratios of lipid biomarkers and sediment maturity. *Geochimica et Cosmochimica Acta* **69**(23), 5517-5530.
- Rao Z., Zhu Z., Jia G., Henderson A. C. G., Xue Q., and Wang S. (2009) Compound specific δD values of long chain n-alkanes derived from terrestrial higher plants are indicative of the δD of meteoric waters: Evidence from surface soils in eastern China. *Organic Geochemistry* **40**(8), 922-930.
- Riederer M. and Markstaedter C. (1996) Cuticular waxes: a critical assessment of current knowledge. In *Plant Cuticles - An Integrated Functional Approach* (ed. K. G. Kerstiens). BIOS Scientific Publishers.
- Sachse D., Billault I., Bowen G. J., Chikaraishi Y., Dawson T. E., Feakins S. J., Freeman K. H., Magill C. R., McInerney F. A., van der Meer M. T. J., Polissar P., Robins R. J., Sachs J. P., Schmidt H.-L., Sessions A. L., White J. W. C., West J. B., and Kahmen A. (2012) Molecular Paleohydrology: Interpreting the Hydrogen-Isotopic Composition of Lipid Biomarkers from Photosynthesizing Organisms. *Annual Review of Earth and Planetary Sciences* **40**(1), 221-249.
- Sachse D., Radke J., and Gleixner G. (2004) Hydrogen isotope ratios of recent lacustrine sedimentary n-alkanes record modern climate variability. *Geochimica et Cosmochimica Acta* **68**(23), 4877-4889.
- Sachse D., Radke J., and Gleixner G. (2006) δD values of individual n-alkanes from terrestrial plants along a climatic gradient - Implications for the sedimentary biomarker record. *Organic Geochemistry* **37**(4), 469-483.
- Samuels L., Kunst L., and Jetter R. (2008) Sealing Plant Surfaces: Cuticular Wax Formation by Epidermal Cells. *Annual Review of Plant Biology* **59**(1), 683-707.
- Sauer P. E., Eglinton T. I., Hayes J. M., Schimmelmann A., and Sessions A. L. (2001) Compound-specific D/H ratios of lipid biomarkers from sediments as a proxy for

- environmental and climatic conditions. *Geochimica et Cosmochimica Acta* **65**(2), 213-222.
- Schefuss E., Schouten S., and Schneider R. R. (2005) Climatic controls on central African hydrology during the past 20,000 years. *Nature* **437**, 1003-1006.
- Schmidt H.-L., Werner R. A., and Rossmann A. (2001) ^{18}O pattern and biosynthesis of natural plant products. *Phytochemistry* **58**(1), 9-32.
- Sessions A. L., Burgoyne T. W., Schimmelmann A., and Hayes J. M. (1999) Fractionation of hydrogen isotopes in lipid biosynthesis. *Organic Geochemistry* **30**(9), 1193-1200.
- Smith F. A. and Freeman K. H. (2006) Influence of physiology and climate on δD of leaf wax n-alkanes from C3 and C4 grasses. *Geochimica et Cosmochimica Acta* **70**(5), 1172-1187.
- Sternberg L., DeNiro M. J., and Savidge R. A. (1986) Oxygen isotope exchange between metabolites and water during biochemical reactions leading to cellulose synthesis. *Plant Physiology* **82**, 423-427.
- Tierney J. E., Russel J. M., Huang Y., Sinninghe Damsté J. S., Hopmans E. C., and Cohen A. S. (2008) Northern Hemisphere Controls on Tropical Southeast African Climate During the Past 60,000 Years. *Science* **322**, 252-255.
- Tipple, B.J., Berke, M.A., Doman, C.E., Khachatryan, S., Ehleringer, J.R., 2013. Leaf-wax n-alkanes record the plant-water environment at leaf flush. *Proceedings of National Academy of Science* **110**, 2659-2664.
- Tuthorn M., Zech M., Ruppenthal M., Oelmann Y., Kahmen A., Valle H. c. F. d., Wilcke W., and Glaser B. (2014) Oxygen isotope ratios ($^{18}\text{O}/^{16}\text{O}$) of hemicellulose-derived sugar biomarkers in plants, soils and sediments as paleoclimate proxy II: Insight from a climate transect study. *Geochimica et Cosmochimica Acta* **126**, 624-634.
- Walker C. D. and Brunel J.-P. (1990) Examining evapotranspiration in a semi-arid region using stable isotopes of hydrogen and oxygen. *Journal of Hydrology* **118**(1-4), 55-75.
- Waterhouse J. S., Cheng S., Juchelka D., Loader N. J., McCarroll D., Switsur V. R., and Gautam L. (2013) Position-specific measurement of oxygen isotope ratios in cellulose: Isotopic exchange during heterotrophic cellulose synthesis. *Geochimica et Cosmochimica Acta* **112**, 178-191.
- Werner R. (2003) The online $^{18}\text{O}/^{16}\text{O}$ analysis: development and application. *Isotopes in Environmental and Health Studies* **39**(2), 85-104.
- Yakir D. (1992) Variations in the natural abundance of oxygen-18 and deuterium in plant carbohydrates. *Plant, Cell & Environment* **15**(9), 1005-1020.

-
- Yakir D. and DeNiro M. J. (1990) Oxygen and hydrogen isotope fractionation during cellulose metabolism in *Lemna gibba* L. *Plant Physiology* **93**(1), 325-332.
- Yang H., Liu W., Leng Q., Hren M. T., and Pagani M. (2011) Variation in n-alkane δD values from terrestrial plants at high latitude: Implications for paleoclimate reconstruction. *Organic Geochemistry* **42**(3), 283-288.
- Zech M. and Glaser B. (2009) Compound-specific $\delta^{18}O$ analyses of neutral sugars in soils using gas chromatography-pyrolysis-isotope ratio mass spectrometry: problems, possible solutions and a first application. *Rapid Communications in Mass Spectrometry* **23**(22), 3522-3532.
- Zech M., Mayr C., Tuthorn M., Leiber-Sauheitl K., and Glaser B. (2014) Oxygen isotope ratios ($^{18}O/^{16}O$) of hemicellulose-derived sugar biomarkers in plants, soils and sediments as paleoclimate proxy I: Insight from a climate chamber experiment. *Geochimica et Cosmochimica Acta* **126**, 614-623.
- Zech M., Pedentchouk N., Buggle B., Leiber K., Kalbitz K., Markovic S. B., and Glaser B. (2011) Effect of leaf litter degradation and seasonality on D/H isotope ratios of n-alkane biomarkers. *Geochimica et Cosmochimica Acta* **75**(17), 4917-4928.
- Zech M., Tuthorn M., Detsch F., Rozanski K., Zech R., Zoeller L., Zech W., and Glaser B. (2013a) A 220 ka terrestrial $\delta^{18}O$ and deuterium excess biomarker record from an eolian permafrost paleosol sequence, NE-Siberia. *Chemical Geology* **360-361**, 220-230.
- Zech M., Tuthorn M., Glaser B., Amelung W., Huwe B., Zech W., Zöller L., and Löffler J. (2013b) Natural abundance of ^{18}O of sugar biomarkers in topsoils along a climate transect over the Central Scandinavian Mountains, Norway. *Journal of Plant Nutrition and Soil Science* **176**(1), 12-15.
- Zech M., Werner R. A., Juchelka D., Kalbitz K., Buggle B., and Glaser B. (2012) Absence of oxygen isotope fractionation/exchange of (hemi-) cellulose derived sugars during litter decomposition. *Organic Geochemistry* **42**, 1470-1475.
- Zech R., Zech M., Markovic S., Hambach U., and Huang Y. (2013c) Humid glacials, arid interglacials? Critical thoughts on pedogenesis and paleoclimate based on multi-proxy analyses of the loess-paleosol sequence Crvenka, Northern Serbia. *Palaeogeography, Palaeoclimatology, Palaeoecology* **387**(0), 165-175.

Study 5

A 16-ka $\delta^{18}\text{O}$ record of lacustrine sugar biomarkers from the High Himalaya reflects Indian Summer Monsoon variability

Michael Zech^{1,2,*}, Mario Tuthorn¹, Roland Zech³, Frank Schlütz^{4,5}, Wolfgang Zech¹, Bruno Glaser²

- ¹) Department of Soil Physics, Soil Science and Soil Geography and Chair of Geomorphology, University of Bayreuth, Universitätsstr. 30, D-95440 Bayreuth, Germany
- ²) Department of Terrestrial Biogeochemistry, Martin Luther University of Halle-Wittenberg, Von-Seckendorff-Platz 3, D-06120 Halle, Germany
- ³) Geological Institute, ETH Zurich, Sonneggstr. 5, CH-8092 Zurich, Switzerland
- ⁴) Lower Saxony Institute for Historical Coastal Research, Viktoriastraße 26/28, D-26382 Wilhelmshaven, Germany
- ⁵) Department of Palynology and Climate Dynamics, Albrecht-von-Haller Institute for Plant Sciences, University of Göttingen, Untere Karspüle 2, 37073 Göttingen, Germany
- *) corresponding author: michael_zech@gmx.de

Journal of Paleolimnology

(2014) 51, 241-251

Abstract

We investigated a late glacial-Holocene lacustrine sediment archive located at 4,050 m a.s.l. in the small carbonate-free catchment of Lake Panch Pokhari, Helambu Himal, Nepal. A $\delta^{18}\text{O}$ sugar biomarker record was established by applying novel compound-specific $\delta^{18}\text{O}$ analysis of plant sugar biomarkers (Zech and Glaser in *Rapid Commun Mass Spectrom* 23:3522-3532, 29). This method overcomes analytical challenges such as extraction and purification faced by previous methods aimed at using $\delta^{18}\text{O}$ of aquatic cellulose as a paleoclimate proxy.

The $\delta^{18}\text{O}$ results for sugar biomarkers arabinose, xylose, and fucose agree well and reveal a pronounced trend towards lower $\delta^{18}\text{O}$ values during the deglaciation and the onset of the Bølling/Allerød interstadial. By contrast, the period of the Younger Dryas is characterized by higher $\delta^{18}\text{O}$ values. The early Holocene again reveals lower $\delta^{18}\text{O}$ values.

We suggest that our lacustrine $\delta^{18}\text{O}$ record reflects coupled hydrological and thermal control. It is strongly related to changes in the oxygen isotopic composition of paleo-precipitation and resembles the $\delta^{18}\text{O}$ records of Asian speleothems. With respect to the ‘amount effect,’ the record is interpreted as reflecting the Indian Summer Monsoon intensity. The precipitation signal is, however, amplified in our record by evaporative ^{18}O enrichment that is controlled by the ratio of precipitation to evaporation (P/E).

We suggest that our $\delta^{18}\text{O}$ record reflects the variability of the Indian Summer Monsoon, which was strong during the Bølling/Allerød interstadial and early Holocene, but weak during the Younger Dryas stadial. This interpretation is corroborated by a pollen-based index for Lake Panch Pokhari that estimated the strength of the Indian Summer Monsoon versus the strength of the Westerlies. Millennial-scale synchronicity with the Greenland $\delta^{18}\text{O}$

temperature records highlights the previously suggested strong teleconnections between the Asian Monsoon system and North Atlantic climate variability.

Keywords: High Himalaya, Late glacial, Indian Summer Monsoon, stable oxygen isotopes, sugar biomarkers

1. Introduction

The oxygen isotopic composition ($^{18}\text{O}/^{16}\text{O}$) of precipitation depends on climate factors such as temperature and precipitation amount (Dansgaard 1964; Araguas-Araguas et al. 2000). Whereas the ‘temperature effect’ predominates at high-latitudes, the ‘amount effect’ generally predominates in monsoonal regions. Similar to speleothems (Wang et al. 2001; Dykoski et al. 2005) and ice cores (Thompson et al. 1997, 2005), lake sediments offer the opportunity to study continuous, high-resolution $\delta^{18}\text{O}$ climate archives. Hence, they are investigated, for instance on the Tibetan Plateau, to reconstruct the Asian Monsoon history. In fact, the Holocene Asian Monsoon history is well documented by numerous $\delta^{18}\text{O}$ records from lake sediments (Zhang et al. 2011). There are, however, a number of problems associated with the construction of lacustrine $\delta^{18}\text{O}$ records. For instance, input of old soil carbon from the catchment and lake reservoir effects can confound chronologies. Furthermore, developing $\delta^{18}\text{O}$ records depends on the occurrence of ostracod- or diatom-containing sediments, and species-specific differences and catchment-specific effects (e.g. meltwater effect) may need to be considered (Lister et al. 1991; Liu et al. 2007; Mischke et al. 2010). With regard to sedimentary cellulose as a recorder of past lakewater $\delta^{18}\text{O}$, there are analytical challenges with respect to extraction, purification and measurement of aquatic cellulose (Saurer and Siegwolf 2004; Kitagawa et al. 2007; Wolfe et al. 2007; Wissel et al. 2008). Recently, Zech and Glaser (2009) and Zech et al. (2012) developed a novel method that is based on compound-specific $\delta^{18}\text{O}$ analyses of sugar biomarkers that are extracted hydrolytically from soils and sediments. This method may help overcome the mentioned analytical challenges and make $\delta^{18}\text{O}$ of sugar biomarkers a valuable new proxy in paleolimnology.

The aim of our study was to test the applicability of the $\delta^{18}\text{O}$ sugar biomarker method proposed by Zech and Glaser (2009) and Zech et al. (2012) to lacustrine sediments. We (i) tested the method on late glacial-Holocene sediments from Lake Panch Pokhari, which is situated at 4,050 m a.s.l. in Helambu Himal, Nepal, (ii) compared our $\delta^{18}\text{O}$ record with other $\delta^{18}\text{O}$ records, and (iii) discuss the factors that influence $\delta^{18}\text{O}$ records in the study area, to better understand the history and forcing mechanisms that influence the Indian Summer Monsoon (ISM).

1.1 Site description and modern climate

Lake Panch Pokhari is located approximately 100 km north of Kathmandu in the Helambu Himal, Nepal, at 4,050 m a.s.l. (28°02.533'N; 85°42.822'E). It is of glacial origin, about 2 m deep and 100 m long and located on a mountain ridge. It is rainwater fed and features a small, non-permanent outflow (Krstic et al. 2012). It is surrounded by a very small (~0.5 km²), carbonate-free catchment (Figs. 1a and b) with sparse alpine vegetation. The catchment bedrock is composed of gneisses and the vegetation belongs to the Central Himalayan Mountain Meadow Zone (Fukui et al. 2007). During summer, the catchment is grazed and pilgrim routes cross the area. The study area receives most of its precipitation from the ISM, with heavy rainfall between May and September and minor winter precipitation from the Westerlies (Fig. 1c). Mean annual precipitation and temperature at the Nyalam meteorological station (3,810 m a.s.l., 28 km northeast) are 650 mm yr⁻¹ and 3.5 °C, respectively (Tian et al. 2003). Lake Panch Pokhari is generally frozen from the end of October until the end of April.

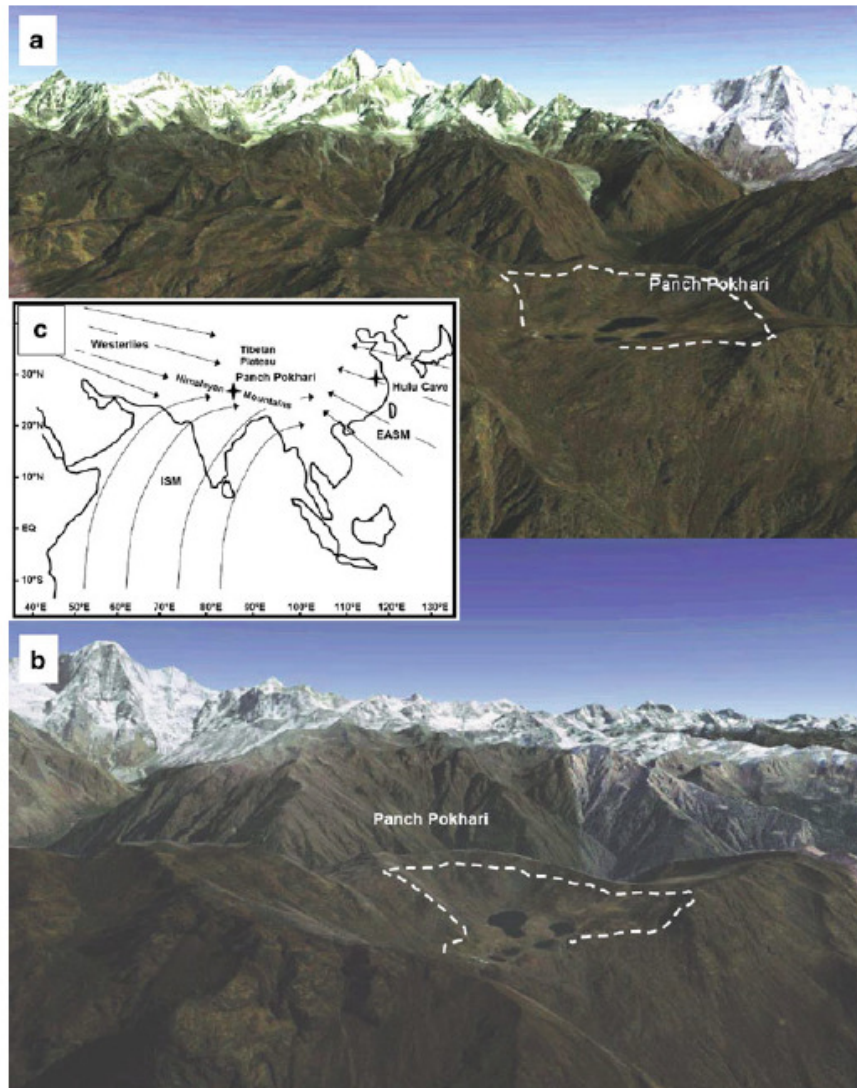


Fig. 1: Location of Lake Panch Pokhari on a mountain ridge in the Helambu Himal, Nepal. a) Northward and b) eastward oblique view over the Panch Pokhari catchment that is indicated by dotted white lines (modified from Google Earth). c) The research area is predominantly influenced by the Indian Summer Monsoon (ISM) and to some degree by winter precipitation provided by the Westerlies. EASM = East Asian Summer Monsoon. The EASM exerts the pivotal climatic influence on Hulu Cave.

2. Materials and methods

2.1 Sampling, TOC analyses and radiocarbon dating

During a field campaign in April 2001, two overlapping sediment cores (N1 and N2) were taken through two neighboring ice boreholes in the middle of Lake Panch Pokhari. Sediment core N1 was opened, described and sampled in the field. The sampling interval was 5 cm in the upper part of the sediment core (0-3.5 m) and 2 cm in the lower, distinctly laminated part (3.5-4.5 m). Samples were air-dried and stored in plastic bags for transport. Core sections N2a to N2g of sediment core N2 were kept intact in plastic tubes and stored in a cooling chamber until they were opened and sampled at 1-cm intervals in the laboratory of the Institute of Soil Science and Soil Geography, University of Bayreuth, Germany.

For total organic carbon (TOC) analyses, sediment samples from cores N1 and N2 were first dried in an oven at 40 °C for several days. Next, finely ground homogenous 50 mg sub-samples were combusted in tin capsules with tungsten oxide added, and TOC was determined by thermal conductivity on a Vario EL elemental analyzer (Elementar, Hanau, Germany). Precision was determined by measuring an acetanilide standard in quadruplicate. Mean standard errors were < 0.02%.

Radiocarbon analyses were carried out on the alkali-insoluble organic matter fractions of nine sediment core samples at the Physics Department of the University of Erlangen, Germany, and at the Poznan Radiocarbon Laboratory, Poland (Table 1). Calibration was done with CalPal Online (Danzeglocke et al. 2012).

Table 1: Radiocarbon data obtained for sediment cores N1 and N2 from Lake Panch Pokhari.

Sample name	Lab reference	Depth (cm)	¹⁴ C-ages (a BP)	Calibrated ¹⁴ C-ages (cal a BP)
Ne03/Panch/N1/107	Erl-6884	107	3,235 ± 61	3,476 ± 69
Ne03/Panch/N1/360	Erl-6886	360	9,864 ± 69	11,311 ± 76
Ne03/Panch/N1/450	Erl-6034	450	12,969 ± 91	15,804 ± 424
Ne03/Panch/N2/4-25	Erl-7686	192	4,054 ± 65	4,597 ± 130
Ne03/Panch/N2/5-40	Erl-7687	234	6,181 ± 93	7,081 ± 118
Ne03/Panch/N2/6-46	Erl-7688	282	8,828 ± 62	9,930 ± 160
Ne03/Panch/N2/7-31	Poz-5961	357	9,900 ± 60	11,349 ± 89
Ne03/Panch/N2/7-03	Poz-5960	385	10,810 ± 60	12,788 ± 73
Ne03/Panch/N2/8-29	Poz-5962	416	12,270 ± 60	14,369 ± 290

Erl = Physical Department of the University of Erlangen, Germany, Poz = Poznan Radiocarbon Laboratory, Poland

2.2 Compound-specific $\delta^{18}\text{O}$ analyses of sugar biomarkers

Monosaccharide sugars from plant-derived hemicelluloses and from algae-derived polysaccharides were released hydrolytically from the sediment samples (sediment core N1) with 4M trifluoroacetic acid (TFA) (105 °C for 4h), using the procedure described by Amelung et al. (1996). After filtering with glass fibre filters, the sugars were purified using XAD and Dowex columns. Derivatization after freeze-drying was done with methylboronic acid (MBA) (Knapp 1979), which ensures that, in contrast to other derivatization methods, the sugars arabinose, fucose and xylose yield only one peak in the chromatograms (Fig. 2), and that all oxygen atoms in the derivatives originate from the sugar molecules and not from derivation reagents (Pizer and Tihal 1992). Oxygen atoms in C1 position of the sugar molecules do not originate from the polysaccharides, but are introduced during the hydrolysis step. These oxygen atoms, however, form a carbonyl group and are therefore easily exchangeable with ambient water. Using water with a known $\delta^{18}\text{O}$ signature during the analytical procedure, and considering an equilibrium fractionation factor of +27‰ (Sternberg and DeNiro 1983), enables measured $\delta^{18}\text{O}$ values to be corrected. For further details on this correction procedure, see Zech and Glaser (2009).

Compound-specific $\delta^{18}\text{O}$ measurements were performed using a GC-Py-IRMS (gas chromatography-pyrolysis-isotope ratio mass spectrometer) consisting of a Trace GC 2000 gas chromatograph (Thermo Fisher Scientific, Bremen, Germany) coupled to a Delta^{plus} isotope ratio mass spectrometer (Thermo Fisher Scientific) via a pyrolysis reactor and a GC/TC III interface (Thermo Fisher Scientific). Sample batches were run in six-fold replication, with replications embedded between standard batches with varying sugar concentrations, as outlined by Zech and Glaser (2009). Mean standard errors for arabinose, fucose and xylose were 1.0‰, 1.4‰ and 1.0‰, respectively. Given that rhamnose often yielded only minor peaks (Fig. 2) and was not detected in some samples, we excluded it from further data evaluation.

The applied novel $\delta^{18}\text{O}$ method circumvents analytical challenges associated with conventional $\delta^{18}\text{O}$ methods used to isolate and measure aquatic cellulose from lake sediments (Saurer and Siegwolf 2004; Wolfe et al. 2007; Wissel et al., 2008). For further details the reader is referred to Zech and Glaser (2009) and to Zech et al. (2012).

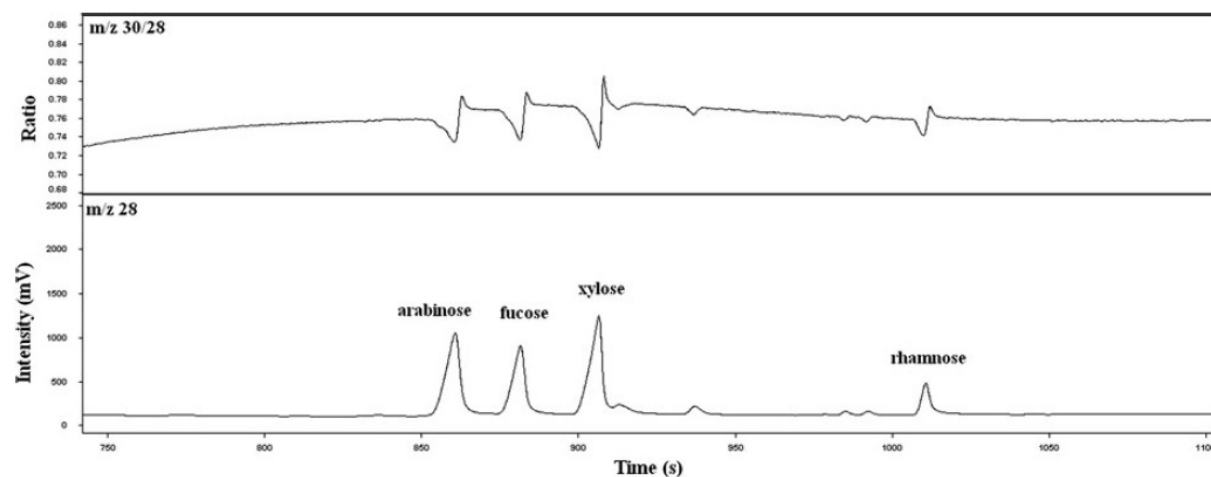


Fig. 2: Typical GC-Py-IRMS chromatogram for the sediment samples from Lake Panch Pokhari (sample 490 cm depth). Whereas the lower part of the figure shows the signal intensity of m/z 28 ($^{12}\text{C}^{16}\text{O}$), the upper part shows the ratio of m/z 30 to m/z 28 ($^{12}\text{C}^{18}\text{O}$ to $^{12}\text{C}^{16}\text{O}$).

2.3 Pollen analyses and calculation of a pollen-based index reflecting the Indian Summer Monsoon (ISM) strengt

For pollen analyses, sediment samples of 1 cc were prepared with HCl, KOH, HF and acetolysis (Erdtman 1960; Moore et al. 1999). Identification of palynological remains was carried out under 500x to 1250x magnification. About 200 pollen types were distinguished using literature and a reference collection of about 5,500 type slides (Beug and Miehle 1999; Beug 2004; Schlütz and Zech 2004). Pollen taxa (i.e. *Picea*, *Engelhardia*, *Shorea*) most likely representing one species in central Nepal are named accordingly (*Picea smithiana*, *Engelhardia spicata*, *Shorea robusta*) (Schlütz and Zech 2004). Calculation of pollen percentages is based on the sum of terrestrial plants, about 360 pollen grains per sample. From the identified arboreal pollen types, those representing one species (i.e. *Engelhardia spicata*) or a group of species (*Acer acuminatum*-type) with a clear geographic preference were identified and assigned to two groups (Table 2).

Table 2: Arboreal pollen taxa grouped according to their modern distribution.

Western Himalaya	Eastern Himalaya
<i>Acer acuminatum</i> -type	<i>Acer campbellii</i> -type
<i>Aesculus hippocastanum</i>	<i>Alchornea</i>
<i>Fraxinus excelsior</i> -type	<i>Castanopsis</i> -type
<i>Phyllanthus</i> -type	<i>Combretaceae</i> / <i>Melastomataceae</i>
<i>Picea smithiana</i>	<i>Engelhardia spicata</i>
<i>Pinus roxburghii</i>	<i>Fraxinus floribunda</i> -type
<i>Pinus wallichiana/gerardiana</i>	<i>Glochidion</i> -type
	<i>Mallotus</i> -type
	<i>Podocarpus neriifolius</i>
	<i>Schima wallichii</i>
	<i>Shorea robusta</i>

One group includes pollen types of trees and shrubs mostly restricted to the western Himalaya, a region with high snowfall in winter and relatively dry summer months. The second group consists of pollen types of trees and shrubs restricted to the eastern Himalaya, where the influence of the ISM is strong (Annotated checklist of the flowering plants of Nepal; Flora of China; Polunin and Stainton 1999). Using these two groups, the percentage contribution of eastern-derived pollen types was calculated for each sample. The percentage contributions were then transformed to a range from 0 to 1, with 1 corresponding to 100% pollen from the eastern part of the Himalaya, and used as index of the ISM strength (Fig. 3).

3. Results

3.1 Chronostratigraphy and TOC contents

Nine radiocarbon (^{14}C) dates were obtained for the alkali-insoluble organic matter fraction in sediment cores N1 and N2 (Table 1). The radiocarbon results suggest that sediments of Lake Panch Pokhari represent a valuable paleoenvironmental and climate archive of the late glacial and Holocene (Fig. 3). Sedimentation began after the cirque became deglaciated approximately 15.8 cal ka BP. The warm Bølling/Allerød interstadial (radiocarbon dates $14,369 \pm 290$ and $12,788 \pm 73$ cal a BP) is characterized by higher TOC content, whereas the colder period of the Younger Dryas is characterized by low TOC content (Fig. 3). The onset of the early Holocene is dated at $11,311 \pm 76$ cal a BP (N1) and $11,349 \pm 89$ cal a BP (N2). TOC contents enable correlation of sediment cores N1 and N2 (Fig. 3). Whereas calibrated ^{14}C ages and errors are illustrated in Fig. 3 in stratigraphic position, they are plotted by age in Fig. 4.

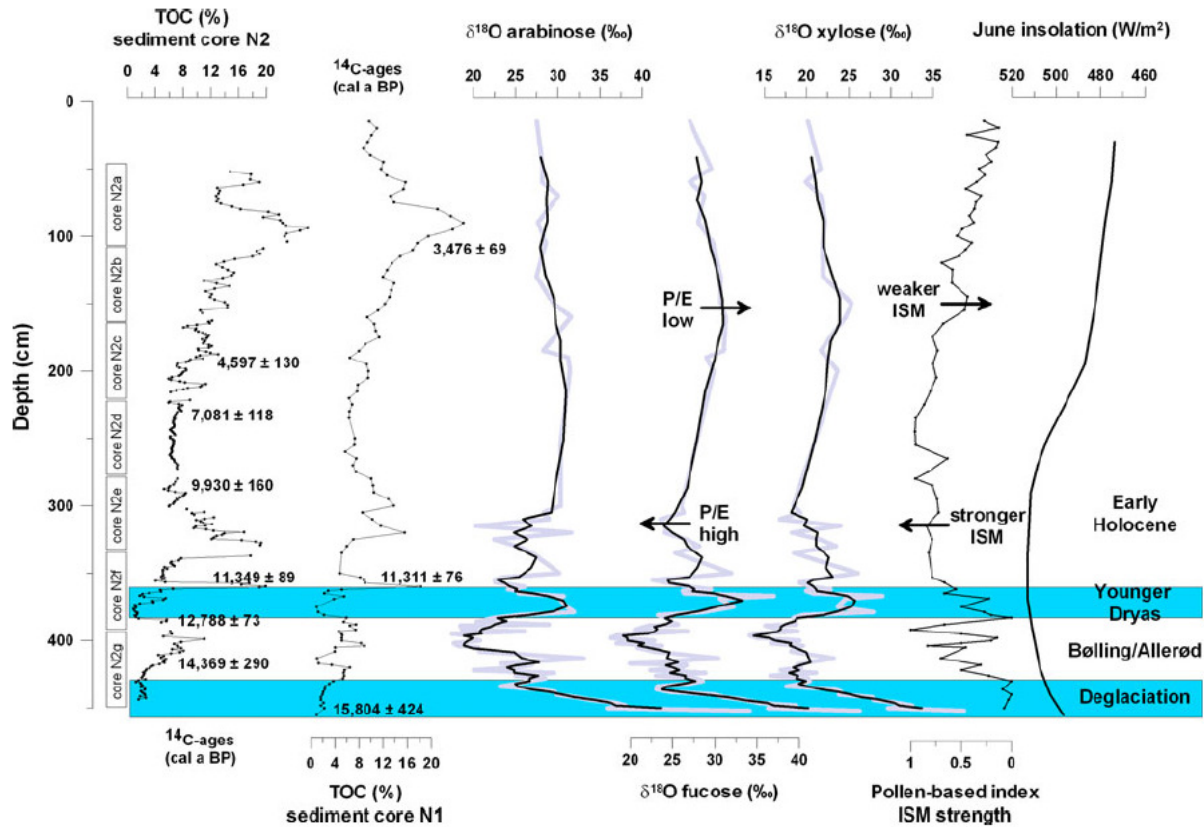


Fig. 3: Depth profiles for analytical results from the sediment cores of Lake Panch Pokhari. Total organic carbon (TOC) contents for sediment cores N1 and N2 are shown with the calibrated radiocarbon data given to the right. The $\delta^{18}\text{O}$ results of hemicellulose and polysaccharide sugar biomarkers (arabinose, fucose and xylose) extracted from core N1 (grey lines show all data, dark lines show the 3-point running mean) reflect the ratio of precipitation to evaporation (P/E). In addition, a pollen-based index of the strength of the Indian Summer Monsoon (ISM) and the July insolation at 30°N (Berger and Loutre 1991) are shown. The periods of deglaciation and Younger Dryas are depicted with horizontal blue bars.

3.2 Lake Panch Pokhari $\delta^{18}\text{O}$ sugar biomarker results

Compound-specific $\delta^{18}\text{O}$ values for sugar biomarkers arabinose, fucose and xylose range from 13.3 to 52.7‰ and reveal similar trends (Fig. 3). The long-term trends reveal dramatically decreasing $\delta^{18}\text{O}$ values during the deglaciation, with minimum values during the Bølling-Allerød interstadial and maximum $\delta^{18}\text{O}$ values during the Younger Dryas. During the

early Holocene, Lake Panch Pokhari $\delta^{18}\text{O}$ values were again lower, although not reaching the minimum values of the Bølling-Allerød. The middle Holocene is characterized by relatively high $\delta^{18}\text{O}$ values. At higher resolution, the individual $\delta^{18}\text{O}$ records of Lake Panch Pokhari are punctuated by numerous centennial-scale $\delta^{18}\text{O}$ shifts, particularly during the late glacial and the early Holocene (Figs. 3 and 4).

4. Discussion

4.1 Interpretation of the $\delta^{18}\text{O}$ sugar biomarker record of Lake Panch Pokhari

Concerning interpretation of the $\delta^{18}\text{O}$ record from Lake Panch Pokhari, we assumed that the sugar biomarkers were produced primarily by aquatic organisms. This is plausible, because the lake catchment is very small, with only scarce vegetation. Carbon/nitrogen ratios are generally ≤ 12 (Krstic et al. 2012) and thus do not indicate a significant input of terrestrial organic matter, which is typically characterized by higher ratios (Meyers and Ishiwatari 1993). Furthermore, the abundance of fucose (Fig. 2) may serve as a proxy for autochthonous organic matter, because fucose is only a minor component of vascular plants (Jia et al. 2008; Zech et al. 2012), whereas it is often very abundant in phytoplankton, zooplankton and bacteria (Hecky et al. 1973, Hicks et al. 1994, Biersmith and Benner 1998, Ogier et al. 2001).

Concerning incorporation of the $\delta^{18}\text{O}_{\text{lake water}}$ signal into the aquatic hemicelluloses and polysaccharides, an ^{18}O enrichment of approximately $+27\text{‰}$ during sugar metabolism has to be considered (DeNiro and Epstein 1981; Schmidt et al. 2001). Although generally determined by studying cellulose rather than hemicelluloses, this $+27\text{‰}$ biosynthetic fractionation factor is confirmed across diverse taxonomic groups and was long assumed not to vary with temperature. Recently, Sternberg and Ellsworth (2011) found evidence for slight, but systematically greater fractionation at lower temperatures. Given the wide range of sugar

biomarkers investigated here ($\delta^{18}\text{O}$ values range from 13.3 to 52.7‰), we suggest that our sedimentary $\delta^{18}\text{O}$ record primarily reflects the variability of $\delta^{18}\text{O}_{\text{lake water}}$. The isotopic composition of the lake water is controlled by the $\delta^{18}\text{O}$ of paleo-precipitation, modified by evaporative ^{18}O enrichment.

4.2 Comparison with other $\delta^{18}\text{O}$ records and modern precipitation

Our $\delta^{18}\text{O}$ sugar biomarker record closely resembles the late glacial Greenland ice core and Chinese speleothem $\delta^{18}\text{O}$ records (Wang et al. 2001; Dykoski et al. 2005; NGRIP members 2005) (Fig. 4). The magnitude of change in Chinese speleothem $\delta^{18}\text{O}$ records over the glacial-interglacial transition ($\sim 4\%$; Dykoski et al. 2005), however, is much smaller than the magnitude of change recorded in our lacustrine sequence. The weighted average for all three biomarkers ranges from 16.8 to 37.5‰ (3-point running mean, Fig. 4).

Excluding the first, high $\delta^{18}\text{O}$ values during deglaciation, the magnitude is 13.1‰. For comparison, the Guliya ice core on the Tibetan Plateau features a $\delta^{18}\text{O}$ shift of $\sim 10\%$ over the last glacial-interglacial cycle (Thompson et al. 2005), the Dasuopu ice core features an interannual $\delta^{18}\text{O}$ magnitude of $\sim 6\%$ from AD 1985 to 1995 (Tian et al. 2003) and the ostracode shells of Lake Qinghai feature a $\delta^{18}\text{O}$ range of $\sim 8\%$ during the late Pleistocene (Liu et al. 2007). It is important to keep in mind that there is strong seasonal $\delta^{18}\text{O}$ variability in modern precipitation from our study area. Data from the nearby Nyalam meteorological station (3,810 m a.s.l., N28°11', E85°58') show $\delta^{18}\text{O}_{\text{precipitation}}$ values greater than +5‰ from March to May and as low as -30‰ from June to September (Tian et al. 2003).

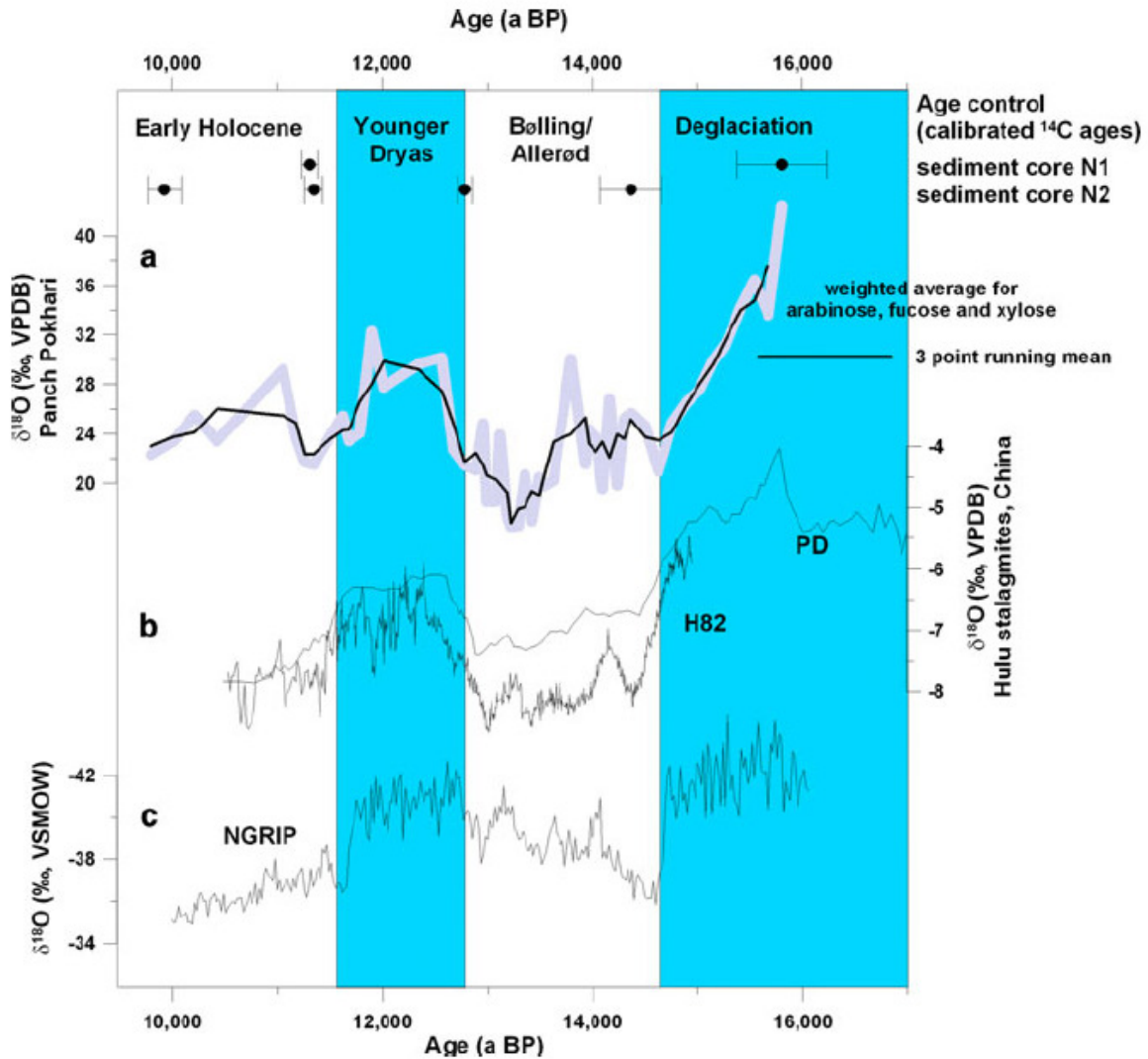


Fig. 4: Comparison of the Lake Panch Pokhari $\delta^{18}\text{O}$ record with other $\delta^{18}\text{O}$ records. a) The grey line shows the weighted average for arabinose, fucose and xylose; the dark line shows the 3-point running mean for the weighted average. b) Hulu stalagmites H82 and PD (Wang et al. 2001) and c) Greenland ice core $\delta^{18}\text{O}$ record (NGRIP members 2005) plotted versus time. Vertical blue bars highlight the periods of deglaciation and the Younger Dryas. Calibrated radiocarbon ages and errors are plotted for sediment cores N1 and N2. VSMOW = Vienna Standard Mean Ocean Water, VPDB = Vienna Pee Dee Belemnite.

4.3 Amount effect and source effect as influencing factors

The modern seasonal pattern, with relatively low $\delta^{18}\text{O}_{\text{precipitation}}$ values during summer, indicates that the ‘temperature-effect’ that predominates at high latitudes (Dansgaard 1964;

Araguas-Araguas et al. 2000) and on the Northern Tibetan Plateau (Tian et al. 2003), is of minor relevance in our study area. Rather, as in other monsoon-influenced regions, modern precipitation in Helambu Himal is characterized by low $\delta^{18}\text{O}$ values when the ISM is active and brings precipitation maxima. This is called the ‘amount-effect.’ The strength of the monsoon, and the area under its influence, has varied in the past. Hence, speleothem $\delta^{18}\text{O}$ records in South Asia (Wang et al. 2001; Fleitmann et al. 2003; Dykoski et al. 2005; Sinha et al. 2005; Shakun et al. 2007) are assumed to reflect $\delta^{18}\text{O}$ variations of precipitation and $\delta^{18}\text{O}$ is often interpreted as a proxy for the intensity of the ISM and the East Asian Summer Monsoon (EASM), respectively (Fig. 1). We therefore highlight the similarities between the Chinese speleothems and our late glacial and Holocene lacustrine $\delta^{18}\text{O}$ record from Panch Pokhari (Fig. 4). Accordingly, we suggest that high $\delta^{18}\text{O}$ values during the deglaciation and the Younger Dryas indicate a weak ISM, whereas lower $\delta^{18}\text{O}$ values during the Bølling-Allerød and the early Holocene indicate a strengthened ISM. This is in agreement with precipitation-controlled glacier advances in the Himalaya during the early late glacial and the early Holocene (Owen 2009). Notably, a Younger Dryas glacier advance has yet to be identified (Owen 2009).

In addition to monsoon strength, it is important to consider two ‘source effects’ when interpreting $\delta^{18}\text{O}$ variability of paleo-precipitation. First, the oxygen isotope composition of the Indian Ocean seawater was not constant during the late Glacial. Schrag et al. (2002) reported an average glacial-interglacial $\delta^{18}\text{O}$ decrease of 1‰ for seawater as a consequence of ^{18}O -depleted glacial meltwater. Assuming a linear relationship between sea level and seawater $\delta^{18}\text{O}$, Dykoski et al. (2005) suggested that the $\delta^{18}\text{O}$ value of the Indian Ocean decreased by ~0.35‰ from 16 to 11 ka, thus accounting for ~15% of the Dongge Cave speleothem $\delta^{18}\text{O}$ variability. This may, however, be an underestimation because this approach presumes a rapid and uniform mixing and distribution of the glacial meltwater via ocean circulation.

Furthermore, we suggest that accumulation of ^{18}O -enriched Indian Ocean sea surface water, as a consequence of evaporative losses, could have been much greater than acknowledged, especially during periods when the thermohaline-driven conveyor belt of deep ocean circulation slowed down, i.e. during the Younger Dryas event. This hypothesis is supported by the occurrence of increased salinity from 18 to 14.5 ka and during the Younger Dryas (Levi et al. 2007).

The second ‘source effect’ is also challenging to test quantitatively. The study area nowadays receives only minor winter precipitation. Given that monsoon precipitation is ^{18}O -depleted compared to winter precipitation brought by the Westerlies (Breitenbach et al. 2010), shifting atmospheric circulation patterns and hence changing ratios of winter to summer precipitation budgets, could yield changing mean annual $\delta^{18}\text{O}$ values of precipitation. This would point to a variability of the area of influence of the ISM, but does not necessarily require variability in the strength of the ISM.

As an additional proxy, we calculated a pollen-based index using pollen from the Eastern Himalaya as an indicator for a strong ISM and pollen from the Western Himalaya as an indicator of stronger Westerlies and therefore a weakened ISM. This index not only shows the orbitally driven, long-term trend of the ISM strength, but also confirms millennial-scale ISM variability, as indicated by our $\delta^{18}\text{O}$ record during the late Glacial (Fig. 3).

4.4 Evaporative ^{18}O enrichment as an influencing factor

Given that the glacial-interglacial transition is recorded by a shift in $\delta^{18}\text{O}$ in the range of $\sim 4\text{‰}$ in Chinese speleothem records, and up to $\sim 10\text{‰}$ in ice cores, we argue that the magnitude of $\delta^{18}\text{O}$ change within the lacustrine sequence cannot be explained by $\delta^{18}\text{O}$ variability of precipitation alone ($\sim 20\text{‰}$ for the weighted mean of all biomarkers, 3-point running mean; Fig. 4).

In particular, the high $\delta^{18}\text{O}$ values during deglaciation and the overall relatively high $\delta^{18}\text{O}$ values during the entire Holocene are unlikely to be explained by $\delta^{18}\text{O}_{\text{precipitation}}$ variability alone. We thus suggest that evaporative ^{18}O enrichment of the lake water was an amplifying factor and that our $\delta^{18}\text{O}$ record is a proxy for the ratio of local precipitation to evaporation (P/E). This is consistent with the interpretation of monsoon-influenced lacustrine $\delta^{18}\text{O}$ records from East Africa (Barker et al. 2011) and the Tibetan Plateau (Lister et al. 1991; Liu et al. 2007). Accordingly, P/E was low during the arid phases of the late glacial, i.e. during the deglaciation and the Younger Dryas. Using the weighted mean annual $\delta^{18}\text{O}_{\text{precipitation}}$ value (-13.6‰) of the nearby Nyalam meteorological station (Tian et al. 2003), it is possible to estimate the isotopic composition of sugar biomarkers during extreme aridity by combining the effects of monsoon precipitation, evaporation-induced isotopic enrichment and metabolic fractionation of hemicelluloses. Absence of summer monsoon precipitation with low $\delta^{18}\text{O}$ values results in $\delta^{18}\text{O}_{\text{precipitation}}$ values of ~0 to -5‰. During the very arid period of deglaciation, evaporative $^{18}\text{O}_{\text{lake water}}$ enrichment of +10‰ is assumed (adapted from the modern $^{18}\text{O}_{\text{lake water}}$ enrichment of Lake Qinghai, NE Tibetan Plateau; Henderson et al. 2010) and a fractionation factor of +27‰ for the hemicellulose metabolism is used. Combining these factors results in calculated $\delta^{18}\text{O}$ values of 32 to 37‰, and for comparison, the measured weighted average is 37.5‰ (3-point running mean).

In contrast, P/E was high during the humid Bølling-Allerød and the early Holocene. Relatively high $\delta^{18}\text{O}$ values during the generally warmer early Holocene, compared to the Bølling-Allerød interstadial (Figs. 3, 4), likely reflect the thermal control on evaporation as opposed to lower precipitation. This interpretation is in agreement with an evaporation-induced shift towards higher δD values of n-alkane biomarkers in lacustrine records from the Tibetan Plateau (Aichner et al. 2010). Both higher temperatures and increasing aridity are likely responsible for the relatively high $\delta^{18}\text{O}$ values during the middle Holocene (Fig. 3).

Enhanced aridity has been linked to the collapse of the Neolithic culture in Central China during this time (Wu and Liu 2004).

4.5 Driving mechanisms and North Atlantic – Indian Summer Monsoon teleconnections

The driving mechanism for the strength of the ISM and the EASM is the pressure gradient between the continental low over Asia and the high-pressure cells over the Southern Indian Ocean and the Western Pacific. Plausible factors affecting the pressure gradients are orbitally controlled changes in insolation (Berger and Loutre 1991) and changing stadial-interstadial or glacial-interglacial boundary conditions (Overpeck et al. 1996; Sirocko et al. 1996; An et al. 2011). Whereas on longer time scales, monsoon history is coupled to insolation changes at 30 °N in June (Leuschner and Sirocko 2003; Yuan et al. 2004; Herzsuh 2006), centennial and millennial changes in monsoon intensity recorded within high-resolution archives (e.g. speleothems and some marine records) are often correlated with North Atlantic climate events. The synchronicity of our High Himalayan lacustrine $\delta^{18}\text{O}$ record with the Greenland $\delta^{18}\text{O}$ record (Fig. 4) corroborates the strong North Atlantic – Indian Summer Monsoon teleconnections. These teleconnections can be explained by atmospheric and ocean circulation mechanisms. Accordingly, a Northern Hemisphere cooling weakens the sea-land pressure gradient in Southern Asia and thus the ISM. Similarly, increasing the Indian Ocean sea surface temperature by a slow-down of the thermohaline-driven conveyor belt of the deep ocean circulation, for instance during the Younger Dryas, weakens the sea-land pressure gradient and thus the ISM as well.

5. Conclusions

Sediments of Lake Panch Pokhari provide a valuable late glacial climate archive for the High Himalaya. A lacustrine $\delta^{18}\text{O}$ record was established by applying novel compound-specific $\delta^{18}\text{O}$ analysis of sugar biomarkers. All three biomarkers, i.e. hemicellulose-derived arabinose and xylose and algae-derived fucose, revealed similar, systematic $\delta^{18}\text{O}$ variations, with low $\delta^{18}\text{O}$ values coinciding with the Bølling-Allerød and the early Holocene and higher $\delta^{18}\text{O}$ values coinciding with the deglaciation and the Younger Dryas. The $\delta^{18}\text{O}$ biomarker record is controlled by both “amount” and “source” effects, as well as evaporative $^{18}\text{O}_{\text{lakewater}}$ enrichment. Overall, our $\delta^{18}\text{O}$ record reflects the ratio of amounts of precipitation and evaporation (P/E) and allows reconstruction of ISM variability.

The Lake Panch Pokhari $\delta^{18}\text{O}$ record largely resembles the East Asian speleothem $\delta^{18}\text{O}$ records, indicating that the ISM and the EASM are driven by the same mechanisms. Importantly, similarities to the Greenland ice core $\delta^{18}\text{O}$ records support the previously suggested strong North Atlantic – Indian Summer Monsoon teleconnections.

Acknowledgements

We thank B. Huwe, K. Kharki, S. Markovic and L. Zöllner for logistic support and discussions and A. Mergner and S. Bösel for laboratory assistance. Proof-reading was kindly provided by C. Gallant and Editor in Chief M. Brenner. We thank three anonymous reviewers and Guest Editor S. Mischke for constructive reviews and valuable comments on our manuscript. This work was partly funded by the German Research Foundation (DFG ZE 844/1-2) and the Volkswagen Foundation. M. Zech also greatly acknowledges the support given by the Alexander von Humboldt-Foundation.

References

- An S, Clemens SC, Shen J, Qiang X, Jin Z, Sun Y, Prell WL, Luo J, Wang S, Xu H, Cai Y, Zhou W, Liu X, Liu W, Shi Z, Yan L, Xiao X, Chang H, Wu F, Ai L, Lu F (2011) Glacial-Interglacial Indian Summer Monsoon dynamics. *Science* 333:719-723
- Annotated checklist of the flowering plants of Nepal. http://www.efloras.org/flora_page.aspx?flora_id=110
- Aichner B, Herzsich U, Wilkes H, Vieth A, Böhner J (2010) δD values of n-alkanes in Tibetan lake sediments and aquatic macrophytes – A surface sediment study and application to a 16 ka record from Lake Koucha. *Org Geochem* 41:779-790
- Amelung W, Cheshire MV, Guggenberger G (1996) Determination of neutral and acidic sugars in soil by capillary gas-liquid chromatography after trifluoroacetic acid hydrolysis. *Soil Biol Biochem* 28:1631-1639
- Araguas-Araguas L, Froehlich K, Rozanski K (2000) Deuterium and oxygen-18 isotope composition of precipitation and atmospheric moisture. *Hydrol Process* 14:1341-1355
- Barker PA, Hurrell ER, Leng MJ, Wolff C, Cocquyt C, Sloane HJ, Verschuren D (2011) Seasonality in equatorial climate over the past 25 k.y. revealed by oxygen isotope records from Mount Kilimanjaro. *Geology* 39:1111-1114
- Berger AL, Loutre MF (1991) Insolation values for the climate of the last 10 million years. *Quat Sci Rev* 10:297-317
- Beug H-J (2004) Leitfaden der Pollenbestimmung für Mitteleuropa und angrenzende Gebiete. Pfeil, München
- Beug H-J, Miehe G (1999) Vegetation history and human impact in the eastern Central Himalaya (Langtang and Helambu, Nepal). *Dissertationes Botanicae* 318:1-98
- Biersmith A and Benner R (1998) Carbohydrates in phytoplankton and freshly produced dissolved organic matter. *Mar Chem* 63:131-144
- Breitenbach S, Adkins J, Meyer H, Marwan N, Kumar K, Haug G (2010) Strong influence of water vapor source dynamics on stable isotopes in precipitation observed in Southern Meghalaya, NE India. *Earth Planet Sci Lett* 292:212-220
- Dansgaard P (1964) Stable isotopes in precipitation. *Tellus* 16:436-468
- Danzeglocke U, Jöris O, Weninger B (2012) CalPal-2007online. Available at: <http://www.calpal.online/> (last access: October 2012)

- DeNiro MJ and Epstein S (1981) Isotopic composition of cellulose from aquatic organisms. *Geochim Cosmochim Acta* 45:1885-1894
- Dykoski CA, Edwards RL, Cheng H, Yuan D, Cai Y, Zhang M, Lin Y, Qing J, An Z, Revenaugh J (2005) A high-resolution, absolute-dated Holocene and deglacial Asian monsoon record from Dongge Cave, China. *Earth Planet Sci Lett* 233:71-86
- Erdtman G (1960) The acetolysis method. *Svensk Botanisk Tidskrift* 54:561-564
- Fleitmann D, Burns SJ, Mudelsee M, Neff U, Kramers J, Mangini A, Matter A (2003) Holocene forcing of the Indian Monsoon recorded in a stalagmite from Southern Oman. *Science* 300:1737-1739
- Flora of China. http://www.efloras.org/flora_page.aspx?flora_id=2.
- Fukui K, Jujii Y, Ageta Y, Asachi K (2007) Changes in lower limit of mountain permafrost between 1973 and 2004 in the Khumbu Himal, the Nepal Himalayas. *Glob Planet Change* 55:251-256.
- Hecky RE, Mopper K, Kilham P, Degens ET (1973) The amino acid and sugar composition of diatom cell-walls. *Mar Biol* 19:323-331
- Hicks RE, Owen CJ, Aas P (1994) Deposition, resuspension, and decomposition of particulate organic matter in the sediments of Lake Itasca, Minnesota, USA. *Hydrobiologia* 284:79-91
- Henderson A, Holmes J, Leng M (2010) Late Holocene isotope hydrology of Lake Qinghai, NE Tibetan Plateau: effective moisture variability and atmospheric circulation changes. *Quat Sci Rev* 29:2215-2223
- Herzschuh U (2006) Palaeo-moisture evolution in monsoonal Central Asia during the last 50,000 years. *Quat Sci Rev* 25:163-178
- Jia G, Dungait JAJ, Bingham EM, Valiranta M, Korhola A, Evershed RP (2008) Neutral monosaccharides as biomarker proxies for bog-forming plants for application to palaeovegetation reconstruction in ombrotrophic peat deposits. *Org Geochem* 39:1790-1799
- Kitagawa H, Tareq SM, Matsuzaki H, Inoue N, Tanoue E, Yasuda Y (2007) Radiocarbon concentration of lake sediment cellulose from Lake Erhai in southwest China. *Nucl Instrum Meth B* 259:526-529
- Knapp DR (1979) *Handbook of analytical derivatisation reaction*. John Wiley & Sons, New York

- Krstic S, Zech W, Obreht I, Svircev Z, Markovic SB (2012) Late Quaternary environmental changes in Helambu Himal, Central Nepal, recorded in the diatom flora assemblage composition and geochemistry of Lake Panch Pokhari. *J Paleolimnol* 47:113-124
- Leuschner DC, Sirocko F (2003) Orbital insolation forcing of the Indian Monsoon - a motor for global climate changes? *Palaeogeogr Palaeoclimatol Palaeoecol* 197:83-95
- Levi C, Labeyrie L, Bassinot F, Guichard F, Cortijo E, Waelbroeck C, Caillon N, Duprat J, Garidel-Thoron T, Elderfield H (2007) Low-latitude hydrological cycle and rapid climate changes during the last deglaciation. *Geochem Geophys Geosys* 8(Q05N12): doi:10.1029/2006GC001514
- Lister GS, Kelts K, Zao CK, Yu J-Q, Niessen F (1991) Lake Qinghai, China: closed-basin lake levels and oxygen isotope record for ostracoda since the latest Pleistocene. *Palaeogeogr Palaeoclimatol Palaeoecol* 84:141-182
- Liu X, Shen J, Wang S, Wang Y, Liu W (2007) Southwest monsoon changes indicated by oxygen isotope of ostracode shells from sediments in Qinghai Lake since the late Glacial. *Chin Sci Bull* 52:539-544
- Meyers P and Ishiwatari R (1993) Lacustrine organic geochemistry - an overview of indicators of organic matter sources and diagenesis in lake sediments. *Org Geochem* 20:867-900
- Mischke S, Aichner B, Diekmann B, Herzsuh U, Plessen B, Wünnemann B, Zhang C (2010) Ostracods and stable isotopes of a late glacial and Holocene lake record from the NE Tibetan Plateau. *Chem Geol* 276:95-103
- NGRIP members (2005) Greenland ice core chronology 2005 (GICC05) and 20 year mean of $\delta^{18}\text{O}$ data from NGRIP and GRIP. Available online at: http://www.gfz.ku.dk/~www-glac/ngrip/index_eng.htm
- Moore PD, Webb JA, Collinson ME (1999) *Pollen analysis*. Blackwell, Oxford
- Ogier S, Disnar J-R, Albéric P, Bourdier G (2001) Neutral carbohydrate geochemistry of particulate material (trap and core sediments) in an eutrophic lake (Aydat, France). *Org Geochem* 32:151-162
- Overpeck J, Anderson D, Trumbore S, Prell WL (1996) The southwest Indian monsoon over the last 18,000 years. *Clim Dynam* 12:213-225
- Owen L (2009) Latest Pleistocene and Holocene glacier fluctuations in the Himalaya and Tibet. *Quat Sci Rev* 28:2150-2164
- Pizer R and Tihal C (1992) Equilibria and reaction mechanism of the complexation of methylboronic acid with polyols. *Inorg Chem* 31:3243-3247

- Polunin O, Stainton A (1999) *Flowers of the Himalaya*. University Press, Oxford
- Saurer M and Siegwolf R (2004) Pyrolysis techniques for oxygen isotope analysis of cellulose. In: de Groot PA (ed) *Handbook of stable isotope analytical techniques*, (vol 1). Elsevier B.V., New York, pp 497-508
- Schlütz F and Zech W (2004) Palynological investigations on vegetation and climate change in the late Quaternary of Lake Rukche area, Gorkha Himal, Central Nepal. *Veg Hist Archaeobot* 13:81-90
- Schmidt, H.-L., Werner, R., Roßmann, A. (2001) ^{18}O Pattern and biosynthesis in natural plant products. *Phytochemistry* 58:9-32
- Schrag D, Adkins J, McIntyre K, Alexander J, Hodell D, Charles C, McManus J (2002) The oxygen isotopic composition of seawater during the Last Glacial Maximum. *Quat Sci Rev* 21:331-342
- Shakun J, Burns S, Fleitmann D, Kramers J, Matter A (2007) A high-resolution, absolute-dated deglacial speleothem record of Indian Ocean climate from Socotra Island, Yemen. *Earth Planet Sci Lett* 259:442-456
- Sinha A, Cannariato KG, Stott LD, Li H-C, You C-F, Cheng H, Edwards RL, Singh IB (2005) Variability of Southwest Indian summer monsoon precipitation during the Bølling-Allerød. *Geology* 33:813-816
- Sirocko F, Garbe-Schönberg D, McIntyre A, Molino B (1996) Teleconnections between the subtropical monsoons and high-latitude climates during the last deglaciation. *Science* 272:526-529
- Sternberg L and Ellsworth PFV (2011) Divergent biochemical fractionation, not convergent temperature, explains cellulose oxygen isotope enrichment across latitudes. *Plos One* 6:e28040. doi:10.1371/journal.pone.0028040
- Sternberg L and DeNiro MJ (1983) Bio-geochemical implications of the isotopic equilibrium fractionation factor between oxygen atoms of acetone and water. *Geochim Cosmochim Acta* 47:2271-2274
- Tian L, Yao T, Schuster P, White J, Ichiyanagi K, Pendall E, Pu J, Yu W (2003) Oxygen-18 concentrations in recent precipitation and ice cores on the Tibetan Plateau. *J Geophys Res* 108(D9), 4293, doi:10.1029/2002JD002173
- Thompson LG, Davis ME, Mosley-Thompson E, Lin P-N, Henderson KA, Mashiotta TA (2005) Tropical ice core records: evidence for asynchronous glaciation on Milankovitch timescales. *J Quat Sci* 20:723-733

- Thompson LG, Yao T, Davis ME, Henderson KA, Mosley-Thompson E, Lin PN, Beer J, Synal HA, Cole-Dai J, Bolzan JF (1997) Tropical climate instability: the last glacial cycle from a Qinghai-Tibetan ice core. *Science* 276:1821-1825
- Wang Y, Cheng H, Edwards RL, An ZS, Wu JY, Shen C-C, Dorale JA (2001) A high-resolution absolute-dated Late Pleistocene monsoon record from Hulu Cave, China. *Science* 294:2345-2348
- Wissel H, Mayr C, Lücke A (2008) A new approach for the isolation of cellulose from aquatic plant tissue and freshwater sediments for stable isotope analysis. *Org Geochem* 39:1545-1561
- Wolfe BB, Falcone M, Clogg-Wright K, Mongeon C, Yi Y, Brock B, Amour N, Mark W, Edwards TWD (2007) Progress in isotope paleohydrology using lake sediment cellulose. *J Paleolimnol* 37:221-231
- Wu W and Liu T (2004) Possible role of the ‘‘Holocene Event 3’’ on the collapse of Neolithic cultures around the central plain of China. *Quat Int* 117:153-166
- Yuan D, Cheng H, Edwards RL, Dykoski CA, Kelly MJ, Zhang M, Qing J, Lin Y, Wang Y, Wu J, Dorale JA, An ZS, Cai Y (2004) Timing, duration, and transition of the Last Interglacial Asian Monsoon. *Science* 304:575-578
- Zech M and Glaser B (2009) Compound-specific $\delta^{18}\text{O}$ analyses of neutral sugars in soils using GC-Py-IRMS: problems, possible solutions and a first application. *Rapid Commun Mass Spec* 23:3522-3532
- Zech M, Werner R, Juchelka D, Kalbitz K, Buggle B, Glaser B (2012) Absence of oxygen isotope fractionation/exchange of (hemi-) cellulose derived sugars during litter decomposition. *Org Geochem* 42:1470-1475
- Zhang J, Chen F, Holmes JA, Li H, Guo X, Wang J, Li S, Lü Y, Zhao Y, Qiang M (2011) Holocene monsoon climate documented by oxygen and carbon isotopes from lake sediments and peat bogs in China: a review and synthesis. *Quat Sci Rev* 30:1973-1987

Study 6

Coupled ^{18}O and ^2H isotopes of biomarkers record lake evaporation history and allow reconstructing the isotopic composition of precipitation

Mario Tuthorn^{1,*}, Johannes Hepp¹, Roland Zech², Ines Mügler³, Wolfgang Zech¹, Michael Zech^{1,4}

¹) Department of Soil Physics and Chair of Geomorphology, University of Bayreuth, Universitätsstrasse 30, D-95440 Bayreuth, Germany

²) Geological Institute, ETH Zurich, Sonneggstrasse 5, CH-8092 Zurich, Switzerland

³) Max Planck Institut for Biogeochemistry, Hans-Knöll Strasse 10, D-07745 Jena, Germany

⁴) Institute of Agronomy and Nutritional Sciences, Soil Biogeochemistry, Martin-Luther University Halle-Wittenberg, von-Seckendorff-Platz 3, D-06120 Halle, Germany

^{*}) corresponding author: mariothrn@windowslive.com, phone: +49 921 55 2178

Submitted to Journal of Hydrology

Highlights

- $\delta^{18}\text{O}$ and $\delta^2\text{H}$ biomarker records were established for a lake sediment archive
- The 16 ka $\delta^{18}\text{O}_{\text{sugar}}$ and $\delta^2\text{H}_{n\text{-alkane}}$ biomarker records are similar but not identical
- Differences are explicable with evaporative isotopic enrichment of lake water
- Reconstructed d-excess of lake water can serve as proxy for evaporative losses
- A coupled $\delta^{18}\text{O}$ - $\delta^2\text{H}$ approach allows a model-based reconstruction of $\delta^{18}\text{O}_{\text{prec}}$

Abstract

Over the past decades, $\delta^{18}\text{O}$ and $\delta^2\text{H}$ analyses of lacustrine sediments became an invaluable tool in paleohydrology and paleolimnology for reconstructing the isotopic composition of past lake water and precipitation. However, based on $\delta^{18}\text{O}$ or $\delta^2\text{H}$ records alone, it can be challenging to distinguish between changes of the precipitation signal and changes of evaporation. Here we propose a coupled $\delta^{18}\text{O}$ - $\delta^2\text{H}$ biomarker approach that offers the possibility to disentangle between these two factors. The isotopic composition of *n*-alkanes were analysed in order to establish a 16 ka Late Glacial and Holocene $\delta^2\text{H}$ record for the sediment archive of Lake Panch Pokhari in High Himalaya, Nepal. The $\delta^2\text{H}_{n\text{-alkane}}$ record generally corroborates a previously established $\delta^{18}\text{O}_{\text{sugar}}$ record reporting on high values characterising the deglaciation and the Older and the Younger Dryas, and low values characterising the Bølling and the Allerød periods. Since the investigated *n*-alkane and sugar biomarkers are considered to be primarily of aquatic origin, they were used to reconstruct the isotopic composition of lake water. The reconstructed deuterium excess of lake water ranges from +57 ‰ to -85 ‰ and can serve as proxy for the evaporation history of Lake Panch Pokhari. Lake desiccation during the deglaciation, the Older Dryas and the Younger Dryas is corroborated by a multi-proxy approach using additionally the Hydrogen Index (HI) and the carbon to nitrogen ratio (C/N) as proxies for lake sediment organic matter mineralisation. Furthermore, the coupled $\delta^{18}\text{O}$ and $\delta^2\text{H}$ approach allows disentangling the lake water isotopic enrichment from variations of the isotopic composition of precipitation. The reconstructed 16-ka $\delta^{18}\text{O}_{\text{precipitation}}$ record of Lake Panch Pokhari is well in agreement with the $\delta^{18}\text{O}$ records of Chinese speleothems and presumably reflects the Indian Summer Monsoon variability.

Keywords: *n*-alkanes, sugars, stable water isotopes, d-excess, evaporation, lake desiccation,

1. Introduction

Biomarker and stable isotope analyses became an indispensable tool in many different scientific fields. In paleohydrology and paleoclimatology, stable oxygen ($^{18}\text{O}/^{16}\text{O}$) and hydrogen ($^2\text{H}/^1\text{H}$) isotopes are of especial interest because the isotopic composition of precipitation is known to depend primarily on climatic conditions such as temperature and precipitation amount (Craig, 1961; Dansgaard, 1964; Craig & Gordon, 1965; Rozanski *et al.*, 1982). Hence, various kinds of archives are investigated in order to reconstruct the isotopic composition of precipitation and thus paleoclimate (Dansgaard *et al.*, 1993; Roden *et al.*, 2000; Cruz *et al.*, 2005; Thompson *et al.*, 2005; Loader *et al.*, 2008; Rao *et al.*, 2009; Li *et al.*, 2011; Zech *et al.*, 2013).

With regard to lacustrine sediments, which have been recognised to be often excellent climate archives, $\delta^{18}\text{O}$ and $\delta^2\text{H}$ analyses are performed for instance on carbonates of ostracod shells, on silica of diatoms, on aquatic cellulose, on hemicellulose-derived sugar biomarkers or on leaf wax-derived *n*-alkanes (Sauer *et al.*, 2001; Huang *et al.*, 2004; Sachse *et al.*, 2004; Wissel *et al.*, 2008; Mischke *et al.*, 2010; Chaplignin *et al.*, 2012; Zech *et al.*, 2014b). All these methods have their own advantages and disadvantages, but overall the results are in many paleoclimate studies considered to reflect primarily the isotopic composition of precipitation. However, lake water does not always simply reflect the isotopic composition of precipitation. Especially under arid and semiarid climatic conditions, lake water is becoming enriched in ^{18}O and ^2H due to evaporation and involving isotopic fractionation processes. While this offers the intriguing possibility to reconstruct lake water evaporation history (e.g. Mayr *et al.*, 2007; Muegler *et al.*, 2008; Aichner *et al.*, 2010a), a major constraint of single isotope studies (based on $\delta^{18}\text{O}$ or $\delta^2\text{H}$ results alone) can be how to distinguish between changes of the precipitation signal and changes of evaporation.

In this study we propose as possible solution for the above presented constraint a coupled $\delta^{18}\text{O}$ and $\delta^2\text{H}$ biomarker approach. We (i) established a lacustrine $\delta^2\text{H}$ record based on *n*-alkane biomarkers for late glacial – Holocene sediments of Lake Panch Pokhari, Nepal. (ii) The $\delta^2\text{H}_{n\text{-alkane}}$ record is compared with a previously published $\delta^{18}\text{O}$ record of sugar biomarkers (Zech *et al.*, 2014b). (iii) Using the biomarker records, the isotopic composition of lake water is reconstructed and the deuterium excess of lake water is evaluated as proxy for lake evaporation history. (iv) Lastly, we present a model-based reconstruction of $\delta^{18}\text{O}$ and $\delta^2\text{H}$ values of paleoprecipitation ($\delta^{18}\text{O}_{\text{prec}}$ and $\delta^2\text{H}_{\text{prec}}$, respectively).

2. Material and methods

2.1 Study area – Lake Panch Pokhari, Helambu Himal, Nepal

A detailed description of the study area was provided previously by Krstic *et al.* (2012) and Zech *et al.* (2014b). In brief, Lake Panch Pokhari is located at 4050 m a.s.l., about 100 km north of Kathmandu in the Helambu Himal, Nepal (28°02.533'N; 85°42.822'E; Fig. 1). It is of glacial origin, became ice-free around 16 cal ka BP when sedimentation started according to radiocarbon data, it is rainwater fed and about 2 m deep. Importantly for this study, Lake Panch Pokhari is surrounded by a very small catchment and it has a small, but non-permanent outflow. The catchment is scarcely vegetated so that in all likelihood the vast majority of the sedimentary organic material of Lake Panch Pokhari is of autochthonous rather than of allochthonous origin.

The study area is influenced by the Indian Summer Monsoon causing heavy rainfall between May and September and the Westerlies causing minor winter precipitation. Modern day mean annual precipitation at the close-by meteorological station Nyalam (3810 m a.s.l., 28 km northeast) is 650 mm and mean annual temperature is about 3.5 °C (Tian *et al.*, 2003).

However, it is widely accepted that monsoon precipitation strongly varied during the past (Wang *et al.*, 2001; Dykoski *et al.*, 2005; Mischke & Chen, 2014).

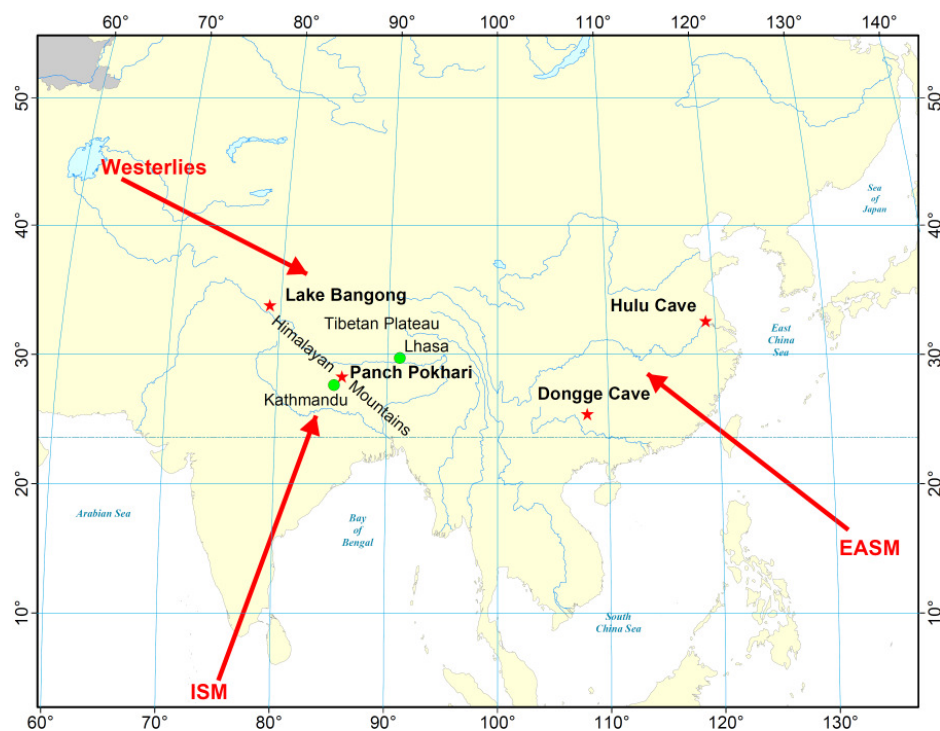


Fig. 1: Location of Lake Panch Pokhari, Helambu Himalaya, Nepal. The most prominent atmospheric circulation pattern influencing the study area are additionally depicted (Westerlies, ISM - Indian Summer Monsoon, EASM - East Asian Summer Monsoon).

Two overlapping sediment cores (N1 and N2) were taken from the middle of Lake Panch Pokhari in April 2001. Already in the field, the N1 sediment core was sampled at 5 cm core intervals in the upper part (0-3.5 m) and at 2 cm intervals in the lower and laminated part (3.5-4.5 m). The N2 sediment cores N2a to N2g were retrieved intact and later on sampled at 1 cm intervals in the laboratory. For the here presented *n*-alkane and sugar biomarker analyses, oven-dried (40 °C) sediment samples of core N1 were investigated.

2.2 Compound-specific $\delta^2\text{H}$ analyses of *n*-alkanes

n-Alkane biomarkers from 38 sediment samples were prepared according to a slightly modified procedure described by Zech and Glaser (2008) in the Laboratory of the Department

of Soil Physics, University of Bayreuth, Germany. Briefly, the procedure involves extraction of lipids with methanol/toluene (7/3) using an accelerated solvent extractor (ASE 200, Dionex, Germering, Germany) and purification of *n*-alkanes on silica/aluminium oxide (both 5% deactivated) columns with hexane/toluene (85/15) as eluent.

$\delta^2\text{H}$ values of the alkanes *n*-C₂₅, *n*-C₂₇, *n*-C₂₉ and *n*-C₃₁ recovered from the sediment samples were determined in the Stable Isotope Laboratory of the Max Planck Institute, Jena, Germany, using a HP5890 gas chromatograph equipped with a DB-5 ms column (30 m × 0.32 mm i.d., 0.5 µm film thickness, Agilent). The gas chromatograph was coupled via a high-temperature conversion oven operated at 1425 °C (Hilkert *et al.*, 1999) to an isotope ratio mass spectrometer (Delta^{plus}XL, Finnigan MAT, Bremen, Germany) for compound-specific $\delta^2\text{H}$ analyses. Each sample was analyzed in triplicate. Note that short- and mid-chained *n*-alkanes were less abundant and therefore did not withstand linearity criteria in most samples.

All $\delta^2\text{H}$ values were normalized to the VSMOW (Vienna Standard Mean Ocean Water) scale using a mixture of *n*-alkanes (*n*-C₁₀ to *n*-C₃₂). The $\delta^2\text{H}$ values of the *n*-alkanes in the standard mixture were calibrated against internal references (NBS-22, IAEA-OH22) using TC/EA-IRMS. The accuracy and drift of the system were evaluated via three standard measurements after every three samples (nine injections). To ensure stable ion source conditions the H_3^+ factor was determined at least once a day. Mean $\delta^2\text{H}$ values and standard deviations for triplicate measurements of the alkanes *n*-C₂₅, *n*-C₂₇, *n*-C₂₉, and *n*-C₃₁ are given in Table 1. Weighted mean $\delta^2\text{H}$ values over all four *n*-alkanes are plotted versus sediment depth in Fig. 2a and against sugar biomarker $\delta^{18}\text{O}$ results (from Zech *et al.*, 2014b) in a $\delta^2\text{H}$ - $\delta^{18}\text{O}$ -diagram in Fig. 3.

3. Theory/calculation

3.1 $\delta^{18}\text{O}$ - $\delta^2\text{H}$ diagram

Precipitation world-wide typically plots along the so-called global meteoric water line (GMWL) in a $\delta^{18}\text{O}$ - $\delta^2\text{H}$ diagram (Fig. 3) (Dansgaard, 1964). Due to fractionation processes, evaporation causes evaporating water to be isotopically depleted in ^{18}O and ^2H . By contrast, residual water, for instance lake water, becomes enriched in ^{18}O and ^2H . However, this enrichment does not follow the GMWL but rather a so-called local evaporation line (LEL) (Fig.3). This is caused by the kinetic effect resulting in slower diffusivity of the $^1\text{H}^1\text{H}^{18}\text{O}$ molecules compared to the $^2\text{H}^1\text{H}^{16}\text{O}$ molecules.

3.2 Model-based reconstruction of $\delta^{18}\text{O}_{\text{prec}}$ and $\delta^2\text{H}_{\text{prec}}$ values

The isotopic evaporative enrichment under steady-state conditions in open water bodies can be described as an isotopic mass balance model (Craig & Gordon, 1965). Assuming equilibrium conditions between isotopic composition of atmospheric vapor and total inflow leads to the following equation (Gat & Bowser, 1991):

$$\delta_{LS} - \delta_{IT} \cong \frac{(1-h_N)\epsilon^* + \Delta\epsilon}{h_N + (1-h_N)\frac{I_{TOT}}{E}} \quad (\text{Eqn. 1})$$

where:

I_{TOT} - total inflow (precipitation, surface water and groundwater inflow),

E - evaporation rate,

h_N - relative humidity normalized to the ground temperature (%),

δ_{LS} - isotopic composition of lake water under steady state conditions (‰),

δ_{IT} - isotopic composition of the total inflow components (‰),

$\Delta\varepsilon$ - kinetic isotopic enrichment,

ε^* - equilibrium isotopic enrichment.

The kinetic isotopic enrichment ($\Delta\varepsilon$) can be expressed according to Gonfiantini (1986) as:

$$\Delta\varepsilon = nC_k\Theta(1-h_N) \quad (\text{Eqn. 2})$$

where n is a turbulence parameter, C_k is kinetic fractionation factor for ^{18}O and/or ^2H and Θ is advection parameter which takes humidity buildup into account (Gibson *et al.*, 2008). Under turbulent conditions, the commonly used value for n equals 0.5 (Merlivat, 1978; Vogt, 1978; Gonfiantini, 1986; Gibson, 2001), whereas Θ can be set to 1 for small water bodies because the influences of the evaporation flux on the surrounding humidity is minor (Gat, 1995). Therefore kinetic fractionation factors reach only half of their maximum extent, 12.4‰ and 14.3‰ for $nC_k^2\Theta$ and $nC_k^{18}\Theta$, respectively (Vogt, 1978; Gonfiantini, 1986; Araguas-Araguas *et al.*, 2000). The equilibrium isotopic enrichment can be calculated as:

$$\varepsilon^* = \left(1 - \frac{1}{\alpha_{L/V}}\right) \cdot 10^3, \quad (\text{Eqn. 3})$$

where $\alpha_{L/V}$ describes the temperature dependent equilibrium fractionation factor for ^{18}O and/or ^2H . Eqn. 3 can be derived by empirical equations after Horita and Wesolowski (1994). We use here a constant temperature of 10°C which results in values of 92.55‰ and 10.67‰ for ε_2^* and ε_{18}^* , respectively. Note that the temperature is negligible compared to the measurement errors of biomarker analyses (Zech *et al.*, 2013).

Using Eqn. 1 and considering the definition of kinetic fractionation, the slope of the local water evaporation line (LEL) can be described as follows:

$$S_{LEL} = \frac{\delta_{LS}^2 - \delta_{IT}^2}{\delta_{LS}^{18} - \delta_{IT}^{18}} = \frac{(1-h_N)\varepsilon_2^* + \Delta\varepsilon_2}{(1-h_N)\varepsilon_{18}^* + \Delta\varepsilon_{18}} = \frac{(1-h_N)(\varepsilon_2^* + nC_k^2\Theta)}{(1-h_N)(\varepsilon_{18}^* + nC_k^{18}\Theta)} = \frac{\varepsilon_2^* + nC_k^2\Theta}{\varepsilon_{18}^* + nC_k^{18}\Theta}. \quad (\text{Eqn. 4}).$$

Given the premise that that paleoprecipitation plotted along the GMWL, Eqn. 3 can be used to reconstruct the isotopic composition of precipitation by calculating the intersection between the individual LELs (for a given lake water data point) and the GMWL. Using the above presented fractionation factors we calculated slope (S_{LEL}) of 4.2 for the LEL.

Note that Eqn. 4 is independent of relative humidity and it only depends on the fractionation factors which are valid under isotopic equilibrium conditions between total inflow and local atmospheric water vapor (Gat, 1971; Gat & Bowser, 1991). However, recent studies suggest that S_{LEL} is not independent of climate, as assumed in the Craig-Gordon model (Gibson *et al.*, 2005; Gibson *et al.*, 2008). Therefore we use additional slopes to reconstruct the isotopic composition of paleoprecipitation. Water samples of the Bangong lake system in western Tibet (Fontes *et al.*, 1996) show a slope of 3.5 for the LEL due to high potential evaporation and low relative humidity. Still, Gibson *et al.* (2008) presents that S_{LEL} in high-latitudes of Himalaya generally ranges from 4 to 5. To cover a possible climatic range we use S_{LEL} values of 5 and 3.5 for additional reconstructions of the isotopic composition of precipitation. This offers a confidence interval for the reconstructed $\delta^{18}\text{O}_{\text{prec}}$ and $\delta^2\text{H}_{\text{prec}}$ values (Fig. 2c and d).

Note furthermore that no reconstruction is calculated for lake water data points lying left of the GMWL (Fig. 3). These data points imply that no evaporation occurred and lake water reflects the isotopic composition of precipitation.

4. Results and Discussion

4.1 Lake Panch Pokhari $\delta^2\text{H}_{n\text{-alkane}}$ record and comparison with the $\delta^{18}\text{O}_{\text{sugar}}$ record

The $\delta^2\text{H}$ values of the four analysed *n*-alkanes *n*-C₂₅, *n*-C₂₇, *n*-C₂₉, and *n*-C₃₁ of Lake Panch Pokhari range from -126 ‰ to -260 ‰ (Table 1) and correlate significantly with each

other. The coefficients of correlation for $\delta^2\text{H}$ of $n\text{-C}_{25}$, $n\text{-C}_{27}$, $n\text{-C}_{29}$, and $n\text{-C}_{31}$ range from 0.84 to 0.96 ($p < 0.001$; $n = 38$). The weighted mean $\delta^2\text{H}$ of all four n -alkanes is plotted versus depth in Fig. 2a. Accordingly, the $\delta^2\text{H}_{n\text{-alkane}}$ record reveals a pronounced trend towards more negative values from the deglaciation to the Early Holocene. This trend is interrupted by two periods showing $\delta^2\text{H}_{n\text{-alkane}}$ maxima, which coincide with the Younger Dryas and presumably the Older Dryas events. For details on the age-depth model, the reader is referred to Zech *et al.* (2014b).

The $\delta^2\text{H}_{n\text{-alkane}}$ record reveals similarities with the $\delta^{18}\text{O}$ record established for the sugar biomarkers arabinose, fucose and xylose from Lake Panch Pokhari (Zech *et al.*, 2014b) (Fig. 2b). Namely, both records show maxima for the deglaciation and the Older and the Younger Dryas, whereas they show minima for the Bølling and the Allerød periods. However, the records also feature clear discrepancies. Particularly, the $\delta^2\text{H}_{n\text{-alkane}}$ record is characterized by very negative values throughout the Holocene, whereas the Holocene $\delta^{18}\text{O}_{\text{sugar}}$ values are well within the range of the Late Glacial $\delta^{18}\text{O}_{\text{sugar}}$ values (Fig. 2a and b).

Study 6

Table 1: $\delta^2\text{H}$ values of individual *n*-alkanes. Measurements were carried out in triplicate (sd = standard deviation).

Depth (cm)	$\delta^2\text{H}_{n\text{-alkanes}}$ (‰)								Chronology
	C ₂₅ mean	sd	C ₂₇ mean	sd	C ₂₉ mean	sd	C ₃₁ mean	sd	
15	-204	2	-206	1	-212	6	-227	1	Holocene
50	-223	0	-219	1	-227	1	-245	0	
60	-223	1	-224	2	-224	2	-234	1	
70	-216	2	-208	2	-218	4	-222	0	
90	-226	5	-209	5	-204	9	-204	4	
130	-200	2	-201	1	-217	5	-211	10	
150	-215	1	-204	1	-207	1	-231	1	
160	-205	2	-198	2	-213	2	-211	3	
190	-220	1	-223	1	-235	2	-245	2	
200	-224	3	-215	1	-223	4	-230	1	
300	-234	3	-217	7	-249	6	-222	8	
305	-192	8	-210	6	-260	6	-235	5	
320	-233	9	-223	8	-250	6	-217	9	
335	-217	2	-203	2	-207	2	-199	3	
360	-206	4	-195	2	-173	3	-166	2	Younger Dryas
375	-147	7	-154	3	-171	2	-172	3	
388	-178	4	-183	3	-192	1	-186	8	Allerød
393	-157	3	-173	2	-202	2	-191	4	
402	-219	1	-211	2	-229	3	-234	4	
408	-175	1	-178	1	-190	2	-198	2	Older Dryas
413	-138	2	-158	1	-172	0	-188	3	
417	-133	2	-145	3	-169	5	-176	4	
418	-171	5	-170	6	-186	1	-182	4	
420	-184	2	-186	2	-192	1	-191	3	
422	-180	6	-184	3	-189	3	-180	1	Bølling
424	-172	4	-171	2	-191	7	-182	2	
426	-182	3	-184	3	-189	6	-182	4	
428	-183	2	-181	1	-199	1	-190	2	
430	-183	3	-178	1	-188	2	-188	4	
432	-158	2	-160	7	-180	1	-178	2	
434	-141	2	-145	1	-157	7	-160	3	
436	-160	4	-166	2	-180	3	-182	2	Deglaciation
438	-147	1	-156	1	-170	2	-172	1	
442	-145	1	-127	1	-146	1	-140	5	
444	-141	3	-146	1	-161	2	-154	3	
446	-151	2	-156	1	-174	2	-157	2	
448	-126	7	-144	4	-161	2	-157	8	
450	-133	5	-140	2	-155	4	-153	1	

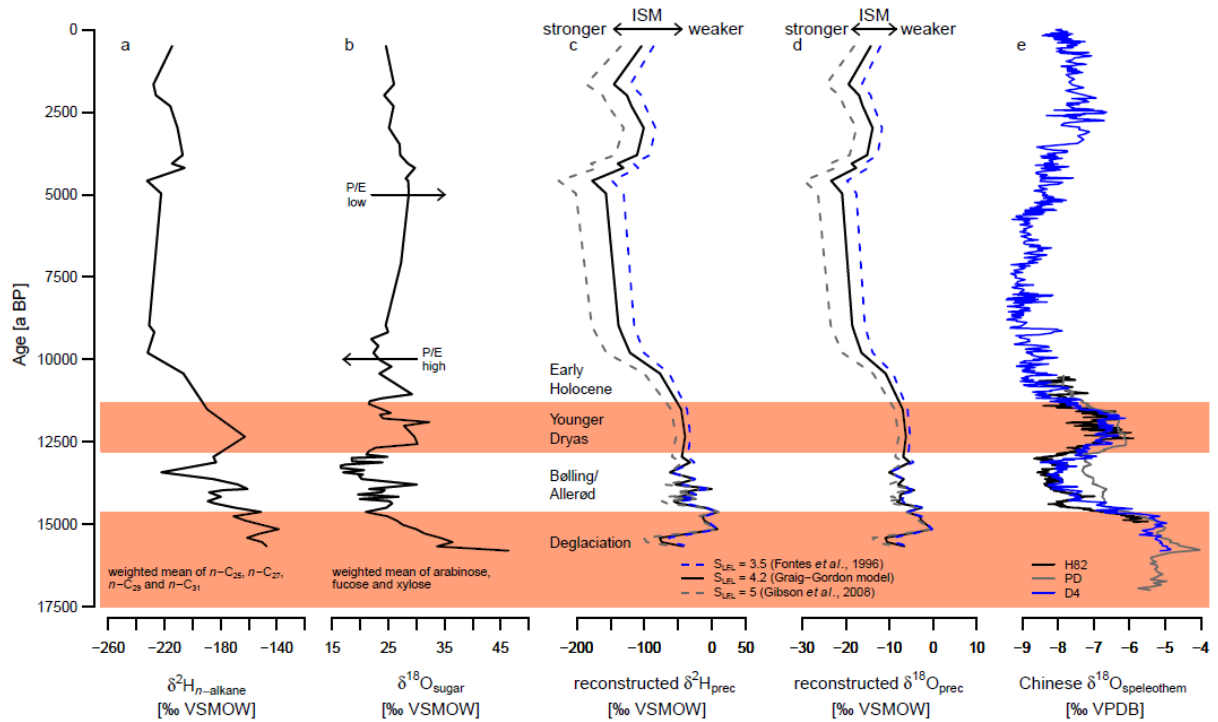


Fig. 2: Comparison of (a) the Lake Panch Pokhari $\delta^2\text{H}_{n\text{-alkane}}$ record (weighted mean of $n\text{-C}_{25}$, $n\text{-C}_{27}$, $n\text{-C}_{29}$, and $n\text{-C}_{31}$) with (b) the $\delta^{18}\text{O}_{\text{sugar}}$ record (from Zech *et al.*, 2014), (c, d) the reconstructed $\delta^2\text{H}_{\text{prec}}$ and $\delta^{18}\text{O}_{\text{prec}}$ records and (e) the $\delta^{18}\text{O}$ records of Chinese speleothems (Wang *et al.*, 2001; Dykoski *et al.* 2005). P/E = ratio of precipitation to evaporation; S_{LEL} = slope of the evaporation line; H82, PD, D4 = identification of Chinese speleothems.

4.2 Interpretation – $\delta^2\text{H}_{n\text{-alkane}}$ and $\delta^{18}\text{O}_{\text{sugar}}$ reflect lake water

A fundamental question for the interpretation of the $\delta^2\text{H}_{n\text{-alkane}}$ and $\delta^{18}\text{O}_{\text{sugar}}$ records is whether the sedimentary biomarkers are autochthonous and of aquatic origin or allochthonous and of terrestrial origin. This is crucial because, albeit with an offset called biosynthetic fractionation factor (Schmidt *et al.*, 2001), aquatic biomarkers can be considered to reflect primarily the isotopic composition of lake water. By contrast, biomarkers produced by terrestrial plants reflect the isotopic composition of leaf water (Tuthorn *et al.*, 2014; Zech *et al.*, 2013), i.e. precipitation modified by evapo(transpi)rative enrichment of soil and leaf water, thus requiring a different interpretation.

Concerning Lake Panch Pokhari, there are several arguments pointing to sedimentary organic matter being primarily of aquatic origin. First, the catchment is very small and sparsely vegetated. Second, carbon and nitrogen ratios (C/N) may serve as proxy for aquatic versus terrestrial organic matter. This is based on the finding that non-vascular aquatic organisms typically have very low C/N ratios of <10, whereas terrestrial vascular plants typically have much higher C/N ratios (Meyers and Ishiwatari, 1993). With C/N ratios of <12 (Krstic *et al.*, 2012) (Fig. 4a), the sediments of Lake Panch Pokhari are well within the range of sedimentary organic matter which has not experienced significant terrestrial input. Third, the sugar biomarker patterns strongly indicate that the sugars are of aquatic origin because of the abundant occurrence of fucose (Zech *et al.*, 2014b). The latter is known to be a major component of phytoplankton, zooplankton and bacteria (Hecky *et al.*, 1973; Biersmith & Benner, 1998; Ogier *et al.*, 2001), whereas it is produced in much lower concentrations by vascular plants (Jia *et al.*, 2008; Zech *et al.*, 2012). Fourth, the *n*-alkanes *n*-C₂₅, *n*-C₂₇, *n*-C₂₉, and *n*-C₃₁ dominate in the sediments of Lake Panch Pokhari. These homologues are often considered to be of terrestrial origin in lacustrine archives because they clearly dominate the *n*-alkane patterns of most higher plant leaf-waxes (Eglinton & Hamilton, 1967; Meyers, 2003). However, long-chained *n*-alkanes are no exclusive biomarkers for terrestrial plants. They have been identified to dominate also in emergent aquatic plants and are reported to be derived from certain microalgae such as *Botryococcus braunii* and diatoms, too (Bradley, 1966; Lichtfouse *et al.*, 1994; Volkman *et al.*, 1998; Ficken *et al.*, 2000; Aichner *et al.*, 2010b Douglas *et al.*, 2012;). Indeed, the sediments of Lake Panch Pokhari are very rich in diatoms, yielding up to ~ 70% diatom abundance and up to ~45% biogenic opal (Krstic *et al.*, 2012; Krstic *et al.*, 2013).

Hence, while we acknowledge that a partial contribution of terrestrial organic matter cannot be excluded, the above arguments suggest that the investigated *n*-alkane and sugar

biomarkers are primarily of aquatic origin. This in turn allows reconstructing the isotopic composition of the paleolake water based on the $\delta^2\text{H}_{n\text{-alkane}}$ and $\delta^{18}\text{O}_{\text{sugar}}$ results by applying biosynthetic fractionation factors. For *n*-alkanes and sugars, biosynthetic fractionation factors of $\sim -160\text{‰}$ (Sessions *et al.*, 1999; Sachse *et al.*, 2006) and $\sim +27\text{‰}$ (Sternberg *et al.*, 1986; Yakir & DeNiro, 1990; Schmidt *et al.*, 2001; Cernusak *et al.*, 2003), respectively, can be assumed. Note that there is an ongoing discussion concerning the temperature dependency of the biosynthetic fractionation factor of sugars. While Sternberg and Ellsworth (2011) suggest that the factor can increase to $\sim +31\text{‰}$ at lower temperatures, this is questioned by Zech *et al.*, (2014a) and further studies, ideally hydroponic culture studies (Ellsworth and Sternberg, 2014), are needed to answer this question.

The reconstructed isotopic composition of the lake water can now be used to draw further paleoclimatic interpretations. It is determined by the isotopic composition of paleoprecipitation on the one hand and by evaporative isotopic enrichment of the lake water on the other hand. While single isotope studies based on $\delta^{18}\text{O}$ or $\delta^2\text{H}$ results alone do not allow distinguishing between these two factors, a coupled $\delta^{18}\text{O}$ and $\delta^2\text{H}$ approach offers this possibility.

4.3 Coupling $\delta^{18}\text{O}_{\text{sugar}}$ and $\delta^2\text{H}_{n\text{-alkane}}$ biomarker results of Lake Panch Pokhari

4.3.1 Deuterium-excess as proxy for lake water evaporation losses

Fig. 3 depicts the $\delta^{18}\text{O}_{\text{sugar}}$ and $\delta^2\text{H}_{n\text{-alkane}}$ biomarker results in a $\delta^{18}\text{O}$ - $\delta^2\text{H}$ diagram. By applying the biosynthetic fractionation factors for *n*-alkanes and sugars, the biomarker results can be converted into paleolake water isotopic composition (Fig. 3). The respective paleolake water data points mostly plot close to the GMWL or right of the GMWL, the latter being attributable to evaporation losses. The distance of the reconstructed paleolake water to the

GMWL can be described as deuterium excess ($d = \delta^2\text{H} - 8 \cdot \delta^{18}\text{O}$; Dansgaard, 1964). The reconstructed d-excess values of Lake Panch Pokhari range from +57 to -85‰ (Figs. 3 and 4).

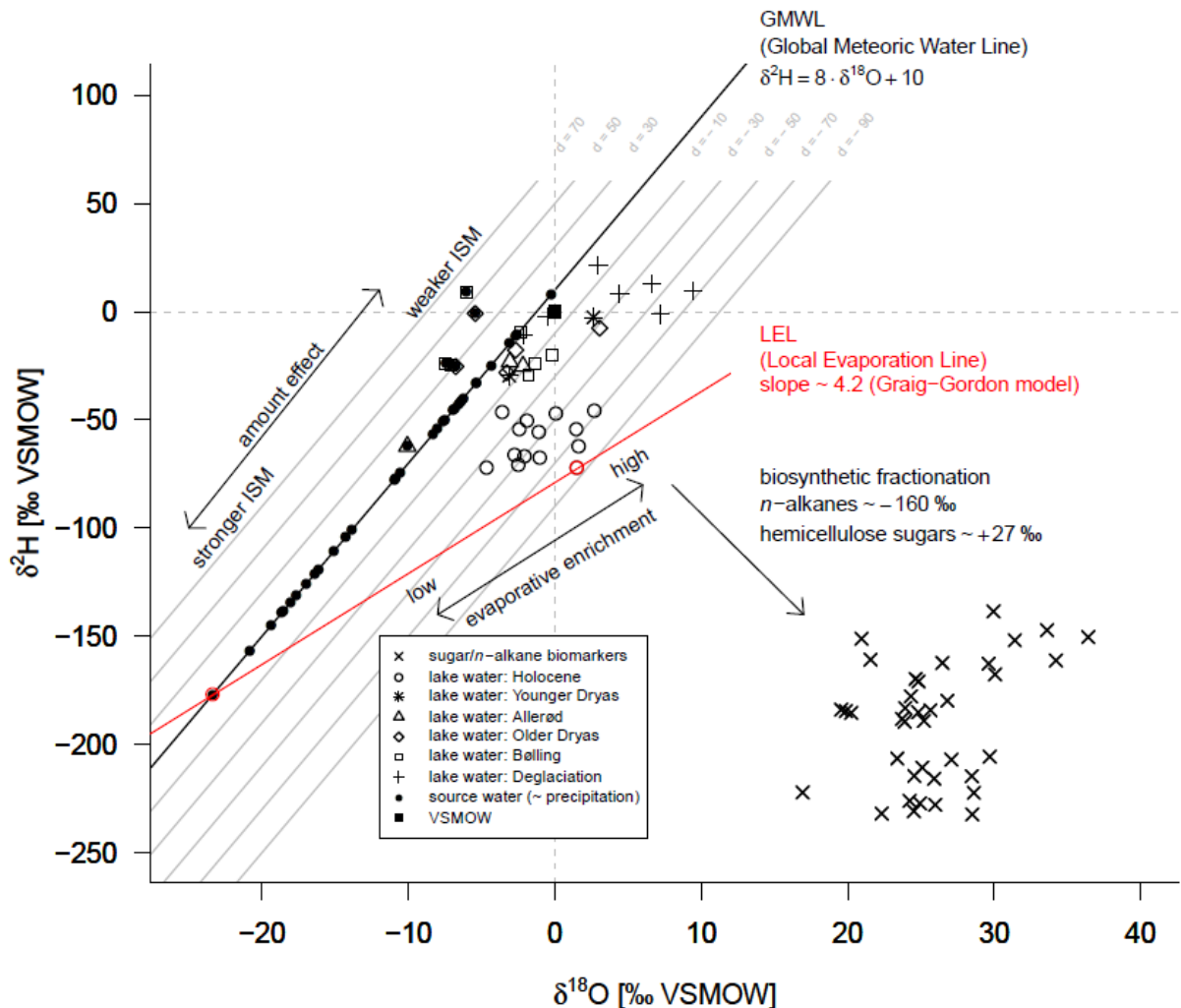


Fig. 3: $\delta^{18}\text{O}$ - $\delta^2\text{H}$ diagram illustrating the isotopic deviation of lake water (defined as deuterium-(d)-excess) from the Global Meteoric Water Line (GMWL). $\delta^{18}\text{O}$ values of hemicellulose-derived sugars (mean of arabinose, fucose, and xylose; from Zech *et al.*, 2014) and $\delta^2\text{H}$ values of wax-derived *n*-alkanes (mean of *n*-C25, *n*-C27, *n*-C29, and *n*-C31) are used for reconstruction of the isotopic composition of Panch Pokhari lake water. $\delta^2\text{H}$ and $\delta^{18}\text{O}$ values of precipitation are calculated as intersections of the individual local evaporation lines (LEL) with the GMWL using a slope value of 4.2.

Note that d-excess values of $> +10\text{‰}$, i.e. data points plotting left of the GMWL in Fig. 3, are not necessarily outliers because such positive d-excess values can occur when there

is strong recycling of rainwater (re-evaporation) and d-excess values of up to +30‰ are reported also from the Tibetan Plateau (Tian *et al.*, 2001).

Given that evaporation causes lake water to become ^{18}O and ^2H enriched along the LELs, the degree of evaporative losses is reflected by the d-excess values (Fig. 3). We therefore suggest that the d-excess, which is reconstructed from the aquatic *n*-alkane and sugar biomarkers, can serve as proxy for the evaporation history of Lake Panch Pokhari (Fig. 4c). For comparison and in addition, Fig. 4 also depicts the C/N ratio and the hydrogen index (HI) as lake level indicators (Talbot and Livingstone, 1989).

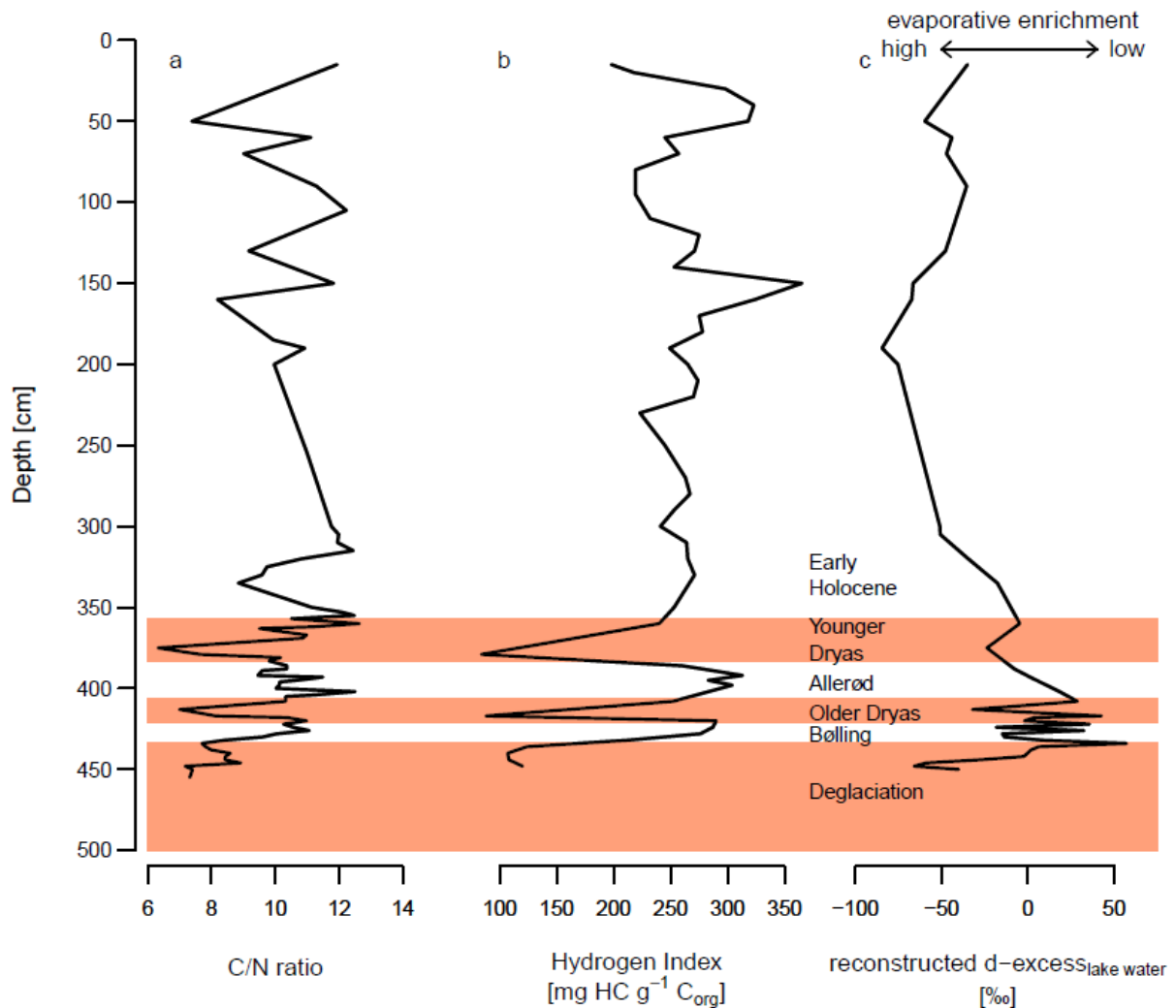


Fig. 4: Comparison of (a) C/N ratio (from Krstic *et al.*, 2011) (b) Hydrogen Index (HI) and (c) deuterium-excess of lake water as proxies for evaporation history of Lake Panch Pokhari.

These indicators are based on the notion, that lake desiccation results in mineralization of the sedimentary organic matter due to subaerial exposure. Thereby, carbon is lost in form of CO₂ causing lower C/N ratios. Furthermore, certain organic compounds are selectively removed and inert organic compounds that are characterized by lower HI values (< 200) become relatively enriched. According to Fig. 4, all three evaporation proxies/lake level indicators reveal distinct minima during the deglaciation, the Older Dryas and the Younger Dryas. The multi-proxy approach hence clearly suggests that during these periods Lake Panch Pokhari desiccated, presumably due to greatly reduced precipitation. This interpretation is in agreement with the generally accepted notion that the Indian Summer Monsoon and the East Asian Summer Monsoon were very weak before ~15 ka BP and during the Younger Dryas, as indicated by maxima of East and South Asian speleothem $\delta^{18}\text{O}$ records (Fig. 2e). While the C/N ratio shows several more minima also during the Holocene, the HI never drops again below 200 (Fig. 4b). This suggests that Lake Panch Pokhari did not desiccate during the Holocene. Also this finding is in agreement with the monsoon history, because more negative $\delta^{18}\text{O}_{\text{speleothem}}$ values during the Holocene are interpreted to reflect intensified monsoon precipitation (Fig. 2e). Nevertheless, the d-excess indicates that relatively high evaporative enrichment of the lake water occurred, especially during the Middle Holocene (Fig. 4c). This can be explained with overall higher temperatures and thus lake water evaporation during the Holocene compared to the Late Glacial.

4.3.2 Reconstructed $\delta^{18}\text{O}_{\text{prec}}$ and $\delta^2\text{H}_{\text{prec}}$ values

As described in section 3.2 and depicted in Fig. 3, the coupled $\delta^{18}\text{O}$ and $\delta^2\text{H}$ biomarker approach furthermore allows reconstructing the isotopic composition of precipitation as intersects of the LELs with the GMWL. Using a slope of 4.2 for the LEL yields $\delta^2\text{H}_{\text{prec}}$ and $\delta^{18}\text{O}_{\text{prec}}$ values which range from -177 ‰ to +7.9 ‰ and from -23.4 ‰ to -0.3 ‰, respectively (Figs. 2c and d). In order to provide a confidence interval, Figs. 2c and d additionally display

$\delta^{18}\text{O}_{\text{prec}}$ and $\delta^2\text{H}_{\text{prec}}$ records obtained when using slopes of 3.5 and 5. The reconstructed $\delta^{18}\text{O}_{\text{prec}}$ values for the uppermost and youngest sediments of Lake Panch Pokhari are well in agreement with modern precipitation of close-by meteorological station Nyalam (weighted $\delta^{18}\text{O}_{\text{prec}} = -13.6\text{‰}$, Tian *et al.*, 2003).

Figure 2 furthermore illustrates that the reconstructed $\delta^{18}\text{O}_{\text{prec}}$ record of Lake Panch Pokhari strongly resembles the $\delta^{18}\text{O}$ records of Chinese speleothems (Wang *et al.*, 2001; Dykoski *et al.*, 2005), thus validating the proposed modeling approach. Especially the pronounced trend towards more negative $\delta^{18}\text{O}$ values at the transition from the late glacial to the Early Holocene is much better reflected by the reconstructed $\delta^{18}\text{O}_{\text{prec}}$ record (Fig. 2d) compared to the $\delta^{18}\text{O}_{\text{sugar}}/\delta^{18}\text{O}_{\text{lake water}}$ record (Fig. 2b). Overall more negative $\delta^{18}\text{O}_{\text{prec}}$ values in the High Himalaya compared to Southern and Eastern China can be attributed to the altitude effect (Meier *et al.*, 2013).

Concerning the paleoclimatic interpretation, the strong resemblance of the $\delta^{18}\text{O}_{\text{prec}}$ record of Lake Panch Pokhari with the Chinese speleothem $\delta^{18}\text{O}$ records supports the idea that the Indian Summer Monsoon and the East Asian Summer Monsoon varied mostly synchronously during the late glacial and the Holocene. Furthermore, the most pronounced intensification of both monsoon systems coincides with the Early Holocene and lasted until approximately 5 ka BP (Fig. 2). Both interpretations are in agreement with the generally accepted knowledge about monsoon history (Zhang *et al.*, 2011).

5. Conclusions

A lacustrine $\delta^2\text{H}$ biomarker record was established for Lake Panch Pokhari. The $\delta^2\text{H}$ values of the *n*-alkanes *n*-C₂₅, *n*-C₂₇, *n*-C₂₉, and *n*-C₃₁ range from -126 ‰ to -260 ‰. The $\delta^2\text{H}_{\text{n-alkane}}$ record resembles the $\delta^{18}\text{O}_{\text{sugar}}$ biomarker record, shows high values for the deglaciation and the Older and the Younger Dryas, but low values for the Bølling and the

Allerød periods. However, the two biomarker isotope records also reveal discrepancies, for instance during the Holocene, when the $\delta^2\text{H}_{\text{n-alkane}}$ record is characterized by the most negative values whereas the $\delta^{18}\text{O}_{\text{sugar}}$ record is characterized by intermediate values.

The investigated biomarkers are primarily of autochthonous, aquatic origin. This seems plausible because (i) the catchment is very small and sparsely vegetated, (ii) the C/N ratios are relatively low (<12), (iii) the sugar biomarker patterns show high abundance of fucose and (iv) the sediments are very rich in diatoms. Hence, their isotopic composition can be used to reconstruct the isotopic composition of lake water by applying biosynthetic fractionation factors. The reconstructed d-excess of lake water ranges from +57 ‰ to -85 ‰ and can serve as proxy for the evaporation history of Lake Panch Pokhari. Distinct minima suggest strong evaporative enrichment during the deglaciation, the Older Dryas and the Younger Dryas, which is corroborated by the lake desiccation proxies C/N and HI and can be attributed to greatly reduced precipitation. The coupled $\delta^{18}\text{O}_{\text{sugar}}$ and $\delta^2\text{H}_{\text{n-alkane}}$ approach furthermore allowed reconstructing $\delta^{18}\text{O}_{\text{prec}}$ and $\delta^2\text{H}_{\text{prec}}$ values using a Craig-Gordon model. The respective precipitation records are well in agreement with Chinese speleothem $\delta^{18}\text{O}$ records suggesting that the Indian Summer Monsoon varied synchronously with the East Asian Summer Monsoon and became strongly intensified during the Early Holocene.

Acknowledgements

We kindly thank Prof. B. Huwe (University Bayreuth) and Prof. L. Zöller (University Bayreuth) for logistic support and Prof. K. Rozanski for having previously introduced M.T., J.H. and M.Z. into water isotope modelling. This study was financed by the German Research Foundation (ZE 844/1-2).

References

- Aichner B., Herzsuh U., Wilkes H., Vieth A., and Boehner J. (2010a) δD values of n-alkanes in Tibetan lake sediments and aquatic macrophytes - A surface sediment study and application to a 16 ka record from Lake Koucha. *Organic Geochemistry* **41**(8), 779-790.
- Aichner B., Wilkes H., Herzsuh U., Mischke S., and Zhang C. (2010b) Biomarker and compound-specific $\delta^{13}C$ evidence for changing environmental conditions and carbon limitation at Lake Koucha, eastern Tibetan Plateau. *Journal of Paleolimnology* **43**(4), 873-899.
- Araguas-Araguas L., Froehlich K., and Rozanski K. (2000) Deuterium and oxygen-18 isotope composition of precipitation and atmospheric moisture. *Hydrological Processes* **14**(8), 1341-1355.
- Biersmith A. and Benner R. (1998) Carbohydrates in phytoplankton and freshly produced dissolved organic matter. *Marine Chemistry* **63**(1-2), 131-144.
- Bradley W. H. (1966) Tropical Lakes, Copropel, and Oil Shale. *Geological Society of America Bulletin* **77**, 1333-1338.
- Cernusak L. A., Wong S. C., and Farquhar G. D. (2003) Oxygen isotope composition of phloem sap in relation to leaf water in *Ricinus communis*. *Functional Plant Biology* **30**(10), 1059-1070.
- Chapligin B., Meyer H., Swann G. E. A., Meyer-Jacob C., and Hubberten H.-W. (2012) A 250 ka oxygen isotope record from diatoms at Lake El'gygytgyn, far east Russian Arctic. *Climate of the Past* **8**(2), 1169-1207.
- Craig H. (1961) Isotopic Variations in Meteoric Waters. *Science* **133**(3465), 1702-1703.
- Craig H. and Gordon L. I. (1965) Deuterium and oxygen-18 variations in the ocean and the marine atmosphere. *Conference on Stable Isotopes in Oceanographic Studies and Paleotemperatures*, 9-130.
- Cruz F. W., Burns S. J., Karmann I., Sharp W. D., Vuille M., Cardoso A. O., Ferrari J. A., Silva Dias P. L., and Viana O. (2005) Insolation-driven changes in atmospheric circulation over the past 116,000 years in subtropical Brazil. *Nature* **434**(7029), 63-66.
- Dansgaard W. (1964) Stable isotopes in precipitation. *Tellus* **16**(4), 436-468.
- Dansgaard W., Johnsen S. J., Clausen H. B., Dahl-Jensen D., Gundestrup N. S., Hammer C. U., Hvidberg C. S., Steffensen J. P., Sveinbjornsdottir A. E., Jouzel J., and Bond G.

- (1993) Evidence for general instability of past climate from a 250-kyr ice-core record. *Nature* **364**, 218-220.
- Douglas P. M. J., Pagani M., Brenner M., Hodell D. A., and Curtis J. H. (2012) Aridity and vegetation composition are important determinants of leaf-wax δD values in southeastern Mexico and Central America. *Geochimica et Cosmochimica Acta* **97**, 24-45.
- Dykoski C. A., Edwards R. L., Cheng H., Yuan D., Cai Y., Zhang M., Lin Y., Qing J., An Z., and Revenaugh J. (2005) A high-resolution, absolute-dated Holocene and deglacial Asian monsoon record from Dongge Cave, China. *Earth and Planetary Science Letters* **233**(1-2), 71-86.
- Eglinton G. and Hamilton R. J. (1967) Leaf Epicuticular Waxes. *Science* **156**(3780), 1322-1335.
- Ellsworth P. V. and Sternberg L. S. L. (2014) Biochemical effects of salinity on oxygen isotope fractionation during cellulose synthesis. *New Phytologist*, DOI: 10.1111/nph.12696.
- Ficken K. J., Li B., Swain D. L., and Eglinton G. (2000) An n-alkane proxy for the sedimentary input of submerged/floating freshwater aquatic macrophytes. *Organic Geochemistry* **31**(7-8), 745-749.
- Fontes J.-C., Gasse F., and Gibert E. (1996) Holocene environmental changes in Lake Bangong basin (Western Tibet). Part 1: Chronology and stable isotopes of carbonates of a Holocene lacustrine core. *Palaeogeography, Palaeoclimatology, Palaeoecology* **120**(1-2), 25-47.
- Gat J. R. (1971) Comments on the Stable Isotope Method in Regional Groundwater Investigations. *Water Resources Research* **7**(4), 980-993.
- Gat J. R. (1995) Stable Isotopes of Fresh and Saline Lakes. In *Physics and Chemistry of Lakes* (ed. A. Lerman, D. Imboden, and J. R. Gat), pp. 139-165. Springer.
- Gat J. R. and Bowser C. (1991) The heavy isotope enrichment of water in coupled evaporative systems. In *Stable Isotope Geochemistry: A Tribute to Samuel Epstein* (ed. H. P. Taylor, J. R. O'Neil, and I. R. Kaplan), pp. 159-168. The Geochemical Society.
- Gibson J. J. (2001) Forest-tundra water balance signals traced by isotopic enrichment in lakes. *Journal of Hydrology* **251**(1-2), 1-13.
- Gibson J. J., Birks S. J., and Edwards T. W. D. (2008) Global prediction of δA and δ^2H - $\delta^{18}O$ evaporation slopes for lakes and soil water accounting for seasonality. *Global Biogeochemical Cycles* **22**(2), GB2031.

- Gibson J. J., Edwards T. W. D., Birks S. J., St Amour N. A., Buhay W. M., McEachern P., Wolfe B. B., and Peters D. L. (2005) Progress in isotope tracer hydrology in Canada. *Hydrological Processes* **19**(1), 303-327.
- Gonfiantini R. (1986) Environmental isotopes in lake studies. In *Handbook of Environmental Isotope Geochemistry*, Vol. 3 (ed. P. Fritz and J. C. Fontes), pp. 113-168. Elsevier.
- Hecky R. E., Mopper K., Kilham P., and Degens E. T. (1973) The amino acid and sugar composition of diatom cell-walls. *Marine Biology* **19**(4), 323-331.
- Hilkert A. W., Douthitt C. B., Schlueter H. J., and Brand W. A. (1999) Isotope ratio monitoring gas chromatography/Mass spectrometry of D/H by high temperature conversion isotope ratio mass spectrometry. *Rapid Communications in Mass Spectrometry* **13**(13), 1226-1230.
- Horita J. and Wesolowski D. J. (1994) Liquid-vapor fractionation of oxygen and hydrogen isotopes of water from the freezing to the critical temperature. *Geochimica et Cosmochimica Acta* **58**(16), 3425-3437.
- Huang Y., Shuman B., Wang Y., and Webb T. (2004) Hydrogen isotope ratios of individual lipids in lake sediments as novel tracers of climatic and environmental change: a surface sediment test. *Journal of Paleolimnology* **31**(3), 363-375.
- Jia G., Dungait J. A. J., Bingham E. M., Valiranta M., Korhola A., and Evershed R. P. (2008) Neutral monosaccharides as biomarker proxies for bog-forming plants for application to palaeovegetation reconstruction in ombrotrophic peat deposits. *Organic Geochemistry* **39**(12), 1790-1799.
- Krstic S. S., Pavlov A., Levkov Z., and Juettner I. (2013) New *Eunotia* taxa in core samples from Lake Panch Pokhari in the Nepalese Himalaya. *Diatom Research* **28**(2), 203-217.
- Krstic S. S., Zech W., Obrecht I., Svircev Z., and Markovic S. B. (2012) Late Quaternary environmental changes in Helambu Himal, Central Nepal, recorded in the diatom flora assemblage composition and geochemistry of Lake Panch Pokhari. *Journal of Paleolimnology* **47**(1), 113-124.
- Li Q., Nakatsuka T., Kawamura K., Liu Y., and Song H. (2011) Regional hydroclimate and precipitation $\delta^{18}\text{O}$ revealed in tree-ring cellulose $\delta^{18}\text{O}$ from different tree species in semi-arid Northern China. *Chemical Geology* **282**, 19-28.
- Lichtfouse É., Derenne S., Mariotti A., and Largeau C. (1994) Possible algal origin of long chain odd n-alkanes in immature sediments as revealed by distributions and carbon isotope ratios. *Organic Geochemistry* **22**(6), 1023-1027.

- Loader N. J., Santillo P. M., Woodman-Ralph J. P., Rolfe J. E., Hall M. A., Gagen M., Robertson I., Wilson R., Froyd C. A., and McCarroll D. (2008) Multiple stable isotopes from oak trees in southwestern Scotland and the potential for stable isotope dendroclimatology in maritime climatic regions. *Chemical Geology* **252**, 62-71.
- Mayr C., Luecke A., Stichler W., Trimborn P., Ercolano B., Oliva G., Ohlendorf C., Soto J., Fey M., Haberzettl T., Janssen S., Schaebitz F., Schleser G. H., Wille M., and Zolitschka B. (2007) Precipitation origin and evaporation of lakes in semi-arid Patagonia (Argentina) inferred from stable isotopes ($\delta^{18}\text{O}$, $\delta^2\text{H}$). *Journal of Hydrology* **334**(1-2), 53-63.
- Meier C., Knoche M., Merz R., and Weise S. M. (2013) Stable isotopes in river waters in the Tajik Pamirs: regional and temporal characteristics. *Isotopes in Environmental and Health Studies* **49**(4), 542-554.
- Merlivat L. (1978) Molecular diffusivities of H_2^{16}O , HD^{16}O , and H_2^{18}O in gases. *The Journal of Chemical Physics* **69**(6), 2864-2871.
- Meyers P. A. (2003) Applications of organic geochemistry to paleolimnological reconstructions: a summary of examples from the Laurentian Great Lakes. *Organic Geochemistry* **34**(2), 261-289.
- Meyers P. A. and Ishiwatari R. (1993) Lacustrine organic geochemistry-an overview of indicators of organic matter sources and diagenesis in lake sediments. *Organic Geochemistry* **20**(7), 867-900.
- Mischke S., Aichner B., Diekmann B., Herzschuh U., Plessen B., Wuennemann B., and Zhang C. (2010) Ostracods and stable isotopes of a late glacial and Holocene lake record from the NE Tibetan Plateau. *Chemical Geology* **276**(1-2), 95-103.
- Mischke S. and Chen F. (2014) Introduction to "Late Pleistocene and Holocene climate change in continental Asia". *Journal of Paleolimnology* **51**(2), 157-159.
- Muegler I., Sachse D., Werner M., Xu B., Wu G., Yao T., and Gleixner G. (2008) Effect of lake evaporation on δD values of lacustrine n-alkanes: A comparison of Nam Co (Tibetan Plateau) and Holzmaar (Germany). *Organic Geochemistry* **39**(6), 711-729.
- Ogier S., Disnar J.-R., Albéric P., and Bourdier G. (2001) Neutral carbohydrate geochemistry of particulate material (trap and core sediments) in an eutrophic lake (Aydat, France). *Organic Geochemistry* **32**(1), 151-162.
- Rao Z., Zhu Z., Jia G., Henderson A. C. G., Xue Q., and Wang S. (2009) Compound specific δD values of long chain n-alkanes derived from terrestrial higher plants are indicative of

- the δD of meteoric waters: Evidence from surface soils in eastern China. *Organic Geochemistry* **40**(8), 922-930.
- Roden J. S., Lin G., and Ehleringer J. R. (2000) A mechanistic model for interpretation of hydrogen and oxygen isotope ratios in tree-ring cellulose. *Geochimica et Cosmochimica Acta* **64**(1), 21-35.
- Rozanski K., Sonntag C., and Muennich K. O. (1982) Factors controlling stable isotope composition of European precipitation. *Tellus* **34**(2), 142-150.
- Sachse D., Radke J., and Gleixner G. (2004) Hydrogen isotope ratios of recent lacustrine sedimentary n-alkanes record modern climate variability. *Geochimica et Cosmochimica Acta* **68**(23), 4877-4889.
- Sachse D., Radke J., and Gleixner G. (2006) δD values of individual *n*-alkanes from terrestrial plants along a climatic gradient - Implications for the sedimentary biomarker record. *Organic Geochemistry* **37**(4), 469-483.
- Sauer P. E., Miller G. H., and Overpeck J. T. (2001) Oxygen isotope ratios of organic matter in arctic lakes as a paleoclimate proxy: field and laboratory investigations. *Journal of Paleolimnology* **25**(1), 43-64.
- Schmidt H.-L., Werner R. A., and Rossmann A. (2001) ^{18}O pattern and biosynthesis of natural plant products. *Phytochemistry* **58**(1), 9-32.
- Sessions A. L., Burgoyne T. W., Schimmelmann A., and Hayes J. M. (1999) Fractionation of hydrogen isotopes in lipid biosynthesis. *Organic Geochemistry* **30**(9), 1193-1200.
- Sternberg L., DeNiro M. J., and Savidge R. A. (1986) Oxygen isotope exchange between metabolites and water during biochemical reactions leading to cellulose synthesis. *Plant Physiology* **82**, 423-427.
- Sternberg L. and Ellsworth P. F. V. (2011) Divergent Biochemical Fractionation, Not Convergent Temperature, Explains Cellulose Oxygen Isotope Enrichment across Latitudes. *PLoS ONE* **6**(11), DOI:10.1371/journal.pone.0028040.
- Talbot M. R. and Livingstone D. A. (1989) Hydrogen index and carbon isotopes of lacustrine organic matter as lake level indicators. *Palaeogeography, Palaeoclimatology, Palaeoecology* **70**(1-3), 121-137.
- Thompson L. G., Davis M. E., Mosley-Thompson E., Lin P.-N., Henderson K. A., and Mashiotta T. A. (2005) Tropical ice core records: evidence for asynchronous glaciation on Milankovitch timescales. *Journal of Quaternary Science* **20**(7-8), 723-733.

-
- Tian L., Yao T., Schuster P. F., White J. W. C., Ichiyanagi K., Pendall E., Pu J., and Yu W. (2003) Oxygen-18 concentrations in recent precipitation and ice cores on the Tibetan Plateau. *Journal of Geophysical Research: Atmospheres* **108**(D9), 4293.
- Tian L., Yao T., Sun W., Stievenard M., and Jouzel J. (2001) Relationship between δD and $\delta^{18}O$ in precipitation on north and south of the Tibetan Plateau and moisture recycling. *Earth Sciences* **44**(9), 789-796.
- Tuthorn M., Zech M., Ruppenthal M., Oelmann Y., Kahmen A., Valle H. c. F. d., Wilcke W., and Glaser B. (2014) Oxygen isotope ratios ($^{18}O/^{16}O$) of hemicellulose-derived sugar biomarkers in plants, soils and sediments as paleoclimate proxy II: Insight from a climate transect study. *Geochimica et Cosmochimica Acta* **126**, 624-634.
- Vogt H. J. (1978) Isotopen trennung bei der Verdunstung von Wasser, University of Heidelberg.
- Volkman J. K., Barrett S. M., Blackburn S. I., Mansour M. P., Sikes E. L., and Gelin F. o. (1998) Microalgal biomarkers: A review of recent research developments. *Organic Geochemistry* **29**(5-7), 1163-1179.
- Wang Y. J., Cheng H., Edwards R. L., An Z. S., Wu J. Y., Shen C.-C., and Dorale J. A. (2001) A High-Resolution Absolute-Dated Late Pleistocene Monsoon Record from Hulu Cave, China. *Science* **294**(5550), 2345-2348.
- Wissel H., Mayr C., and Luecke A. (2008) A new approach for the isolation of cellulose from aquatic plant tissue and freshwater sediments for stable isotope analysis. *Organic Geochemistry* **39**(11), 1545-1561.
- Yakir D. and DeNiro M. J. (1990) Oxygen and hydrogen isotope fractionation during cellulose metabolism in *Lemna gibba* L. *Plant Physiology* **93**(1), 325-332.
- Zech M. and Glaser B. (2008) Improved compound-specific $\delta^{13}C$ analysis of n-alkanes for application in palaeoenvironmental studies. *Rapid Communications in Mass Spectrometry* **22**(2), 135-142.
- Zech M., Mayr C., Tuthorn M., Leiber-Sauheitl K., and Glaser B. (2014a) Oxygen isotope ratios ($^{18}O/^{16}O$) of hemicellulose-derived sugar biomarkers in plants, soils and sediments as paleoclimate proxy I: Insight from a climate chamber experiment. *Geochimica et Cosmochimica Acta* **126**, 614-623.
- Zech M., Tuthorn M., Detsch F., Rozanski K., Zech R., Zoeller L., Zech W., and Glaser B. (2013) A 220 ka terrestrial $\delta^{18}O$ and deuterium excess biomarker record from an eolian permafrost paleosol sequence, NE-Siberia. *Chemical Geology* **360-361**, 220-230.

- Zech M., Tuthorn M., Zech R., Schluetz F., Zech W., and Glaser B. (2014b) A 16-ka $\delta^{18}\text{O}$ record of lacustrine sugar biomarkers from the High Himalaya reflects Indian Summer Monsoon variability. *Journal of Paleolimnology* **51**(2), 241-251.
- Zech M., Werner R. A., Juchelka D., Kalbitz K., Buggle B., and Glaser B. (2012) Absence of oxygen isotope fractionation/exchange of (hemi-) cellulose derived sugars during litter decomposition. *Organic Geochemistry* **42**, 1470-1475.
- Zhang J., Chen F., Holmes J. A., Li H., Guo X., Wang J., Li S., Lue Y., Zhao Y., and Qiang M. (2011) Holocene monsoon climate documented by oxygen and carbon isotopes from lake sediments and peat bogs in China: a review and synthesis. *Quaternary Science Reviews* **30**(15-16), 1973-1987.

Additional peer-reviewed publications

Zech M., Saurer M., Tuthorn M., Rinne K., Werner R. A., Siegwolf R., Glaser B., and Juchelka D. (2013a) A novel methodological approach for delta O-18 analysis of sugars using gas chromatography-pyrolysis-isotope ratio mass spectrometry. *Isotopes in Environmental and Health Studies* **49**(4), 492-502.

Zech M., Tuthorn M., Detsch F., Rozanski K., Zech R., Zoeller L., Zech W., and Glaser B. (2013b) A 220 ka terrestrial $\delta^{18}\text{O}$ and deuterium excess biomarker record from an eolian permafrost paleosol sequence, NE-Siberia. *Chemical Geology* **360-361**, 220-230.

(Eidesstattliche) Versicherungen und Erklärungen

(§5 Nr. 4 PromO)

Hiermit erkläre ich, dass keine Tatsachen vorliegen, die mich nach den gesetzlichen Bestimmungen über die Führung akademischer Grade zur Führung eines Doktorgrades unwürdig erscheinen lassen.

(§8 S. 2 Nr. 5 PromO)

Hiermit erkläre ich mich damit einverstanden, dass die elektronische Fassung meiner Dissertation unter Wahrung meiner Urheberrechte und des Datenschutzes einer gesonderten Überprüfung hinsichtlich der eigenständigen Anfertigung der Dissertation unterzogen werden kann.

(§8 S. 2 Nr. 7 PromO)

Hiermit erkläre ich eidesstattlich, dass ich die Dissertation selbständig verfasst und keine anderen als die von mir angegebenen Quellen und Hilfsmittel benutzt habe.

Ich habe die Dissertation nicht bereits zur Erlangung eines akademischen Grades anderweitig eingereicht und auch nicht bereits diese oder eine gleichartige Doktorprüfung endgültig nicht bestanden.

(§8 S. 2 Nr. 9 PromO)

Hiermit erkläre ich, dass ich keine Hilfe von gewerblichen Promotionsberatern bzw. –vermittlern in Anspruch genommen habe und auch künftig nicht nehmen werde.

Ort, Datum, Unterschrift